UNIVERSITEIT GENT

Academiejaar 2008-2009
Faculteit Wetenschappen

Comparative and phylogenetic analysis of the early embryonic development in the phylum Nematoda

Vergelijkende en fylogenetische analyse van de vroege embryonale ontwikkeling in het fylum Nematoda

PART I: TEXT

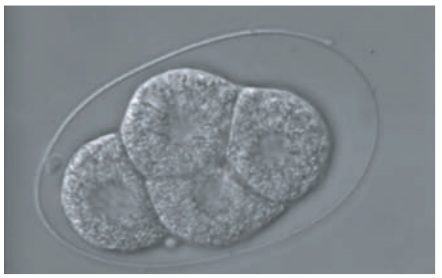
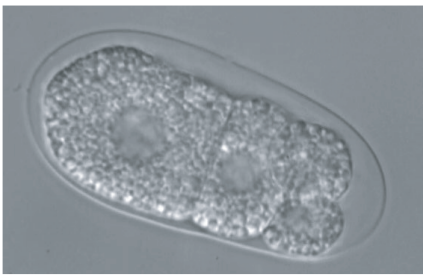


Sandra Vangestel

Promotor: Prof. dr. G. Borgonie

Co-promotors: dr. W. Houthoofd and Prof. dr. T. Artois

Thesis submitted to obtain the degree of Doctor in Sciences (Biology)

Proefschrift voorgelegd tot het bekomen van de graad van Doctor in de Wetenschappen (Biologie)

Voor ons ma en onze pa

MEMBERS OF THE READING COMMITTEE

Prof. dr. Gaetan BORGONIE, Promotor (Ugent)

dr. Wouter HOUTHOOFD, co-promotor (Ugent)

Prof. dr. Tom ARTOIS, co-promotor (Uhasselt)

Prof. dr. Einhard SCHIERENBERG (Zoologisches Instut der Universität Köln, Germany)

Prof. dr. Wilfrida DECRAEMER (Koninklijk Belgisch Instituut voor Natuurwetenschappen and Ugent)

MEMBERS OF THE EXAMINATION COMMITTEE

Prof. dr. Wim VYVERMAN, chairman (Ugent)

Prof. dr. Gaetan BORGONIE, Promotor (Ugent)

dr. Wouter HOUTHOOFD, co-promotor (Ugent)

Prof. dr. Tom ARTOIS, co-promotor (Uhasselt)

Prof. dr. Einhard SCHIERENBERG (Zoologisches Instut der Universität Köln, Germany)

Prof. dr. Wilfrida DECRAEMER (Koninklijk Belgisch Instituut voor Natuurwetenschappen and Ugent)

Prof. dr. Ann HUYSSEUNE (Ugent)

Prof. dr. Jacques VANFLETEREN (Ugent)

DANKWOORD - ACKNOWLEDGEMENTS

Voor velen is het schrijven van een doctoraat een zeer stresserende periode, omdat het meestal op een paar maanden tijd geschreven wordt... Maar doordat ik het helemaal op mijn manier gedaan heb, kijk ik er dan ook op terug als één van de mooiste periodes uit mijn leven... Niet dat het altijd even plezant was... want voor mij is het schrijven van een doctoraat te vergelijken met de beklimming van de Mont Ventoux (ik heb hem al echt beklommen, het was wel vanuit de volgwagen achter mijn schoonbroer Frank, maar soit...)... je kan de top af en toe zien en dan ben je hoopvol en optimistisch, maar helaas zie je de top meestal niet en moet je gewoon blijven trappen tegen beter weten in... tot je eindelijk de top bereikt! En nu ik bovenaan de top sta, wordt het dan ook tijd om de mensen te bedanken die me mee boven gebracht hebben... want de Ventoux beklimmen, dat doe je niet in je eentje!

Eerst en vooral mijn promoter. Gaetan, 8 jaar geleden bleek je ineens opgescheept te zitten met ééntje van t Boerekot... In de rode stoeltjes, op een bruine enveloppe, deed je uit de doeken waarmee ik mij de komende 6 jaar zou bezighouden... op het einde van je enthousiaste uiteenzetting kon je geen letter meer lezen van wat erop gekriebeld stond, maar ik was vertrokken! Toen ik na 2 jaar besliste om mijn onderzoek een beetje in een andere richting te duwen, was je de eerste om me te steunen en mee te zoeken naar alternatieven. Ik wil je vooral bedanken dat ik het op mijn manier (lees mijn tempo) heb mogen afwerken en dat ik heel mijn hebben en houden van het labo naar mijn kamertje in Geel heb mogen verhuizen. En zeker ook bedankt voor de peptalks als het even wat minder ging...

En dan mijn begeleider: Wouter, je was nog thesisstudent, toen ik als assistent begon, maar je hebt me pijlsnel voorbij gestoken. Een mens kan zich echt geen betere begeleider wensen dan jij: ongelooflijk enthousiast, maar ook superkritisch als het moet... na elke discussie met jou, kon ik niet wachten om er terug in te vliegen! Jij bent echt wel de drijvende kracht achter dit project geweest! Echt merci voor alles... in de eerste plaats voor je vriendschap, maar ook voor al de tijd die je in mij gestoken hebt met discussiëren en met nalezen, om niet zot te worden als je ’s avonds weer eens 15 mails van mij in je mailbox vond, om me op te monteren als ik het niet goed meer zag zitten, maar vooral om in mij te geloven dat ik dit tot een goed einde zou kunnen brengen...zonder jou was het zeker nooit gelukt!!!

En mijn begeleider van het fylogenstisch luik: Tom, bedankt om mij bij te staan bij het klaarheid scheppen in al die bomen! Er is niemand die moeilijke materie zo boeiend en duidelijk kan uitleggen als jij!

Prof. Schierenberg, thanks for the very interesting discussions during the last few months, especially about the plectids. It was really inspiring!

En ook een welgemeend dankjewel aan alle juryleden voor het grondig nalezen van deze tekst en voor hun waardevolle suggesties!

En dan het labo. Ik heb er ongelooflijk veel plezier gemaakt, zeker in de beginjaren, toen onze petri-platen gewoon op de vensterbank mochten staan, er gewoon pizza uit de flow gegeten mocht worden en er elke week wel een reden was om een receptie te geven. Tom, bedankt om me tijdens mijn moleculaire hoogdagen met raad en daad bij te staan en vooral voor de geweldige rustpauzes, waarin we de hele wereld afreisden. Liesbeth, in jou vond ik een Kempens maatje en een vaste partner voor de geweldige recepties uit de oude tijd, waarbij iedereen naar iedereens receptie kwam. Ook Kim zou ik willen bedanken voor de vele geweldige babbels en natuurlijk ook voor de onvergetelijke momenten tijdens ons congres in Taos. Maxime, merci voor de discussies die we gevoerd hebben, want ook al heb je de nematoden ingeruild voor platwormen, je bleef betrokken bij mijn project. Zeker Rita mag ik niet vergeten: altijd even nieuwsgierig naar wat wij allemaal uitspoken en altijd paraat als er weer eens gefotoshopt moest worden... Marjolein, merci voor alle babbels en ons fantastisch verblijf in Leeds. Al degenen die ondertussen het labo verlaten hebben: Clarinda, Joeri, Ruben: merci voor de ongelooflijk toffe sfeer! Verder wil ik zeker ook de nieuwe lichting niet vergeten: Hanne, Mieke, Pamela, Stijn, Freija, Katrien: bedankt om zo te supporteren de laatste maanden!

Ik mag zeker ook Alexander niet vergeten, mijn enige thesissudent in al die jaren. Bedankt voor de opnames en volledig je plan te trekken tijdens mijn zwangerschapsverlof!

Miranda, bedankt voor het gieten van duizenden platen!

En Andy, bedankt voor evenveel DNA-sequenties (voooral dan van *Pristionchus*)!

Onze Kris en Liza: merci voor al de berekingen bij het *Pristionchus*-artikel!

Mijn zeer kritische nalezers van de verschillende hoofdstukken: Liesbeth, Tom Tytgat, Tom Gheskiere, Hanne en Mieke, bedankt! Zeker Liesbeth, merci om gans de tekst en de referenties door te nemen op zo'n korte tijd en vooral om zo mee te leven! Ge zijt ne schat!

Kikke, merci voor de vertalingen van al die Duitse artikels! En mijn broer voor de talrijke statistische berekeningen, die al dan niet de uiteindelijke versie van dit

doctoraat gehaald hebben. Merci, he Caje! Als ik ergens iets terug kan doen en ergens pietevogelkes moet gaan observeren, ik heb tijd nu, he...en nu is het aan jullie!

Verder al mijn vrienden en familie, die voor me supporterden! Ima, merci om zo mee te leven! Stien, merci voor de ontspannende weekendjes in Amsterdam! Debby, Kathleen, Cristel, Isa, Ils, Tessa, Marleen, Christel, Petra... merci voor al de ontspannende momenten! Mijn buurvrouw Leen wil ik zeker ook bedanken om mij af en toe vanachter mijn buro te halen om wat te kletsen... al durfden die pauzes nogal eens uitlopen...

Tenslotte zijn er 2 mensen zonder wie dit werk er nooit had geweest en die mijn doctoraat (soms tegen wil en dank) van heel dichtbij meegemaakt hebben. Aan hen draag ik dit doctoraat dan ook op. Ma en pa, waar moet ik in hemelsnaam beginnen...??? Want als ik alles moet opnoemen, gaat dat hier langer worden dan mijn tekst! Merci om jullie leven de voorbije 2 jaar helemaal in het teken van mijn doctoraat te stellen: merci om Seppe en Sara altijd en altijd bij te houden, op al die onaangekondigde momenten... merci om al de beelden mee te helpen digitaliseren, toen de 4D-computer crashte... merci voor het intikken van al die datamatrices, voor het opstellen van mijn referentielijst... maar vooral om mij aan te moedigen dit huzarenwerk te ondernemen! Nooit ga ik kunnen terugdoen wat jullie allemaal voor mij gedaan hebben...

Gezien het feit dat ik er zolang aan bezig geweest ben, vragen velen of ik het allemaal opnieuw zou doen ... en natuurlijk is mijn antwoord ja! Want buiten dit doctoraat heeft mijn verblijf in de Ledeganck mij nog iets veel belangrijkers opgeleverd en dat ben jij, Wim! Je gaf je huisje in Heusden op om mijn ding te kunnen doen en dat zal ik nooit vergeten... de voorbije maanden waren best wel zwaar, maar we zijn er geraakt! Merci voor het opvangen van al mijn buien en om zoveel ‘huispapa’ te spelen, voor de hulp bij het maken van de moleculaire bomen, voor het editen van mijn figurenboek, voor al je kritische opmerkingen en de talloze fylogenetische discussies op onmenselijk late uren... maar vooral om mij te blijven aanmoedigen en mij te overtuigen dat ik echt wel goed bezig was... ik zie je graag... en nu gaan we eindelijk genieten!!!!

Het laatste woord wil ik richten tot mijn kindjes... Seppe en Sara, mama’s boekje is eindelijk af en ik beloof jullie plechtig: ik maak er nooit nog een opnieuw!!!

Sandra Vangestel

Geel, 1 september 2008

TABLE OF CONTENTS

Chapter 1 Introduction

1.1 Why study the embryonic development of nematodes?

Nothing in Biology makes sense except in the light of evolution (Dobzhansky, 1964). The evolution of several developmental processes has been studied in detail in a small number of model organisms. However, to fully understand these developmental processes, an understanding of their evolutionary origin and variation is necessary. As a model of a developmental process, we have chosen the early embryonic development. Nematodes are excellent models to study the evolution of this developmental phase, because eggs are transparent so we can follow the development from fertilized egg to hatched juvenile directly under the light microscope. Representatives of nematodes can be found everywhere in nature, thus substantial variation may be expected. Moreover, by screening all over the phylum, it will be possible to reconstruct the evolution of these developmental events and assess the phylogenetic significance of these events.

1.2 Historical overview of nematode embryology

The ancient and species-rich phylum Nematoda has been the object of embryonic studies since the 19th century (zur Strassen, 1896, 1959; Boveri, 1899, 1910; Müller, 1903). The first descriptions and explanations of fertilization and meiosis were accomplished by research on the nematode egg. In 1883 Van Beneden, a Belgian embryologist, published a series of important papers on the fertilized egg of *Ascaris megalocephala*, an intestinal worm found in horses. He showed that fertilization occurred by the union of two nuclei, one from the sperm cell and one from the egg, and that each contained half the number of chromosomes, found in body cells of the nematode. The German biologist Boveri (1887) first described the process of chromatin diminution in early cleavage divisions of the *Parascaris equorum* embryo. During chromatin diminution, the soma is separated from the germline, because the germline daughter cell always preserves its full chromatin content, in contrast to the somatic daughter cell, which loses part of its genome. This process was later also described in some other parasitic nematodes, copepods and ciliates. During these studies he also observed that a maturing egg cel disposes of half of the amount of nucleic material through the polar bodies by two divisions, thus reducing the chromosome number by half, thereby describing meiosis. The concept of mosaic development and the determination of blastomeres were also based on studies of nematodes (Boveri, 1887; zur Strassen 1896; Müller, 1903). All these studies were primarily done on parasitic nematodes, while the

study of embryonic development of free-living nematodes only took off in the 1970's (Malakhov and Cherdantsev, 1975). Early embryonic studies on different marine nematodes were done by the Russian embryologists Drozdovskii, Malakhov and their co-workers in the late 1960s. With the English translation of their work in 1994 (Malakhov, 1994) the information on the early embryonic development of these nematodes became worldwide. In 1983 Sulston and co-workers established the complete embryonic cell lineage of *Caenorhabditis elegans*. The cell lineage of an organism is the pattern of cell divisions and cell fates produced by an ancestral blast cell. With this, the timing, location and ancestral relationship of each division during development, is known. A major conclusion from these studies was that *Caenorhabditis elegans* shows a strict invariant cell lineage that generates a fixed number of cells with a fixed cell type (Sulston and Horvitz, 1977; Sulston *et al.*, 1983), which is in contrast to *Drosophila* and vertebrates. Because of its reproducibility, the embryonic development of *Caenorhabditis elegans* has been used in all fields of biology and medicine (Stent and Weisblat, 1982). In 2002, Brenner, Horvitz and Sulston received the Nobel Prize for Medicine for their work on the genetics of organ development and programmed cell death in *Caenorhabditis elegans*. Because of its importance as a model organism, and because it is our reference nematode, a thorough description of this nematode will be given.

1.3 The model organism *Caenorhabditis elegans*

In 1965, Sydney Brenner chose the small soil nematode *Caenorhabditis elegans* as a model to study the genetics of development and neurobiology. This free-living, bacteriovorous nematode, belonging to the family Rhabditidae, is often found in compost heaps and other nutrient rich environments. Since then, the knowledge of this nematode has expanded greatly. In 1998, the complete genome was sequenced, covering more than 19000 genes (*Caenorhabditis elegans* Sequencing Consortium, 1998). For more than 40 percent of the predicted protein products, orthologues in other organisms can be found. In addition, detailed genetic mapping, cloning and analysis of mutationally defined genes and physical mapping of the entire genome have become available.

Until the late 1980's it was generally believed that the development in *Caenorhabditis elegans* was mosaic and cell specification in embryos occurred cell autonomous, where cytoplasmic determinants specify the fate of blastomeres by differential segregation (Laufer *et al.*, 1980; Cowan and McIntosh, 1985; Edgar and McGhee, 1986; Schierenberg, 1988). However, later, cases of inductive interactions between individual blastomeres were revealed that were necessary for the correct

specification of these blastomeres (Priess and Thompson, 1987; Priess *et al.*, 1987; Schierenberg, 1987; Schnabel, 1991; Wood, 1991; Bowerman *et al.*, 1992).

1.4 The early embryonic development in *Caenorhabditis elegans*

The embryonic development of this model organism has been studied in great detail. As such, it forms an excellent reference system to reveal variations from this system. Therefore, the early embryonic development of this nematode will be discussed thoroughly, from fertilization until the process of gastrulation. Whenever relevant, the underlying molecular processes will be discussed as well.

1.4.1 The formation of 6 founder cells

Embryogenesis in *Caenorhabditis elegans*, from fertilization until hatching, takes 14 hours at 22°C (Sulston *et al.*, *1983*). After fertilization in the spermatheca, the eggshell, which consists of an outer vitelline membrane, a middle chitinous layer and an inner layer consisting of lipids and collagenous cross-linked proteins, is formed (Bird and Bird, 1991). During this time, a process called pseudocleavage can be observed: a pronounced constriction of the membrane near the equator and the formation of a cleavage furrow, followed by its regression. At the same time, the egg pronucleus migrates posteriorly towards the sperm nucleus and they meet in the posterior half of the egg. The first cleavage starts 35 min after fertilization and is asymmetrical with the formation of a larger anterior founder cell AB and a smaller posterior germline cell P1 (Fig. 1.1, Fig. 1.2, Fig. 1.3). Then the AB blastomere divides in a direction perpendicular to the longitudinal axis into two AB daughter cells, while P1 divides in the direction parallel to the longitudinal axis into an anterior somatic cell, EMS, which determines the future ventral side of the embryo, and a posterior germline cell, P_2. One AB cell migrates to the anterior pole (ABa) and the other AB cell migrates to the future dorsal side of the embryo (ABp). These rearrangements result in a rhomboidal configuration. Further asymmetric divisions of EMS into MS and E, of P2 into C and P3, and then of P3 into D and P4, complete the generation of six founder cells whose descendants each produce a specific subset of cell types (Sulston *et al.*, 1983) (Fig. 1.2; Fig. 1.4). The E cell exclusively forms the endoderm. The D cell is strictly mesodermal, producing 20 body wall muscle cells while the P4 cell only gives rise to the germline. This is in contrast to the other 3 founder cells (Fig. 1.2), which all produce a mix of ectoderm and mesoderm, although the AB founder cell produces primarily ectodermal cells and MS primarily mesodermal cells. Seventy percent of all the generated cells are derived from AB progeny. Cells forming mesoderm (i.e. body muscle and part of the pharynx) are derived

from four different lineages (Fig. 1.2, Fig. 1.4). In *Caenorhabditis elegans* most cells are placed close to their final position and long-range migrations are not frequently observed.

1.4.2 Cleavage directions are highly regulated

In contrast to somatic cells, the germline cells P0, P1, P2 and P3 divide asymmetrically. Cowan and Hyman (2004) discuss the steps necessary to establish an asymmetric division. First, a polarity cue coming from the sperm centrosome determines the position of the cell axis (Goldstein and Hird, 1996). Secondly, this polarity cue triggers the formation of an anterior and a posterior cortical domain, defining the polarity of the cell. The formation of these cortical domains regulates the segregation of determinants along the antero-posterior (a-p) axis and the orientation and translocation of the mitotic spindle (Cowan and Hyman, 2004). P granules are a component of the egg cytoplasm and segregate to the posterior pole during the first cell cycle and to the germline P lineage in subsequent divisions. P granules contain proteins that can bind to RNA and thus control the trafficking, translation and stability of mRNAs in the germline. Cytoplasmic streaming appears to play a major role in localizing these germline-specific P granules to the posterior cortex of the one-cell embryo (Hird *et al.*, 1996). Genes that play an essential role in the segregation of these P granules are the *par*-genes (Kemphues *et al.*, 1988; Kemphues, 1989; Kirby *et al.*, 1990; Morton *et al.*, 1992, 2002; Cheng *et al.*, 1995).

In contrast to P0-P3, P4 divides symmetrically, as it is the first cell giving rise exclusively to germ cells by clonal mitotic divisions. In addition, most of the somatic cells divide equally and orthogonally to the previous division during the first divisions. This somatic pattern is essentially the default pattern. Successive orthogonal division axes are typical during embryogenesis of many organisms (Wilson, 1925 in Hyman and White, 1987). The explanation for this default pattern of division (90^{o} to the previous division axis), lies in the movements of centrosomes; prior to mitosis, the centrosome in a cell duplicates, and the two daughter centrosomes migrate away from each other to opposite sides of the nucleus (for review, see Strome, 1993). In the P cells, the division axes are oriented along the A-P axis, so an additional rotation of the centrosome-nucleus complex is required. Besides intact microtubules and an intact microfilament skeleton (Hyman and White, 1987), the *par* gene products also participate in controlling rotation of the centrosome-nucleus complex (Cheng *et al.*, 1995).

A characteristic developmental event, named *reversal of cleavage polarity*, was first described by Schierenberg (1987) in the *Caenorhabditis elegans* embryo.

Schierenberg generated partial embryos by puncturing the eggshell with a laser micro-beam and gently removing the anterior AB cell in order to give space for the posterior germline cells. In the divisions of P0 and P1, the somatic sister cell lies anteriorly to the new germline cell, while in the divisions of P2 and P3 the somatic sister of the new germline cell lies posteriorly. When P2 divides in intact embryos of *Caenorhabditis elegans*, the anterior P3 cell is pushed to the ventral side and C is pushed to the dorsal side. P3 also gives rise to a germline cell P4 at the ventral side and a somatic cell D, located at the dorsal side of the embryo. In this way, the resulting configuration of the posterior cells from ventral to dorsal is E-P4-D-C.

1.4.3 Inductions in early embryogenesis

The invariant lineage and the strict regulation of cleavage directions assure a stereotyped spatial configuration in the early stages of embryonic development. This configuration is a prerequisite for inductions.

The three principal axes of the body plan are established early in development. Establishment of the a-p axis is initiated after fertilization in the one-cell stage with the sperm-derived centrosome breaking down the symmetry of the oocyte. The cleavage of the AB blastomere occurs parallel to the future dorso-ventral axis (d-v) of the embryo. However, as AB completes division, cells are rearranged so that one daughter (ABa) is more anterior than the other (ABp). The left-right (l-r) axis can be observed after the division of 2AB, since the spindles of ABa and ABp are set up orthogonal with respect to the a-p and d-v axes. However, the daughters on the left side (ABal and ABpl) are skewed towards to the anterior and thus have different cell-cell contacts than their right-hand counterparts (Sulston *et al.*, 1983; Wood, 1991).

1.4.3.1 Specification of cell fates in the AB lineage

The fate of the eight AB great-granddaughters is established by four inductions (Fig. 1.5). First, in the four-cell stage, an interaction between P2 and ABp is necessary to break the initial equivalence between ABa and ABp (Bowerman *et al*., 1992; Hutter and Schnabel, 1994; Mango *et al*., 1994b; Mello *et al*., 1994; Moskowitz *et al*., 1994, Priess, 2005). Similarly, the left and right daughters of ABa and ABp are initially equivalent. However, signaling from MS results in most of the left-right asymmetries in the early embryo (Hutter and Schnabel, 1994; Mango *et al*., 1994a). When signaling from MS is prevented, the blastomere ABara adopts the fate of its bilateral homolog, ABala and ABalp adopts the fate of its bilateral homolog ABarp (Hutter and Schnabel, 1994). An analysis of cell-cell contacts revealed that the cells ABara and ABalp always contact the

MS cell, while their bilateral counterparts do not (Hutter and Schnabel, 1994). Two other important cell-cell contacts in the 24-cell-stage of *Caenorhabditis elegans* embryogenesis that are essential for induction have been described by Hutter and Schnabel (1995b) and Priess (2005). These contacts (ABalap-ABplaa and ABplpa-MSap) induce further left-right asymmetries in the AB lineage. In all cases signalling occurs by means of the Notch pathway. In this mechanism of signal transduction, contact between ligand and receptor (GLP-1 or LIN-12) initiates a series of cleavage events that liberate the intracellular domain of the receptor. This domain then enters the nucleus, where it activates gene expression (Priess, 2005).

From then on, most cleavages within the AB lineage occur along the a-p axis. Bischoff and Schnabel (2006a) postulated that in the *Caenorhabditis elegans* embryo P_2 and its descendants constitute a polarising centre in the posterior of the embryo which orientates the cell cleavages of AB-derived blastomeres along the a-p axis. These (a/p) divisions result in sister cells with different fates. In fact, Kaletta *et al.* (1997) showed that the invariant lineage of *Caenorhabditis elegans* is established by a stepwise bifurcation of blastomere specification at a-p divisions. The molecular components of this a/p system have been studied in detail (Lin *et al.*, 1995; Rocheleau *et al.*, 1997; Thorpe *et al.*, 1997; Lin *et al.*, 1998, Menegheni *et al.*, 1999; Korswagen *et al.*, 2000; Maduro *et al.*, 2002; Korswagen, 2002; Park and Priess, 2003; Huang *et al.*, 2007). An important gene involved in generating a-p asymmetries is POP-1, a TCF protein (Lin *et al.*, 1995). After each (a/p) cell division, the anterior daughter cell invariably shows a higher level of nuclear POP-1 compared to its posterior daughter (Lin *et al.*, 1995; Lin *et al.*, 1998). When high levels of POP-1 are induced in the posterior daughter cell, its fate is transformed to the anterior fate. Similarly, the absence of POP-1 in the anterior daughter cell leads to a transformation to the posterior fate (Park and Priess, 2003).

1.4.3.2 Specification of cell fates in the P1 lineage

Germ-line blastomeres can be distinguished from somatic blastomeres by several characteristics. A germ-line blastomere is born from an unequal cleavage. Before each unequal cleavage, P granules move toward the side of the blastomere from which the germline blastomere will be born (Strome and Wood, 1983). As a consequence, at all stages of embryogenesis, P-granules are localized exclusively in germline blastomeres. Besides the presence of these P-granules, the germ cells are characterized by a repression of transcription, mediated by PIE-1 (Seydoux *et al.*, 1996). In *pie-1* mutants, P_4 and D both contain P-granules and both blastomeres can produce intestinal cells (Mello *et a*l.

1992). In addition, four MES-proteins, although not specifically partitioned to the germline blastomeres, are crucial for their subsequent development (Strome, 2005).

The fate of the E cell is specified in the four cell stage, when Wnt signalling from the P2 blastomere induces the EMS blastomere to form gut by regulating β-catenin levels and activating transcription (Schierenberg 1987; Goldstein 1992, 1993, 1995; Rocheleau *et al.*, 1997; Thorpe *et al.*, 1997). If P_2 is removed from the embryo during this early period, EMS divides into daughter blastomeres that both have characteristics of MS blastomeres, but have no apparent characteristics of E blastomeres. A gene, called *pop-1* was found to be the repressor of the E fate in the MS blastomere (Lin *et al.*, 1995, Rocheleau *et al.*, 1997; Thorpe *et al.*, 1997; Calvo *et al.*, 2001) and later also as the promoter of endoderm formation of E (Maduro *et al.*, 2005; Shetty *et al.*, 2005). Other genes that are essential for endoderm development have been identified (McGhee et al., 1990; Hawkins and McGhee, 1995; Zhu *et al*., 1997; Fukushige *et* al., 1998; Marshall and McGhee, 2001, McGhee *et al*., 2006).

The C, MS, and D blastomeres each produces body-wall muscles through distinct patterns of division and differentiation. Schnabel (1994, 1995) showed that cell-cell interactions are important for muscle production from MS and D. The D blastomere, derived from the P_2 lineage, appears to exert an inhibitory effect on muscle development from MS that, in normal embryogenesis, is blocked by AB descendants: only when both P_2 and AB are killed does MS produce muscles. The genes pal-1 and mex-3 were found to be important for the specification of C and D blastomeres (Hunter and Kenyon, 1996; Draper *et* al., 1996; Edgar *et al*., 2001; Huang *et al*., 2002; Baugh *et al*., 2005)

1.4.4 The process of gastrulation

During gastrulation, the morphology of the embryos is restructured by cell migration. The purpose of gastrulation is to position the 3 embryonic germ layers: the endoderm, ectoderm and mesoderm. Gastrulation in *Caenorhabditis elegans* starts at the 26-cell stage. At this point, the 16AB descendants lie anteriorly and laterally, and the four C descendants lie posteriorly and dorsally. The four MS cells lie ventrally in the middle of the embryo. The two endodermal precursors, D and the germline precursor P4 lie ventrally in the posterior half of the embryo. In *Caenorhabditis elegans*, gastrulation has been studied in detail (Nance and Priess, 2002, Lee and Goldstein, 2003, Nance *et al.*, 2003). Gastrulation starts (90 min after the first cell division of the embryo) when the two endodermal precursor cells Ea and Ep constrict their apical surfaces as they ingress into a small interior cavity called the blastocoel (Sulston *et al.*, 1983). As they ingress, their

apical surfaces (outer surface that faces the vitelline envelope) move away from the vitelline envelope and are covered by 6 neighbouring cells: 3 MS granddaughters (MSap, MSpa, MSpp), 2 AB progeny (ABplpa, ABplpp) and P4. Junkersdorf and Schierenberg (1992) showed that when the E cell was irradiated and hence its division delayed, the E cell itself migrated to the interior of the embryo. Their results also showed that specific neighbouring cells are not required to initiate gastrulation. Myosin and PAR-proteins were found to play an essential role in ingression (Nance and Priess, 2002). After the endodermal cells have completed ingression, mesodermal and germline cells ingress from various positions on the ventral surface over the following 200 min. After the cell ingressions are complete, gastrulation culminates with the epiboly of the hypodermal cells. Lee and Goldstein (2003) showed that the eggshell and the vitelline envelope do not provide signals or surfaces essential for ingression. They also demonstrated that the neighbouring cells do not push the E cells internally.

1.5 Early embryonic development of other nematodes

Although well studied, the embryonic development of the model organism *Caenorhabditis elegans* is not a good representative for many species within the phylum. Comparative embryological analyses have revealed much more diversity in developmental mechanisms than previously thought. The most important differences to *Caenorhabditis elegans* will be discussed. Here, nematodes are assigned to clades, according to the phylogeny of Holterman *et al.* (2006), which will be discussed in 1.6. For an overview of the clades, we refer to Fig. 1.6.

In contrast to *Caenorhabditis elegans*, which has a fixed cell lineage, in nematodes of the orders Enoplida and Triplonchida (clade 1), no indication for a fixed cell lineage was found (Malakhov, 1994; 1998; Voronov and Panchin, 1998; Voronov *et al.*, 1998; Voronov, 1999; Schierenberg, 2005). In both marine free-living nematodes *Enoplus brevis* (Voronov and Panchin, 1998; Voronov *et al.*, 1998) and *Pontonema vulgara* (Malakhov, 1994; 1998; Voronov and Panchin, 1998; Voronov *et al.*, 1998; Voronov, 1999) (order Enoplida) blastomeres cannot be distinguished from one another at the 2-8 cell stage and divisions are usually synchronous. The first visible cell lineage is the gut lineage (E-lineage). By injecting single blastomeres with a fluorescent tracer dye and following their progeny, it was shown that, with the exception of the endodermal lineage, the fates of the early blastomeres are not specified and embryos possess a considerable regulative potential (Voronov *et al.*, 1998). One of the two first formed blastomeres may contribute to anterior or posterior, left or right, or intermediate parts of

the embryo and the endodermal precursor cell may derive from either two blastomeres (Voronov *et al.*, 1998). A characteristic feature, eutely (fixed cell number), is not present in Enoplida (Malakhov, 1998). Schierenberg (2005) found the same symmetric cleavage and the absence of distinct cell lineages in the freshwater nematode *Tobrilus diversipapillatus* (order Triplonchida). Moreover, this nematode differed from all studied nematodes so far, in that a large blastocoel is formed (Schierenberg, 2005).

This type of development with a variable cleavage is in strong contrast to the invariant lineage found in nematodes belonging to all other clades, which mostly show asymmetric cleavages in the first divisions of early embryonic development. Despite the fact that all these nematodes show a fixed cell lineage, there are some important differences in the potential to establish gut. Early embryonic studies on different marine nematodes belonging to the family Mermithidae (clade 2) revealed that in the 2-cell embryo, the gut lineage comes from the anterior somatic founder cell AB (Malakhov, 1994), while in all other clades (3-12) the gut is derived from the posterior P1 cell. Schulze and Schierenberg (2008) published the same findings on *Romanomermis culicivorax*, another member of the family Mermithidae: gut is derived from the anterior blastomere. In this nematode, the establishment of polarity, the formation of embryonic axes and the pattern of asymmetric cleavages, are different from *Caenorhabditis elegans*. A polarity reversal in the germline takes place already in P1 and the dorso-ventral axis appears to be inverted. At the four-cell stage two daughters of different blastomeres behave like AB descendants, while the other two resemble the descendants of P1. Schulze and Schierenberg (2008) also showed that the midbody region has a prominent role in spindle orientation, positioning, and cytoplasmic segregation. A feature not observed in any other nematode so far is the presence of coloured cytoplasm and its segregation into the EMS cell and its descendants. This coloured component probably has no role in cell specification, but probably controls the exposure to light, since it is found in cells contributing to the hypodermis (Schulze and Schierenberg, 2008).

Within clades 3-12, the early embryonic development of several nematodes has been studied. The oldest descriptions of the embryonic development of nematodes come from animal parasitic nematodes. Free-living or plant parasitic nematodes, did not receive much attention. At the end of the 19th century, the classical model system for developmental studies was *Ascaris.* Apart from its slow development, cleavage patterns are similar to the ones found in *Caenorhabditis elegans* (zur Strassen, 1896; Boveri, 1899).

In the sixties and seventies, much more plant parasitic nematodes were described, because of their economical importance. However, these studies were not performed in great detail and due to lack of adequate instrumentation, cells could be followed only until very early stages. Moreover, in some of these studies the assignment of the anterior and posterior side in the two-cell stage was clearly switched. For instance, Roman and Hirschmann (1969) described the early division pattern of *Pratylenchus scribneri*. They state that they cannot distinguish the anterior from the posterior blastomere at the two-cell stage, but assume that this nematode has the same pattern of division as *Parascaris equorum* (Boveri, 1892). Hence, they consider the first blastomere that divides as the anterior blastomere (which they called the S1 blastomere instead of the AB according to *Caenorhabditis elegans* nomenclature). This seems very unlikely, as this leads to spatial configurations that were never again observed when modern techniques allowed to follow division after division of cells with great precision. The same can be concluded for the study of a member of the Cephalobidae, *Acrobeles complexus*, by Thomas (1965). By switching anterior and posterior cell names, the same division pattern as in other cephalobids can be found.

Schierenberg and co-workers expanded micromanipulation experiments on *Caenorhabditis elegans* to other nematodes and were the first to report a strategy for cell fate specification, which was very different from *Caenorhabditis elegans*. Wiegner and Schierenberg (1999) examined the mechanism of cell specification experimentally in *Acrobeloides nanus* (Cephalobidae) and showed that this nematode has a considerable regulative potential: after the elimination of the AB cell, its posterior neighbour EMS adopts an AB-like fate and this EMS cell in turn is replaced by the C cell. Their results show that in the *Acrobeloides nanus* embryo inhibiting interactions between neighbouring somatic cells specify the fates of primarily multipotent blastomeres in a hierarchical and sequential manner. This is in contrast to *Caenorhabditis elegans*, where none of the cells are individually able to generate gut and therefore need induction (Wiegner and Schierenberg, 1999). The induction from the germline cell P2 to EMS to specify EMS as gut precursor has not been observed in *Acrobeloides nanus*: when P2 is removed, EMS will still produce gut cells (Wiegner and Schierenberg, 1999). Bossinger and Schierenberg (1996a+b) had already demonstrated that differences in the pattern of intercellular communication exist between these two species. In contrast to *Caenorhabditis elegans*, where blastomeres become dye-coupled with lucifer yellow simultaneously, cells in *Acrobeloides nanus* become stained progressively along the antero-posterior axis in the sequence in which they were born (Bossinger and

Schierenberg, 1992). In addition, the pattern of high molecular weight molecules such as dextranes, is different in both nematodes. In *Caenorhabditis elegans* dextranes do not diffuse between blastomeres, except between sister cells before the closure of cell membranes after mitosis. In *Acrobeloides nanus* however, this dye quickly diffuses between somatic cells in the sequence in which they were born, although, never passing into the germline cells (P1-P4), suggesting the presence of large communication channels, originating from midbodies (midbody-like channels) (Bossinger and Schierenberg, 1996b). Another difference between *Caenorhabditis elegans* and *Acrobeloides nanus* lies in the timing of endocytotic activity. After injection of Lucifer Yellow and transferrin, these dyes accumulate in the gut primordium, visualizing a transfer from yolk into the gut through receptor-coupled endocytosis. In *Caenorhabditis elegans* this process takes place in the 16E stage, while in *Acrobeloides nanus* this process is already observed in the 2E stage (Bossinger *et al*., 1996). Yet another difference with *Caenorhabditis elegans* is that *Acrobeloides nanus* shows no reversal of cleavage polarity in the germline, as shown by Skiba and Schierenberg (1992), using experimental interference. Consequently, cells are arranged in a different configuration compared to *Caenorhabditis elegans*. Ultimately cell migrations lead to a pattern similar to that of *Caenorhabditis elegans*. After inhibition of zygotic transcription, development arrests very soon in *Acrobeloides nanus* (5-cell stage), suggesting that maternal supplies are low in this nematode (Wiegner and Schierenberg, 1998). This is in contrast to *Caenorhabditis elegans*, where development continues until the 100-cell stage, because embryos are equipped with a large maternal pool (Edgar et al., 1994).

Table 1.1 presents an overview of nematodes in which early embryonic development has been studied. However, in most cases, data are fragmentary and often only one specific parameter of the nematode was studied. In other cases, a more detailed description of the early embryonic development is available.

1.6 Nematode phylogeny

These studies of the embryonic development of nematodes from different branches in the phylogenetic tree show that there is a large variability in the way a juvenile worm is generated. Therefore characteristics of early development can possibly be used to study phylogenetic relationships. In the past different phylogenies of the phylum Nematoda have been established. Until recently, phylogenies within the phylum Nematoda were based on comparative morphology of adult structures only (Micoletzky, 1922; Chitwood, 1937; Maggenti, 1963; 1983; Andrassy, 1976; Lorenzen, 1981; 1994).

The first molecular phylogenetic framework of the phylum Nematoda where major clades are identified based on small subunit rDNA sequences, was established in 1998 by Blaxter and co-workers. An overview of the most important molecular phylogenies is given below and differences between the phylogenies are discussed.

Blaxter *et al.* (1998) analyzed 53 small subunit (SSU) ribosomal DNA sequences, covering the major parasitic and free-living taxonomic groups. They identified five major clades within the phylum, all of which include parasitic species (Fig. 1.6). Clade I comprises the vertebrate parasitic Trichinellida, the insect parasitic Mermithida, the plant parasitic Dorylaimida and the freeliving Mononchida. In clade II, the plant parasitic Triplonchida and the free-living Enoplida are found. Clade III represents mostly vertebrate and arthropod parasitic taxa, including the Ascaridida. The order Rhabditida is present in both clades IV and V and is hence paraphyletic. Clade IV includes the predominantly plant-parasitic Tylenchida and Aphelenchida and the free-living bacteriovores of Cephalobidae and Panagrolaimidae. Clade V groups Rhabditina (including *Caenorhabditis elegans*) with the vertebrate parasitic Strongylida, the entomopathogenic genus *Heterorhabditis* and the Diplogastrida, including the satellite model organism, *Pristionchus pacificus*. Taxa not assigned to one of the clades in the phylogeny of Blaxter *et al*. (1998), but positioned in between clades 2 and 3, include plectids, chromadorids and monhysterids.

A review, proposing a revised classification based on molecular as well as traditional systematic methods, has been published by De Ley and Blaxter (2002). Major parasitic groups were downgraded in their hierarchical position to a level that conforms better to their phylogenetic history. In this new classification, the morphological dissimilar panagrolaimids, steinernematids, strongyloids, tylenchids and cephalobids are included in a single suborder Tylenchina because of moderate support of their common origin in SSU rDNA inferred phylogenies.

More recently, Holterman *et al.* (2006) and Meldal *et al.* (2007) produced phylum-wide SSU rDNA phylogenies based on a wider sampling, compared to the first molecular phylogenetic framework from Blaxter *et al.* (1998). While previous phylogenies were mainly based on terrestrial and parasitic taxa, Meldal *et al.* (2007) especially added sequences of marine taxa to resolve relationships between several major taxa (e.g. Chromadorida, Monhysterida and Enoplida). Both phylogenies largely agree, however in contrast to the phylogeny of Holterman *et al*. (2006) based on Bayesian inference, there was no clear evidence for the relationship between the three classes,

Enoplia, Dorylaimia, and Chromadoria in the consensus tree of Meldal *et al*. (2007). Therefore, we favour the phylogeny of Holterman *et al*. (2006), based on Bayesian inference, because here the basal radiation of the phylum is resolved. Holterman *et al*. (2006) subdivided the phylum in 12 clades (Fig. 1.6), which are numbered with numbers 1, 2,…12. With "basal" clades, we indicate clades that are placed closest to the ancestor of the phylum Nematoda, while with "derived" clades, we mean clades that are separated at a later stage. The most basal[1] clade - clade 1- is dominated by nematodes from the orders Enoplida (marine nematodes) and Triplonchida (mainly freshwater nematodes, also including the plant parasitic Trichodoridae), but also contains two Plectida families (terrestrial nematodes). Embryological support for this clade was found in the absence of both an asymmetrically dividing germline and a bilateral symmetry during early embryogenesis (Malakhov, 1994; Voronov *et al.*, 1998; Voronov, 1999; Schierenberg, 2005). Clade 2 comprises nematodes from the orders Trichinellida (animal parasites), Mononchida (predaceous and cannibalistic nematodes), Mermithida (insect-parasites) and Dorylaimida (nematodes feeding on algae, fungi or other nematodes; but also nematodes from Longidoridae (plant-parasitic that have the ability to transmit plant viruses). Chromadorida (marine, freshwater and soil nematodes) and Desmodorida (marine nematodes) are paraphyletic: members of these orders can be found in both clades 3 and 4. However, in a more recent phylogeny presented by Holterman *et al*. (2008), Chromadorida is considered monophyletic, with the exclusion of Selachinematidae. Clade 5 includes the orders Monhysterida (marine, freshwater and soil nematodes), Araeolaimida (bacteriovores in marine or brackish water) and one family of the order Plectida. Clade 6 contains most families within the order Plectida (freshwater and soil nematodes). Clade 7 covers only one family, the Teratocephalidae, a sister to all other Secernentea (clades 8-12). The latter is in contrast to Meldal *et al*. (2006) who found variable relationships between Rhabditida, Teratocephalidae and Plectida depending on the analysis used: Plectidae as a sister taxon to both *Teratocephalus lirellus* and the Rhabditida; or Plectidae as a sister taxon to *Teratocephalus lirellus,* both within Rhabditida. Clade 8 is dominated by animal parasitic nematodes and includes the suborder Spirurina (including e.g. *Ascaris* and *Brugia*). Clade 9 predominately consists of bacteriovores, including the Rhabditomorpha, Bunonematomorpha, Diplogasteromorpha and Myolaimina but also of a few animal (Strongyloidea) and insect parasites

1 The terms basal and derived are strictly spoken not correct to appoint clades of a phylogenetic tree, but these generally used terms will be used in this thesis to retain clearness

(Heterorhabditidae). Mainly bacteriovores and a few parasites of animals (Strongyloididae) and insects (Steinernematidae) are present in clade 10. This clade comprises the Panagrolaimorpha, the family Brevibuccidae, and a taxon belonging to the Tylenchomorpha (Aphelenchoididae). Clade 11 solely comprises bacterial feeding families of the Cephalobomorpha. Clade 12, dominated by plant parasitic nematodes, comprises the Tylenchomorpha.

1.7 Overview of the investigated families and notes on their phylogenetic position

In this doctoral thesis seven families are examined, belonging to clade 6 (family Plectidae), clade 9 (family Rhabditidae, Neodiplogasteridae), clade 10 (Panagrolaimidae, Alloionematidae), clade 11 (Cephalobidae) and clade 12 (Meloidogynidae).

Plectidae (clade 6) are free-living bacteriovores found in soil, decaying substrates, decomposed wood, moss and aquatic habitats. Chitwood (1937, 1958) considered the family Plectidae as a member of the Adenophorea (clade 1-7 in the phylogeny of Holterman *et al.*, 2006). Moreover, they were presumed to have preserved the morphology of the earliest Adenophorea. Later, Maggenti (1963) concluded that Plectidae could not be close to the common ancestor of all nematodes based on pharynx structure and placed them closer to the ancestor of all Secernentea (= Rhabditida = clade 8-12 in the phylogeny of Holterman et al., 2006). In 1976, Andrassy, who subdivided the phylum into three major nematode groups, placed the Plectidae as a sister taxon to all Secernentea. This position for the Plectidae has been maintained in the phylogenies of Fürst von Lieven (2003), Blaxter *et al.* (1998) and De Ley and Blaxter (2002). Meldal *et al.* (2006) found that the Plectidae, *Teratocephalus lirellus* and Rhabditida always form a well supported clade, although variable relationships were found, depending on the analysis used. Holterman *et al.* (2006) placed the family Plectidae in clade 6, sister to all Rhabditida (including Teratocephalidae). They found that clade 7, comprising the family Teratocephalidae, is most close to the origin of Secernentean radiation (clade 8-12). It should be noted that also in clade 1, two Plectida families -Rhabdolaimidae and Bastianiidae- are found next to Enoplida and Triplonchida. This agrees with the findings of De Ley and Blaxter (2002) who considered Plectida as an amalgam of paraphyletic and misplaced families.

Rhabditidae (clade 9) encompass a large number of ecologically and genetically diverse free-living nematodes. Nematodes belonging to this family are usually specialized to feed on bacteria (decaying organic matter), although some are associated with animal

hosts or vectors. For instance, *Pelodera strongyloides* has been reported to be a facultative parasite of mammals (Sudhaus and Schulte, 1988; Jones *et al.*, 1991). The life-cycle can be as short as 3.5 days, but these worms can also develop through an alternative larval stage, the dauer larva, that is specialized to disperse or to resist harsh conditions. Several scientific, agricultural, and medical important nematodes can be found in the family Rhabditidae. Without a doubt, the best known nematode in this family is *Caenorhabditis elegans*. Traditional long-standing classifications have unified (e.g. Andrassy, 1976) the Rhabditidae with the bacteriovore cephalobids and panagrolaimids together with the parasitic strongyloids and steinernematids, while the mainly plant-parasitic aphelenchids and tylenchids were considered as a separate order, the Tylenchida. De Ley and Blaxter (2002) have however included the morphological dissimilar panagrolaimids, steinernematids, strongyloids, tylenchids and cephalobids in a single suborder Tylenchina because of moderate support of their common origin in SSU rDNA inferred phylogenies. This support has been affirmed in recent phylogenetic analyses (Holterman *et al.*, 2006; Meldal *et al.*, 2006).

Neodiplogasteridae (clade 9) contain bacteriovores, fungivores, entomopathogenic parasites and predators (Fürst von Lieven and Sudhaus, 2000). The closest relatives of diplogasterids appear to be species exhibiting a typical Rhabditid morphology (Sudhaus and Fitch, 2001), but also the bunonematids (Fürst von Lieven, 2002). The exact phylogenetic relationship of Neodiplogasteridae to Rhabditidae is still subject to debate and several studies suggest that the Neodiplogasteridae are part of the Rhabditidae (Sudhaus and Fürst von Lieven, 2003; Holterman *et al*., 2006; Kiontke *et a*l., 2007). Studies on the embryonic development in the family Neodiplogasteridae (clade 9) mostly concern the satellite organism, *Pristionchus pacificus*. Comparative studies between *Pristionchus pacificus* and *Caenorhabditis elegans* have revealed differences in the regulation of developmental processes such as the development and genetic analysis of sex determination (Pires-daSilva and Sommer, 2004), vulva development (Sommer and Sternberg, 1994; 1996; Sigrist and Sommer, 1999; Sommer, 2005) and gonad formation (Rudel *et al*., 2005; Sommer, 2005). Recently, developmental and molecular studies of *Pristionchus pacificus* have been complemented with genomic data comprising the genetic linkage map (Srinivasan *et al*., 2002), the physical map (Srinivasan *et al*., 2003), and whole genome sequencing, which is approaching its completion. In addition, the ecology and the specific ecological niche of *Pristionchus pacificus* have been studied. Herrmann *et al.* (2006) showed that *Pristionchus* species are often associated with scarabaeoid beetles and the Colorado potato beetle.

The family **Panagrolaimidae** (clade 10) are mostly bacteriovorous nematodes, only rarely associated with animal hosts or vectors. They are grouped together with insect pathogens (Steinernematidae), amphibian-reptilian parasites (Rhabdiasidae) and parasites of other vertebrates (Strongyloididae) into the Panagrolaimomorpha. Large subunit (LSU) rDNA sequences have been used to infer relationships within Panagrolaimomorpha (Nadler *et al.,* 2006). In the phylogeny of Holterman *et al.* (2006), Panagrolaimomorpha can be found in clade 10. Bert *et al.* (2003) have formulated a revision of the family Panagrolaimidae based on a new genus *Baujardia*. One panagrolaimid we studied, *Halicephalobus gingivalis,* is classified in most countries as a free-living bacteriovorous nematode, but in fact is a facultative parasite of horses and occasionally humans (Gardiner *et al.*, 1981; Blunden *et al.*, 1987; Nadler *et al.*, 2003). Panagrolaimidae include many opportunists (e.g. species of *Panagrolaimus*) as well as several genera specifically associated with fermentation, decaying wood and wood-boring insects (Bert and Borgonie, 2006). Furthermore, many Panagrolaimidae are capable of withstanding a wide range of chemically harsh environments; for example *Turbatrix aceti* and *Panagrellus redivivus,* can be found in vinegar, while *Panagrellus silusiae*, *Panagrellus nepenthicola* and *Baujardia mirabilis* inhabit bookbinder's paste, beer filters and pitcher plants respectively (Bert and Borgonie, 2006).

Alloionematidae (clade 10) are free-living bacteriovores. Within this family we examined one species, *Rhabditophanes* sp. Based on SSU rDNA this family has been placed within the Panagrolaimorpha (clade 10) (De Ley and Blaxter, 2002), together with parasitic nematodes with alternating life cycles, such as *Strongyloides, Parastrongyloides* and *Rhabdias* (Dorris *et al*., 2002). As such, *Rhabditophanes sp*. represents the first known example of reversal of parasitism within the Metazoa (Dorris *et al*., 1999). Detailed morphological analysis of the intestine revealed unusual intestinal lamellae along the entire intestinal tract of *Rhabditophanes sp*. Willems *et al.* (2005) suggest that the reversal to a free living lifecycle coincided with a drastic reduction in the availability of food and that this was the driving force for these adaptations.

Cephalobidae (clade 11) are bacteriovores, not closely associated with animal hosts or arthropod vectors and include some of the most widespread opportunists, but also numerous specialists of sandy soils and extreme temperatures. In desert and mountain soils, Cephalobomorpha may constitute more than half of the total nematode density (De Ley, 1992). Cephalobomorpha are considered to have a sister group relation with the Tylenchomorpha (Holterman *et al*., 2006; Meldal *et al*., 2006; Bert *et al.*, 2008).

Relationships among Cephalobomorpha have been recently inferred by LSU rDNA sequences (Nadler *et al.*, 2006).

The family **Meloidogynidae (clade 12)** comprises the largest and economically most important group of plant parasitic nematodes. Tylenchomorpha have exploited all plant organs including flowers and seeds, although they mostly attack roots. The evolution of plant-parasitic Tylenchomorpha is of particular interest because associations range from transitory grazing by root-hair feeders to the highly complex host-pathogen interactions of gall-inducing nematodes and their hosts. Non plant-parasitic Tylenchomorpha feed on fungi, algae, lichens, mosses, insects, mites, leeches or frogs (Siddiqi, 2000). Bert *et al.* (2008) studied the evolution and phylogenetic relations of these rich and complex feeding traits. In the phylogeny of Holterman *et al.* (2006) Tylenchomorpha can be found in clade 12. In this thesis we will study the root-knot nematode *Meloidogyne incognita*, an economically important plant parasitic nematode with a wide host range. Females lay up 1000 eggs, which have a highly resistant and transparent chitin-containing shell and which are deposited in a gelatinous matrix that protects them from desiccation. Second-stage infective juveniles hatch from the eggs in about 18 days. After penetrating the plant roots, they induce a feeding site consisting of several giant cells embedded in a gall-like structure. Infected roots are knarled or nodulated, forming galls, hence the term "root-knot" nematode.

1.8 The use of embryology in phylogenetics

Interest in the relationship between embryonic development and phylogeny extends back to the 19th century (see introduction). However, the controversy about certain concepts (e.g. phylotypic stage) makes it clear that the phylogenetic importance of developmental processes is subject to debate. Nevertheless, comparative analysis of the early embryonic development of nematodes from various clades of the phylogenetic tree, suggests that the developmental mechanisms are very flexible (e.g. “indeterminate” development of nematodes belonging to clade 1, compared to the strict determinate development found in other clades) and makes early embryonic variations useful for assessing evolution.

Although researchers have made several attempts to trace the evolution of embryonic diversity within nematodes, the potential significance of embryonic development in the phylogeny of the phylum Nematoda is little recognized. Drozdovsky (1967) assessed the arrangement of the blastomeres in the four-cell stage to postulate phylogenetic relationships. Voronov *et al.* (1998) pointed out that three distinct patterns

of early embryonic development reported for nematodes are in good agreement with the classification of Blaxter *et al.* (1998), who divide the phylum into three big groups (clade I, clade II and clade III-V). Nematodes from clade II (= clade 1 in phylogeny of Holterman *et al*., 2006) have an early embryonic development that is different from all other nematodes, because up until the 8-cell stage blastomeres are indistinguishable from each other. This is in contrast to nematodes from clade III-V (= clade 3-12 in phylogeny of Holterman *et al*., 2006), where blastomeres are distinguishable from another even after the first division, based on size or appearance (the AB and P1 cell). In nematodes from clade I (= clade 2 in phylogeny of Holterman et al., 2006), the two daughter cells of the zygote can also be distinguished from each other, but they are not homologous to AB and P1.

Goldstein *et al.* (1998) and Goldstein (2001) mapped several early developmental characters, such as a-p axis specification, onto the molecular phylogeny of Blaxter *et al.* (1998). They analyzed how asymmetry is generated along the a-p axis in 30 species by analyzing the presence of a cytoplasmic rearrangement in the uncleaved embryo, and whether the site of sperm entry predicts the posterior of the embryo. A-p asymmetry in *Acrobeloides* sp. is generated differently compared to *Caenorhabditis elegans*: the sperm is not used to specify a-p asymmetry, there are no signs of cytoplasmic movements, and P-granules are segregated differently (Goldstein *et al*., 1998). They found that this mechanism of a-p symmetry is an apomorphic character, which may have arisen once in an ancestor of clades 10, 11 and 12. However, they examined the scored characters in only a limited number of clades (9-12).

Dolinski *et al.* (2001) were the first to map the evolution of some early developmental characters on a large scale. They scored the spatial arrangement of the four-cell stage, whether the AB and P1 lineages proceed at a synchronous or asynchronous rate, and the time when the germ founder cell P4 is established for 70 species.

In 2000, Schierenberg identified features that are typical for specific taxa: the timing of early cleavages, timing of gastrulation and establishment of bilateral symmetry. Recently, Schierenberg and Lahl (2004) investigated two developmental events, namely, the establishment of a visible germline and the type of gastrulation. They found four taxon-specific character combinations that could be used to infer phylogenetic information. In another study Schierenberg (2005) gives an overview of embryological variation in several parameters of early embryonic development and discusses their use as a potential phylogenetic marker. Earlier Schierenberg and co-workers described

differences in embryonic development between nematode species, which were observed after experimental interference with the developmental process. His work provides great insight into intercellular communication, specification of gut fate, compensation of lost cells and timing of endocytotic activity (Bossinger and Schierenberg, 1992; 1996a+b; Bossinger *et al.*, 1996; Wiegner and Schierenberg, 1998; 1999).

1.9 Objectives of this thesis:

All the above data clearly suggest that early embryonic variations are potential phylogenetic markers. Therefore we analyzed the early embryonic development of 21 species belonging to different clades within the phylum. Because a large number of nematodes are non-culturable, most of the chosen species were restricted to clade 9-11, comprising free-living bacteriovorous nematodes. One species from clade 6 was included and besides these bacteriovorous nematodes, one plant-parasitic nematode from clade 12 was also studied.

This thesis has two main objectives. The first is to make a comparative analysis of the early stages in embryonic development of these nematodes. This will allow us to gain insight in the variation in embryonic development present in the examined clades, but also between the examined clades. Furthermore, by analyzing a larger number of individuals for some species, we will gain insight in the variation that naturally occurs in these species. This will give an indication how conserved certain developmental pathways are in nematodes other than *Caenorhabditis elegans*. This analysis will possibly reveal other developmental patterns and may appoint which nematode taxa are interesting for further molecular and experimental analysis. However, since no experimental interference is used in this work, certain differences in developmental patterns will remain undetected.

The second goal is to examine which events in the early embryonic development of nematodes are potential phylogenetic markers. After analyzing the early embryonic development for all species, we will thoroughly map the evolution of some early developmental traits onto a molecular phylogeny, based on the phylogeny of Holterman *et al.* (2006). This will allow us to evaluate the level of congruence (and thus the phylogenetic value) of each character with phylogeny. Moreover, this will enable us to identify more precisely when in evolution modifications to development have occurred and whether these modifications reflect different developmental strategies, arising as a consequence of different phylogenetic histories or as a consequence of other parameters.

Chapter 2 Material and Methods

2.1 Strains analyzed

Because a large number of nematodes are non-culturable, most of the chosen species were restricted to clade 9-11, comprising free-living bacteriovorous nematodes. One species from clade 6 was included and besides these bacteriovorous nematodes, one plant-parasitic nematode from clade 12 was also studied. The analyzed strains can be found in Table 2.1. The number between brackets is the number of lineages which were established for that species. For the calculation of the egg shape index (ESI) sometimes more individuals were examined, but this number will be given in the corresponding table of ESI. In chapter 4 (phylogenetic analysis) some data were obtained from literature, to cover representatives from all clades. In Table 2.2 the reference for each cited species is included.

2.2 Taxonomy of nematodes

A historical overview of nematode taxonomy was presented by Coomans (2000). De Ley and Blaxter (2002) outlined comprehensively the history of past phylogenetic frameworks and discussed how these phylogenies were translated into classifications. This classification from De Ley and Blaxter (2002) is followed throughout this thesis. The applied classification and the studied species are presented below:

Phylum Nematoda Potts, 1932
Class Enoplea Inglis, 1983
Subclass Dorylaimia Inglis, 1983
Order Mononchida Jairajpuri, 1969
Suborder Mononchina Kirjanova and Krall, 1969
Superfamily Mononchoidea Chitwood, 1937
Family Mononchidae Chitwood, 1937
Prionchulus punctatus (Cobb, 1917) Andrássy, 1958
Class Chromadorea Inglis, 1983
Subclass Chromadoria Pearse, 1942
Order Plectida Malakhov, 1982
Superfamily Plectoidea Örley, 1880
Family Plectidae Örley, 1980
Plectus aquatilis Andrássy, 1985
Order Rhabditida Chitwood, 1933
Suborder Tylenchina Thorne, 1949
Infraorder Panagrolaimomorpha De Ley & Blaxter 2002
Superfamily Panagrolaimoidea Thorne, 1937
Family Panagrolaimidae Thorne, 1937

Halicephalobus gingivalis (Stefanski, 1954) Andrássy, 1984
Panagrolaimus detritophagus Fuchs, 1930
Panagrolaimus rigidus (Schneider, 1866) Thorne, 1937
Panagrellus redivivus Goodey, 1954
Procephalobus sp. Steiner, 1934
Family Alloionematidae
Rhabditophanes sp. Fuchs, 1930
Infraorder Cephalobomorpha De Ley & Blaxter, 2002
Superfamily Cephaloboidea Filipjev, 1934
Family Cephalobidae Filipjev, 1934
Acrobeloides butschlii (de Man, 1885) Steiner & Buhrer, 1933
Acrobeloides maximus (Thorne, 1925) Thorne, 1937
Acrobeloides nanus (de. Man, 1880) Anderson, 1968
Acrobeloides thornei Brzeski, 1962
Cephalobus cubaensis Steiner, 1935
Infraorder Tylenchomorpha De Ley & Blaxter 2002
Superfamily Tylenchoidea Örley, 1880
Family Meloidogynidae Scarbilovich, 1959
Meloidogyne incognita (Kofoid and White, 1919) Chitwood 1949
Suborder Rhabditina Chitwood, 1933
Infraorder Diplogasteromorpha De Ley & Blaxter 2002
Superfamily Diplogasteroidea Micoletzky, 1922
Family Neodiplogasteridae Paramonov, 1952
Pristionchus pacificus Sommer, Carta, Kim, and Sternberg 1996
Infraorder Rhabditomorpha De Ley & Blaxter 2002
Superfamily Rhabditoidea Örley, 1880
Family Rhabditidae Örley, 1880
Caenorhabditis elegans (Maupas, 1900) Dougherty, 1955
Caenorhabditis remanei (Sudhaus, 1974) Andrassy, 1983
Rhabditella axei (Cobbold, 1884) Chitwood, 1933
Oscheius dolichuroides (Anderson & Sudhaus, 1985)
Pellioditis marina (Bastian, 1865) Andrássy, 1983
Pelodera Strongyloides Pelodera strongyloides (Schneider, 1860) Schneider, 1866
Mesorhabditis longespiculosa (Schuurmans Stekhoven, 1951) Dougherty, 1955
Mesorhabditis miotki (Sudhaus, 1978) Andrassy, 1983
Teratorhabditis palmarum Gerber & Giblin-Davis, 1990

2.3 Nematode culture

Acrobeloides butschlii, Acrobeloides maximus, Acrobeloides nanus, Acrobeloides thornei, Caenorhabditis elegans, Cephalobus cubaensis, Caenorhabditis remanei, Halicephalobus gingivalis, Mesorhabditis longespiculosa, Mesorhabditis miotki, Oscheius dolichuroides, Panagrolaimus detritophagus, Pristionchus pacificus, Panagrellus redivivus, Panagrolaimus rigidus, Procephalobus sp., *Pelodera strongyloides, Rhabditella axei, Rhabditophanes* sp. *and Teratorhabditis palmarum* were cultured on 1% agar plates. *Pellioditis marina* was cultured on artificial sea agar plates

(solution A: 23.9 g NaCl, 10.8 g $MgCl_2.6H_20$, 1.52 g $CaCl_2.2H_20$, 0.004 g $SrCl_2.6H_20$, 0.68 g KCl and 0.01 g KBr; dilute to 856 ml; solution B: 40 g Na_2SO_4, 0.2 g $NaHCO_3$, 0.003 g NaF and 0.027g H_3BO_3 dilute to 1000 ml. Mix solution A and solution B; buffer with TRIS-HCl to keep a neutral pH if necessary). This solution was used to make 1% agar plates (1/3 nutrient agar/agar); 1 ml cholesterol (5 mg/ml in EtOH) was added. *Escherichia coli* OP50 was used as a food source. *Plectus aquatilis* was cultured on low salt agar plates made from 10g agar / 500 ml distilled water. All agar plates contained 5 mg/l cholesterol. The uracil-requiring strain of *E. coli* OP50 was used as a food source. *Prionchulus punctatus*, a predator on other nematodes, was cultured on humus extract based agar plates; the prey species used was *Oscheius* sp. (Rhabdititidae). Humus extracts were made by cooking decaying leaves in distilled water for 45 minutes in a microwave oven and filtering them through coffee filters. Humus extracts were stored at –20°C. 1% humus agar was made with nutrient agar diluted with 2/3 distilled water and 1/3 humus extract. Handling was as described by Brenner (1974). *Meloidogyne incognita* was cultured in vitro on *Pisum sativum* on Knop medium (Sijmons *et al*., 1991) under sterile conditions.

2.4 Slide preparation

For *Meloidogyne incognita,* galls were collected from the roots 4-6 weeks after the initial inoculation and gently cut in M9 buffer with a scalpel to release the eggs/embryos. The embryos of the other examined species were collected by either cutting open gravid females in a drop of distilled water with a scalpel, or by flooding agar plates with distilled water using a drawn-out Pasteur pipette. Embryos in the one- or two-cell stage were transferred to a microscope slide carrying a thin pad of 5% agar. Embryos were covered with a coverslip and sealed with Vaseline (Sulston and Horvitz, 1977).

2.5 4D microscopy

All recordings of the embryos were obtained using 4D microscopy (Hird and White, 1993), a multi-focal plane and a time-lapse recording system. Depending on the developmental tempo, every 30-60 seconds, a Hamamatsu Newvicon camera (C2400-07) recorded 30 focal planes through the embryos (with a distance between 1 and 1.2 µm between two focal planes), and the software Simple PCI 5.3/6.1.0 (Compix, Inc., USA) stored the images on disk. The lineage of each recording was constructed using the Simi Biocell software (version 4.0, Simi Gmbh, D-85705 Unterschleissheim, Germany) (Schnabel *et al.*, 1997). The recordings could be replayed at will for further analysis. The embryonic cell lineage was established by identifying all cells and cell divisions in space

and time. By clicking with the mouse pointer on the nucleus of the cell in the window displaying the digitized image, the cell positions were marked and stored in a file. By establishing the positions of each cell, 3D reconstructions of the embryo were made and cellular migrations could be followed. All embryos were recorded at 20°C, except for *Pellioditis marina, Halicephalobus gingivalis* and *Rhabditophanes* sp., which were recorded at 25°C within the framework of another project. Since we found that temperature only has an effect on developmental tempo and not on all the other examined parameters, we used these recordings for our analysis (see 3.3.2).

Recordings of *Meloidogyne incognita* were done by Bartel Vanholme at the Department of Molecular Biotechnology, Faculty of Bioscience Engineering, Ghent University. Developing embryos (n=5) were observed at room temperature (22+/-1°C) by Nomarski (Differential Interference Contrast microscopy) optics using a Nikon inverted microscope with a 40x oil objective (NA 1.3). A motorised stage controller and automatic shutter were incorporated in the system to create a 4D-imaging capacity. The essential software to control both the stage and the shutter was written in JAVA and integrated in Lasersharp 2000 v5.2 software (BioRad, Hercules, CA). These adaptations provided a fully autonomous working system. Images (800x600 pixels; 468kb) of developing embryos were taken every 15 or 30 minutes in 20 different focal planes during the first 2 weeks and every 12 hours during the remaining period using a CoolSNAP HQ CCD camera (Photometrics, Tucson, AZ). To create time-lapse movies the optical section of interest for each time point was manually selected. Subsequent imaging procedures were performed using ImageJ version 1.371 (available via http://rsb.info.nih.gov/ij/).

2.6 Nomenclature

The cells are named according to the nomenclature of Sulston and Horvitz (1977), Deppe *et al*. (1978) and adapted by Sulston *et al.* (1983). This nomenclature is repeated briefly for better readability of the text. Founder cells formed in the first division rounds are given arbitrary names in capital letters according to Deppe *et al.* (1978). When a founder cell divides, each daughter is named by adding to the name of the mother cell a single low-case letter representing its position immediately after division relative to its sister cell. For divisions in anterior-posterior direction the anterior and posterior daughter are indicated respectively with an ‘a’ and ‘p’, dorso-ventral divisions are indicated with ‘d’ and ‘v’, left-right divisions are indicated with ‘l’ and ‘r’. However, we encountered some problems when naming cells in other species than *Caenorhabditis elegans* and for a discussion on this matter, we refer to p. 64.

2.7 Phylogenetic analysis

To study character evolution based on a phylogenic hypothesis, separate trees were assembled (a “supertree” approach). The presented phylogenetic tree's backbone was based on the framework presented by Holterman *et al.* (2006) which largely agreed with Meldal *et al.* (2006). This was done because not for all analyzed nematodes sequences were available and we preferred to use well established phylogenetic hypotheses based on many taxa. However, *de novo* phylogenetic analyses were made for the taxon dense clades Rhabditomorpha (clade 9), Panagrolaimorpha-Aphelenchoidea (clade 10) and Tylenchomorpha-Cephalobomorpha (clades 11 and 12), based on seven new and 20 GenBank SSU sequences. DNA amplification and sequencing were done as described by Bert *et al.* (2008). The sequences were aligned with Clustal W (Thompson *et al.*, 1997), manually checked and edited. Bayesian inference (BI) was performed with MrBayes v3.1.2 (Ronquist and Huelsenbeck, 2003) with a general time-reversible model with rate variation across sites and a proportion of invariable sites (GTR + I + Γ), as estimated by PAUP/Mr Modeltest 1.0b (Nylander *et al.*, 2004). Analyses were run for four million generations and trees were generated using the last three million generations, well beyond the burn-in value. LogDet-transformed distance analyses (LogDet; Lockhart *et al.*, 1994) were performed using PAUP* 4.0b10 (Swofford, 2002), especially to cope with the possible effects of compositional heterogeneity across taxa. Strict consensus trees were built from the outcome of both analyses based on a pronounced conservative approach; conflicts from both analyses and/or branches with lower than a 95 Bayesian posterior probability were presented as unresolved. Finally, our own analyses and the Holterman (2006) framework were combined into a single tree in Mesquite v1.11 (Maddison and Maddison, 2006). Character evolution of developmental character states was traced using parsimony reconstruction. The character states at the internal nodes were reconstructed with the "reconstruct Ancestral States" module implemented in Mesquite.

2.8 Phylogenetic analysis of cell-cell contacts

A phylogenetic analysis of the cell-cell contact matrix was performed using PAUP* 4.0b10 (Swofford, 2002). Maximum parsimony (MP) analyses consisted of a heuristic search with Tree Bisection Reconnection (TBR) with default options. A majority-rule consensus tree was computed from the resulting trees.

2.9 Statistical analysis

Differences in developmental tempo and shape of the egg between the observed character states were analyzed for each character using a non-parametric Kruskal-Wallis test. Subsequently post hoc comparisons between each pair of character states were made using a non-parametric Mann-Whitney test and values were adjusted using a sequential Bonferoni method (values shown between brackets). When analyzing the division sequence, character states which occurred only once, were omitted.

The relationship between developmental tempo and the time of establishment of P4 was examined using a general linear mixed model. The variables were logtransformed and degrees of freedom were estimated using the Satterthwaite's correction.

2.10 Which parameters of early embryonic development will be studied?

2.10.1 Egg shape index (ESI)

The Egg Shape Index was measured on three recordings and calculated as follows: ESI = 100 x A/B, with A= egg width and B = egg length.

2.10.2 Relative early developmental tempo

For all recorded nematodes the early developmental tempo, measured as the time between the second division of the zygote (AB in case of *Caenorhabditis elegans, Caenorhabditis remanei, Oscheius dolichuroides, Panagrellus redivivus, Panagrolaimus rigidus, Pellioditis marina, Pelodera strongyloides, Plectus aquatilis, Pristionchus pacificus, Rhabditophanes* sp., *Rhabditella axei, Teratorhabditis palmarum*; and P1 in case of *Acrobeloides butschlii, Acrobeloides maximus, Acrobeloides thornei, Cephalobus cubaensis, Halicephalobus gingivalis, Meloidogyne incognita, Mesorhabditis longespiculosa, Mesorhabditis miotki, Panagrolaimus detritophagus* and *Procephalobus sp.*), and the division of the endodermal precursor cell E, was calculated. This time was divided by the time *Caenorhabditis elegans* needed to develop from the division of AB until the division of E at 20°C, and was called the relative early developmental tempo.

Another way to measure early developmental tempo is to take the time for a 2-cell stage embryo to establish 50 cells relative to the time *Caenorhabditis elegans* needs to establish 50 cells.

2.10.3 Synchronous versus asynchronous rate

Synchronous development is defined when the first four blastomeres in the early embryo are from the same second generation cleavage (ABa, ABp, EMS, P2) and asynchronous development when the first four blastomeres are of different generations (and hence all differ in size) (Dolinski *et al*., 2001).

2.10.4 The spatial configuration of the 4-cell embryo

In the 4-cell stage of the early embryo 4 different configurations can be observed. When synchronous development is observed, there are 3 possible configurations depending on the spindle orientation of AB and P1. When the mitotic spindle of AB and P1 is oriented along the long axis of the embryo, a **linear** configuration is reached (Fig 2.1A). When the spindle of AB is set up perpendicularly to the spindle of P1, two different configurations are possible: tetrahedral and rhomboidal. In a **tetrahedral** configuration each of the blastomeres of the embryo is in contact with three others (Fig. 2.1D), while in the **rhomboidal** configuration, two of the four blastomeres are each in contact with two other blastomeres (Fig. 2.1C). When asynchronous development is observed, the cleavage of AB is delayed and the configuration of AB, EMS, C and P3 is assessed. Besides a linear arrangement, a **partial linear** arrangement is defined (Fig. 2.1B). This partial linear arrangement refers to the linear arrangement of EMS and P2 (Dolinski *et al*., 2001).

2.10.5 The spatial configuration of the posterior cells after the division of P3

The posterior cells' final configuration from ventral to dorsal was scored as follows: after P3 divided, we looked at the configuration of the following cells: the endodermal precursor (EMS or E), C, D and P4. When a nematode shows no polarity reversal the posterior cells' configuration from ventral to dorsal is C-D-P4. When a nematode has a single polarity reversal the posterior cells' configuration from ventral to dorsal is either P4-D-C or C-P4-D. When a double polarity reversal occurs, the posterior cells' spatial configuration from ventral to dorsal is D-P4-C (Fig. 2.2).

Note that the endodermal precursor cell is not always born from the P1 cell. In clade 2 it was shown that this endodermal precursor cell is derived from the AB lineage (Malakhov, 1994; Schulze and Schierenberg, 2008 and our unpublished data from *Prionchulus punctatus*).

2.10.6 Gastrulation

In all nematodes the start of gastrulation (time and cell stage) and how many endodermal precursor cells gastrulate, will be determined. The start of gastrulation is determined using the 3D function of Simi Biocell as follows: right before gastrulation, MS and P4 are arranged linearly at the ventral side of the embryo. The time, when the centre of (one of) the endodermal precursor cells cross the line that runs through the centres MS and P4, by migrating interiorly, is appointed as the start of gastrulation.

2.10.7 Cell-cell contact in the 8AB cell stage

To compare the cellular arrangements of different embryos the 3D option was used. This shows a three-dimensional view of all cells present at a particular point in time and allows embryos to be rotated. Cell cell contacts in the 8AB stage were assessed, because this stage stage provides a useful reference point for summarizing the effects of Notch signaling on the fates of AB descendants (Priess, 2005).

The 8AB stage corresponds to the 12-or 13-cell stage, depending on whether P3 had already divided or not. Cell cell contacts were assessed in all species and presented in Fig. 3.23, Fig. 3.31, Fig. 3.42, Fig. 3.47, Fig. 3.57 and Fig. 3.63 (1 = contact is present, 0 = contact is absent). Cell contacts were scored as ‘present’ if the cells had contact in the period that the embryos were in the 12 (or 13) cell stage, even if this contact was subsequently lost. Variable contacts were marked by a yellow square. With respect to the absence of cell-cell contacts we should note that we cannot claim this with certainty, since we cannot exclude the presence of small phylopodia, which allow transmission of signals between cells, because of resolution restrictions of our 4D-system.

2.10.8 Cleavage orientation

The cleavage orientation of AB cells in the 4AB and the 8AB stage and their deviation from the a-p axis was calculated. The a-p axis was defined by the centres of P_2 in the 4-cell-stage and the AB-derived blastomere, which is placed farthest from P_2 in the 16-AB cell stage. Both centres defined a vector p1p2. When a cell divided, approximately 120 seconds after the furrow started to ingress, a vector p3p4 was drawn between the centres of both daughter cells. 120s was taken as time point for *Caenorhabditis remanei*, *Caenorhabditis elegans*, *Pelodera strongyloides*, *Rhabditella axei* and *Rhabditophanes* sp. 180s was taken as time point for *Pristionchus pacificus, Teratorhabditis palmarum, Pellioditis marina, Panagrellus redivivus, Mesorhabditis miotki, Halicephalobus gingivalis, Procephalobus sp., Panagrolaimus detritophagus* and *Oscheius dolichuroides.*

In all the slowly developing species of Cephalobidae and *Mesorhabditis longespiculosa* 240s after the furrow started to ingress, the vector p3p4 was drawn.

The cleavage angle (θ) with respect to the a-p axis was calculated using the following equation: p1p2 x p3p4= || p1p2|| || p3p4|| cos θ. To obtain angles between 0°-90°, p1 and p2 were sometimes switched, depending on the orientation of the embryo on the slide. Since we cannot deduce from an angle of 90°, whether this as along the d-v axis or the l-r axis, we just want to make conclusions whether cells divide along the a-p axis (<45°) or not (>45°), since in *Caenorhabditis elegans* all AB blastomeres in the 8AB stage divide mainly along the a-p axis (Bisschoff and Schnabel, 2006b). Therefore we divide them in ‘mainly along the a-p’ or mainly ‘more skewed’.

Chapter 3 Comparative analysis of early embryonic developmental characters

3.1 Description of early embryonic development in the examined families

3.1.1 The early embryonic development within the Plectida: family Plectidae

3.1.1.1 Introduction

Within this family one species was studied: *Plectus aquatilis*. The embryonic development of this species, together with 6 other plectids was already analyzed by Lahl *et al.* (2003). They described that gastrulation occurs with one endodermal precursor cell. They also found a bilateral symmetry which becomes obvious very early in development (Lahl *et al.*, 2003). However their analysis was done using video-microscopy and an analysis of cell cycle patterns and the spatial organization of blastomeres within the embryo was not included in their study. Therefore we re-analyzed this species by means of 4D microscopy. Using this technique we observed a variable arrangement of AB cells in the 16AB cells, which they could not have seen using video-microscopy. For its potential use as phylogenetic marker, comprehensiveness and the ability to compare between other species, a description of the process of gastrulation and the early establishment of bilateral symmetry in the MS and C lineage is given, although this was already reported by Lahl *et al*. (2003).

3.1.1.2 Egg characteristics

The ESI was calculated and was found to be 87 ± 2 (n = 5). In combination with data from literature (Lahl *et al.*, 2003), we conclude that Plectidae are characterized by more rounded eggs.

3.1.1.3 General features of embryogenesis

The early embryonic development of *Plectus aquatilis* showed a fixed cleavage pattern (Fig. 3.1). The early development of *Plectus aquatilis* started with a series of unequal, asynchronous cell divisions, during which a larger somatic founder cell and a

smaller germline precursor cell is formed. The zygote, $P_{0,}$ divided into an anterior somatic cell, AB and a posterior germline cell, P_1. First, the AB cell divided in a perpendicular direction. Since both AB and P1 cleaved prior to the second generation cleavages, the development is described as being synchronous. Then, the germline cell, P_1 divided into an anterior somatic cell, EMS, and a posterior germline cell, P_2. One AB cell migrated to the anterior side (ABa) and the other AB cell migrated to the future dorsal side of the embryo (ABp) resulting in a rhomboidal configuration. However, in two out of five recordings the spindles of AB and P1 were oriented perpendicular to one another, but in different planes, resulting in a tetrahedral configuration. After the division of the 2 AB cells, P_2 divided into a somatic cell, C, and a germline precursor cell, P_3. Following this stage, the EMS divided into an anterior founder cell MS (mainly mesoderm in *Caenorhabditis elegans*) and a posterior founder cell E (endoderm). Then the 4 AB cells divide, followed by the division of C and MS. From here on, variation in the division sequence within different individuals was found (Table 3.1).

3.1.1.4 The early embryogenesis is characterized by complex movements within the eggshell

In the spacious eggshell complex movements of the complete embryo were observed. After the division of P1, a tetrahedral (Fig. 3.2A) configuration is rearranged to a rhomboidal configuration (Fig. 3.2B) After the division of the 2 AB cells (6-cell stage), the whole embryo rotated in all recordings, changing the orientation of the a-p axis of the embryo, relative to the eggshell (Fig 3.2C). The MS blastomere is positioned more anteriorly compared to *Caenorhabditis elegans*. As a result, the spatial arrangement of early blastomeres in the 8 cell stage differs considerably between *Plectus aquatilis* and *Caenorhabditis elegans* (Fig 3.3). After the division of the four AB cells the embryo rotated again (Fig 3.2D). Another rotation of the complete embryo was observed after the division of 8AB (Fig 3.2E, F).

3.1.1.5 Division sequence

The division sequence in three embryos was analysed and compared to that of *Caenorhabditis elegans* (Table 3.1). The division sequence of the three recordings of *Plectus aquatilis* were found to be identical up to the 13-cell stage. Subsequently, intraspecific variation was observed: in embryo 1 there is a temporal separation of MS and E divisions, in contrast to the other two embryos, where MS and E divide after each other. From the 6 cell stage onwards differences in the division sequence between *Plectus aquatilis* and *Caenorhabditis elegans* are found and include a switch between EMS and

P2. The division sequence of embryo 1 is identical to the one published by Lahl *et al*. (2003), while the sequences of embryo 2 and 3 differ from them in a switch between 8AB and E.

3.1.1.6 Developmental tempo

The members of each cell lineage cleave synchronously with cell cycle periods different from those in other lineages. The relative developmental tempo, expressed as the time between the division of the AB blastomere and the division of the endodermal precursor cell E, was calculated. *Plectus aquatilis* develops 4.5 times slower than *Caenorhabditis elegans* at 20°C. Taken the time to establish 50 cells, *Plectus aquatilis* develops 3 times slower than *Caenorhabditis elegans* (Fig 3.4).

The mean cell cycle length in the AB lineage was compared for 4 cycles in 3 recordings of *Plectus aquatilis* (Fig. 3.5). In all recordings the same pattern was observed: the mean cell cycle length extended and then became shorter. However in 2 out of 3 embryos the longest cell cycle was found at the 8AB cell stage whereas in one embryo (embryo 3) a plateau in 4AB and 8AB was found.

In all 3 embryos the lengths of early cell cycles in the other lineages were studied (Fig. 3.6). After birth, the descendants of each founder cell divide with characteristic periods.

With the exception of the C lineage, the division rate is proportional to the time of the first division of the founder cell. AB, which divided firstly, divided the fastest and E the slowest. C is an exception: it divided before the MS and E lineage, but with a division rate which is slower than MS and E. In all cells the length of division rounds, that is the time between the first and the last division of each division round, increased with developmental time (Fig. 3.6), except for embryo 3, where the division round of 4AB is larger than 8AB and 16AB. The lengths of the division rounds for the AB founder cell are larger in embryo 3 than in the other 2 recordings, which explains the early peak in 4AB for this recording in Fig. 3.5.

3.1.1.7 Configuration of the posterior cells

One reversal of polarity, placing the P4 cell closest to the endodermal precursor E (configuration P4-D-C) was observed in all 5 recordings. For a detailed discussion, we refer to chapter 4.

3.1.1.8 Gastrulation

In *Plectus aquatilis* gastrulation starts in the 12-or 13 cell stage. The gut founder cell E itself migrated towards the centre of the embryo (Fig. 3.7A) and divided 120 min (embryo 1), 100 min (embryo 2) and 80 min (embryo 3) later in the interior of the embryo (Fig 3.7B). In all recordings the P4 cell followed the E cell immediately into the interior of the embryo as soon as it was formed. As in *Caenorhabditis elegans*, in *Plectus aquatilis* embryos the 2 E cells divide into 4E cells in the 44 cell stage (Fig. 3.7C). Since gastrulation occurred much earlier in *Plectus aquatilis* than in *Caenorhabditis elegans*, the spatial arrangement of the 12-cell stage is different in both embryos. In *Plectus aquatilis* the endodermal precursor E has started to ingress at this moment and is located more interiorly in the embryo.

3.1.1.9 Bilateral symmetry in MS and C lineage

In the species studied, bilateral symmetry becomes obvious in the very early stage. Fig. 3.8 (A-D) clearly demonstrates the symmetrical pattern of the MS and C cells.

3.1.1.10 Bilateral symmetry in the AB lineage

In contrast to *Caenorhabditis elegans*, an early bilaterally symmetrical pattern was also found in the AB lineage: a dorsal view of the 16AB cell stage shows a complete bilaterally symmetrical configuration of the embryo in all 5 recordings. Two pairs of AB sister cells form a mirror image axis, while 6 pairs are positioned contralateral symmetrically. However, colour coding the descendants of AB in 3D reconstructions reveals that cells occupying the same position in the embryo do not originate from the same mother cell. Three different configurations were observed.

In the first configuration the mirror image axis is built by the descendants of ABarp and ABplp (2/5 embryos) and the pairs ABala-ABara, ABalp-ABprp and ABpla-ABpra descendants form contralateral partners (Fig. 3.9A). In the second configuration, the axis is built by the descendants of ABpra and ABprp (2/5 embryos) and the pairs ABala-ABalp, ABplp-ABarp and ABpla-ABara descendants form contralateral partners (Fig. 3.9B). In the third configuration, the axis is built by the descendants of ABpla and ABplp and ABara-ABarp, ABalp-ABprp and ABala-ABpra form contralateral partners (Fig. 3.9C).

Fig. 3.10 reveals why these 3 different patterns are observed. In two recordings the left daughters of the 2AB cells, ABal and ABpl, are shifted to the anterior direction (Fig. 3.10A), as is the case for *Caenorhabditis elegans* embryos. In two other recordings

the right daughters of the 2AB cell stage, ABar and ABpr are shifted to the anterior direction (Fig. 3.10B). In the 5th embryo, the division of ABa and ABp did not occur in a left-right direction, positioning ABar and ABpr as the most anterior blastomeres (Fig. 3.10C).

In contrast to *Caenorhabditis elegans*, where the third division of AB occurs along the a-p axis, in *Plectus aquatilis* most divisions occur along the dorsoventral axis or the left-right axis. Moreover, divisions seem to be more variable, with no clear predisposition. For instance, in two recordings the division of ABpr occurs in a dorsoventral orientation while in the other cases this division is oriented along the left-right axis.

3.1.1.11 Cell-cell contacts

We analyzed the number of AB cells which are in contact with the MS cell in the 8AB cell stage and found that in 3 out of 5 embryos 4AB cells contacted the MS cell, while in the other 2 embryos 5 AB descendants had contact with the MS cell. Only the contacts ABala-MS and ABalp-MS were found in all 5 recordings. The other contacts were variable among the 5 recordings. Based on this and on the variable positioning of the 16AB cells, we have to conclude that homologous cells and thus homologous cell-cell contacts in the 8AB cell stage cannot be identified and analyzed.

3.1.1.12 Cleavage orientation

Similarly, because of homology problems the cleavage orientation of the 8AB cells could not be determined.

3.1.2 The early embryonic development within the Rhabditomorpha: family Rhabditidae

3.1.2.1 Introduction

In this chapter the model organism *Caenorhabditis elegans* and 8 other species within Rhabditidae were selected and several parameters of the early embryonic development were studied in detail. Most parameters in *Caenorhabditis elegans* are already thoroughly studied. However, we included this nematode in our study, because data on the division angles in the 4AB and 8AB cell stage (absolute numbers) could not be deduced from literature and also cell-cell contacts of the descendants of P1 in the 12-cell stage were not described yet. Therefore we re-analysed this species and these two aspects will be new. However, for comprehensiveness, we reanalyzed and described all the other parameters as well and they confirm earlier studies on this nematode (Deppe *et al*., 1978; Sulston *et al*., 1983; Schierenberg, 1987; Skiba and Schierenberg, 1992). Also the complete cell lineage of *Pellioditis marina* was already published (Houthoofd *et al*., 2003). Since their focus was on the comparison of fate and lineage homology between *Pellioditis marina* and *Caenorhabditis elegans*, a thorough analysis of the early embryonic development was not included. The division sequence, the developmental tempo, the division rounds of the different blastomeres, the establishment of bilateral symmetry and the process of gastrulation was described by these authors, but was re-analyzed and will be included here for comprehensiveness. The analysis of the cell-cell contacts in the 12-cell stage, the division angles in the 4AB and the 8AB stage and an analysis of the cell cycle lengths in the AB lineage are new for this species.

3.1.2.2 Egg characteristics

The ESI was calculated for all species (Table 3.2). Elongated eggs were produced by *Mesorhabditis miotki* (ESI=53 ± 2, n = 6) and *Pelodera strongyloides* (ESI=56 ± 5, n = 3). The most rounded eggs were produced by *Pellioditis marina* (ESI=84 ± 5, n = 2).

3.1.2.3 General features of embryogenesis

The early embryonic development of all members of the family Rhabditidae showed a fixed cleavage pattern (Fig. 3.11-3.19). In all examined species the early development started with a series of unequal, asynchronous cell divisions, during which a larger somatic founder cell and a smaller germline precursor cell is formed. The zygote, $P_{0,}$ divided into an anterior somatic cell AB and a posterior germline cell P_1. In all species, with the exception of *Mesorhabditis miotki* and *Mesorhabditis longespiculosa*,

the AB blastomere divided before the P1 blastomere. The AB blastomere divided in a direction perpendicular to the longitudinal axis. Then, the germline cell P_1 divided into an anterior somatic cell EMS and a posterior germline cell P_2. Since both AB and P1 cleaved prior to the second generation cleavages, the development is described as being synchronous. One AB cell migrated to the anterior side (ABa) and the other AB cell migrated to the future dorsal side of the embryo (ABp). These rearrangements resulted in a rhomboidal configuration that was found to be typical for members of the Rhabditidae family. In *Mesorhabditis longespiculosa* the P1 blastomere divided first with a division axis parallel to the longitudinal axis of the embryo, resulting in 3 cells in a row. AB divided in a perpendicular direction to the longitudinal axis of the egg. With the migration of ABp to the dorsal side, EMS is pushed to the ventral side, leading to the rhomboidal pattern. In *Mesorhabditis miotki* these 2 blastomeres divide at the same time. In *Mesorhabditis miotki, Oscheius dolichuroides, Pelodera strongyloides* and *Pellioditis marina* the AB division occurred in a direction perpendicular to the longitudinal axis and the division of P1 parallel to the longitudinal axis, leading to a transient T-shape that immediately converts to the rhomboidal configuration.

3.1.2.4 Division sequence

The division sequence of the 9 analyzed species within the family Rhabditidae can be found in Table 3.3. Essential differences between species exist in the timing of the divisions of the germline precursor cells. In most species within Rhabditidae this primordial germ cellis established relatively late, at the 15 or 16-cell stage (or in the 24 cell stage, depending whether P3 divides before 8AB) (Table 3.4). This is the case for *Caenorhabditis elegans, Caenorhabditis remanei, Rhabditella axei, Pellioditis marina and Pelodera strongyloides*. In *Teratorhabditis palmarum* the P4 cell was present in the 13-cell stage or in the 14 cell stage when MS had already divided. In *Oscheius dolichuroides, Mesorhabditis miotki* and *Mesorhabditis longespiculosa* the divisions of the germline precursor cells have shifted to an earlier phase, so that P4 is already present in the 8 or 9-cell stage.

Intraspecific variation was observed for several species (Table 3.3). In *Rhabditella axei* differences in division sequence occur from the 28 cell stage on: a switch between 2E and 16AB and between D and MS could be observed. In *Mesorhabditis longespiculosa* differences are identified much earlier: in the 8-cell stage a switch between P3 and EMS occurs. In *Mesorhabditis miotki* the division sequence remains identical in all three recordings until the 32-cell stage. From then on switches between P_4, 2C, 4MS and 2E were observed. In *Caenorhabditis remanei* differences are

found from the 14-cell stage on: a switch between MS and C was observed and also one division later a switch between P3 and 8AB. In *Pellioditis marina* differences in division sequence are found from the 13-cell stage on: P3, MS, E, C and 8AB all occupy different positions in the division sequence when comparing two recordings. In *Teratorhabditis palmarum* the first difference in division sequence between recordings is found from the 13-cell stage on: a switch between P3 and MS and later in the 28 cell stage a switch between D and 16AB is observed. In *Pelodera strongyloides* intraspecific variation is found from the 28 cell stage on: a switch between 16AB and 2C is observed. From then on division sequences vary between recordings.

3.1.2.5 Developmental tempo

The relative developmental tempo of all analyzed species, expressed as the time between the division of the AB *(Caenorhabditis elegans, Caenorhabditis remanei, Oscheius dolichuroides, Pellioditis marina, Pelodera strongyloides, Rhabditella axei and Teratorhabditis palmarum)* or P1 *(Mesorhabditis longespiculosa and Mesorhabditis miotki)* and the division of the endodermal precursor cell E was calculated and normalized to the tempo of *Caenorhabditis elegans* (Table 3.5). All rhabditids develop 1-7.2 times slower than *Caenorhabditis elegans* at 20°C, with the exception of *Caenorhabditis remanei*, which develops even faster than *Caenorhabditis elegans*. *Rhabditella axei* develops at the same tempo as *Caenorhabditis elegans*. We can divide our data set in 3 groups: nematodes with a **fast** development at 20°C, including *Caenorhabditis elegans, Caenorhabditis remanei, Rhabditella axei* and *Pelodera strongyloides* (relative developmental tempo between 0.7 and 1.1). Then there is a group with an **intermediate** development (relative developmental tempo between 2.2 and 2.7), including *Pellioditis marina, Teratorhabditis palmarum* and *Mesorhabditis miotki*. And finally there is a group, existing of nematodes with a **slow** early embryonic development at 20°C (relative developmental tempo between 5.6 and 7.2), including *Oscheius dolichuroides* and *Mesorhabditis longespiculosa.*

Secondly we looked at the number of cells during embryonic development until the 50 cell stage and measured the time to achieve 50 cells as a measurement of developmental tempo. Ordered with increasing relative tempo we see that *Caenorhabditis remanei* < *Caenorhabditis elegans* < *Pelodera strongyloides* < *Rhabditella axei*< *Teratorhabditis palmarum* < *Pellioditis marina* < *Mesorhabditis miotki* < *Mesorhabditis longespiculosa.* Taking the number of cells in time until the 50 cell stage at 20°C, we see that this is in agreement with the classification found using relative early developmental

tempo. Only *Rhabditella axei*, is switched from position 4 (using relative early developmental tempo) to position 2 (time to establish 50 cells) (Fig. 3.20).

The mean cell cycle duration in the AB lineage was compared for all species (Fig. 3.21). Four different patterns can be observed. The **first** pattern can be found in *Caenorhabditis elegans*: cell cycles increased slowly at an equal rate (Fig. 3.21A). For *Caenorhabditis elegans* the cell cycles are shorter at 25°C than at 20°C. The same pattern was observed for *Caenorhabditis remanei* (Fig. 3.21B), *Pelodera strongyloides* (Fig. 3.21G) and *Teratorhabditis palmarum* (Fig. 3.21I). The **second** pattern was found in *Rhabditella axei* (Fig. 3.21H). In early development the mean cell cycle length extended, but from the 4AB stage on the cell cycle length remained constant. The **third** pattern was found in *Mesorhabditis longespiculosa.* This nematode showed long cell cycles compared to the other species, which continued to decrease in time (Fig 3.21C). The **fourth** pattern was found in *Mesorhabditis miotki* (Fig. 3.21D), *Oscheius dolichuroides* (Fig. 3.21E) and *Pellioditis marina* (Fig. 3.21F). The mean cell cycle length extended and then became shorter. The longest cell cycle was found at the 4AB cell stage.

Also the lengths of early cell cycles in the other lineages were studied (Fig. 3.22 A-I). After birth, the descendants of each founder cell divide with characteristic periods. For some nematodes the following correlation was found: the division rate is proportional to the time of the first division of the founder cell. This was found to be true for *Teratorhabditis palmarum*. This correlation was also found in the following nematodes, but with the exclusion of the E cell: *Pellioditis marina, Pelodera strongyloides and Rhabditella axei*. In these nematodes AB, which divided first, divided the fastest and C, which divided last, divided the slowest. In *Mesorhabditis miotki* the P1 blastomere, which divided first (together with AB) divided the fastest and C the slowest. In all these nematodes E is an exception: it arises earlier but divides slower: the third generation of E divides later than the third generation of C, as can be seen in one recording of *Rhabditella axei*.

In *Mesorhabditis longespiculosa* no clear correlation could be found. P1, which divided first developed the fastest, but the second blastomere which divided, AB, did not divide as fast as the MS lineage. Also in *Oscheius dolichuroides* no clear correlation could be found. AB, which divided first, divided not as fast as P lineage.

In general, the length of division rounds, that is the time between the first and the last division of each division round increased with developmental time. Exception to this is the division round of 8AB in one recording of *Caenorhabditis remanei*, which is

shorter than 4AB. Also in *Mesorhabditis longespiculosa* exceptions are found: the division round of 4AB is shorter than the 2AB stage and the division round of 16AB, which is shorter than 8AB. In one recording of *Mesorhabditis miotki* the division round of 8AB is shorter than 4AB.

Intraspecific variation can be found. For instance in *Mesorhabditis miotki* there is a difference in length of the division rounds in the AB lineage but also in the timing of the division of the blastomeres. This is also demonstrated in *Teratorhabditis palmarum*.

There is clearly an effect of temperature on the length of division rounds (Fig. 3.22A). In *Caenorhabditis elegans* cell division rounds at 25°C are much shorter than at 20°C, but show the same pattern. Divisions of the different founder cells occur sooner at 25°C than at 20°C.

3.1.2.6 Configuration of the posterior cells

The spatial configuration of the posterior cells in the embryo after the division of P3 was analyzed for all species. One reversal of polarity, placing the P4 cell closest to the endodermal precursor E (configuration P4-D-C) was observed in all species. For a detailed discussion, we refer to chapter 4.

3.1.2.7 Gastrulation

In all species gastrulation started with the inward migration of two gut precursor cells, Ea and Ep from the ventral side of the embryo into the interior of the embryo. Only minor differences (24-28 cell stage) existed between species, regarding the number of cells present when gastrulation started. In C. *elegans, Caenorhabditis remanei, Mesorhabditis miotki, Oscheius dolichuroides* and *Pelodera strongyloides* gastrulation started in the 26-cell stage. As the two endodermal precursor cells ingress, they are covered by 3 MS granddaughters in the anterior of the embryo (MSap, MSpa, MSpp) and P4 in the posterior of the embryo. When the two E cells have reached their destination, they divide in 4 E cells. In *Oscheius dolichuroides* there was a temporal separation of 11 min between the division of Ea and Ep, which was observed in no other recording. In *Teratorhabditis palmarum* and *Rhabditella axei* gastrulation started at the 28-cell stage. As the two endodermal cells ingress into the interior of the embryo, they are covered by 4 MS granddaughters at the anterior of the embryo and P4 and D at the posterior end of the embryo. In *Pellioditis marina* and *Mesorhabditis longespiculosa* gastrulation started at the 24-cell stage, before the division of the 2 MS cells. After the division of 2 MS, the 4

MS granddaughters in the anterior part of the embryo and P4 and D at the posterior part of the embryo migrate toward each other.

3.1.2.8 Bilateral symmetry

The left-right division of the 2AB cell stage shows different patterns. In *Caenorhabditis elegans, Caenorhabditis remanei, Mesorhabditis miotki, Pellioditis marina, Pelodera strongyloides, Rhabditella axei* and *Teratorhabditis palmarum* the anterior daughters, ABal and ABpl, are skewed into the anterior direction. In *Mesorhabditis longespiculosa* the left-right division of the 2AB cell stage shows different patterns. In two recordings the left daughters of the 2AB cells, ABal and ABpl, are skewed into the anterior direction, as is the case for *Caenorhabditis elegans* embryos, while in another recording the right daughters of the 2AB cell stage, ABar and ABpr are shifted to the anterior direction. Also in *Oscheius dolichuroides* different patterns were found. In one recording the left daughters of the 2AB cells, ABal and ABpl, are skewed into the anterior direction, while in the other two recordings the right daughters of the 2AB cell stage, ABar and ABpr are shifted to the anterior direction. However, before the division of 4AB, cells are reorganized to the same configuration as in cases where the left daughters are positioned more anteriorly.

Because of this shift to the anterior of 2 daughter cells, bilateral symmetry does not become obvious in early embryonic development; Although the first division (MS, C and D) and the second division (E and AB) in somatic lineages separate the future left from right, the divisions occur mostly with a predominant antero-posterior orientation of the cleavage spindle, as is the case for the MS and C lineage. Since recordings were not followed until the end, it was not possible to determine how bilateral symmetry in the juvenile body plan was achieved. The establishment of bilateral symmetry in *Pellioditis marina* was previously studied by Houthoofd *et al*. (2003).

3.1.2.9 Cell-cell contacts

Cell-cell contacts in the 8AB cell stage were analyzed for all species. Variable cell-cell contacts were marked in yellow (Fig. 3.23).

The cell-cell contacts MS-ABara and MS-alp, which induce induce pharyngeal potential in those cells in the *Caenorhabditis elegans* embryo, were found in *Caenorhabditis remanei, Mesorhabditis miotki, Mesorhabditis longespiculosa, Oscheius dolichuroides, Pellioditis marina, Pelodera strongyloides, Rhabditella axei* and *Teratorhabditis palmarum*. As in *Caenorhabditis elegans*, only one member of two

bilateral homologs of blastomeres come into contact with the blastomere MS, except in *Mesorhabditis miotki* and *Mesorhabditis longespiculosa*, where both members of one bilateral homolog, ABalp and ABarp, come into contact with the blastomere MS and in *Teratorhabditis palmarum*, where both members of one bilateral homolog, ABala and ABara, come into contact with the blastomere MS. In *Teratorhabditis palmarum* MS is located much more anteriorly compared to *Caenorhabditis elegans*, leading to different cell-cell contacts (Fig. 3.24).

Other important cell-cell contacts in the 24-cell-stage of *Caenorhabditis elegans* embryogenesis that are essential for induction have been described by Hutter and Schnabel (1995b), Moskowitz *et al.* (1994) and Priess (2005). These contacts (ABalap-ABplaa and ABplpa-MSap) were analysed in all species and found to be present.

3.1.2.10 Cleavage orientation

The cleavage orientation of the 4AB and the 8AB-cell stages was analysed for all species, except *Oscheius dolichuroides*. Eggs were too dark to follow the divisions with great precision in the 16AB stage (Table 3.6).

In *Caenorhabditis elegans* the AB granddaughter cell ABpl divided mainly along the a-p axis, with an angle of 39° ± 5° compared to the a-p axis. ABal and ABpr, on the other hand, had a more skewed orientation (division angles of more than 45° compared to the a-p axis) In the 8 AB-cell stage cells divided mainly along the a-p axis (average of the mean division angles is 22 ±2 °), with the exception of ABala and ABalp, which division had a more skewed orientation (63° ± 6° and 56°± 7°).

In *Caenorhabditis remanei* the anterior granddaughters, ABal and ABar, divided in a more skewed direction (average of the mean division angles is 63 ± 5°) than the posterior granddaughters, ABpl and ABpr (average of the mean division angles is 46 ± 8°), where much more variation of the division angles could be observed. In the 8 AB-cell stage cells divided mainly along the a-p axis (average of the mean division angles is 31 ±2 °).

In *Mesorhabditis longespiculosa* all AB granddaughter cells divided mainly along the antero-posterior axis (average of the mean division angles is 24 ± 7°), with the exception of ABal (61± 9°), (Table 3). In the 8 AB-cell stage cells divided mainly along the a-p axis (average of the mean division angles is 32 ± 5°).

In *Mesorhabditis miotki t*he anterior granddaughters of AB (ABal and ABar) in *Mesorhabditis miotki* divided mainly along the antero-posterior axis (average of the mean

division angles is 29 ± 6°), while the posterior granddaughters of AB (ABpl and ABpr) mainly divided in a more skewed direction (average of the mean division angles is 53 ± 9°). In the 8 AB-cell stage cells divided mainly along the a-p axis (average of the mean division angles is 19 ±2 °).

In *Pellioditis marina* the anterior granddaughters, ABal and ABar, divided in a more skewed direction (average of the mean division angles is 65 ± 7°) in contrast to the posterior granddaughters, ABpl and ABpr (average of the mean division angles is 42 ± 2°) with a more anteroposterior division. In the 8 AB-cell stage in *Pellioditis marina* cells divided mainly along the a-p axis (average of the mean division angles is 29 ±2°), with the exception of the division of ABalp (68±3°) and ABara (68±2°), which was more skewed.

In *Pelodera strongyloides* the granddaughters of AB divided in a more skewed direction (average of the mean division angles is 51 ± 9°), with the exception of ABpl, which had a more anteroposterior direction (mean division angle is 35 ±11°). In the 8 AB-cell stage in *Pelodera strongyloides* cells divided mainly along the a-p axis (average of the mean division angles is 32 ±3°), with the exception of ABalp and ABara, which divided in a more skewed direction (average of the mean division angles is 57 ± 4°).

All AB granddaughter cells in *Rhabditella axei* divided nearly perpendicular to the a-p axis (average of the mean division angles is 76 ± 4°), with the exception of ABpl (45± 10°). In the 8 AB-cell stage cells divided mainly along the a-p axis (average of the mean division angles is 25 ±2 °), with the exception of ABalp, which division had a more skewed orientation (50 ± 2°).

In *Teratorhabditis palmarum* the granddaughters of AB divided in a more skewed direction (average of the mean division angles is 62 ± 4°). In the 8 AB-cell stage cells divided mainly along the a-p axis (average of the mean division angles is 27 ±4°).

3.1.3 The early embryonic development within the Diplogasteromorpha: family Neodiplogasteridae

Part of this chapter was published in:

Vangestel, S., Houthoofd, W., Bert, W. and Borgonie, G. (2008). The early embryonic development of the satellite organism *Pristionchus pacificus*: differences and similarities with *Caenorhabditis elegans*. *Nematology* 10, 301-312.

3.1.3.1 Introduction

As a representative of this family we have chosen *Pristionchus pacificus*, which has been established as a satellite organism in evolutionary developmental biology in the last 10 years (Eizinger *et al*., 1999; Sommer, 2000). In this chapter, 12 individuals of *Pristionchus pacificus* were analysed to gain insight into the naturally occurring variation in the division sequence, the spatial arrangement of blastomeres and the cell cycle patterns of the AB lineage. In addition, cell-cell contacts in different cell stages were examined since in *Caenorhabditis elegans* several cell-cell contacts have been described that are essential, through inductions, for blastomere fate specification. Also the influence of temperature on early embryonic development was studied, by recording embryos at 15°C, 20°C and 25°C.

3.1.3.2 Egg characteristics

The ESI was calculated and was found to be 63 ± 3 (n=12). *Pristionchus pacificus* is characterized by relatively elongated eggs.

3.1.3.3 General features of embryogenesis

The early embryonic development of *Pristionchus pacificus* showed a fixed cleavage pattern (Fig. 3.25 A-L). Development started with a series of unequal cleavages during which a larger somatic founder cell and a smaller germline precursor cell were formed. Subsequent divisions resulted in the formation of five somatic founder cells (AB, MS, E, C and D) and one germline precursor P_4.The zygote, $P_{0,}$ divided into an anterior somatic cell, AB, and a posterior germline cell, P_1. First, the AB cell divided in a perpendicular direction. Then the germline cell P_1 divided into an anterior somatic cell, EMS, which determined the future ventral side of the embryo, and a posterior germline

cell, P_2. One AB cell migrated to the anterior side (ABa) and the other AB cell migrated to the future dorsal side of the embryo (ABp). These rearrangements resulted in a rhomboidal configuration. The two AB cells divided into four AB cells in an identical fashion to *Caenorhabditis elegans*, where the left-right axis was established at this moment and where the left granddaughters of AB lay anteriorly compared to their sister cells. However, since embryos were not followed beyond the 50-cell-stage, it is not known if this division also establishes the left-right axis in *Pristionchus pacificus*. Following this stage, the EMS cell divided into an anterior founder cell MS (mainly mesoderm in *Caenorhabditis elegans*) and a posterior founder cell E (endoderm). After the division of P_2 into a somatic cell, C, and a germline precursor cell, P_3, and after the division of 4AB, variation in the division sequence within different individuals was found.

3.1.3.4 Division sequence

The division sequence of the 12 analyzed recordings can be found in Table 3.7. One prominent deviation from the pattern found in *Caenorhabditis elegans* was a temporal separation between the MS and E divisions in all individuals. This has also been observed for several members of the family Plectidae (Lahl *et al*., 2003). From the 13-cell-stage (8^{th} division) onwards, differences in the division sequence between individuals were found: a switch between MS and C was found in two out of ten individuals. From the 44-cell stage onwards, the sequences showed a higher variation and switches between 4MS, 2E, D and 4C could be found. The lineages (Fig. 3.25 A-L) showed considerable variability in the timing of cell divisions in all founder cells within individuals and this variability increased with developmental time. The pattern of the 16AB cells was studied in detail and extracted below each lineage. In embryo 4, the divisions of the 16 AB cells occurred, on average, at 212 min, while in embryo 8, they occurred at 182 min (Fig. 3.26C, D). In embryo 4 and embryo 8, the cell cycle of 8AB lasted 41 min and 49 min, respectively (Fig. 3.29). The eight posterior AB cells divided, on average, 6 min (embryo 8) and 5 min (embryo 4) earlier than the anterior AB cells. This delay in division timing of the anterior cells was already visible when 8AB divided. Recordings made at other temperatures showed the same variability.

3.1.3.5 Developmental tempo

The early embryonic development of *Pristionchus pacificus* was relatively slower in comparison to *Caenorhabditis elegans*: the relative early developmental tempo was 2.1. Embryogenesis (time until hatching) took 24 h in *Pristionchus pacificus*, compared

to 18 h in *Caenorhabditis elegans* at 20°C (Félix *et al*., 1999). However, this time cannot be used unequivocally as a comparative parameter for developmental speed since *Pristionchus pacificus* undergoes one embryonic moult from J1 to J2 before hatching (Félix *et al*., 1999).

When looking at the number of cells in time, we see that *Pristionchus pacificus* needs 1.7 times as much time to establish 50 cells compared to *Caenorhabditis elegans* (Fig. 3.27).

The mean cell cycle lengths in the AB lineage were compared for four cycles in all recordings (Fig. 3.28). All recordings of *Pristionchus pacificus* showed the same pattern. The mean cell cycle length extended and then became shorter, with a peak in the 8AB generation. In recordings at 25°C, there was an overall shorter mean cell cycle length in AB than in recordings at 20°C or 15°C. The longest mean cell cycle length in AB was found at 15°C.

The length of division rounds, that is the time between the first and the last division of each division round, increased for the AB cells with developmental time in all 12 recordings (Fig. 3.29). At 25°C the length of the division rounds was shorter than the average length at 20°C. However, a great deal of variation could be found at 20°C. For instance, the 8 AB cell stage divided in the fifth division round with periods ranging from 5-13 min.

Also the lengths of early cell cycles in the other lineages were studied in one recording (Fig. 3.30). After birth, the descendants of each founder cell divide with characteristic periods. The correlation that the division rate is proportional to the time of the first division of the founder cell, which was found in most nematodes, does not seem to apply in *Pristionchus pacificus*. Ranked according to increasing time of birth we obtain MS-C-D. However when ranked according to increasing division rate, we obtain: E-MS-C.

3.1.3.6 Configuration of the posterior cells

The spatial configuration of the posterior cells in the embryo after the division of P3 was analyzed for all 12 recordings. One reversal of polarity, placing the P4 cell closest to the endodermal precursor E (configuration P4-D-C) was observed in all recordings. For a detailed discussion on this matter, we refer to chapter 4.

3.1.3.7 Gastrulation

In *Pristionchus pacificus* gastrulation started in the 28-cell stage with the inward migration of the two intestinal precursors, Ea and Ep. As in *Caenorhabditis elegans*, these precursor cells divided in the 44-cell stage after they had reached their final destination. The P_4 cell always stayed in close proximity to the Ep cell and they moved inward side-by-side during gastrulation. This is in contrast to *Caenorhabditis elegans*, where the daughters of P_4 do so around the 100-cell stage.

3.1.3.8 Cell-cell contacts

Both poles of the embryo contained a remarkably large perivitelline space compared to *Caenorhabditis elegans*. As a consequence, the early blastomeres were very motile during early embryogenesis leading to variable transient configurations in the early embryo. Therefore, we analysed cell contacts in the 12-cell stage for all recordings. Fifty-nine out of 66 possible cell-cell contacts in the 12-cell-stage (8AB cell stage) were found to be invariant in all 12 embryos (Fig. 3.31). Seven cell-cell contacts were found to be variable (indicated by a grey square) and three of these variable contacts were also variable in *Caenorhabditis elegans*.

Within the AB lineage, two contacts were found to be different in *Caenorhabditis elegans* (in all recordings): the contacts ABala-ABarp and ABpla-ABprp were present in *Pristionchus pacificus*, but not in *Caenorhabditis elegans* (Fig. 3.32). As in *Caenorhabditis elegans*, cell-cell contacts between AB and P1 descendants also showed variability, contacts ABpla-MS and ABpra-E being found in three of 12 embryos.

The cell-cell contacts MS-ABara and MS-alp, which induce pharyngeal potential in those cells in *Caenorhabditis elegans*, were present in *Pristionchus pacificus*. Other important cell-cell contacts in the 24-cell-stage of *Caenorhabditis elegans* embryogenesis that are essential for induction have been described by Hutter and Schnabel (1995b), Moskowitz and Rothman (1996) and Priess (2005). These contacts (ABalap-ABplaa and ABplpa-MSap) were analysed in *Pristionchus pacificus* and found to be present.

3.1.3.9 Cleavage orientation

The cleavage orientation of the 4AB and the 8AB-cell stages was analyzed (Table 3.8). All AB granddaughter cells divided nearly perpendicular to the a-p axis (average of the mean division angles is 83 ± 1°), with the exception of ABpl, which had a more skewed orientation (mean division angle of is 57 ± 5°). In the 8 AB-cell stage cells

divided mainly along the a-p axis (average of the mean division angles is 28 ± 1°), with the exception of ABalp, which division had a more skewed orientation (65 ± 3°).

3.1.4 The early embryonic development within the Panagrolaimomorpha: family Panagrolaimidae

3.1.4.1 Introduction

In this chapter the early embryonic development of *Halicephalobus gingivalis, Panagrellus redivivus, Panagrolaimus detritophagus, Panagrolaimus rigidus* and *Procephalobus* sp. was analyzed. The complete lineage of *Halicephalobus gingivalis* was recently analyzed by Houthoofd *et al*. (2007). However, a thorough analysis of the early embryonic development of this nematode, including the analysis of cell-cell contacts in different cell stages and a determination of the division angles of early blastomeres was not done and will be presented here. The configuration of the posterior cells and the process of gastrulation in this species were already described in Houthoofd *et al*. (2007). However, for comprehensiveness and the ability to compare between other species, these two features are described here as well.

3.1.4.2 Egg characteristics

The ESI was calculated for all species (Table 3.9). Panagrolaimidae are characterized by relatively elongated eggs (ESI between 47 and 65). *Procephalobus sp*. has the most elongated eggs (ESI = 47 ± 4, n = 3) of all nematodes in this study.

3.1.4.3 General features of embryogenesis

The early embryonic development of all members of the family Panagrolaimidae showed a fixed cleavage pattern (Fig. 3.33- Fig. 3.37). In all examined species the early development started with a series of unequal, asynchronous cell divisions, during which a larger somatic founder cell and a smaller germline precursor cell is formed. The zygote, $P_{0,}$ divided into an anterior somatic cell, AB and a posterior germline cell, P_1. In 2 species, *Panagrellus redivivus* and *Panagrolaimus rigidus*, the AB blastomere divided before the P1 blastomere. In the other 3 examined species the P1 blastomere divided firstly.

For *Halicephalobus gingivalis, Panagrolaimus rigidus, Panagrellus redivivus, Panagrolaimus detritophagus* and *Procephalobus* sp. the division of AB occurred in a direction perpendicular to the longitudinal axis of the embryo, while the division of P1 was parallel to the longitudinal axis (Fig. 3.38). In all examined nematodes this lead to a short transient T-shape that immediately converted to the rhomboid configuration when the anterior daughter cell of AB migrated to the anterior side (ABa) and the other AB

daughter cell migrated to the future dorsal side of the embryo (ABp). In *Panagrolaimus detritophagus* there is a time gap of 30 min between the division of P1 and AB and during this period the AB, EMS and P1 are linearly arranged. Since both AB and P1 cleaved prior to the second generation cleavages, the development is described as being synchronous.

3.1.4.4 Division sequence

The division sequence of the 5 analyzed species within the family Panagrolaimidae was analyzed (Table 3.10). Essential differences between species exist in the timing of the divisions of the germline precursor cells. With the exception of *Halicephalobus gingivalis*, this germline precursor cell is established at the 9-cell stage. In *Halicephalobus gingivalis* the divisions of the germline precursor cells have shifted to a later phase, so that P4 is present at the 14-cell stage.

Intraspecific variation was observed for several species. In *Halicephalobus gingivalis* differences in division sequence occur from the 5 cell stage on: a switch between 2AB and P2 was observed. Much later, from the 34 cell stage on there is a switch between 4MS and 2E. In *Panagrolaimus rigidus* intraspecific variation was observed from the 15 cell stage on: a switch between E and C. The same intraspecific variation was observed in *Panagrellus redivivus.* From then on the sequence is different for all recordings of *Panagrellus redivivus*. In *Procephalobus* sp. Intraspecific variation was observed concerning the timing of the germline precursor cell P4. Later from the 26 cell stage on, a switch between 16AB and 2C was observed. The division sequence of *Panagrolaimus detritophagus* shows the least intraspecific variation. Only the timing of the division of the P4 germline precursor cell is different in all recordings.

3.1.4.5 Developmental tempo

The relative developmental tempo of all analyzed species, expressed as the time between the division of the AB blastomere (*Panagrolaimus rigidus* and *Panagrellus redivivus*) or P1 (*Panagrolaimus detritophagus* and Proce*phalobus* sp.) and the division of the endodermal precursor cell E, can be found in Table 3.11. All studied panagrolaimids develop 2.6 – 4.6 times slower than *Caenorhabditis elegans* at 20°C. Ordered with increasing relative tempo we see that *Panagrellus redivivus* < *Procephalobus* sp. < *Panagrolaimus rigidus* < *Panagrolaimus detritophagus.* However, taking the number of cells in time until the 50 cell stage at 20°C, we see that *Panagrolaimus detritophagus* develops faster than *Panagrolaimus rigidus* (Fig. 3.39). *Halicephalobus gingivalis* was not included, since this recording was done at 25°C.

The mean cell cycle duration in the AB lineage was compared for all species (Fig. 3.40). Three different patterns can be observed. The **first** pattern can be found in *Halicephalobus gingivalis* (Fig. 3.40A). The cell cycle lengths stayed constant from the 2AB until the 16AB cell stage. The **second** pattern was found in *Panagrellus redivivus*, *Panagrolaimus rigidus* and in *Procephalobus sp* (Fig. 3.40B, D, E). The mean cell cycle length extended and then became shorter. The longest cell cycle was found at the 4AB cell stage. In *Panagrellus redivivus* and *Panagrolaimus rigidus* this peak in cell cycle length is much more pronounced than in *Procephalobus* sp. The **third** pattern was found in *Panagrolaimus detritophagus.* This nematode showed longer cell cycles compared to the other species, which continued to decrease in time (Fig 3.40C).

Also the lengths of early cell cycles in the other lineages were studied (Fig. 3.41). After birth, the descendants of each founder cell divide with characteristic periods. In *Procephalobus sp*. the division rate is proportional to the time of the first division of the founder cell. The P1 blastomere, which divided first, divides the fastest and the E lineage, which divided last, divides the slowest. This is also observed in *Panagrolaimus detritophagus*, with the exception of E. This blastomere divided before C, but has a slower division rate than C. In *Halicephalobus gingivalis* there is no clear correlation between the division rate and the time of the first division of the founder cell. Here, the P lineage divided before the AB lineage, but with a slower division rate then AB. The E lineage which divided before the C lineage had a slower division rate than the C lineage. In *Panagrolaimus rigidus* this correlation is not observed as well. Here the AB lineage divided before the P lineage but at a slower rate than the P lineage. In *Panagrellus redivivus* there is a time gap between the division of 2AB and 4AB. In this nematode the C blastomere divides before the E cell, but at a slower rate than the E lineage. Thus, the correlation is not valid in *Panagrellus redivivus.*

In general, the length of division rounds, that is the time between the first and the last division of each division round increased with developmental time, although two exceptions to this were observed. In one recording of *Panagrolaimus rigidus* the division round of 16AB is smaller than those of 8AB and in another recording of *Panagrolaimus rigidus* the division round of 8AB is smaller than those of 4AB. Extremely long division rounds in the AB lineage were observed in one recording of *Procephalobus* sp., where there is a time gap between the divisions of the two branches of the Ab lineage: ABal and ABar divide much later than ABpl and ABpr.

Also intraspecific variation was found for all nematodes, except for *Panagrolaimus rigidus*, where there are only minor variations in the timing of the

divisions in MS, C and E. In all other nematodes more pronounced differences in length of the division rounds or in the timing of the division of the founder cells were observed between recordings.

3.1.4.6 Configuration of the posterior cells

The spatial configuration of the posterior cells in the embryo after the division of P3 was analyzed for all species. One reversal of polarity, placing the P4 cell closest to the endodermal precursor E (configuration P4-D-C) was observed in all species, with the exception of *Halicephalobus gingivalis*, where the configuration D-P4-C was observed (double reversal of polarity). In this species contact between germline and the endodermal progenitor is restored when the two primordial germ cells migrate between the two daughter cells of D, after which they migrate inwards together. For a detailed discussion on this matter, we refer to chapter 4.

3.1.4.7 Gastrulation

Gastrulation in *Halicephalobus gingivalis* starts in the 29-cell stage with the two intestinal precursors Ea and Ep ingressing into the interior of the embryo. The anterior daughter of E gastrulates first in between MSap and MSpp, before the second division round of E. These MS cells gastrulate little after the two daughters of Ea. After the division of 2E, the two Ep daughters start to gastrulate, followed by Da and Dp.

In *Panagrellus redivivus* gastrulation starts in the 24-cell stage with the two intestinal precursors Ea and Ep ingressing into the interior of the embryo. The posterior daughter of E gastrulates first, just before the second division round of MS. After the division of the 2E cells, the two descendants of Ea further ingress. After the division of P4, gastrulation proceeds and the 4MS cells in front of the E cells and the two P4 cells and D cell at the posterior end migrate towards each other.

In *Panagrolaimus detritophagus* gastrulation starts at the 35-cell stage with the ingression of the intestinal precursors derived from the E-lineage. At this time the four granddaughters of E lie in a square at the ventral side of the embryo. First, the posterior cells Epl and Epr ingress to the interior of the embryo, while the anterior cells stay at the ventral side of the embryo. At that time, 8 daughter cells of MS are present. MSaaa, MSaap, MSpaa and MSpap lie in front of the 4E cells, while MSapa, MSapp, MSppa and MSppp lie lateral from the E cells. As gastrulation proceeds the 4 MS descendants in front of the 4 E cells and the two daughter cells of D migrate towards each other.

In *Panagrolaimus rigidus* gastrulation starts in the 24-cell stage with the two intestinal precursors Ea and Ep ingressing into the interior of the embryo. The anterior daughter of E gastrulates first in between MSa and MSp, before the second division round of MS. After the division of the C blastomere, the posterior daughter of E follows to the anterior of the embryo, with the germline precursor cell P4 firmly attached to it.

In *Procephalobus* gastrulation starts in the 45 cell stage with the two intestinal precursors Ea and Ep ingressing into the interior of the embryo. The anterior daughter of E gastrulates first in between MSap and MSpa, just before the second division round of MS. After the ingression of Ep, the two E cells divide and the MS descendants in front of the 2 E cells and the two daughter cells of D migrate towards each other.

3.1.4.8 Bilateral symmetry

In *Halicephalobus gingivalis* at the second division round of AB into a left pair and a right pair, the anterior daughters, ABal and ABpl, are skewed into the anterior direction. This is also the case for *Panagrellus redivivus*, *Panagrolaimus rigidus*. However, in *Procephalobus* sp. and *Panagrolaimus detritophagus* this shift to the anterior is not observed immediately, since ABa divides in a strict left-right division. However, this configuration is later restored to the *Caenorhabditis elegans* configuration.

Because of this shift to the anterior, bilateral symmetry does not become obvious in early embryonic development. Although the first division (MS, C and D) and the second division (E and AB) in somatic lineages separate the future left from right, the divisions occur mostly with a predominant antero-posterior orientation of the cleavage spindle, as is the case for the MS and C lineage. Since recordings were not followed until hatching, it was not possible to determine how bilateral symmetry in the juvenile body plan was achieved. The establishment of bilateral symmetry in *Halicephalobus gingivalis* was previously studied by Houthoofd and Borgonie (2007).

3.1.4.9 Cell-cell contacts

Cell-cell contacts in the 12 cell stage (*Halicephalobus gingivalis*) or the 13-cell stage if P3 had already divided (*Panagrellus redivivus*, *Panagrolaimus rigidus*, *Panagrolaimus detritophagus* and *Procephalobus sp*.) were analyzed for 3 recordings for all species. Variable cell-cell contacts were marked in yellow (Fig. 3.42).

The cell-cell contacts MS-ABara and MS-alp, which induce which induce pharyngeal potential in those cells in *Caenorhabditis elegans* were found in *Halicephalobus gingivalis*, *Panagrolaimus rigidus*, *Panagrellus redivivus*,

Panagrolaimus detritophagus and *Procephalobus sp*. As in *Caenorhabditis elegans*, only one member of two bilateral homologs of blastomeres come into contact with the signaling blastomere MS.

Other important cell-cell contacts in the 24- and 26-cell-stage of *Caenorhabditis elegans* embryogenesis that are essential for induction have been described by Hutter and Schnabel (1995b). These contacts (ABalap-ABplaa and ABplpa-MSap) were analysed in all species and found to be present.

3.1.4.10 Cleavage orientation

The cleavage orientation of the 4AB and the 8AB-cell stages was analysed for all species (Table 3.12).

In *Halicephalobus gingivalis* the anterior granddaughters, ABal and ABar, divided in a more skewed direction (average of the mean division angles is 80 ± 3°) than the posterior granddaughters, ABpl and ABpr (average of the mean division angles is 44 ± 9°). In the 8 AB-cell stage 4 of the 8 AB cells (ABarp, ABpla, ABplp, ABpra) divided mainly along the a-p axis (average of the mean division angles is 25 ±2 °), while the other 4 ABala, ABalp, ABara and ABarp had a more skewed direction (average of the mean division angles is 65 ± 4°).

In *Panagrellus redivivus* the right anterior granddaughter ABar, divided perpendicular to the a-p axis (mean division angle of 87 ± 3°), while the other 3 granddaughters divided mainly along the a-p axis (average of the mean division angles of 33 ± 6°). In the 8 AB-cell stage cells divided mainly along the a-p axis (average of the mean division angles is 21 ± 3°), with the exception of ABala, ABalp and ABarp, which had a more skewed direction (average of the mean division angles is 59 ± 8°).

In *Panagrolaimus detritophagus* the anterior granddaughters, ABal and ABar, divided in a more skewed direction (average of the mean division angles is 69 ± 3°) than the posterior granddaughters, ABpl and ABpr (average of the mean division angles is 31 ± 3°). In the 8 AB-cell stage cells divided mainly along the a-p axis (average of the mean division angles is 27 ± 2 °), with the exception of ABala, ABalp and ABara, which had a more skewed direction (average of the mean division angles is 75 ± 3°).

In *Panagrolaimus rigidus* the left posterior granddaughter ABpl, divided mainly along the a-p axis (mean division angle of 44 ± 3°), while the other 3 granddaughters had a more skewed direction compared to the a-p axis (average of the mean division angles of 69 ± 3°). In the 8 AB-cell stage cells only 3 cells (ABara, ABarp and ABplp) divided

mainly along the a-p axis (average of the mean division angles is 28 ± 5°), while the other 5 AB cells had a more skewed direction (average of the mean division angles is 56 ± 4°),

In *Procephalobus* sp. the anterior granddaughters, ABal and ABar, divided in a more skewed direction (average of the mean division angles is 74 ± 4°) than the posterior granddaughters, ABpl and ABpr (average of the mean division angles is 38 ± 10°). In the 8 AB-cell stage cells divided mainly along the a-p axis (average of the mean division angles is 27 ± 3 °), with the exception of ABalp and ABara, which had a more skewed direction (average of the mean division angles is 58 ± 7°).

3.1.5 The early embryonic development within the Panagrolaimomorpha: family Alloionematidae

3.1.5.1 Introduction

Within this family one species was analyzed: *Rhabditophanes sp*. The nearly complete cell lineage of *Rhabditophanes* sp. was analyzed by Houthoofd *et al.* (2008). They showed that cells are built in a similar way as in *Caenorhabditis elegans*: fate similarity between both species is 88%. Nevertheless, minor differences in the cellular composition of the intestine were observed (Houthoofd *et al*., 2006). However, a thorough analysis of the early embryonic development of this nematode, including the analysis of cell-cell contacts in different cell stages, the configuration of the posterior cells and a determination of the division angles of early blastomeres was not done and will be presented here. The process of gastrulation was already described in Houthoofd *et al*. (2008), but for comprehensiveness and the ability to compare between other species, this feature is described here as well.

3.1.5.2 Egg characteristics

The ESI was calculated based on 2 recordings of *Rhabditophanes* sp. and was found to be 89 ± 2, thus *Rhabditophanes* sp. is characterized by relatively round eggs.

3.1.5.3 General features of embryogenesis

The early development started with a series of unequal, asynchronous cell divisions, during which a larger somatic founder cell and a smaller germline cell is formed (Fig. 3.43). The zygote, $P_{0,}$ divided into an anterior somatic cell, AB and a posterior germline cell, P_1. The division of AB occurred in a direction perpendicular to the longitudinal axis of the embryo, while the division of P1 was parallel to the longitudinal axis. The division of the two blastomeres AB and P1 occurred simultaneously and resulted in a short transient T shape which immediately converted into the rhomboid pattern when the anterior daughter cell of AB migrated to the anterior side (ABa) and the other AB daughter cell migrated to the future dorsal side of the embryo (ABp). Since both AB and P1 cleaved prior to the second generation cleavages, the development is described as being synchronous.

3.1.5.4 Division sequence

The division sequence of the 2 recordings of *Rhabditophanes* sp. was determined (Table 3.13). The division sequence is very similar to *Caenorhabditis elegans*, only

minor differences concern switches between two or three blastomeres. The P4 cell is established earlier in *Rhabditophanes sp*. than in *Caenorhabditis elegans*, in one recording it was established at the 9 cell stage, while in another the division of the germline precursor cell P3 had shifted to a later phase (15-cell stage).

Intraspecific variation was observed from the 9 cell stage on: a switch between 4AB, E and P3 was observed.

3.1.5.5 Developmental tempo

Rhabditophanes sp. has a relative fast developmental tempo of 1.1. When looking at the number of cells in time, we see that *Rhabditophanes* sp. needs 1.1x as much time to establish 50 cells compared to *Caenorhabditis elegans* (Fig. 3.44).

The mean cell cycle duration in the AB lineage was compared (Fig. 3.45). The mean cell cycle length shortened until the 4AB cell stage and then became longer with a peak at the 8AB cell stage. After the 8AB cell stage the cell cycles showed a constant length.

Also the lengths of early cell cycles in the other lineages were studied (Fig. 3.46). After birth, the descendants of each founder cell divide with characteristic periods. The division rate of each founder cell is proportional to the time of the first division of the founder cell. The AB blastomere, which divided firstly (together with P1), divided the fastest and the C lineage, which divided lastly, divided the slowest. E is an exception: it divided before the C blastomere, but with a division rate which is larger than that of the C blastomere.

In general, the length of division rounds, that is the time between the first and the last division of each division round increased with developmental time, although two exceptions to this were observed. In one recording the division round of 8AB is shorter than that of 4AB and in another recording the division round of 4E is shorter than that of 2E. Intraspecific variation was limited.

3.1.5.6 Configuration of the posterior cells

One reversal of polarity, placing the P4 cell closest to the endodermal precursor E (configuration P4-D-C) was observed in all recordings. For a detailed discussion on this matter, we refer to chapter 4.

3.1.5.7 Gastrulation

Gastrulation starts in the 32-cell stage with the ingression of 4 intestinal precursors (Eal, Ear, Epl, Epr) lie in a square at the ventral side of the embryo. First the posterior cells Epl and Epr ingress into the interior of the embryo. After the division of the 4E cells, the four anterior descendants still stay at the ventral side until the 52 cell stage. At this point the 4 MS descendants (MSaaa, MSaap, MSpaa, MSpap) at the anterior and the 2 daughter cells of P4 also move inwards.

3.1.5.8 Bilateral symmetry

In *Rhabditophanes* sp. at the second division round of AB into a left pair and a right pair, the anterior daughters, ABal and ABpl, are skewed into the anterior direction. Because of this shift to the anterior, bilateral symmetry does not become obvious in early embryonic development. Although the first division (MS, C and D) and the second division (E and AB) in somatic lineages separate the future left from right, the divisions occur mostly with a predominant antero-posterior orientation of the cleavage spindle, as is the case for the MS and C lineage. Since recordings were not followed until the end, it was not possible to determine how bilateral symmetry of the juvenile body plan was achieved. For a detailed description of the establishment of bilateral symmetry in *Pellioditis marina*, we refer to Houthoofd *et al*. (2003).

3.1.5.9 Cell-cell contacts

Cell-cell contacts in the 8AB cell stage were analyzed in 2 recordings. Variable cell-cell contacts were marked in yellow (Fig. 4.47).

The cell-cell contacts MS-ABara and MS-ABalp, which induce pharyngeal potential in those cells in *Caenorhabditis elegans*, were found in *Rhabditophanes* sp. ABarp also contacts the MS blastomere, in contrast to *Caenorhabditis elegans*, where only one member of two bilateral homologs of blastomeres come into contact with the signaling blastomere MS. Other important cell-cell contacts in the 24-cell-stage of *Caenorhabditis elegans* embryogenesis that are essential for induction have been described by Hutter and Schnabel (1995b), Moskowitz and Rothman (1996) and Priess (2005). These contacts (ABalap-ABplaa and ABplpa-MSap) were analysed in *Rhabditophanes* sp. and found to be present.

3.1.5.10 Cleavage orientation

The cleavage orientation of the 4AB and the 8AB-cell stages was analysed (Table 3.14). In *Rhabditophanes* sp. the anterior granddaughters, ABal and ABar, divided in a

more skewed direction (average of the mean division angles is 78 ± 3°) than the posterior granddaughters, ABpl and ABpr (average of the mean division angles is 24 ± 10°). In the 8 AB-cell stage cells divided mainly along the a-p axis (average of the mean division angles is 21 ± 2°), with the exception of ABala, ABalp and ABplp, which had a more skewed direction (average of the mean division angles is 55 ± 7°).

3.1.6 The early embryonic development within the Cephalobomorpha: family Cephalobidae

3.1.6.1 Introduction

Within the family Cephalobidae the early embryonic development of *Acrobeloides butschlii*, *Acrobeloides nanus*, *Acrobeloides thornei* and *Cephalobus cubaensis* was studied. Specific features of embryogenesis in *Acrobeloides nanus* have been studied in detail. These include developmental tempo, division sequence, gastrulation, the spatial configuration in the four-cell stage and after the division of P3 (Skiba and Schierenberg, 1992; Lahl *et al.*, 2003), intercellular communication and timing of endocytotic activity (Bossinger and Schierenberg (1992, 1996a+b), specification of gut fate and compensation for lost cells (Wiegner and Schierenberg, 1998, 1999), a-p axis specification (Goldstein *et al.* (1998); Goldstein, 2001; Lahl *et al.*, 2006) and the establishment of diploidy (Lahl *et al.*, 2006). However, a thorough analysis of cell-cell contacts in different cell stages and a determination of the division angles of early blastomeres have not been described for this species and therefore it is included in our dataset. For comprehensiveness and the ability to compare between other species, the above features already described in literature, are included here as well.

3.1.6.2 Egg characteristics

The ESI was calculated for all species and can be found in Table 3.15. Cephalobidae are characterized by relatively elongated eggs (ESI between 53 and 60). *Acrobeloides thornei* has the most elongated eggs (ESI = 53 ± 4, n = 5).

3.1.6.3 General features of embryogenesis

The early embryonic development of all members of the family Cephalobidae showed a fixed cleavage pattern (Fig. 3.48-3.51). In all examined species the early development started with a series of unequal, asynchronous cell divisions, during which a larger somatic founder cell and a smaller germline precursor cell was formed. The zygote, $P_{0,}$ divided into an anterior somatic cell, AB, and a posterior germline cell, P_1. In all examined nematodes the division of the germline blastomere P1 is followed by the division of its daughter germline cell P2. As such, the four first blastomeres are of different generations and therefore of different size. This development is being described as asynchronous development. In all studied Cephalobidae, the AB blastomere divided next, followed by the P3 germline precursor cell. The division of AB always occurred in a direction perpendicular to the longitudinal axis of the embryo, while for the division

axis of P2 several possibilities were found. Fig. 3.52 shows a schematic representation of the division axes found in every species. In *Acrobeloides butschlii* the division of P2 occurred in an antero-posterior direction (3/3), with P3 being the most posterior daughter cell (Fig. 3.52 A). In one recording of *Acrobeloides nanus* the division of P2 occurred in a dorsoventral direction with P3 as the ventral daughter cell, while in another recording the division occurred in an antero-posterior direction, with P3 being the ventral daughter cell (Fig. 3.52B). In *Acrobeloides thornei* 3 different spatial patterns were found in the 5-cell stage (Fig. 3.52C). In one recording the division of P2 occurred in a dorsoventral direction with P3 as the ventral daughter cell, in the other recordings (n=4) the division occurred in the antero-posterior direction. In 3 out of 4 recordings the P3 cell was the posterior daughter cell, while in the other it was the anterior daughter cell. In C. *cubaensis* two different patterns were found. In one recording the division of P2 occurred in a dorsoventral direction with P3 as the ventral daughter cell, while in the other two recordings P3 was the most dorsal cell (Fig. 3.52D).

3.1.6.4 Migrations of the C blastomere to the ventral side in *Acrobeloides thornei*

In two out of 5 recordings of *Acrobeloides thornei* remarkable migrations of the C blastomere were observed. After the division of P2 the configuration was EMS-P3-C. Then the C blastomere which was located at the future dorsal side started to migrate to the ventral side. After 24 minutes migration was completed and C was positioned in between the endodermal precursor cell EMS and the germline precursor cell P3, so that there was no contact between these two cells. After the division of P3, the spatial configuration was EMS-C-P4-D. Then P4 and D started to migrate so that 200 minutes after the division of P3 the *Caenorhabditis elegans* configuration E-P4-D-C was reached. The same migration of the C blastomere was observed in another recording, the only difference was that after the division of P3 the spatial configuration of the posterior cells was E-C-D-P4. In this case migrations of P4 and D restore the *Caenorhabditis elegans* configuration with the C blastomere at the dorsal side of the embryo, before the onset of gastrulation.

3.1.6.5 Division sequence

The division sequence of the 4 analyzed species within the family Cephalobidae can be found in Table 3.16. The division sequence of all species is the same until the 42 cell stage (except for the switch between C and 8AB in one recording of *Acrobeloides butschlii*). The P4 germline precursor cell is present in the 6-cell stage in all nematodes. Intraspecific variation was observed in the 16-cell stage of *Acrobeloides butschlii* with a

switch between C and 8AB in the 42 cell stage of all studied species with a switch between 2C and 4MS. No division of the P4 germline was observed during the time of the recording (50 cell stage). The division sequence of *Acrobeloides nanus* is equal to the one described in Skiba and Schierenberg (1992) (division described until the 15-cell stage), but shows a shift between the divisions of 16AB, 2E, 2C and 4MS compared to the one described in Laugsch and Schierenberg (2004) (division described until the 46-cell stage).

3.1.6.6 Developmental tempo

The descendants of each founder cell cleave synchronously with cell cycle periods different from those of other founder cells. The relative developmental tempo of all analyzed species, expressed as the time between the division of the P1 blastomere and the division of the endodermal precursor cell E, was calculated (Table 3.17). All cephalobids develop 7.1-9.5 times slower than *Caenorhabditis elegans* at 20°C. Ordered with increasing relative tempo we see that *Acrobeloides thornei* < *Acrobeloides nanus* < *Cephalobus cubaensis* < *Acrobeloides butschlii*. Looking at the number of cells in time until the 50 cell stage at 20°C, we see the same ordering of the species, except that *Acrobeloides nanus* needs a little less time to establish 50 cells than *Acrobeloides thornei* (Fig. 3.53).

The mean cell cycle duration in the AB lineage was compared for all species (Fig. 3.54 A-D). All examined species within Cephalobidae showed the same pattern: cell cycles which continued to decrease in time.

The lengths of early cell cycles in the other lineages were studied (Fig. 3.55). After birth, the descendants of each founder cell divide with characteristic periods. With the exception of the E blastomere, in all nematodes the division rate is proportional to the time of the first division of the founder cell. The P1 blastomere, which divides first, divides the fastest and the C lineage, which divided last, divides the slowest. The E blastomere is an exception: it divided before the C blastomere, but has a slower division rate than C.

In general, the length of division rounds, that is the time between the first and the last division of each division round increased with developmental time, although one exception to this was observed. In one recording of *Acrobeloides thornei* the division round of 8AB is smaller than that of 4AB. Also intraspecific variation was found for all nematodes. In one recording of *Acrobeloides thornei* the division of EMS coincided with

the division of the MS cells in the two other recordings. In this recording also the divisions of the other blastomeres showed a delay compared to the other.

3.1.6.7 The spatial configuration of the posterior cells

The spatial configuration of the posterior cells in the embryo after the division of P3 was analyzed for all species. In the family Cephalobidae the configuration C-D-P4 was prevalent. Remarkably, there was considerable intraspecific variation in cellular positioning and subsequent rearrangements within this family. *Acrobeloides butschlii* showed two possible configurations: D-P4-C (3/4; double polarity reversal) and P4-D-C (1/4; the *Caenorhabditis elegans* configuration). In the three cases of double polarity reversal, subsequent migration of P4 over D resulted in the *Caenorhabditis elegans* configuration before gastrulation started. The other case exhibited the *Caenorhabditis elegans* pattern immediately and no migrations were observed. In two recordings of *Acrobeloides nanus*, we observed the configuration C-D-P4. Migrations were observed, where C migrated from its ventral position toward the dorsal side, and P4 and D switched positions. For *Acrobeloides thornei* we observed three different configurations. The configuration C-D-P4 was evident in three out of five cases. All three cases displayed intense cellular migrations, in which C migrated from its ventral position toward the dorsal side, and P4 and D switched positions (Fig. 3.56). While P4 migrated over the D cell ventrally, D translocated to a more dorsal position. One specimen was found with the configuration P4-D-C, showing no cellular migrations. In one recording the configuration C-P4-D was found. After the division of EMS, C started to migrate toward the dorsal side, leading to the *Caenorhabditis elegans* configuration. For *Cephalobus cubaensis* we found three configurations: C-D-P4 (1/3), D-P4-C (1/3) and C-P4-D (1/3). In all cases migrations of the P4 and D blastomeres were observed, until the *Caenorhabditis elegans* configuration was reached.

3.1.6.8 Gastrulation

Gastrulation in *Acrobeloides butschlii*, *Acrobeloides nanus* and *Acrobeloides thornei* starts in the 26 cell stage with the inward migration of the two endodermal precursor cells Ea and Ep ingressing into the interior of the embryo (early in the 2E generation). In *Acrobeloides butschlii* and *Acrobeloides thornei* the anterior daughter Ea gastrulates first when the 4 MS descendants in front of the endodermal precursors and the germline precursor cell P4 and the D blastomere migrate towards each other. In *Acrobeloides nanus* the posterior daughter Ep gastrulates first, after the division of the 4 MS cells. Gastrulation proceeds and the 8MS cells in front of the E cells, which lie

arranged in two rows, and the germline precursor P4 cell and D cell at the posterior end migrate towards each other.

In *Cephalobus cubaensis* gastrulation starts around the 42 cell stage with the stepwise ingression of the intestinal precursors derived from the E-lineage (late in the 2E generation). At this time the two granddaughters of E lie at the ventral side of the embryo. First, the anterior cell Ea ingresses into the interior of the embryo, while the posterior cell stays at the ventral side of the embryo. At that time, 4 daughter cells of MS lie in front of the endodermal precursor cells. As gastrulation proceeds the 4 MS descendants in front of the 2 E cells and the two daughter cells of D migrate towards each other.

3.1.6.9 Bilateral symmetry

In all cephalobids the 2 daughters of AB divide into a left pair and a right pair, the anterior daughters, ABal and ABpl, are skewed into the anterior direction. Because of this shift to the anterior, bilateral symmetry does not become obvious in early embryonic development. Although the first division (MS, C and D) and the second division (E and AB) in somatic lineages separate the future left from right, the divisions occur mostly with a predominant antero-posterior orientation of the cleavage spindle, as is the case for the MS and C lineage. Since recordings were not followed until hatching, it was not possible to determine how bilateral symmetry in the juvenile body plan was achieved.

3.1.6.10 Cell-cell contacts

Cell-cell contacts in the 13 cell stage were analyzed in all recordings. Variable cell-cell contacts were marked in yellow (Fig. 3.57).

The cell-cell contacts MS-ABara and MS-alp, which induce pharyngeal potential in those cells, were found in all examined nematodes. As in *Caenorhabditis elegans*, only one member of two bilateral homologs of blastomeres come into contact with the signaling blastomere MS. Other important cell-cell contacts in the 24-cell-stage of *Caenorhabditis elegans* embryogenesis that are essential for induction have been described by and Schnabel (1995b), Moskowitz and Rothman (1996) and Priess (2005). These contacts (ABalap-ABplaa and ABplpa-MSap) were analysed in all species and found to be present.

3.1.6.11 Cleavage orientation

The cleavage orientation of the 4AB and the 8AB-cell stages was analysed for all species (Table 3.18).

In *Acrobeloides butschlii* the anterior granddaughters, ABal and ABar, divided in a more skewed direction (average of the mean division angles is 77 ± 0°) than the posterior granddaughters, ABpl and ABpr (average of the mean division angles is 37 ± 4°). In the 8 AB-cell stage cells divided mainly along the a-p axis (average of the mean division angles is 20 ±2°), with the exception of ABala, ABalp and ABara, which had a more skewed direction (average of the mean division angles is 70 ± 1°).

In *Acrobeloides nanus* the 4 AB granddaughters divided in a more skewed direction (average of the mean division angles is 71 ± 2°). In the 8 AB-cell stage cells divided mainly along the a-p axis (average of the mean division angles is 21 ±7 °), with the exception of ABala, ABalp and ABara, which had a more skewed direction (average of the mean division angles is 62 ± 7°).

In *Acrobeloides thornei* the 4 AB granddaughters divided in a more skewed direction (average of the mean division angles is 70 ± 2°). In the 8 AB-cell stage cells divided mainly along the a-p axis (average of the mean division angles is 25 ±4 °), with the exception of ABala, ABalp and ABara, which had a more skewed direction (average of the mean division angles is 64 ± 5°).

In *Cephalobus cubaensis* the anterior granddaughters, ABal and ABar, divided in a more skewed direction (average of the mean division angles is 75 ± 6°) than the posterior granddaughters, ABpl and ABpr (average of the mean division angles is 39 ± 6°). In the 8 AB-cell stage cells divided mainly along the a-p axis (average of the mean division angles is 24 ± 5 °), with the exception of ABala, ABalp and ABarp, which had a more skewed direction (average of the mean division angles is 66 ± 9°).

3.1.7 The early embryonic development within the Tylenchomorpha: family Meloidogynidae

3.1.7.1 Introduction

As a representative of this family the root-knot nematode *Meloidogyne incognita* was chosen.

3.1.7.2 Egg characteristics

The average ESI was 44 ± 4 (n = 5). Eggs of *Meloidogyne incognita* were the most elongated eggs of all studied nematodes in this thesis.

3.1.7.3 General features of embryogenesis

Meloidogyne incognita eggs show a large perivitelline space at both poles of the egg. Prior to the first cell division, there was high cytoplasmic streaming and active nuclear movement, accompanied with membrane ruffling of the single cell. The duration of this period was extremely variable, lasting less than one hour in some eggs to several days in others.

The early embryonic development of *Meloidogyne incognita* showed a fixed cleavage pattern (Fig. 3.58, Fig. 3.59). The early development of *Meloidogyne incognita* starts with a series of unequal, asynchronous cell divisions, during which a larger somatic founder cell and a smaller germline precursor cell is formed. In one embryo the first division of the *Meloidogyne incognita* zygote was unequal and resulted in the formation of an anterior somatic cell AB and a slightly smaller posterior germline precursor cell P1. In the other 2 embryos no size difference in the AB and P1 cell could be observed. Both daughter cells cleaved anterior-posteriorly, resulting in four cells in a linear pattern. Since AB cleaved prior to the second generation cleavages, the development is described as being synchronous. This linear pattern is rearranged into a rhomboidal pattern by the migration of the posterior AB daughter cell to the future dorsal side and migration of EMS to the future ventral side of the embryo. This rearrangement of cells was followed by the cleavage of the posterior P2 germline cell producing the C founder cell and the germline cell P3. At this point we observed variations in spatial patterns (Fig. 3.60). After the division of P2, P3 could either be in ventral (n=2) or dorsal position (n=3). This does not depend on the orientation of AB's cleavage spindle because two AB cells are already present when P2 divides. In the next round of cleavage the somatic AB cells divided, immediately followed by the division of the EMS cell. This resulted in the creation of

two additional founder cells, MS and E. The last founder cells were formed by the next cell division, where the germline cell P3 produced the germline cell P4 and the somatic cell D.

3.1.7.4 Division sequence

The division sequence of the first 17 cell cycles was analysed and compared to that of *Caenorhabditis elegans* (Table 3.19). In embryo 2 P4 divided before MS and E, in contrast to the 2 other recordings, where P4 divided after these cells had divided. Essential differences with *Caenorhabditis elegans* exist in the timing of germline divisions. While in *Caenorhabditis elegans* the primordial germ cell P4 is present in the 24 cell stage, P4 is already present in the 9 cell stage in *Meloidogyne incognita.*

3.1.7.5 Developmental tempo

Meloidogyne incognita is characterized by an extreme slow embryonic development compared to the other nematodes studied. The development from first cell cleavage to hatching took almost 3 weeks in *Meloidogyne incognita* at room temperature, while looking at the relative developmental tempo, expressed as the time between the division of the P1 blastomere and the division of the endodermal precursor cell E, *Meloidogyne incognita* develops 64 times slower than *Caenorhabditis elegans*.

The mean cell cycle length in the AB lineage was compared for 4 cycles in all 3 recordings of *Meloidogyne incognita* (Fig. 3.61). In all recordings the same pattern was observed: the mean cell cycle length extended and then became shorter. However differences are found concerning which cell stage has the longest cell cycle. In 2/3 embryos the longest cell cycle was found at the 4AB cell stage whereas in one embryo this was at the 8AB stage. The embryos with a maximum cell length at 4AB had general longer cell cycles and developed slower.

Also the lengths of early cell cycles in the other lineages were studied (Fig.3.62). After birth, the descendants of each founder cell divide with characteristic periods. The division rate is proportional to the time of the first division of the founder cell. The P1 blastomere, which divided firstly, divides the fastest and the C lineage, which divided lastly, divides the slowest.

In general, the length of division rounds, that is the time between the first and the last division of each division round increased with developmental time, although one exception to this was observed. In one recording the division round of 8AB is smaller than that of 4AB.

Intraspecific variation could be observed. In recording 1 all lineages developed faster than in recording 2, while the embryo in this recording developed faster than recording 3.

3.1.7.6 Configuration of the posterior cells

We found variations in spatial patterns in the 5-cell stage (Fig. 3.60). As mentioned above, after the division of P2, P3 could either be in ventral (n=2) or dorsal position (n=3). In embryos with P3 in ventral position, the division of P3 resulted in a dorsal D cell and a ventral P4 cell, leading to the configuration E-P4-D-C (n=2) as described for *Caenorhabditis elegans*. Alternatively, in embryos with P3 in dorsal position the cleavage polarity of P3 was reversed, leading to the configuration E-C-D-P4 (n=3). In this species contact between germline and the endodermal progenitor is restored when C started to migrate more dorsally and P4 and D switch place, until the configuration P4-D-C is reached. For a detailed discussion on this matter, we refer to chapter 4.

3.1.7.7 Gastrulation

In *Meloidogyne incognita* gastrulation starts around 131 hours, in the 26-cell stage. Like in *Caenorhabditis elegans*, the two daughter cells of the E cell are translocated from the ventral side to the centre of the embryo. The posterior endodermal precursor cell Ep migrates inwards firstly in between the four MS granddaughters MSaa, MSap, MSpa and MSpp, followed by its anterior sister cell, after which they divide left–right. Tracking individual cells beyond this stage (48 cells) was difficult because heavy granulation of the different cells obscured details.

3.1.7.8 Bilateral symmetry

In *Meloidogyne incognita* at the second division round of AB into a left pair and a right pair, the anterior daughters, ABal and ABpl, are skewed into the anterior direction. Because of this shift to the anterior, bilateral symmetry does not become obvious in early embryonic development. Since recordings could not be followed until the end, it was not possible to determine how bilateral symmetry in the juvenile body plan was achieved.

3.1.7.9 Cell-cell contacts

Cell-cell contacts in the 8AB cell stage were analyzed for 3 recordings for all species. Variable cell-cell contacts were marked in yellow (Fig. 3.63).

The cell-cell contacts MS-ABara and MS-alp, which induce pharyngeal potential in those cells in the *Caenorhabditis elegans* embryo, were found in *Meloidogyne incognita*. As in *Caenorhabditis elegans*, only one member of two bilateral homologs of blastomeres come into contact with the signaling blastomere MS.

3.1.7.10 Cleavage orientation

The cleavage orientation of the AB cells up to the 16 AB-cell stages could not be determined since eggs were too dark to follow the daughter cells with great precision after the division of 16AB.

3.2 Discussion

Some characteristics of early embryonic development were valuable to infer phylogenetic relationships, because variations existed in two or a few distinct states that can be unequivocally separated from each other and no intraspecific variation was observed. These characters include the division sequence of the first three divisions, the occurrence of an asynchronous versus synchronous development, the spatial configuration of the embryo in the 4-cell stage and the 8AB stage and the spatial configuration of the posterior cells in the embryo. The evolution of these parameters will be reconstructed on a molecular tree or used to reconstruct a phylogeny and these results will be further discussed in chapter 4. Other characteristics of early embryonic development were not coded into a data-matrix because of intraspecific variation or because the data could not be coded unambiguously into distinct characters states (e.g. division sequence of the first 10 divisions). These characters were excluded from the phylogenetic analysis and will be discussed here.

3.2.1 Remark on the nomenclature used

The cells are named according to the nomenclature of Sulston and Horvitz (1977) and Deppe *et al*. (1978) and adapted by Sulston *et al.* (1983). This nomenclature was established, based on the divisions of cells in the model organism *Caenorhabditis elegans*. However, divisions do not always occur in a similar way in other nematodes and hence sometimes difficulties arise when using this nomenclature. For instance, in *Caenorhabditis elegans* ABal and ABar divide mainly along the anterior-posterior axis and ABala and ABara are clearly positioned more anteriorly than their sister cells ABalp and ABarp. Although the division occurs mainly along the a-p axis, a small dorsoventral component is present: ABala is positioned more dorsally from its sister ABalp, and ABara is positioned more ventrally from its sister cell ABarp. However, in *Teratorhabditis palmarum*, the division of ABal and ABar is orientated mainly along the dorsoventral axis, with only a small a-p component. If we use the *Caenorhabditis elegans* nomenclature, we would have to name the most anterior cells ABala, and ABara respectively; but these cells are positioned ventrally, respectively dorsally from their sister cell, which is the opposite of the *Caenorhabditis elegans* configuration. The same variability was also observed within one species (e.g. *Pristionchus pacificus*). Hence, if we use this nomenclature very strictly, we would find a very different spatial configuration of blastomeres for these two nematodes. However, if we appoint the most dorsal cell ABala (in the division of ABal) and the most ventral cell ABara (in the

division of ABar) we observe that the same cells occupy the same places in the embryo during further development. Therefore, we can use the *Caenorhabditis elegans* nomenclature for other nematodes, although always validating that homologous cells are involved.

3.2.2 The influence of temperature on the early embryonic development

The influence of temperature (15°C, 20°C and 25°C) on early embryonic development was studied in *Pristionchus pacificus* (Neodiplogasteridae). The only observed difference between the three recordings, was the developmental tempo. Embryos recorded at 15°C developed almost twice as slow compared to embryos developing at 25°C. The same influence can be observed for cell cycle rhythms: in embryos developing at 25°C an overall shorter mean cell cycle length in AB was observed compared to embryos developing at 20°C or 15°C. In recordings of *Caenorhabditis elegans*, development at 20°C was 1.7 times slower than development at 25°C, based on early development. Based on total embryogenesis Schnabel *et al.* (1997) mentioned that *Caenorhabditis elegans* develops 1.2 times slower at 20°C than at 25°C.

Vancoppenolle *et al.* (1999) studied the generation times of 11 species belonging to the family Rhabditidae at 3 different temperatures (18, 25 and 30°C) and found that temperature greatly influences the generation time. Most species did not survive at 30°C and, with the exception of *Teratorhabditis* sp., all species developed faster at 25 than at 18°C. They found that the studied nematodes belonging to Cephalobidae and Panagrolaimidae prefer higher temperatures and reach their optimal generation time at 30°C.

Other authors have studied the influence of temperature on several other nematodes. Shafquat *et al.* (1991) showed that embryos of *Dorylaimus stagnalis* did not hatch at 5 and 10°C, while the time until hatching was 24 hours at 40°C. Hasegawa *et al.* (2004) showed that in the pinewood nematode *Bursaphelenchus xylophilus*, the time to establish 46 cells was heavily dependent on temperature. Although early embryonic development was much faster at 35°C, compared to 30, 25 and 20°C, embryos hatched with a lower frequency at this temperature.

Besides developmental tempo, all the other examined parameters were found to be similar at different temperatures (division sequence, time of establishment of the P4 cell, gastrulation, cell-cell contacts, division angles). Thus, with the exception of division

rate, there was no influence of temperature on all the studied parameters. Schnabel *et al.* (1997) showed the absence of temperature influence (20°C versus 25°C) on the variability of cell positions as well.

3.2.3 The early embryonic developmental tempo

Since recordings were not done at each specific optimal temperature, no absolute comparisons of developmental timing can be established. Still, our comparative analysis of nematode development has revealed considerable variations in developmental tempo. *Meloidogyne incognita* is characterized by an extremely slow development, compared to *Caenorhabditis elegans*. Considering the time from the first cell cleavage until hatching *Meloidogyne incognita* develops at least 35 times slower compared to *Caenorhabditis elegans*. For the early embryonic events this difference is even higher: here, *Meloidogyne incognita* develops 64 times slower than *Caenorhabditis elegans*. Similarly, the completion of a cell cycle during early embryogenesis requires several hours in *Meloidogyne incognita*, whereas in *Caenorhabditis elegans* cells divide approximately every 10 minutes in the early stages. Most of the species belonging to the family Rhabditidae develop fast at 20°C (developmental tempo between 0.7 and 5), in contrast to species within Cephalobidae. However, as demonstrated by Vancoppenolle *et al.* (1999) the latter family prefers higher temperatures (30°C).

Nevertheless all these nematodes, with the exception of *Meloidogyne incognita*, develop much faster than nematodes found in the most basal clades. The marine nematode *Enoplus brevis* (clade 1) is characterized by a very slow embryonic development: at 25°C the time until hatching is 16-20 days (Voronov and Panchin, 1998), compared to 800 min for *Caenorhabditis elegans* (Sulson *et al.*, 1983). Another studied member of the Enoplida develops even slower: in *Pontonema vulgare* the time until hatching is 30 days at 16°C (Voronov, 1999). These nematodes are found in a stable marine habitat. Schierenberg (2001) formulated that this slow development was probably necessary to preserve aspects of regulative development. Associated with the colonization of freshwater and terrestrial habitats, nematodes possibly needed to react to the more rapidly changing environment and thus nematodes that developed faster, or nematodes that are more tolerant to changing environmental conditions, have a selective advantage (Schierenberg, 2001). Houthoofd *et al*. (2003) mapped the generation time (time between the first egg laying of the parental generation and the first egg laying of the F1 generation) of 31 nematode species onto the molecular phylogeny of Blaxter *et al*. (1998) and found that the speed of development seemed to have increased during the

course of evolution. So based on their data, a relationship appears between developmental tempo and phylogenetic position. Nevertheless, also very slow developing nematodes are found in clade 12 that comprise terrestrial nematodes. In clade 12, for the plant parasitic nematode *Meloidogyne incognita*, the time from the division of the zygote until hatching is 18 days at room temperature (RT). However not all plant parasitic nematodes develop this slowly: for *Tylenchorhynchus claytoni* the time from the first division of the zygote until hatching is 5.6 days (Wang, 1971). In other clades more slowly developing nematodes were found as well (e.g. *Parascaris equorum* (clade 8) with an embryonic development of 1-2 weeks at RT). So it appears that the speed of development has changed independently in several taxa.

These observed differences in developmental tempo are reflected in other examined parameters as well, such as the observed patterns of cell cycle rhythms and the moment of establishment of the germline precursor cell (numbers of cells present). These characteristics are more valuable for a comparative analysis, since they are not directly influenced by temperature.

3.2.4 The early embryonic development of nematodes displays both interspecific and intraspecific variation

Comparing the embryonic development of nematodes belonging to different clades of the molecular tree shows that prominent differences exist between nematodes. Interspecific variations include differences in cleavage order of the blastomeres, spatial configuration of the early embryo, cell cycle rhythms, establishment of bilateral symmetry and the process of gastrulation. However, also intraspecific variation was observed for several species in the following parameters: division sequence of the early blastomeres, cell cycle rhythms and the spatial configuration in the early embryo (both deduced from cell-cell contacts in the 8AB stage and division angles in the 4AB and 8AB stage).

3.2.4.1 Intraspecific variation

Comparison of the **division sequence** in different recordings of one species revealed the remarkable variability in cleavage timing. In *Halicephalobus gingivalis* intraspecific variation is already observed from the 5-cell stage onwards. In most other nematodes, especially those that develop fast, intraspecific variation was observed from the 13 cell stage onwards and this variation was even more pronounced in later divisions. Our data show that a change in the order of cell divisions is compatible with development

into a hatching juvenile and that a very precise timing of blastomeres is not a prerequisite for normal development.

Minor variations in division sequence were previously observed in other studies, but never as early as in *Halicephalobus gingivalis*. Spieler and Schierenberg (1995) studied the development of the alternating free-living and parasitic generations of the nematode *Rhabdias bufonis* (Rhabdiasidae). This nematode is an anuran lung parasite with a heterogonic life cycle, characterized by the alternation of gonochoristic (free-living) and hermaphroditic (parasitic at late larval and adult stages) generations. Both in the lineage of the free-living and the parasitic embryo variations were observed in the early cleavages (from the 13-cell stage onwards). Also minor variations in division sequence after the 26-cell stage were reported for *Acrobeloides nanus* (Lahl *et al*., 2003). The division sequence of several *Rhabditis species* also displayed minor variations (Laugsch and Schierenberg, 2004), as did *Pellioditis marina* (15-cell stage, Houthoofd *et al*., 2003). Also Sulston *et al.* (1983) previously mentioned a variation in the timing of cell divisions (10%) during the early embryogenesis of *Caenorhabditis elegans* (and 2% in late embryogenesis).

In addition, the lengths of the division rounds within the sublineage of an established founder cell seemed to be variable and this variability increased with developmental time. For instance, in one recording of *Procephalobus* sp. descendants of ABa develop at a different rate than those of ABp, leading to an extremely long division round for 4AB. Yet, these alterations in cell cycle length appear to have no impact on the developing nematode. Junkersdorf and Schierenberg (1992) found that slowing down of cell cycle periods in certain cell lineages and thus a change in the normal order of cell divisions, still results into a hatching juvenile. Their results demonstrate that a strict timing of cell divisions in early nematode embryogenesis is not a prerequisite for normal development. Lahl *et al*. (2003) irradiated the endodermal precursor cell E of *Caenorhabditis elegans* embryos with low doses, resulting in a delayed division and hence in an altered division sequence. In 50 percent of the cases a moving larva was observed, suggesting that alterations in the division order are tolerated in *Caenorhabditis elegans* with its essential invariant cell lineage.

In our analysis of **cell cycle rhythms**, we have found two species showing intraspecific variation in this parameter. In *Meloidogyne incognita,* the first recorded embryo has the longest cell cycle in the 8AB stage, while the other two recorded embryos have the longest cell cycle in the 4AB stage. In *Plectus aquatilis,* embryo 1 and 2 have the longest cell cycle in the 8AB stage, while in embryo 3 cell cycles in the 4AB stage

are as long as in the 8AB stage. Possibly these eggs did not receive the same amount of maternal supplies, resulting in different cell cycle rhythms. It is well known that the hatching time of *Meloidogyne incognita* is extremely variable (Perry and Wesemael, 2008). By increasing variation in embryonic development, the nematode increases the chance that some of its offspring will hatch at the time when a suitable host plant is in the neighbourhood. Doing so, the nematode increases its success as a parasite.

The **spatial configuration** of the embryo showed intraspecific variation for all species. **Cell-cell contacts** were analyzed in a large number of individuals belonging to two species: *Caenorhabditis elegans* (n=8) and *Pristionchus pacificus* (n=12). In *Pristionchus pacificus* seven out of 66 possible cell-cell contacts in the 12-cell stage (8AB cell stage) were found to be variable and three of these variable contacts were also variable in *Caenorhabditis elegans*. As in *Caenorhabditis elegans*, cell-cell contacts between AB and P1 descendants also showed variability, contacts ABpla-MS and ABpra-E being found in three of the 12 embryos. For all the other examined species at least 3 individuals (with the exception of *Teratorhabditis palmarum*, *Rhabditophanes* sp. and *Acrobeloides nanus*) were studied and for none of them 66 identical cell-cell contacts were observed in the three recordings, showing that the spatial configuration is not identical per species. The regulation of **division angles** appeared to be not that strict in all examined nematodes either, since intraspecific variation was observed for every species. Standard deviations greater than 20° were observed for several cells in different species, both at the division of 4AB and the 8AB cell stage. In the 4AB stage the division of ABpr was the most variable. In the 8AB stage, the blastomeres ABpla and ABplp showed the most variation in division angle (4 out of 19 species had a standard deviation of at least 20°). The largest variation was observed in *Cephalobus cubaensis* in the division of ABara (SD = 38).

Using the 4D system, Schnabel *et al.* (1997) studied the natural variability of cleavages in *Caenorhabditis elegans*. They followed the descendants of the AB blastomeres in the 12-cell stage until the premorphogenetic stage. The AB descendants established discrete regions in the embryo and extensive cell migrations were necessary to establish these regions. They also examined the environment of cells, which later produce the hypodermal seam cells at the 50-, 100- and 400- cell stage. Striking differences were found at the 50- and 100- cell stage; however in the 400- cell stage the environment of these cells was identical in the 3 examined embryos. It therefore appears that embryos have the capability of assembling a very precise arrangement of cells in the premorphogenetic stage from variable earlier stages. They suggested that cells that

acquire variable positions during embryogenesis (partly due to the variability of cleavage timing) are later tied together by a sorting process, a new mechanism of pattern formation, which they called “cell focusing” (Bischoff and Schnabel, 2006b; Schnabel *et al*., 2006). The reason why *Caenorhabditis elegans* has an invariant lineage, despite this regionalisation, is because inductions occur on a small number of cells in the early embryo, in contrast to other organisms such as *Drosophila* or *Xenopus* where inductions occur on a large group of cells, inducing a natural variability and hence precluding an invariant lineage (Schnabel *et al.*, 1997).

3.2.4.2 Interspecific variation

Variability in cell cycle rhythms

For all nematodes studied the pattern of early cell cycle lengths in the AB lineage was examined. Four different patterns were observed (Fig. 3.64). The **first pattern** is that of *Caenorhabditis elegans*, where cell cycles gradually increase in length. Laugsch and Schierenberg (2004) described variations in several species and suggested that this may be caused by a differential supply of maternal gene products. In *Caenorhabditis elegans* the increase in cell cycle length is correlated with the diminishing amounts of maternal gene products. It is known that in *Caenorhabditis elegans*, where cell cycles of 12-20 min are found, early embryogenesis is heavily dependent on maternal gene products synthesised during oogenesis (Edgar *et al*., 1994; Bowerman, 1998). The *Caenorhabditis elegans* pattern was also observed in *Caenorhabditis remanei*, *Pelodera strongyloides* and *Teratorhabditis palmarum.*

This pattern is in contrast to the **second pattern** (*Acrobeloides nanus)*, which has longer cell cycles decreasing in time. Since this nematode receives less maternal material, at first this nematode has a slow developmental tempo, but when newly zygotic gene products become available, an increase in developmental tempo is observed (Wiegner and Schierenberg, 1999). This *Acrobeloides nanus* pattern was observed in all members of the family Cephalobidae (*Cephalobus cubaensis*, *Acrobeloides thornei* and *Acrobeloides butschlii*), but also in one species belonging to Rhabditidae (*Mesorhabditis longespiculosa*) and in one species within the Panagrolaimidae (*Panagrolaimus detritophagus*).

A **third pattern** is found to be an intermediate between these two extremes. Laugsch and Schierenberg (2004) found species such as *Rhabditis belari* and *Rhabditis dolichura*, where the development first slows down and then accelerates, presumably

because maternal supply is decreasing and zygotic supply is increasing. An extreme case was found in *Rhabditis dolichura*, where there is a cleavage pause during embryonic development, because zygotic transcription has not started before maternal supplies get depleted (Laugsch and Schierenberg, 2004). The *Rhabditis belari* pattern was also observed in *Mesorhabditis miotki*, *Oscheius dolichuroides*, *Pellioditis marina*, *Plectus aquatilis*, *Meloidogyne incognita* and *Procephalobus* sp. The *Rhabditis dolichura* pattern was observed in *Pristionchus pacificus*, *Panagrellus redivivus* and *Panagrolaimus rigidus*. In *P. pacificus* this peak occurred one cell cycle later than in *Mesorhabditis miotki*, *Oscheius dolichuroides*, *Pellioditis marina*, *Procephalobus* sp., *Panagrellus redivivus* and *Panagrolaimus rigidus* (8AB instead of 4AB), indicating that there is probably a larger amount of maternal supplies present in *Pristionchus pacificus*. In two nematodes (*Plectus aquatilis* and *Meloidogyne incognita*) intraspecific variation in the AB generation, at which this local optimum (4AB or 8AB) occurred, was observed. This suggests that not all embryos receive the same amount of maternal gene products.

A **fourth pattern** that is characterised by a constant cell cycle length, was found in *Rhabditella axei* and *Halicephalobus gingivalis*. It is likely that zygotic gene products become available just in time to compensate for the depletion of the maternal gene products.

Rhabditophanes sp. shows a mix of several patterns. First, the mean cell cycle length shortens until the 4AB cell stage and subsequently becomes longer with a peak at the 8AB cell stage. After the 8AB cell stage the cell cycles show a constant length.

To determine the exact contribution of maternal pools to early embryonic development, zygotic transcription can be blocked with α-amanitin in the early 1-4 cell embryo. Under these conditions *Caenorhabditis elegans* develops until the 120-150 cell stage because a lot of maternal products are present (Edgar *et al*., 1994; Wiegner and Schierenberg, 1998), while the cephalobid *Acrobeloides nanus* arrests in the 5-cell stage, indicating that development at this stage is already dependent on zygotic gene expression (Wiegner and Schierenberg, 1998).

These four patterns do not follow unequivocally the phylogenetic diversification since the four different patterns were found both in the family Panagrolaimidae and the family Rhabditidae. Only the family Cephalobidae appears to be characterized by the *Acrobeloides nanus* pattern. Apparently the observed patterns are associated with the developmental tempo (Fig. 3.65).

Differences in developmental tempo between the four observed patterns were analyzed using a non-parametric Kruskal-Wallis test (Table 3.20). Subsequently, post hoc comparisons between each pair of patterns were done using a non-parametric Mann-Whitney test and values were adjusted using a sequential Bonferoni method (values shown between brackets) (see materials and methods).

Significant differences in developmental tempo, were recorded between pattern 1 (*Caenorhabditis elegans* pattern) and pattern 3 (*Rhabditis belari* pattern) and between pattern 1 (*Caenorhabditis elegans* pattern) and pattern 2 (*Acrobeloides nanus* pattern). When Bonferoni correction was not included, also significant differences between pattern 2 (*Acrobeloides nanus* pattern) and pattern 3 (*Rhabditis belari* pattern) were observed. Thus, the patterns 1, 2 and 3 are apparently associated with developmental tempo.

Variability in early division sequence

Analysis of the division sequence of early blastomeres in different species shows that the order of somatic cell divisions is very similar, but the pace of somatic cell division versus the pace of germline cell divisions varies considerably. As a result, the time of establishment of the germline precursor cell P4 varies between different species. As a measurement of the time at which the P4 cell becomes established, the number of cells present at that time could be used. Since this cell stage is variable among nematodes this would be a potential phylogenetic marker. In *Prionchulus punctatus* (clade 2) the P4 cell divides in two unequal cells, suggesting that one is a somatic cell and the other one a primordial germ cell, which is called P5 (= the first cell that will give rise exclusively to germ cells by clonal mitotic divisions) (W. Houthoofd, pers. comm.). Data for nematodes belonging to clades 3 and 4 are not available. Establishment of the P4 cell at a very early cell stage (P4 cell present in the 5 or 6-cell stage or before) was found in all species of Cephalobidae. Presence of the P4 cell in the 7-, 8- or 9- cell stage was observed for *Axonolaimus paraspinosus* (clade 5), based on drawings of Malakhov (1994), in three species in Rhabditidae (clade 9), one species in Diploscapteridae (clade 9), one species in Aphelenchidae (clade 10) , four species of Panagrolaimidae (clade 10) and one species within Aphelenchoididae (clade 12). Presence of the germline precursor cell at 13 cell stage or later was observed in clade 2, clade 6, clade 7, clade 8, clade 9 and 10. However, our data show that intraspecific variation occurs in several nematodes (*Plectus aquatilis, Caenorhabditis elegans, Caenorhabditis remanei, Pellioditis marina, Teratorhabditis palmarum, Mesorhabditis longespiculosa and Rhabditophanes sp.*). Moreover there is the problem of homology assessment: two nematodes with a P4 cell present in the 12-cell stage do not necessarily have the same cellular composition. In conclusion, this parameter

expressed as number of cells present when P4 is established, cannot be used to infer phylogenetic information.

Nevertheless, Dolinski *et al.* (2001) mapped this parameter on a molecular phylogeny, by subdividing their data into two groups: nematodes with an early and nematodes with a late establishment of the P4 cell. Doing so, the problem of homology assessment is avoided. Early establishment was evaluated by the 6^{th} cleavage (the 7-cell stage or earlier, leading to the presence of the P4 cell in the 8-cell stage or before); versus postponement of P4 until a later cleavage (the 9-cell stage or later, leading to the presence of the P4 cell in the 10-cell stage or later). However, some of their data proved to be different from our results. Our data on *Meloidogyne incognita* show that the P4 cell was established by the 7^{th} cleavage, leading to the presence of the P4 cell in the 9 cell stage. A time gap of 16h, 17h and 20h, respectively for embryo 1, 2 and 3, between the division of EMS and P3, was observed. Thus, in none of the recordings, a simultaneous division of EMS and P3 was observed. *Meloidogyne incognita* is thus characterized by a late establishment of the P4 cell, instead of an early one. In two out of three recordings of *Teratorhabditis palmarum* the P4 cell was established by the 6^{th} cleavage (in the third recording by the 7^{th} cleavage), resulting in the presence of P4 in the 8-or 9-cell stage. Therefore both early and late establishment were observed within one species. Lahl *et al.* (2003) showed that in *Teratocephalus lirellus* the P4 cell was established by the 8^{th} cleavage, corresponding to the presence of the P4 cell in the 13-cell stage. According to the definition of Dolinski *et al.* (2001), *Teratocephalus lirellus* is therefore characterized by a late establishment. Lahl *et al.* (2007) showed that in *Diploscapter coronatus* the P4 cell is established by the 6^{th} cleavage, corresponding to the presence of P4 in the 8-cell stage. This corresponds to an early establishment instead of late, as suggested by Dolinski *et al.* (2001). Furthermore, we fail to see the rationale to appoint the 6^{th} cleavage as the distinction between early and late development. Our data show that they are continuous and there is no clear gap between two groups. Moreover, further analysis demonstrated that this parameter is associated with the developmental tempo of the embryo.

A general linear mixed model was used to examine the relationship between developmental tempo and the number of cells present when the P4 cell was established. Therefore, our data were log-transformed and the number of recordings was implemented as a random factor in the model. Degrees of freedom were estimated using the Satterthwaite's correction (see Material and methods). Considering *Meloidogyne incognita* and *Rhabditophanes* sp. as outlier, this variation is negatively associated (slope is -0.4817 ± 0.1701) with the developmental tempo ($F_{1, 58.4} = 8.02$; p=0,0063) (Fig. 3.67).

So the earlier the P4 cell is established, the more slowly the early embryonic development proceeds. This observation is in accordance with the formulated model of Skiba and Schierenberg (1992), which predicts a relative earlier separation of the germline in slow developing nematodes. It is thought that the early separation of germline from somatic cells is a necessary process to preserve germline quality (Skiba and Schierenberg, 1992). This hypothesis was based on a limited number of species. Here we find a clear association between the relative early developmental tempo and the number of cells present when the P4 cell was established, based on a much larger number of nematodes from different families, found in different clades of the phylum (Fig. 3.66).

An early establishment of the P4 cell and an asynchronous development (i.e. a delay in the development of the AB lineage), which characterizes all members of the Cephalobidae, are both examples of heterochrony. In the broadest sense, heterochrony refers to a change in the relative timing of developmental events in one species relative to an ancestral species (Smith, 2001). Haeckel first launched this term to explain exceptions to his theory of recapitulation: heterochrony is a temporal shift of the appearance of an organ relative to other organs of the same organism. (Smith, 2001). Besides series of morphological states nowadays, sequence heterochrony studies also analyze events like the onset of expression of genes (Smith, 2001).

Germ cell specification is an important issue in developmental biology, as from then on, germ cells can be distinguished from somatic cells. The timing and mechanism of this segregation imposes selective pressures on the germ cells; and hence may have important evolutionary consequences. In *Caenorhabditis elegans* the germ cell precursor cell can easily be identified very early in embryogenesis, in the 16-24 cell stage (depending on whether AB divides before P3 or not), as the specification of germ cells goes along with the localization of maternally inherited determinants, the P-granules. This is called preformation. The process in which germ cells cannot be observed until later in development and arise as a result of inductive signals from surrounding tissues is named epigenesis. Extavour and Akam (2003) reviewed data on 28 metazoan phyla and found that although preformation is seen in most model organisms (fruitfly *Drosophila melanogaster*, frog *Xenopus laevis*, zebrafish *Danio rerio*), it is rather an exception than a rule to specify germ cells in this way. For instance, preformation is seen in all Diptera, to which the fruitfly belongs, but is not representative for all insects. Similarly, preformation may be the common mechanism for all teleosts, to which the zebrafish belongs, but not necessarily for all fish. They also demonstrated that epigenetic germ cell specification may be the ancestral mechanism for the phylum Metazoa.

Variability in bilateral symmetry

Two different patterns in the establishment of bilateral symmetry were observed: a pattern that resembles that of *Caenorhabditis elegans* (displayed by all examined nematodes, except *Plectus aquatilis*) and a different pattern, found in the family Plectidae.

The *Caenorhabditis elegans* juvenile shows an overall left-right symmetry (Sulston *et al.*, 1983). This bilateral symmetry is reflected in the somatic lineages of the P1 descentants: the first division (MS, C and D) or the second division (E) separates the future left from right. However, this is not always very obvious, because some divisions occur mostly with a predominant antero-posterior orientation of the cleavage spindle (MS, C). This bilateral symmetry in the early 6-cell embryo is disturbed by the topological left-right asymmetry of the division of ABa and ABp along the left-right axis. In all nematodes, except *Mesorhabditis longespiculosa* and *Oscheius dolichuroides*, immediately after division, the left daughter cells clearly shift anteriorly, relative to the right daughter cells. In *Mesorhabditis longespiculosa* and *Oscheius dolichuroides* this shift of the left daughter cells is not so clear-cut, but before the division of the 4AB cells, the left daughters are in anterior position as is the case in all other nematodes examined. The left-right asymmetry of cell fates is set up at the 12-cell stage when an induction of MS breaks the left-right equivalence of the four anterior AB-derived blastomeres (Hutter and Schnabel, 1994; Wood, 1991). From this asymmetric early embryo, a complete symmetrical hatchling is generated stepwise in a complex pattern: contralaterally analogous cells arise from different lineages on the two sides of the embryo.

In *Plectus aquatilis* however, a strict bilateral symmetry was observed during early embryonic development. In this nematode MS and C divide into strict left and right daughter cells. Lahl *et al.* (2003) found the same strict left-right divisions in other Plectidae and called this a “strong symmetry”. The same “strong symmetry” was found in *Ascaris* by zur Strassen (1896) and Boveri (1899). This is in contrast to *Caenorhabditis elegans*, where left-right decisions are also made early but do not become obvious, because spindles in MS and C are predominantly orientated along the antero-posterior axis. This could be called “weak symmetry”.

In Plectidae a complete symmetrical configuration in the 16AB cell stage can be observed. However, this is not the result of strict left-right divisions, since different configurations, comprising cells from different mother cells can be found. In two recordings the 4 lateral cells at the anterior side of the embryo are ABala and ABalp

descendants, in two other recordings they are descendants of ABala and ABara, while in another recording they are descendants of ABpla and ABplp. This variability in the positioning of the AB blastomeres is already observed in the 6-cell stage where the left pair of AB descendants is not always placed more anterior than the right pair (1/4), and positioning seems to occur random. This is in contrast to *Caenorhabditis elegans*, where the left pair of AB descendants is always placed more anterior than the right pair during the third cleavage round, leading to different cell-cell contacts on the left and the right side and hence to fate differences in bilateral pairs of blastomeres by inductions. In plectids, it seems that cells are not specified before the 16AB cell stage and no fixed cell lineage pattern can be found. Possibly all 16AB cells are still equivalent at this stage and need induction in a later stage. In *Caenorhabditis elegans* the early AB divisions are also equal and sister cells ABa and ABp have equivalent developmental potentials, until an induction from P2 breaks this equivalence. If the positions of ABa and ABp are interchanged before this induction occurs, the embryo develops normally and hatches into a fertile worm (Priess and Thomson, 1987). Also in the 4AB cell stage the initial pair of anterior AB blastomeres on the right is equivalent to the pair on the left. If the relative left-right positions of the daughters of ABa and ABp, are switched, the embryo hatches into a larva that grows to a fertile adult with an inverted left-right axis (Wood, 1991). It would be very interesting to test at what time point cells in *Plectus aquatilis* become committed through inductions, correlated with specific cell-cell contacts. Whether the same inductions as in *Caenorhabditis elegans* also take place in *Plectus aquatilis*, remains to be analyzed by ablation experiments as done in Hutter and Schnabel (1994, 1995b). However, this will only be possible when a complete lineage is available and until then, immunostaining will be a helpful tool to explain the observed patterns. Nevertheless, we think it is highly unlikely that the same inductions as in *Caenorhabditis elegans* take place in *Plectus aquatilis*, since a variable number of AB cells contacts the MS cell. So possibly the specification of the AB lineage occurs completely different compared to *Caenorhabditis elegans*, and in a later phase of embryonic development.

Hutter and Schnabel (1994, 1995b) studied the establishment of embryonic axes in *Caenorhabditis elegans* and found that MS induces left-right asymmetry in the AB lineage in the anterior part of the embryo. They found that cell-cell contacts between MS and ABara and between MS and ABalp are needed to create differences in equivalent blastomere pairs. They found that after ablation of MS the ABara blastomere executes the ABala fate and the ABalp blastomere adopts the ABarp-fate. The major part of the ABp lineage remained symmetrical and was not affected by the ablation of MS. (Hutter and

Schnabel, 1995b). In the *Caenorhabditis elegans* embryo the physical constraint of the vitelline membrane controls the stereotypic cleavages seen in the early embryo (Schierenberg and Junkersdorf, 1992). These cleavages lead to an asymmetric arrangement of blastomeres in the 12-cell embryo, resulting in only one member each of two bilateral homologs of blastomeres coming into contact with the signaling blastomere, initiating inductions required to establish the left-right asymmetry of the embryo. However, in *Plectus aquatilis*, possibly these constraints are not present in the early stages leading to variable cleavage directions and hence to different spatial configurations, with always both members of two bilateral homolog blastomeres (ala-ara and alp-arp) coming into contact with the MS cell. Therefore, possibly in *Plectus aquatilis* a different specifying mechanism must exist where an induction from MS still takes place, but is not based on differential cell-cell contacts. Lahl *et al*. (2003) showed that *Plectus* sp., another plectid, behaved like *Caenorhabditis elegans* with respect to regulation: it has no potential to replace eliminated early blastomeres.

Variability in gastrulation

The timing of gastrulation and the number of intestinal precursors that migrate into the interior of the embryo varies considerably between different species. We refer to chapter 4 (4.5) for a detailed discussion on this matter.

Variability in cell-cell contacts

Variations in the cell division timing of early embryogenesis may result in an altered spatial arrangement of blastomeres. The cell-cell contacts in the 8AB cell stage (this is 12-or 13-cell stage, depending on whether P3 has divided or not) were assessed in nematodes belonging to the family Rhabditidae, Neodiplogasteridae, Panagrolaimidae, Alloionematidae, Cephalobidae and Meloidogynidae. These cell-cell contacts were mapped onto a phylogenetic tree and also used to generate a phylogenetic tree (see chapter 4). 42 out of 90 contacts were invariant among the examined nematodes (parsimony uninformative, see chapter 4), thus as much as 48 contacts showed variation between the analysed species. But are these differences in cell-cell contacts meaningful?

In *Caenorhabditis elegans* several cell-cell contacts are necessary to specify the fate of blastomeres. A series of four Notch mediated inductions is responsible for establishing the different fates of the 8AB blastomeres (reviewed in Priess, 2005). Notch signalling occurs when one cell, expressing the receptor, comes into contact with a neighbouring cell, expressing the ligand. The intracellular domain of the receptor then enters the nucleus, where it activates gene expression and thereby regulating its fate

(Priess, 2005). A first induction occurs in the four-cell stage. Because the Notch ligand producing cell P2 only contacts ABp and not ABa, a different fate is established in ABp, although these cells are initially equivalent (Priess and Thomson, 1987), and both express the Notch receptor (Evans *et al*., 1994). A second induction occurs in the 12-cell stage, where a signal from MS to ABalp and ABara induces pharyngeal potential in these cells (Hutter and Schnabel, 1994). Both cell-cell contacts were found in all examined nematodes. As in *Caenorhabditis elegans*, only one member of two bilateral homologs of blastomeres comes into contact with the signaling blastomere MS; except in *Rhabditophanes sp*., *Mesorhabditis miotki* and *Mesorhabditis longespiculosa*, where both members of one bilateral homolog, ABalp and ABarp, come into contact with the signaling blastomere MS. In *Teratorhabditis palmarum* MS contacts all four anterior granddaughters of AB. Possibly, in these nematodes a different specifying mechanism exists where an induction from MS is still established, but one that is not based on differential cell-cell contacts. Bischoff and Schnabel (2006b) propose a relay mechanism, where a signal is transduced from cell to cell over larger distances.

Another important induction establishes left-right asymmetry in the ABpla/pra lineage and requires cell-cell contact between the ABalap and ABplaa blastomeres in the 24-cell-stage of the *Caenorhabditis elegans* embryo (Hutter and Schnabel, 1995b). Lastly, a final induction in *Caenorhabditis elegans* by MSap concerns the production of the excretory cell by a descendant of ABplpa and requires contact between ABplpa and MSap in the 26-cell-stage (Hutter and Schnabel, 1995b). Both cell-cell contacts were present in all examined embryos (Fig. 3.68). Therefore, an analogous mechanism to specify the different fates of the AB descendants is feasible**.** However, cell ablation experiments in addition to a study of these inductions on a molecular level to identify the receptors and ligands active in this interaction, should provide more insight into this process.

Variability in the cleavage orientation in the AB lineage

In the 4AB cell stage of all the studied species a dominant division axis was not found. The two anterior granddaughters of AB divided with a division angle that was on average more than 45° relative to the a-p axis in 16 out of 19 species. In 13 out of 19 species the division of ABpl occurred with a predominantly anterio-posterior orientation (average division angle was less than 45°). For ABpr this was observed in 7 out of 19 species.

In *Caenorhabditis elegans* (n=8) we found that only the division of ABpl has a predominantly antero-posterior character (average division angle = 39 ± 5), all other AB granddaughters divide in a more oblique orientation compared to the a-p axis. However, this is in contrast to what has been described in literature. According to Hutter and Schnabel (1995a) in *Caenorhabditis elegans* the division axes of the third cleavage of the descendants of the anterior blastomere AB occur along the a-p axis, with the exception of ABar, which divides mainly along the d-v axis with only a small a-p component. According to our dataset, the division of ABar is the most perpendicular of all four granddaughters. The divisions of ABal and ABpr do not occur along the a-p axis, but oblique (68 ± 4° and 56 ± 5°). In the POP-1 study of Park and Priess (2003) the division of ABpr in wild-type embryos of *Caenorhabditis elegans* also appears to occur in a more oblique manner.

Walston *et al*. (2004) studied the division orientation of ABar in *Caenorhabditis elegans* in detail and showed that the spindle orientation, which is perpendicular to the other three AB granddaughters, depends on contact with the C blastomere. In some nematodes however, contact between ABar and C was not observed (*Mesorhabditis longespiculosa*; *Mesorhabditis miotki* and *Teratorhabditis palmarum*). In other species this contact was observed only in some recordings prior to the division of ABar (*Pristionchus pacificus* 8/12, *Caenorhabditis remanei* 1/3, *Cephalobus cubaensis* 1/2, *Panagrolaimus rigidus* 1/3, *Procephalobus* sp. 1/3), so the contribution of this pathway to the polarisation of ABar in those species remains unclear. It is possible that another mechanism, not dependent on contact with the C blastomere, is operational.

In the 8AB stage most cells divided along the a-p axis, however in a varying degree in the studied species. In 3 species (*Mesorhabditis miotki*, *Caenorhabditis remanei* and *Teratorhabditis palmarum*) all 8 AB cells divided with an average angle relative to the a-p axis which was less than 45°. In *Pristionchus pacificus*, *Rhabditella axei* and *Mesorhabditis longespiculosa* 7 out of 8 AB cells divided mainly along the a-p axis. In *Caenorhabditis elegans* (and *Procephalobus* sp., *Pellioditis marina* and *Pelodera strongyloides*) 6 of 8 AB cells (not always the same) divided along the antero-posterior axis. Our results for *Caenorhabditis elegans* are in contrast to the results of Hutter and Schnabel (1995a); they showed that the division of 8AB occurs mainly along the a-p axis in *Caenorhabditis elegans*. Our data show that this is the case for 6 out of 8 AB blastomeres, that have an average division angle of less than 45°. However, Bischoff and Schnabel (2006a) mention that AB-derived cells during early development (from 4AB-64AB) do not strictly cleave along the a-p axis, but deviate on average 45° ± 20° from the

a-p axis. Based on our 8 recordings of *Caenorhabditis elegans*, we find a deviation from the a-p axis for AB descendants (4AB-8AB) of 41 ± 23°, which corresponds to the data of Bischoff and Schnabel (2006a).

If division angles are not tightly regulated, is it possible that the shape of the egg has an influence on the division axes of the developing embryo? One could expect that in more elongated eggs more divisions would occur along the a-p axis because of constraints imposed by the vitelline membrane, while in more round eggs there would be more divisions perpendicular to the a-p axis. Indeed, in nematodes with more round eggs, such as *Rhabditophanes* sp. and *Pellioditis marina*, 3 resp. 2 blastomeres in the 8AB stage divide in a more skewed direction. However, for nematodes with more elongated eggs (ESI between 47 and 57) only for one species (*Mesorhabditis miotki*) it was observed that all 8 AB cells divide along the a-p axis. In 4 species (*Halicephalobus gingivalis, Acrobeloides nanus, Acrobeloides butschlii, Acrobeloides thornei*) at least 3 cells in the AB stage have a more oblique division. Hence, it appears that the shape of the egg has no influence on the direction of the division axes. Schierenberg and Junkersdorf (1992) already demonstrated that the complete removal of the eggshell does not interfere with successful development into a normal worm.

The importance of the precise orientation of cell division axes in embryos for partitioning segregated cytoplasmic components to particular daughter cells was illustrated by Hutter and Schnabel (1995a). They suggested a model whereby an induction from P_1 to AB in the two-cell-stage is necessary to specify the fates of the four posterior AB cells in the 12-cell-stage. It is essential that the third cleavage of AB occurs along the a-p axis so that a polarisation between posterior and anterior cell is possible. When cells divide along the d-v axis, the establishment of a graded cytoplasmic content is not possible, suggesting another mechanism to specify AB-derived blastomeres in these nematodes where a division axis perpendicular to the a-p axis was found.

Most anterior/posterior divisions result in sister cells with different fates in the early embryo. It has been suggested that cells throughout the embryo somehow recognize a common anterior/posterior axis of polarity (Way *et al*., 1994). The molecular components that play a role in establishing this a-p system are discussed in the introduction. It would be interesting to examine the levels of POP-1, LIT-1 (and other proteins involved in this pathway) in the daughter cells of blastomeres with a division axis perpendicular to the a-p axis since these proteins have a asymmetric distribution during an a-p division (e.g. POP-1 levels are high in the anterior daughter cells, while LIT-1 levels are high in posterior daughter cells).

The importance of a stereotyped cleavage pattern and hence cellular polarity in *Caenorhabditis elegans* pattern formation was questioned by Schnabel *et al.* (2006) and Bischoff and Schnabel (2006b). They demonstrated that after gastrulation, cells move extensively relative to each other before they reach their final destination. This sorting process of cells into regions, which they called “cell focusing”, is coupled to their particular cell fate and occurs before morphogenesis. According to this hypothesis, cells autonomously generate a positional value on their surface and by comparing the values of surrounding cells, cells move relative towards each other until they reach their final destination. If the cell fate is experimentally changed, cells move towards positions, which are in accordance with their new fates. By removing the eggshell and combining blastomeres *in vitro* Bischoff and Schnabel (2006b) showed that the direction of cell movement depends on local cell-cell interactions in the embryo and not on cellular polarity.

According to Schnabel *et al*. (2006) this sorting process is only active after gastrulation. However, the migrations from the C blastomere, observed in *Acrobeloides thornei* might be an example of cell sorting in a much earlier stage of embryogenesis. Here, the C blastomere rearranges its position by extensive migrations from the dorsal to the ventral side, until it is positioned in between the EMS and the P3 blastomere. However, why its position is changed for a second time (after 30 minutes, when the P4 and D rearrange), so that C is again positioned dorsally, remains unanswered. Experimental interference in this process should give insight into this matter.

Bischoff and Schnabel (2006a) postulated that in the *Caenorhabditis elegans* embryo P_2 and its descendants constitute a polarising centre in the posterior of the embryo that orientates the cell cleavages of AB-derived blastomeres along the a-p axis. This polarization depends on a MOM-2/Wnt signalling pathway. However, in at least four nematodes (*Pristionchus pacificus, Acrobeloides nanus, Acrobeloides thornei* and *Teratorhabditis palmarum* all cleavages of the 4AB stage occurred along the dorsoventral axis and an active polarizing centre seems not to be involved. In the next division round, divisions of AB blastomeres mainly occurred along the a-p axis; hence, the relay mechanism is possibly delayed for one division round.

3.3 Conclusions

Our comparative analysis of nematodes from clade 6 and clade 9-12 shows that an astonishing amount of intraspecific variation is observed for all species in the early stages of embryonic development, this for several analyzed parameters. This natural variability in the early stages of embryonic development was never thoroughly analyzed before, except in *Caenorhabditis elegans* by Schnabel *et al.* (1997), however they focused on later stages (50, 100 and 200 cells) of the premorphogenetic phase.

Comparing the embryonic development of nematodes belonging to different lineages shows that also prominent developmental differences exist between nematode taxa. However, this diversity in early embryonic development does not result in a corresponding degree of diversity in the morphology of hatched juveniles. Thus, modifications of these early developmental mechanisms have apparently only limited impact on the adult morphology. If an adaptive value is apparently lacking, what could be the grounds for this diversity in embryonic pattern formation? One explanation could be that the embryological program is constantly altered, because some of the signaling pathways, such as Wnt and Notch signaling are involved in many other aspects of development (Eisenman, 2005; Greenwald, 2005), some of which are under selection. As such, as a secondary effect the pathways active in early embryonic development are altered as well.

Another explanation is that these variations probably do not affect the fitness of the species and are the result of neutral evolution. This would explain the large amount of intraspecific variation in some parameters. Moreover, many structures are determined during postembryonic development (e.g. vulva), so selection occurs in this stage of development. However, Schierenberg (2001) opted that apparently neutral morphological changes may also affect fitness. By experimentally repositioning the blastomeres in the 4AB stage, the handedness of the embryo and the adult body plan can be altered (Wood, 1991). It has been suggested that mating success may depend on the ratio of left-handed to right-handed individuals (zur Strassen, 1951 in Schierenberg, 2001).

It is obvious that variations in the cell division timing of early embryogenesis and differences in cell division angles result in an altered spatial arrangement of blastomeres. However, despite this variability in cell-cell contacts, it seems that cell-cell contacts that are necessary for early inductions in *Caenorhabditis elegans*, both in the 12-cell stage and later in embryogenesis, showed no variability and were present in all examined nematodes. Therefore, it appears that variability is low enough for crucial cell-cell

contacts that are possibly relevant for cell fate specifications via inductions, to be maintained, while others, which are not important for inductions, are more variable and are likely to be restored later by the cell focusing mechanism, as described by Bischoff and Schnabel (2006b). However, the existence of such inductions needs to be experimentally confirmed.

Our thorough analysis of the early embryonic development of nematodes within clade 6 and clades 9-12 may be a starting point to pinpoint which groups might be most interesting to unravel developmental mechanisms of the early embryonic development, both on a molecular and an experimental level.

As such the Plectidae (clade 6) and Cephalobidae (clade 11) are excellent candidates for further investigation. Plectidae appear to have a different mechanism to specify AB cells, compared to *Caenorhabditis elegans*, since cleavages in the AB lineage do not lead to fixed cellular arrangements. Executing laser-ablation experiments in combination with immuno-histochemical analysis could provide improved insight into the formation of this complete bilateral symmetrical configuration at a very early stage.

In addition, nematodes from more basal clades appear interesting to identify new specification mechanisms. Preliminary analysis of a nematode belonging to the family Cyatholaimidae (genus *Acanthonchus*, clade 3) reveals that the specification in the AB lineage must occur in a completely different manner: a complete symmetrical configuration is observed (up to the 32AB cell stage) comparable to what was observed in our analyzed species within Plectidae. However, no intraspecific variation in cellular positioning of the AB cells was observed in this species (W. Houthoofd, pers. comm.). Laser-ablation experiments could unravel the formation of this complete bilateral symmetrical configuration at a very early stage in development.

Chapter 4 Phylogenetic analysis of early embryonic characters

Part of this chapter is accepted as:

Vangestel, S., Houthoofd, W., Bert, W., Vanholme, B., Calderón-Urrea, A., Willems, M., Artois, T. & Borgonie G. (2008). The assessment of the configuration of the posterior cells of the nematode embryo as a potential phylogenetic marker. *Russian Journal of Nematology*.

Part of this chapter is in preparation as:

Vangestel, S., Houthoofd, W., Bert, W. & Borgonie, G. (2008). The assessment of the early embryonic development of the nematode embryo as a potential phylogenetic marker (in prep).

4.1 Introduction

In the previous chapter, we presented several nematodes with an embryonic development that differs from that of *Caenorhabditis elegans*. Therefore, it is clear that the embryonic development of the model organism *Caenorhabditis elegans* is not representative for the embryonic development of all nematodes. We found large differences in developmental tempo, cell cycle rhythms and time of establishment of the P4 cell. In addition, differences in the establishment of bilateral symmetry were observed. Based on a comparative analysis of division angles in the AB lineage from the 4AB until the 8AB stage and cell-cell contacts in the 8AB stage, the spatial configuration within the embryo of *Caenorhabditis elegans* appears not to be characteristic for all nematodes. Moreover, the examined parameters in the previous chapter are all characterized by considerable intraspecific variation, consistent with neutral evolution.

On the other hand, several characters of early embryonic development, which showed no intraspecific variation, were found. All these characters are related (directly or indirectly) to the timing of developmental processes. Heterochrony is believed to be a major force in developmental evolution (Gould, 1977). The observed characters are related to two features: the timing of early cleavages and the timing of gastrulation. Other characters are the indirect consequence of these heterochronies and concern the spatial arrangement of blastomeres. In this chapter, the evolution of the following characters was

traced along the phylogram: asynchronous versus synchronous development (for definition see material and methods, 2.10.3), the division sequence of the first three divisions, the number of gastrulating cells, the spatial configuration of the 4- and the 8AB cell stage and the spatial configuration of the posterior cells in the early embryo. In general, many features of development are interdependent. However, a useful approach to interpret the evolution of these interdependent characters is to map them on phylogenetic trees, based on independent characters, such as DNA.

Furthermore, we analysed whether these characters have changed according to stochastic or deterministic processes. In case of stochastic processes (drift and absence of selection-independent constraints), we would observe unbiased changes between character states and reversals would be expected. Alternatively, when variation is the result of deterministic processes (selection or constraints), biased changes would be expected as unidirectional evolutionary trends in independent lineages.

4.2 Molecular phylogeny of the phylum Nematoda

A phylogenetic context of the analyzed organisms is a prerequisite to determine which features of early embryonic development are primitive and which features are derived (e.g., convergent or novel). We used a “super-tree approach” to generate a molecular phylogeny of the whole phylum. The presented phylogenetic tree's backbone was based on the framework presented by Holterman *et al.* (2006) and agreed with Meldal *et al.* (2006). However, *de novo* phylogenetic analyses were performed for the taxon-dense clades Rhabditomorpha (clade 9), Panagrolaimorpha-Aphelenchoidea (clade 10) and Tylenchomorpha-Cephalobomorpha (clades 11 and 12). For references to data that were obtained from literature, we refer to the Material and Methods section and to the legends of the figures. Strict consensus trees were constructed from the outcome of both Bayesian inference and LogDet-transformed distance analyses. Conflicts from both analyses and/or branches with lower than a 95 Bayesian posterior probability were presented as unresolved (see Material and methods).

Within clade 9 three major sub-clades can be distinguished (Fig. 4.1). Sub-clade 1 comprises the Neodiplogasteridae. Sub-clade 2, “Pleiorhabditis’ comprises the *Mesorhabditis*-group and *Pelodera*. Sub-clade 3 “Eurhabditis” includes the genera *Caenorhabditis*, *Diploscapter* and nematodes belonging to the *Rhabditis*-group. Because of conflicts between the two analyses, the relationships between these three sub-clades are unresolved. Within sub-clade 3 relationships between *Rhabditis terricola*, *Rhabditella*

axei, *Pellioditis marina* and *Oscheius dolichuroides* + *Rhabditis dolichura* are unresolved.

Based on our two analyses, we found the phylogenetic relationship between Rhabditomorpha and Neodiplogasteridae as unresolved. Our LogDet analysis placed Neodiplogasteridae outside Rhabditomorpha. However, this is in contradiction with Meldal *et al.* (2006), Holterman *et al.* (2006) and Kiontke *et al*. (2007) based on multiple genetic analyses. They all considered the Neodiplogasteridae to be nested within the Rhabditomorpha. In contrast, the placement of Neodiplogasteridae outside Rhabditomorpha, which agrees with classical views, is apparently supported –among others- by morphological data of the pharynx: pharyngeal structures are highly different between and highly conservative within both groups. Our subdivision of clade 9 in three sub-clades confirms the study of Kiontke *et al*., (2007). The position of *Rhabditella axei*, *Pellioditis marina* and (*Oscheius dolichuroides* + *Rhabditis dolichura*) is also unresolved in the study of Sudhaus and Fitch (2001) (Fig. 4.1).

According to our analysis, Panagrolaimidae forms a monophyletic group within clade 10 (Fig. 4.2). This is in agreement with Nadler *et al*. (2006) and Bert *et al*. (2008). The placement of Aphelenchoididae (*Bursaphelenchus xylophilus*) outside the Tylenchomorpha (clade 12) has already been described by Blaxter *et al*. (1998). However, this is probably because of long branch attraction and/or an elevated AT-content (De Ley and Blaxter, 2002; Holterman *et al*., 2006; Bert *et al*., 2008).

4.3 Coding of developmental characters and the problem of homology

In phylogenetics, recognizing homology is a 2-step process involving both similarity and congruence. In the first step, similarity is used to postulate homology (= primary homology assessment). The most important similarity criteria are topographical position, special similarity and ontogeny (Richter, 2005). Congruence tests whether such similarity may be explained by common ancestry (i.e., synapomorphy) or not (i.e., homoplasy). According to this view, homology is simply a character that defines a branch on the tree. In other words it is synonymous with synapomorphy (Hennig, 1966) and relies on tree topology (Patterson, 1988). Tree topology may be altered by adding taxa or characters, and characters considered homologous in previous analyses may come to be considered homoplastic and *vice versa* (Rieppel, 1996, 2007).

Apart from this phylogenetic definition of homology, there are alternative visions on this concept. Brigandt (2003) stated that that the concept of homology has underwent a sort of adaptive radiation, away from the original definition, stating that common evolutionary origin is a prerequisite for homologous structures. Originally, the concept of homology was used in comparative anatomy, where it referred to topological similarity, similarity in structural detail and histology and correspondence of developmental origin. In this field of biology these homologous characters provide the data for classification. However, in other biological disciplines the role of the homology concept has somewhat changed in accordance with theoretical aims and interests of these disciplines. In evolutionary developmental biology, the goal is to explain the origin and the formation of structures. In developmental explanations the focus is on considerations of corresponding causal origin, or a comparable developmental role or behaviour of structures. Some even support the idea of process homology, i.e. the homology between developmental processes (Gilbert et al, 1996, Gilbert and Bolker, 2001; Minelli 2003). Recently Heijnol *et al.* (2006) investigated the germ band in an isopod crustacean and found that, based on similarity of the formation of genealogical units in the anterior part, Ianaidacea and Isopoda have a sister group relationship. In their study they show that cell origin, gene expression and cell fate can be separated at different stages of development but converge at a later stage to produce one homologous stage. Although the studied structures are formed by cells of different origin, they homologize these structures between different taxa.

Following the logic, we have coded in current study the character ‘number of endodermal cells involved in gastrulation’ by focussing on the process of gastrulation. Thus, whether or not these gastrulating cells originate from the same cell, we code this character in every clade. As described in the introduction, in clade 1 it is unknown from which cell the endodermal precursor cell is derived, since these nematodes are characterized by symmetrical cleavages (Malakhov, 1994; 1998; Voronov and Panchin, 1998; Voronov *et al.*., 1998; Voronov, 1999, Schierenberg, 2005). In clade 2 the endodermal precursor cell is derived from the anterior cell in the two-cell stage, while in nematodes from clade 3-12, it is derived from the posterior cell in the two-cell stage (Malakhov, 1994; Schulze and Schierenberg, 2008; our data of *Prionchulus punctatus*). Thus, since the same process is observed, this character is coded in every clade. However, when coding the character ‘configuration of the posterior cells’ we argue that in clade 1 and 2 this character cannot be coded, because the cells of interest are not homologous. In this character the focus is specifically on the spatial configuration of

these cells in the early embryo, after the division of P3. Therefore, we consider this character as non-applicable in these clades. When coding non-applicable data into a data-matrix, a "-" is placed in the column. However, the program Mesquite, which reconstructs ancestral states makes no distinction between missing data caused by failure to observe (coded with a "?") and non-applicable data (coded with a "-"); Thus, a careful interpretation of the character evolution within these basal clades is warranted. The obtained data-matrix can be found in Table 4.1

4.4 Phylogenetic analysis of characters related to timing of cell divisions

4.4.1 Synchronous versus asynchronous development

Synchronous development is defined when the first four blastomeres in the early embryo are from the same second generation cleavage (ABa, ABp, EMS, P2) and asynchronous development when the first four blastomeres are of different generations (and hence all differ in size) (Dolinski *et al*., 2001).

Mapping our data clearly shows that a synchronous development is the ancestral state in the phylum and also the most prevalent state in the phylum: in most nematodes both daughter cells of P0 cleaved prior to the second generation cleavage (Fig. 4.2). An asynchronous development appears to be a synapomorphy for the family Cephalobidae (clade 11): the division of P1 is followed by the division of P2 and as a consequence the four blastomeres (AB, EMS, C and P3) are of different size. However, Dolinski *et al.* (2001) also found an asynchronous development in some species belonging to Aphelenchoididae (clade 10) and in all species belonging to Tylenchidae and Anguinidae (clade 12). Following the hypothesis of the polyphyletic state of Aphelenchoidea (= Aphelenchidae + Aphelenchoididae), an asynchronous development has arisen at least three times independently: in Aphelenchoididae (clade 10), in Cephalobidae (clade 11) and in Anguinidae + Tylenchidae (clade 12) (Fig. 4.3). An asynchronous development is a synapomorphy for Cephalobidae and for Anguinidae + Tylenchidae.

4.4.2 The division sequence of the first 3 divisions

4.4.2.1 Tracing the evolutionary history of the first 3 divisons

The order of somatic cell divisions in all examined species is very similar, but the pace of somatic cell division versus the pace of germline cell divisions varies considerably. Schierenberg (2000) already suggested that this sequence heterochrony

might be a potential phylogenetic marker. Here we analyzed the division order of the first three blastomeres (P0 not included). It should be noted that in the division sequence here described, “EMS cell” accounts for the cell that is derived from the posterior daughter cell of the zygote P0. In clade 3-12, the gut is derived from this EMS cell. In clade 2 however, the gut is derived from the anterior daughter cell of the zygote (Schulze and Schierenberg, 2008). Therefore, if in the division sequence of the first three divisions of nematodes from this clade EMS is included, EMS is not the gut producing cell, but simply the anterior daughter cell of P1.

In Fig. 4.4 the evolutionary history of the order of the first 3 divisions of blastomeres is traced along the phylogeny. Six different character states of the division sequence were observed. The ancestral state within the phylum is not unequivocal: either AB-P1-2AB or P1/AB-EMS/ABa. The sequence AB-P1-2AB was most prevalent in the phylum. The sequence AB-P1-P2 arose at least twice independently in the phylum: once in an ancestor of *Oscheius dolichuroides* + *Rhabditis dolichura* and once in *Teratocephalus lirellus*. The sequence, in which these first 2 blastomeres switch place, P1-AB-P2, has arisen three or four times independently in the phylum: either in *Meloidogyne incognita, Mesorhabditis longespiculosa* and an ancestor of *Halicephalobus gingivalis* + *Procephalobus* sp. + *Panagrolaimus rigidus* + *Panagrolaimus detritophagus* with a reversal to the sequence AB-P1-2AB in *P.* rigidus; or in *Meloidogyne incognita*, *Mesorhabditis longespiculosa*, *Panagrolaimus detritophagus* and an ancestor of *Halicephalobus gingivalis* + *Procephalobus* sp. Notice that in *Halicephalobus gingivalis* intraspecific variation was observed: in one recording the sequence P1-AB-2AB was observed, not shown in Fig. 4.4). An intermediate state, in which the first two blastomeres divide at the same time, the character state P1/AB-P2 is an autapomorphy for *Mesorhabditis miotki*. The sequence P1-P2-AB appears to be characteristic for the Cephalobomorpha (clade 11), since it was not observed in the remainder of the taxa. However, Dolinski *et al*. (2001) showed that *Aphelenchoides* sp. (clade 10) also has this early division pattern. The occurrence of the division sequence P1-P2-AB is linked to the occurrence of an asynchronous development, because in the latter case the division of the AB lineage is slowed down.

4.4.2.2 Reconstructing a phylogeny based on large division sequences

One approach to infer phylogenetic information from developmental data, is to code these sequences into a data-matrix and generate a phylogeny based on this data-matrix. This has been done in other phyla, since these division sequences are easy to determine and can help to clarify problems in systematics. Several methodologies were

developed to code cell lineage data into a data-matrix, but several important issues have to be considered when using division sequences to infer phylogenetic relationships. Developmental sequences have several properties that make their appropriate translation into characters problematic, especially when the sequence is coded in more than one character.

Guralnick and Lindberg (2001) examined the division sequence of a number of spiralian taxa and concluded that such differences were relevant to the study of spiralian phylogeny. They used a coding scheme, called *the relative timing* coding method. In this method, each column in the data-matrix corresponds to a cell (AB, P1, EMS,…) and the different character states are the number of cells present when this cell is formed. Nielsen and Meier (2002) criticized this method for several reasons. When two cells are present in the same cell stage, this does not imply that the same cellular composition of the two embryos is assured, and hence homologous stages are not considered. Moreover, the logical dependency of the characters is large using this method: if a character shifts in the division sequence, the relative position of other cells is changed as well. They concluded that these cell division patterns must be known in greater detail and that the coding methods need more refining before a possible phylogenetic signal can be identified. They also proposed an alternative method: *the delayed event* coding method where each character represents a shift of a division of each cell (e.g. AB $_{3\text{-}2}$, meaning that AB has shifted from position 3 to position 2 in the division sequence). In this way the problem of homology assessment is overruled and logical dependency of the characters is less, but still present.

The event pairing coding method was independently developed by Mabee and Trendler (1996), Smith (1996, 1997) and Velhagen (1995, 1997). In this method developmental sequences are recoded in all possible pair-wise combinations of events to form characters. The character states of each character describe the relative order of the two events in the pair. For instance, the character AB-P1 has 3 character states: 0=divides before, 1 = divide at the same time and 2 = divides after. This method was originally developed only for comparative analyses. However, when used to reconstruct phylogeny, Schulmeister and Wheeler (2004) have shown that this method leads to the establishment of impossible hypothetical ancestral sequences and as a consequence to an underestimation of the tree length, because data (the relative order of A and B and the relative order from B and C in the division sequence ABC) are treated as if they were independent.

In response to this and in contrast to all methods described before, Schulmeister and Wheeler (2004) proposed a method where the entire developmental sequence was coded as a single character. So the data-matrix contains one single character and the different division sequences are all different characters states of this character. Their method applies Search-based character optimization (Wheeler, 2003), an algorithm that uses an edit cost function, which calculates the cost to transform from one character state to another. Using this method logically impossible sequences are excluded, however, biologically impossible sequences are not taken into account (for instance the division of 2AB before AB) and should still be filtered out. We used here a similar approach in our analysis by considering the sequences as one character.

From the discussion above it is obvious that a phylogenetic analysis of larger ontogenetic sequences requires an appropriate methodological approach. In the current study, because of its variable nature in nematodes, this larger division sequence (e. g. 10 divisions instead of 3), cannot be used in this way to determine which sequences are ancestral and which are derived. In fact, for only 8 out of 21 examined species no intraspecific variation in the first 10 divisions was observed (in *Acrobeloides nanus*, *Acrobeloides thornei*, *Panagrellus redivivus*, *Panagrolaimus detritophagus*, *Mesorhabditis miotki*, *Oscheius dolichuroides*, *Pelodera strongyloides* and in *Rhabditella axei*). In all other nematodes intraspecific variation was seen before the 10^{th} division, occasionally even from the third division on: in *Halicephalobus gingivalis* a switch between P2 and 2AB was observed.

4.5 Phylogenetic analysis of characters related to timing of gastrulation: the number of endodermal precursor cells involved in gastrulation

In nematodes cells move only over a small distance (single cell diameters) during gastrulation, compared to other animals. Nevertheless, gastrulation plays an essential role in development, internalizing endodermal, mesodermal, and germline precursors. Our comparative analysis clearly shows that the timing of gastrulation and the number of intestinal precursors that migrate into the interior of the embryo varies considerably between different species.

In Fig. 4.5 the evolution of the number of endodermal precursor cells involved in gastrulation was traced along the molecular phylogeny. Four different character states were observed: gastrulation with 1, 2 and 4 cells were observed in our dataset.

Gastrulation with a large group of endodermal precursor cells was observed in *Tobrilus diversipapillatus* (clade 1, E. Schierenberg, pers. comm.).

The ancestral state in the phylum is not unequivocal: either gastrulation with 1, 2 or a large group of cells, could be characteristic for the ancestor of nematodes. Gastrulation with one endodermal precursor cell is found in all species of clade 3, 4, 5 and 6, but was also observed in one member of clade 2 (family Trichuridae; Malakhov, 1994). Lahl and Schierenberg (2003) analyzed 6 species of Plectidae and found that gastrulation with one endodermal cell was typical for all analyzed Plectidae. They named the gastrulation observed in all plectids “early” and the one seen in all other nematodes “late”. Recent analysis of one species belonging to the family Cyatholaimidae (clade 3) shows that gastrulation in this species occurs with two endodermal precursor cells (W. Houthoofd, pers. comm.). Gastrulation with 4 endodermal precursors is observed in one species in clade 2 (Malakhov, 1994) and in several species in clade 10 (Spieler and Schierenberg, 1995 and our data on two species). All other examined species in clade 10 showed an invagination of the 2 gut founder cells. However, there is variation in the order of cells that undergo gastrulation. In some nematodes with two ingressing endodermal precursor cells, the anterior endodermal precursor cell gastrulates first, while in others it is the posterior endodermal precursor cell. After both cells have reached their final position, they divide into four endodermal precursor cells.

In *Tobrilus diversipapillatus* (clade 1) gastrulation starts in the 64-cell stage with the invagination of approximately 10 cells from the anterior pole (E. Schierenberg, pers. comm.). Schierenberg (2005) found that a large blastocoel was formed, surrounded by a single layer of blastomeres. This is in contrast to all studied nematodes so far. A complex of cells that gastrulates, after the formation of a coeloblastula has also been described for the Nematomorpha (sister to Nematoda, according to ML and Bayesian analyses in Dunn *et al*., 2008) and Priapulida (sister to Nematoda + Nematomorpha, according to Bayesian analysis in Dunn *et al*., 2008) (Malakhov, 1994). Based on this feature Triplonchida should be considered as the earliest branch within the nematode tree and this type of gastrulation as the archetypical state for the phylum (Schierenberg, 2005). This agrees with Holterman *et al.* (2006) who places the Enoplida + Triplonchida at the root of the nematode tree. Other major nematode phylogenies were not able to resolve the basal radiation of the nematode tree (Blaxter *et al*., 1998; Meldal *et al*., 2006). Thus, embryological data could provide here pivotal information to resolve the nematode phylogeny.

4.6 Phylogenetic analysis of characters concerning the spatial configuration of the embryo

4.6.1 The cell-cell contacts in the 8AB cell stage

4.6.1.1 Tracing the evolutionary history of cell-cell contacts in the 8AB cell stage

Cell-cell contacts were assessed in the 8AB cell stage for all examined families (except in the family Plectidae), since it is known in *Caenorhabditis elegans* that in this stage stereotyped cell-cell contacts are a prerequisite for Notch mediated inductions, which are responsible for establishing the different fates of the 8AB blastomeres (Priess, 2005). Depending on whether P3 had divided or not, this resembles the 12-or 13- cell stage in the embryo. Our focus is on these cell-cell contacts that show no intraspecific variation, because these contacts possibly can be used to infer phylogenetic information. However, for completeness, all theoretically possible cell-cell contacts were assessed, so in total 90 characters were scored, each with the character state "1" = contact is present, "0" = contact is absent and "-" = cell-cell contact cannot be scored (Table 4.2). Character 90 is whether P3 has already divided or not. This division took place in the following species: *Meloidogyne incognita, Acrobeloides butschlii, Acrobeloides thornei, Acrobeloides nanus, Cephalobus cubaensis, Procephalobus* sp., *Panagrolaimus detritophagus, Panagrellus redivivus, Panagrolaimus rigidus, Oscheius dolichuroides, Mesorhabditis longespiculosa and Mesorhabditis miotki.* From these 90 characters 42 characters were parsimony uninformative and include both the cell-cell contacts of sister cells, such as ABala-ABalp, which are always present (character 1, 26, 47, 64, 77, 80 and 86), as the cell-cell contacts which were invariant among the examined nematodes(characters 4, 6, 7, 9, 10, 11, 12, 13, 18, 19, 20, 22, 23, 24, 25, 31, 34, 35, 36, 37, 39, 42, 44, 45, 46, 49, 53, 54, 55, 64, 70, 72, 79, 80, 81, 83 and 87). All other examined cell-cell contacts varied between species.

The parsimony reconstruction of the evolution of cell-cell contacts in the 8-AB stage showed that most cell-cell contacts are not typical for specific families. For instance, the contact between ABarp and C is found in 2 of the 5 examined species in Cephalobidae (*Acrobeloides butschlii* and *Acrobeloides thornei*), in *Rhabditophanes sp*., in 3 of 5 species in Panagrolaimidae (*Halicephalobus gingivalis*, *Panagrolaimus rigidus* and *Panagrolaimus detritophagus*) and in 5 of 9 examined species in Rhabditidae (*Rhabditella axei*, *Oscheius dolichuroides*, *Pellioditis marina*, *Caenorhabditis remanei* and *Pelodera strongyloides*) (Fig. 4.6). Another example is the contact between ABpla

and MS, which is found in *Meloidogyne incognita*, *Rhabditophanes sp*. in 3 of 5 examined species in Panagrolaimidae (*Procephalobus* sp., *Halicephalobus gingivalis* and *Panagrellus redivivus*) and in 3 of 9 examined species in Rhabditidae (*Mesorhabditis longespiculosa*, *Mesorhabditis miotki* and *Pelodera strongyloides*) (Fig. 4.7).

In all recordings of *Teratorhabditis palmarum* contacts were found that were not observed in other species: contact between ABala and MS, between ABpla and E and between ABara and E. This is due to the more anterior position of MS, compared to other nematodes. Thus, alteration of the position of one cell, results in the alteration of three cell-cell contacts, illustrating the interdependency of these characters.

Some characters were typical for only very few nematodes. For instance, the contact between ABpra and C (character 67) and between ABpra and E (character 66) was a synapomorphy for *Meloidogyne incognita* and *Mesorhabditis longespiculosa*.

As discussed in the previous chapter, some contacts showed intraspecific variability. In most cases variable contacts in one species were different from those in another species. The most variable contact is ABarp-ABplp (character 38), which is found to be variable in 7 out of 21 examined species (Fig. 4.8).

4.6.1.2 Generating a phylogeny based on cell-cell contacts in the 8AB stage

From the previous analysis we conclude that specific cell-cell contacts cannot be used to delineate taxa on the family level. But do species exhibit a combination of cell-cell contacts that are specific for them? Therefore we considered our recordings as operational taxonomical units and generated a phylogeny based on the observed cell-cell contacts in the 8AB stage. The cell-cell contacts in the family Plectidae could not be determined because AB cells seemed not to be specified in the 16AB cell stage, thus an appropriate outgroup was not available when generating this phylogeny. As a consequence no conclusions about monophyly can be deduced.

According to the resulting tree topology, the families Rhabditidae, Panagrolaimidae and Cephalobidae appear to be polyphyletic. Furthermore, the genus *Caenorhabditis* does not form a monophyletic group. Thus the tree topology obtained from cell-cell contacts is not in agreement with molecular based tree topologies.

On the species-level, recordings of *Pristionchus pacificus* and *Panagrolaimus rigidus* form polyphyletic groups, while recordings of *Caenorhabditis remanei*, *Panagrolaimus detritophagus*, *Procephalobus sp.*, *Acrobeloides thornei*, *Acrobeloides butschlii* and *Rhabditophanes* sp. form paraphyletic groups. Recordings of *Rhabditella*

axei, Oscheius dolichuroides, Panagrellus redivivus, Acrobeloides nanus, Halicephalobus gingivalis, Pelodera strongyloides, Pellioditis marina, Teratorhabditis palmarum, Mesorhabditis miotki, Mesorhabditis longespiculosa, Meloidogyne incognita, Caenorhabditis elegans and *Cephalobus cubaensis* appear to form monophyletic groups. However, since no outgroup was available, no conclusions about monophyly can be formulated (Fig. 4.9). A general remark is that variation within species is smaller than variation between species.

From both analyses (ancestral state reconstruction and *de novo* phylogeny reconstruction) we can conclude that the examined nematodes show intraspecific variability in their cell-cell contacts in the 8AB stage. In the previous chapter we have shown that, with the exception of *Plectus aquatilis,* all contacts in the 8AB stage, which are a prerequisite for Notch mediated inductions, are present in all the examined species and thus are very conservative.

4.6.2 The spatial configuration of the four-cell embryo

Four different configurations were observed in our dataset (Fig. 4.10). The rhomboidal configuration can be established in different manners. First, the anterior AB cell can position its mitotic spindle parallel to the short axis of the embryo and the posterior cell P1 parallel to the long axis of the embryo, ultimately resulting in a rhomboidal configuration. In some nematodes (*Rhabditophanes* sp., *Halicephalobus gingivalis, Panagrellus redivivus, Panagrolaimus detritophagus, Procephalobus* sp., *Rhabditella axei, Mesorhabditis miotki* and *Teratorhabditis palmarum*) these perpendicular division axes are particularly visible through the short transient T-configuration, which immediately converts into the rhomboidal configuration. In other nematodes the spindle in the AB blastomere is established parallel to the short axis of the embryo, but already at the metaphase stage the spindle is turned and becomes diagonal. The mitotic spindle of P1 is positioned parallel to this terminal position of the AB spindle. In this way a parallel cleavage is observed, as described by Ziegler (1895, in Malakhov, 1994), but in fact this is only a variant of a T-shaped cleavage: in both configurations spindles of AB and P1 are set up perpendicular to each other. In *Meloidogyne incognita,* both AB and P1 position their spindles along the long axis of the embryo producing a linear four-cell stage. This linear pattern is later rearranged into a rhomboidal pattern by the migration of the posterior AB daughter cell to the future dorsal side and migration of EMS to the future ventral side of the embryo. In some recordings of the plectids (clade 6) the spindles of the AB and the P1 blastomeres are orientated

mutually perpendicular to form a tetrahedral configuration (here, the spindles are not in the same plane as the plane of observation). Finally, a last configuration was observed in the Cephalobidae: a partially linear pattern. This partial linear arrangement refers to the linear arrangement of EMS and P2 (Dolinski *et al*., 2001).

The parsimony reconstruction of the evolution of the spatial configuration of the four-cell embryo along the phylogram (Fig. 4.11) suggests that a rhomboidal configuration is the ancestral state in the phylum. A partial linear configuration is a synapomorphy for clade 11. In clade 1 the geometric form of cleavage in nematodes is variable: either the rhomboidal or tetrahedral geometry is established in nematodes from this clade. Malakhov (1994) examined several species within clade 2-5 and found that some species formed a tetrahedral configuration. Some of these embryos undergo transformation to the rhomboidal configuration, while others do not. According to our analysis a rhomboidal configuration is the most prevalent state among nematodes from clade 7-10, only *Diploscapter coronatus* displays a linear pattern.

According to literature data a linear pattern was also observed in *Protorhabditis sp*. (clade 9) (Dolinski *et al*., 2001), *Diploscapter orientalis* (clade 9) (Tahseen *et al*., 1991), some members of the Aphelenchoididae (clade 10) (Dolinski *et al*., 2001), some members of Aphelenchidae (clade 12) (Dolinski *et al*., 2001) and in other more derived Tylenchomorpha (clade 12). (Shahina and Maqbool, 1989; Roman and Hirschmann, 1969; Clark, 1967; van Weerdt, 1960; Vovlas, 1977; Dasgupta and Raski, 1968; Fassuliotis, 1975; Sarr *et al*., 1987; Seshadri, 1965; Fassuliotis, 1962). A linear pattern in these derived Tylenchomorpha is in contrast to the configuration of the more basal Tylenchomorpha, which are characterized by a partial linear arrangement of the 4-cell stage (Anderson and Darling, 1964; Yuksel, 1960; Brun and Carol, 1970). Dolinski *et al.* (2001) suggested that this configuration of the embryos is correlated with the diversification of the Tylenchomorpha, especially the division "basal" *vs.* "derived" tylenchid nematodes. Taxa with plesiomorphic morphological characters of Tylenchomorpha (see Luc et al., 1987) include Tylenchidae and Anguinidae (referred to as Tylenchina A in Dolinski *et al.*, 2001) and the more derived groups include the Meloidogynidae, Pratylenchidae, Hoplolaimidae, Criconematoidea and the Belonolaimidae (referred to as Tylenchina B in Dolinski et al, 2001). This subdivision is substantiated with 18S rRNA based phylogenies (Bert *et al*., 2008). A partial linear configuration was also observed in some Aphelenchoididae (clade 10).

Literature data, combined with ancestral state reconstruction on family-level reveal two possibilities (Fig. 4.12). Firstly, the ancestor of clade 11+12 could be

characterized by a linear pattern. In this case a partial linear pattern has arisen independently in Anguinidae+Tylenchidae, in Cephalobidae and in some members of Aphelenchoididae. Secondly, if the ancestor of clade 11+12 is characterized by a partial linear pattern, a linear pattern has arisen multiple times in the phylum: in some species in clade 9, in the more derived Tylenchomorpha (including *Meloidogyne incognita*, clade 12), in some members of Aphelenchoididae (clade 10) and in some members of the Aphelenchidae (clade 12).

4.6.3 The spatial configuration of the posterior cells

In two clades the spatial configuration of the posterior cells after the division of P3 cannot be coded. As discussed in the introduction, the early embryonic development of nematodes from clade 1 differs from the other clades. Malakhov (1994) first showed that marine nematodes of the order *Enoplida* lack early asymmetric cleavages and a recognizable germline. Schierenberg (2005) studied another member of clade 1, belonging to the order Triplonchida, and confirmed the symmetric cleavage and the absence of distinct cell lineages. Therefore this character cannot be determined in this clade. Malakhov (1994) revealed that in *Prionchulus* sp. (Mononchidae, clade 2) the intestine is derived from the anterior instead of the posterior blastomere. Schulze and Schierenberg (2008) observed the same in *Romanomermis culicivorax* (Mermithidae). As a result, because of homology problems (cells with a similar fate and position in the embryo have a different lineal origin) this character cannot be coded in this clade.

All four theoretically possible character states (Fig. 2.2) were observed in our dataset. However, with the exception of *Diploscapter coronatus* (Lahl, 2007) all nematodes belonging to clades 3-10 had one fixed configuration, while in species from clade 11 and 12 variable configurations were observed. In nematodes with a fixed configuration, two different states were observed. The configuration P4-D-C was observed in most of the examined nematodes. Descriptions of five species within clades 3-5, observed by Malakhov (1994), suggest that also in these species a small primordial germ cell at the ventral side is in contact with the intestinal precursor, thus leading to the pattern P4-D-C. We exclude prior cell rearrangements because cell migrations are nowhere mentioned in the text. The D-P4-C configuration was found in one species within clade 10: *Halicephalobus gingivalis* (Houthoofd and Borgonie, 2007).

In contrast, nematodes belonging to clade 11 and 12 showed considerable intraspecific variation in cellular positioning and subsequent rearrangements. As discussed in the introduction, this phenomenon was already observed by Skiba and

Schierenberg (1992) for *Acrobeloides nanus* (clade 11). Also a variable configuration was observed for *Meloidogyne incognita* (clade 12), which contrasts with the observations of Goldstein *et al.* (1998), who mentioned an absence of polarity reversal for *Meloidogyne incognita*. Using experimental interference, Laugsch and Schierenberg (2004) also found variable configurations within clade 9 using experimental interference. They analyzed three *Rhabditis* species (family Rhabditidae) in this way and found that in two of them, *Rhabditis belari* (2/4) and *Rhabditis dolichura* (9/11), a reversal of polarity in P3 was seen in some cases, resulting in the configuration C-P4-D.

In all cases where the *Caenorhabditis elegans* configuration is not reached after the division of P3, subsequent cellular migrations restore the contact between the germline and the endodermal precursors, leading to the *Caenorhabditis elegans* spatial arrangement (P4-D-C) before the onset of gastrulation. This suggests that this configuration is needed for normal further development (Skiba and Schierenberg, 1992). Contact between germline and gut is a common feature in many species, and is likely to be required for normal germline development. Primordial germ cells have a similar pattern of migration in *Drosophila*, *Xenopus*, chick and mouse. In each case the primordial germ cells associate with the developing gut, from which they migrate to the gonads during organogenesis (Wylie, 1999). Possibly these migrations of the C, D and P4 cell are also a form of cell sorting, as discussed in the previous chapter. By comparing their positional value on their cell surfaces, the C, D and P4 blastomeres start migrating to their final destination. A nice experiment would be to experimentally modify the position of these blastomeres in the embryo and observe whether these cells still move to the same positions.

The parsimonious reconstruction of the evolution of the configuration of the posterior cells along the phylogram (Fig. 4.13) suggests that a fixed configuration of the posterior cells and, more precisely, the configuration P4-D-C, is the ancestral state for the phylum. From this configuration the pattern D-P4-C evolved once in *Halicephalobus gingivalis*. According to our reconstruction (Fig. 4.13), a variable configuration of the posterior cells evolved at least twice independently, once in an ancestor of clades 11 and 12 and once in *Diploscapter coronatus* (clade 9). This leads to an important question: why would this variable patterning evolve with no apparent evolutionary consequence, since the change is neutralized by compensatory migrations? The variable polarity of the germline divisions suggest that in these nematodes, a mechanism which was originally tightly regulated, is lost in an ancestor from clade 11+12 and in *Diploscapter coronatus*; and time consuming migrations to restore the needed *Caenorhabditis elegans*

configuration before gastrulation are no obstacle. This agrees with the low maternal control in *Acrobeloides nanus* (clade 11), in which early development proceeds very slowly and speeds up later when zygotic expression becomes active (Wiegner and Schierenberg, 1998). In the fast developing *Caenorhabditis elegans* however, essential decisions, including fixed division axes which assure the correct positioning of early blastomeres, have shifted to a very early phase of development in conjunction with the early segregation of maternal factors. For instance, in *Caenorhabditis elegans* the MES-1 protein, which is localized to the boundary between the germline and gut cells, is required for unequal divisions of the germline and EMS (Berkowitz and Strome, 2000; Bei *et al.*, 2002). In embryos with a mutation in this maternal-effect gene, P_0 and P_1 divide normally, but P2 and P3 partition P-granules to both daughters, leading to defects in cleavage asymmetry. The variable polarity in germline divisions in clades 11-12 and *Diploscapter coronatus* indicates that no tightly regulated molecular MES-1-like mechanism is present in these species, and that the posterior cells' ultimate position must be regulated later during the compensatory migrations. Moreover, the observed variable arrangements of blastomeres within one species suggest that certain inductive cell interactions found in *Caenorhabditis elegans* probably do not take place in these nematodes, and cell fates are specified in a different way. Wiegner and Schierenberg (1998, 1999) demonstrated that *Acrobeloides nanus* shows aspects of regulative development. Whether other members of the family *Cephalobidae* also exhibit this regulative fate specification mechanism is not clear yet. Schierenberg (2000) mentioned that other *Cephalobidae* behave similarly, but until now experimental confirmation is missing.

We have shown that *Meloidogyne incognita* and Cephalobidae both have a similar variable positioning of their posterior cells. This is in agreement with the sister relationship of the Tylenchomorpha and the Cephalobidae (Holterman *et al.*, 2006; Bert *et al.*, 2008). Other parameters typical of clades 11 and 12 were described by Goldstein *et al.* (1998), who analyzed how asymmetry is generated along the a-p axis by analyzing the presence of a cytoplasmic rearrangement in the uncleaved embryo, and whether the site of sperm entry predicts the posterior end of the embryo. They found that the mechanism, typical of *Acrobeloides sp*., is an apomorphic character, which may have arisen once in an ancestor of clades 10, 11 and 12. In addition, Dolinski *et al.* (2001) described similar early developmental characters for Cephalobidae and some Tylenchomorpha. For Cephalobidae (clade 11) and the Tylenchomorpha with ancestral morphological characters (Tylenchidae and Anguinidae) they found an asynchronous cleavage of the

early blastomeres and early establishment of the P4 cell. In contrast, typical for *Meloidogyne incognita* is a synchronous cleavage of its early blastomeres and late establishment of P4 cell (our unpublished data), similar to *Caenorhabditis elegans*. Hence, in this derived group of Tylenchomorpha early developmental characteristics were observed, which are not found in Cephalobidae.

4.7 Is the variation in early embryonic development the result of stochastic or deterministic processes?

Table 4.3 provides an overview of the examined characters and their evolutionary changes within the phylum. There is an extensive evolutionary bias in most characters: there are multiple changes to the same character state in independent lineages (e.g. P1-AB-P2 has arisen 4 times independently, the tetrahedral pattern has arisen at least 4 times independently). Reversals, however, were not observed. This suggests that the variation observed in the early embryonic development of nematodes is determined by deterministic processes (Kiontke *et al*., 2007). Both deterministic processes of selection or developmental constraints could be causal factors.

Character states, unique to a single taxon (autapomorphies) or clade (synapomorphies) are possible candidates for hypotheses regarding adaptation, while symplesiomorphies (shared primitive characters) are not. In addition, homoplasious characters are also potential candidates to define adaptations, since the multiple appearance of a character on different branches of the cladogram suggests similarity due to independent evolution rather than ancestry.

The relative amount of homoplasy can be measured using the consistency index (**CI**). This is calculated as the minimum number of steps expected given the number of character states in the data, divided by the actual number of steps. Consistency indices were calculated for the 5 characters.

Character 1 (synchronous versus asynchronous development): 1/1 =1

Character 2 (division sequence) = 5/9 = 0.55

Character 3 (number of gastrulating cells) = 3/8 =0.38

Character 4 (configuration in the four-cell stage) = 3/10 =0.3

Character 5 (configuration of the posterior cells) = 1/2 =0.5

For character five (configuration of the posterior cells) we suppose that the occurrence of a variable pattern is associated with the loss of a mechanism which was originally tightly regulated. As such, we consider two character states for this character: a fixed and a variable configuration. Based on our data set, character 2, 3 and 4 contains multiple homoplasies.

In the following we assessed a possible relation of the observed character evolutions and potential adaptive forces. We only tested the possible relation of the five characters with developmental tempo and shape of the egg for all the examined nematodes. We restricted ourselves to these two parameters, because other evident parameters such as feeding type showed no variability in the examined species or could not be determined unequivocally (ecological niche). With the exception of *Meloidogyne incognita*, all examined nematodes were bacteriovorous, hence the feeding type has no testable relation with these characters. Similarly, all examined nematodes are terrestrial nematodes. However, there are some differences concerning temperature sensitivity. Vancoppenolle *et al.* (1999) concluded that Cephalobidae and Panagrolaimidae tend to prefer higher temperatures than Rhabditidae, Diploscapteridae and Neodiplogasteridae, but no species within Tylenchomorpha were included. However, species of *Meloidogyne* are cosmopolitan, but found more frequent in areas with warm and hot climates. Thus, an equivocal relation between temperature and the analyzed characters is absent.

4.7.1 Are the analysed character states related to developmental tempo?

According to our statistical analysis (Table 4.4), there is a significant difference in developmental tempo between species with an asynchronous and a synchronous rate (character 1). For the division sequence (character 2) we found a significant difference in developmental tempo between the sequence AB-P1-2AB and P1-P2-AB. Apparently these sequence switches are related to developmental tempo. A relation between the developmental tempo and the number of endodermal cells that gastrulate (character 3) was not observed. For the configuration in the four-cell stage (character 4) we found a significant difference in developmental tempo between a rhomboidal and a partial linear configuration and the occurrence of these patterns was found to be related to the developmental tempo. For the configuration of the posterior cells we found a significant difference in developmental tempo between a variable and a fixed configuration.

However, Gittleman and Luh (1992) put forward the necessity to test for phylogenetic correlation when analysing such comparative studies. But statistical

methods that count for phylogenetic relations, such as nested analysis of covariance (Bell, 1989) cannot be implemented in this study, because of the non-parametric nature of the data. Taking into account this limitation of our statistical analysis, a careful interpretation is required.

Fig. 4.14 shows that nematodes with an asynchronous development have a slow developmental tempo. However, *Mesorhabditis longespiculosa* (Rhabditidae), which develops as slow as *Acrobeloides thornei*, is nevertheless characterized by a synchronous development. Furthermore, *Meloidogyne incognita* (clade 12), which has a synchronous rate, develops more slowly than the Cephalobidae. *Romanomermis culicivorax*, which has a fixed configuration, develops at least 20 times more slowly than *Caenorhabditis elegans* (based on total embryogenesis,Ginarte & Mijares, 1994). So we can conclude that all nematodes with an asynchronous development are slow developing nematodes, but not all slow developing nematodes have an asynchronous development. Since within Cephalobidae only slow developing species were observed, the current analysis cannot determine whether the observed pattern is linked to developmental tempo or historical determinants.

Fig. 4.15 suggests that nematodes with a division sequence AB-P1-2AB all have a fast developmental tempo. All nematodes with the division sequence P1-P2-AB are characterized by a slow developmental tempo, but *Mesorhabditis longespiculosa* shows that nematodes with a comparable developmental tempo as the Cephalobidae, can have a different division sequence (P1-AB-P2).

Fig. 4.16 suggests that nematodes with a partial linear configuration are slow developing nematodes, while nematodes with a rhomboidal configuration are fast developing nematodes. However, *Mesorhabditis longespiculosa* shows that not all nematodes with a comparable developmental tempo as the Cephalobidae have a partial linear configuration.

Fig. 4.17 suggests that nematodes with a fixed configuration of their posterior cells have a fast developmental tempo. As such, rapidly developing nematodes tend to show a strict regulation of the division axes of the germline divisions. With the exception of *Diploscapter coronatus*, all nematodes with a variable configuration are slow developing nematodes. However, not all slow developing nematodes have a fixed configuration. *Romanomermis culicivorax*, which has a fixed configuration, develop at least 20 times more slowly than *Caenorhabditis elegans* (based on total embryogenesis, Ginarte & Mijares, 1994).

Thus, a careful interpretation of the available statistical data shows that relations of the analysed character states and developmental tempo, which are supported by correlation statistics, need to be assessed with tests that account for their phylogenetic relations.

4.7.2 Are the analysed character states related to the shape of the egg?

According to our statistical analysis the shape of the egg has no relation with the occurrence of a synchronous versus asynchronous rate (character 1) (Table 4.5). For the division sequence (character 2) we found a significant difference in egg shape between the sequence AB-P1-2AB and P1-P2-AB and between AB-P1-2AB and P1-AB-P2, hence these sequences are related to the shape of the egg (Fig. 4.18). The shape of the egg appeared to have no relation with the number of endodermal cells that gastrulate (character 3). For the configuration in the four-cell stage (character 4) we found a significant difference in shape of the egg between a rhomboidal and a linear configuration. Fig. 4.19 reveals that nematodes with the most elongated eggs all have a linear configuration in the 4-cell stage embryo. Literature pictures of *Diploscapter*, *Protorhabditis*, *Belonolaimus*, *Pratylenchus*, and *Nacobbus* suggest that the occurrence of a linear pattern might be related to the shape of the egg, since all these nematodes produce elongated eggs (Dolinski *et al.*, 2001). The shape of the egg is related to the configuration of the posterior cells (character 5), since significant differences in egg shape were found between a variable and a fixed configuration. However, long nematode eggs, with an egg shape index around 40, have both variable (*Meloidogyne incognita and Diploscapter coronatus*) and fixed (*Procephalobus sp*.) configurations. More round eggs with an egg shape index around 60 also display both variable (*Cephalobus cubaensis*) and fixed (*Oscheius dolichuroides*) configurations (Fig. 4.20).

4.8 Conclusions

Many features of embryonic development are difficult to isolate as independent, since many features are linked in time and space. Therefore a useful approach to interpreting the evolution of interdependent characters is to map them on phylogenetic trees based on independent character sets, such as molecular data.

From our comparative analysis (chapter 3) we have distilled 5 characters, which are potentially useful to infer phylogenetic information. Ancestral state reconstruction of these characters onto a molecular phylogeny revealed the following synapomorphies:

1. an asynchronous development (when the first four blastomeres are of different generations) for Cephalobidae (clade 11) and Anguinidae + Tylenchidae (clade 12)
2. the division sequence P1-P2-AB for Cephalobidae (clade 11)
3. a partial linear configuration in the 4-cell stage for Cepahlobidae (clade 11) and Anguinidae + Tylenchidae (clade 12) if a linear pattern for the ancestor of clade 11+12 is assumed
4. a variable configuration of the posterior cells for clades 11+12

Our analysis revealed that especially Cephalobidae (clade 11) display features that are shared by all species within this family. In total 4 synapomorphies were found for this family: an asynchronous development, a division sequence P1-P2-AB, a partially linear arrangement in the 4-cell stage and a variable configuration of the posterior cells after the division of P3. Possibly all Cephalobidae display an additional feature that is not found in other clades, i.e. the potential of regulative development. Until now this was only demonstrated for *Acrobeloides nanus* (Wiegner and Schierenberg, 1999), but the very similar patterns of embryonic development suggest that also other nematodes from this clade may possess the potential to compensate for lost cells However, this has to be confirmed by ablation experiments.

We demonstrated that the evolution of all characters was biased and studied the relation between developmental tempo or egg shape and these 5 characters. Our dataset shows that nematodes which are characterized by an asynchronous development, the division sequence P1-P2-AB, a partial linear configuration in the four-cell stage and a variable configuration (with the exception of *Diploscapter coronatus*) are all slow developing nematodes. Further analysis on a large number of species in this clade, that account for their phylogenetic relationships, could reveal whether these features are determined by developmental tempo or by historical determinants. Our analysis, combined with data from literature further suggests that the occurrence of a linear pattern might be related to the shape of the egg, since all nematodes with a linear arrangement produce elongated eggs.

General conclusions

In order to assess the value of embryonic data in nematode phylogeny we made a comparative analysis of the early stages in the embryonic development of 21 species of nematodes, belonging to clade 6 and clades 9-12 and searched for taxon-specific characters. With the aid of 4D microscopy the early cell divisions, cell cycle rhythms, the process of gastrulation and the establishment of bilateral symmetry were analyzed. In addition, the spatial configuration of the embryo at different time points by determining cell-cell contacts and division angles, were examined. These analyses revealed that most characters of early embryonic development were not suitable to delineate taxa in the examined clades, since a large amount of intraspecific variation was observed for all species. This intraspecific variation shows that a “strict invariant” lineage, with a strict timing of cell divisions and stereotyped cell contacts in the early phase of embryonic development, is not a prerequisite to develop into a worm. Besides this intraspecific variation, coding early developmental data proved to be problematic, because of interdependency of the data, since most early developmental characters are linked in time and space. Moreover, we encountered some problems in the primary homology assessment. For instance, when coding the number of endodermal cells that gastrulate, an identical process is considered, yet the cells that do gastrulate are derived from different precursors in the embryo.

Our comparative analysis showed that the early embryonic development of two families showed prominent differences to that of *Caenorhabditis elegans.* Nematodes from clade 6 (Plectidae) appeared to have a different mechanism to specify the AB cells, compared to *Caenorhabditis elegans*. Further analysis should include laser-ablation experiments in combination with immuno-histochemical analysis to give more insight into the formation of this complete bilateral symmetrical configuration at a very early stage in development.

Ancestral state reconstruction of 5 characters (asynchronous versus synchronous development, division sequence of the first 3 divisions, number of gastrulating cells, configuration in the four cells stage and configuration of the posterior cells after the division of P3) onto a phylogenetic tree revealed 4 synapomorphies for the Cephalobidae (clade 11: an asynchronous development, a division sequence P1-P2-AB, a partially linear arrangement in the 4-cell stage and a variable configuration of the posterior cells after the division of P3. Unravelling the molecular mechanisms underpinning the establishment of these features will be an exciting future challenge.

Ancestral state reconstruction further revealed that several characters showed a biased evolution as they arose multiple times in independent lineages. Statistical tests indicate possible relationships with developmental tempo and egg shape. However, further analysis on a larger number of species in this clade and the inclusion of statistical tests that account for phylogenetic relationships, should reveal whether these features are due to directional selection or other constraints, or whether the occurrence of these features are merely due to common ancestry.

Thus, is nematode embryology valuable for nematode phylogeny? Although in the examined clades in this thesis the proportion intraspecific versus interspecific variation was relatively high, preliminary analyses of the early embryonic development of a species within clade 2 (Mermithida and Mononchida) and 3 (Chromadorida) revealed that cells in this species seem to be specified in a completely different manner than in *Caenorhabditis elegans*. Thus it is very likely that more prominent differences will be found in the more basal clades and hence possible phylogenetic markers.

Summary

Nematodes are excellent models to study early embryonic development, because – at least for many nematodes- eggs are transparent and the development from fertilized egg to hatched juvenile can be visualized directly under the light microscope. 4D-microscopy, a multi-focal plane and time-lapse recording system, allows to make recordings of developing embryos and follow each cell in time and space. By identifying cell divisions, a division pattern or cell lineage can be established and a 3D reconstruction of the embryos can be generated at all times.

In a first part (chapter 3) a comparative analysis of the early embryonic development was done on 21 nematode species belonging to clade 6 and clades 9-12 (phylogeny of Holterman *et al.*, 2006). This allowed to gain insight into the variation in embryonic development of the examined clades and to explore possible phylogenetic markers. The following parameters were analyzed for all examined species: egg characteristics, division sequence, developmental tempo, the spatial configuration of blastomeres in the embryo, the process of gastrulation, the establishment of bilateral symmetry, cell-cell contacts in the 8AB stage and cleavage orientations of the 4AB and 8AB stage.

Comparing the early embryonic development of nematodes belonging to these clades revealed prominent differences between nematodes. Variations include differences in cell cycle rhythms, cleavage order of the blastomeres, spatial configuration of the early embryo (based on cell-cell contacts and division angles), establishment of bilateral symmetry and the process of gastrulation. However, this diversity in early embryonic development does not result in a corresponding degree of diversity in the morphology of hatched juveniles. Thus, modifications of these early developmental mechanisms have apparently no impact on the adult morphology and are probably the result of neutral evolution.

Our comparative analysis revealed that most characters of early embryonic development cannot be used as phylogenetic markers, since also a large amount of intraspecific variation was observed for all species. This intraspecific variation shows that a “strict invariant” lineage, with a strict timing of cell divisions and stereotyped cell contacts in the early phase of embryonic development, is not a prerequisite to develop into a worm. Besides this intraspecific variation, coding early developmental data proved to be problematic, because of interdependency of the data, since most early

developmental characters are linked in time and space. Moreover, we encountered some problems in the primary homology assessment. For instance, when coding the number of endodermal cells that gastrulate, an identical process is considered, yet the cells that do gastrulate are derived from different precursors in the embryo.

From the comparative analysis five 5 characters, which are potentially useful to infer phylogenetic information were distilled. In a second part of this thesis (chapter 4) ancestral state reconstructions of these characters onto a molecular phylogeny revealed the following synapomorphies:

1. an asynchronous development (when the first four blastomeres are of different generations) for Cephalobidae (clade 11) and Anguinidae + Tylenchidae (clade 12)

2. the division sequence P1-P2-AB for Cephalobidae (clade 11)

3. a partial linear configuration in the 4-cell stage for clade 11 and Anguinidae + Tylenchidae (clade 12) if a linear pattern for the ancestor of clade 11+12 is assumed

4. a variable configuration of the posterior cells for clades 11+12

Some characters proved to have a biased evolution as they have arisen multiple times in independent lineages. Statistical tests indicate possible relationships with developmental speed and egg shape. In addition, our comparative analysis revealed that the time of establishment of the P4 cell appeared to be related to the developmental tempo. However, further analysis on a larger number of species and the inclusion of statistical tests that account for phylogenetic relationships should reveal whether these features are due to directional selection or other constraints, or whether the occurrence of these features is due to common ancestry.

This thorough analysis of early embryonic development of nematodes within clade 6 and clades 9-12 may be a start point to pinpoint which groups might be most interesting to unravel developmental mechanisms of the early embryonic development, both on a molecular or experimental level. As such the Plectidae (clade 6) and Cephalobidae (clade 11) are excellent candidates for further investigation. Plectidae appear to have a different mechanism to specify AB cells, compared to *Caenorhabditis elegans*, since cleavages in the AB lineage do not lead to fixed cellular arrangements.

Executing laser-ablation experiments in combination with immuno-histochemical analysis could provide improved insight into the formation of this complete bilateral symmetrical configuration at a very early stage in plectid development.

Furthermore, for Cephalobidae (clade 11) four synapomorphies were found: an asynchronous development, the division sequence P1-P2-AB, a partially linear arrangement in the 4-cell stage and a variable configuration of the posterior cells after the division of P3. Unravelling the molecular mechanisms underpinning the establishment of these features will be an exciting future challenge.

In conclusion, early embryonic development of nematodes in the examined clades showed relatively high intraspecific variation versus interspecific variation, Hence, the use of embryonic data to infer phylogenetic information was rather limited. However, preliminary analyses of the early embryonic development of species within clade 2 (Mermithida and Mononchida) and 3 (Chromadorida) reveals clearly more pronounced differences: cells in these species appear to be specified completely differently compared to *Caenorhabditis elegans*. Thus, most likely more prominent differences will be found in the more basal clades and hence possible phylogenetic markers to delineate nematode lineages, especially on order-level.

.

Samenvatting

Nematoden zijn een goed model om de vroege embryonale onwtikkeling te bestuderen, omdat, althans voor sommige nematoden, eitjes doorzichtig zijn en de ontwikkeling van embryo tot juveniele worm kan gevolgd worden met behulp van lichtmicroscopie. Met behulp van 4D microscopie, een time-lapse opname-systeem dat opnames kan maken op verschillende coupes doorheen het embryo, is het mogelijk om iedere cel in het embryo tijdens de ontwikkeling nauwgezet te volgen in ruimte en tijd en alle celdelingen vast te leggen. Zo kan de celgenealogie opgesteld worden en kan op ieder moment een driedimensionale reconstructie van het embryo gemaakt worden.

In een eerste luik (hoofdstuk 3) werd een vergelijkende analyse gedaan van de vroege embryonale ontwikkeling van 21 soorten, behorende tot clade 6 en clades 9-12 (fylogenie van Holterman *et al.*, 2006). Hierdoor kregen we een idee van de aanwezige variatie in vroege ontwikkeling, die aanwezig was in de onderzochte clades. Deze analyse gaf aan welke parameters mogelijke fylogenetische merkers zijn. De volgende parameters werden hierbij onderzocht in alle soorten: eivorm, het ontwikkelingstempo, de spatiale configuratie van het embryo, het gastrulatieproces, de vorming van bilaterale symmetrie, celcontacten in het 8AB stadium en delingshoeken van de 4AB en 8AB cellen.

Vergelijking van de vroege embryonale ontwikkeling van nematoden behorende tot deze clades toonde aan dat er opvallende verschillen in ontwikkeling tussen nematoden zijn. Er werden verschillen gevonden in celcyclus-ritme, delingsvolgorde van de blastomeren, spatiale configuratie van het vroege embryo (gebaseerd op zowel celcontacten als delingshoeken), vorming van bilaterale symmetrie en gastrulatie-proces. Deze diversiteit in vroege ontwikkelingspatronen leidt echter niet tot een diversiteit in morfologische kenmerken van de juveniele worm. Modificaties aan deze vroege ontwikkelingsmechanismen hebben blijkbaar maar een beperkte impact op de juveniele morfologie en zijn mogelijk het gevolg van neutrale evolutie.

Deze vergelijkende analyse toonde aan dat de meeste karakters van de vroege ontwikkeling van nematoden niet gebruikt kunnen worden als fylogenetische merkers, aangezien ze intraspecifieke variatie vertonen in de meeste soorten. Deze intraspecifieke variatie toont aan dat een “strict invariante” genealogie, met een stricte timing van celdelingen en stereotype celcontacten geen voorwaarde zijn om tot een worm te ontwikkelen. Naast deze intraspecifieke variatie, werd het coderen van vroege embryonale data eveneens bemoeilijkt doordat vele parameters gelinkt zijn in tijd en ruimte en moeilijk als onafhankelijke karakters kunnen beschouwd worden. Bovendien

werden er problemen ondervonden bij het opstellen van de primaire homologie. Bijvoorbeeld, bij het coderen van het aantal endodermale precursorcellen dat gastruleert, wordt hetzelfde proces van gastrulatie beschouwd, hoewel deze endodermale cellen niet afkomstig zijn van dezelfde cel in het embryo (AB of P1).

Uit de comparative analyse werden 5 karakters weerhouden , die potentieel waardevolle fylogenetische merkers zijn. In een tweede luik (hoofdstuk 4) toonde reconstructies van de ancestrale toestand op een moleculaire boom, de volgende synapomorfieën:

1. een asynchrone ontwikkeling voor de Cephalobidae (clade 11) en de Anguinidae + Tylenchidae (clade 12)

2. de delingssequentie P1-P2-AB voor de Cephalobidae (clade 11)

3. een partieel lineaire configuratie in het viercellig stadium voor Cephalobidae (clade 11) en Anguinidae + Tylenchidae (clade 12), wanneer de voorouder van clade 11+12 een lineaire configuratie zou hebben

4. een variabele configuratie van de achterste cellen van het embryo na de deling van P3, voor clades 11+12

De evolutie van sommige karakters lijkt niet random te zijn, aangezien deze meerdere keren onafhankelijk onststaan zijn. Statistische tests geven aan dat er mogelijk een verband is tussen deze karakters en het ontwikkelingstempo en de eivorm. Om met grotere zekerheid uit te maken of deze effectief het gevolg zijn van gestuurde selectie of andere ‘constraints’, of daarentegen het gevolg zijn van gemeenschappelijke voorouders, moeten tests op een groter aantal soorten uitgevoerd worden. Bovendien dienen tests ingecorporeerd te worden die rekening houden met fylogenetische verwantschappen.

Deze grondige analyse van de vroege ontwikkeling van nematoden in clade 6 en clades 9-12 is een vertrekpunt om uit te maken welke taxa de meest interessante zijn om nog ongekende ontwikkelingsmechanismen verder uit te diepen met behulp van moleculaire en experimentele analyses. Zo moeten de Plectidae (clade 6)en de Cephalobidae (clade 11) absoluut verder onderzocht worden. Plectidae lijken een ander mechanisme te bezitten om de AB cellen te specifiëren, in vergelijking met *Caenorhabditis elegans*. Bij Plectidae leiden de delingen in de AB lineage niet tot een vaste configuratie, wat doet veronderstellen dat ze nog niet gespecifieerd zijn. Laser-

ablatie experimenten, in combinatie met antilichaamkleuringen kan hier meer inzicht verschaffen in de vorming van deze compleet bilateraal symmetrische configuraties in een zeer vroeg stadium.

Voor de Cephalobidae werden 4 synapomorfieën gevonden: een asynchrone ontwikkeling, de delingssequentie P1-P2-AB, een partiëel lineaire configuratie in het viercellig stadium en een variabele configuratie van de achterste cellen na deling van P3. Het ontrafelen van de moleculaire mechanismen, die aan de basis liggen van al deze karakters, is een grote uitdaging voor toekomstig onderzoek.

Samenvattend, kunnen we stellen dat een relatief hoge verhouding intraspecifieke versus interspecifieke variatie in de onderzochte parameters van vroege embryonale ontwikkeling gevonden werd. Bijgevolg was hier het gebruik van embryologischa data als fylogenetische merker eerder beperkt. Voorlopige analyses van nematodes in clade 2 (Mermithida en Mononchida) en clade 3 (Chromadorida) tonen echter aan dat in deze nematoden cellen op een compleet andere manier gespecifieerd worden. Dus het is zeer waarschijnlijk dat in deze basale clades nog meer grote verschillen gevonden zullen worden, die gebruikt kunnen worden als fylogenetsiche merkers om op orde-niveau taxa af te bakenen.

List of publications

VANGESTEL, S., HOUTHOOFD, W., BERT, W., VANHOLME, B., CALDERÓN-URREA, A., WILLEMS, M., ARTOIS, T. & BORGONIE, G. Assessment of the configuration of the posterior cells of the nematode embryo as a potential phylogenetic marker. *Russian Journal of Nematology* (accepted).

VANGESTEL, S., HOUTHOOFD, W., BERT, W. AND BORGONIE, G. (2008). The early embryonic development of the satellite organism *Pristionchus pacificus*: differences and similarities with *Caenorhabditis elegans*. *Nematology* 10, 301-312.

HOUTHOOFD, W., WILLEMS, M., VANGESTEL, S., MERTENS, C., BERT, W. & BORGONIE, G. (2006). Different roads to form the same gut in nematodes. Evolution & Development 8, 362–369.

HOUTHOOFD, W., JACOBSEN, K., MERTENS, C., VANGESTEL, S., COOMANS A. & BORGONIE, G. (2003). Embryonic cell lineage of the marine nematode *Pellioditis marina*. *Developmental Biology* 258, 57-69.

VANGESTEL, S., HOUTHOOFD, W., BERT & BORGONIE, G. The value of early embryonic development of nematodes in phylogenetic studies. (in prep).

List of publications not directly related to this research

MEESEN, G., POFFIJN, A., VANGESTEL, S. & VAN OOSTVELDT, P. (1999). Feasibility study for the use of PADC as a radiation detector for living cell cultures. *Radiation Measurements*, 31, p471-474.

VAN OOSTVELDT, P., VANGESTEL, S., MEESEN, G., POFFIJN, A., COENE, L., SCHELFHOUT, V. & DE POTTER, C. (1999). Single cell tissue specific methods for evaluation of radiation and microgravity effects. *Mutation Research*, 430, p235-240.

BERT, W., VANGESTEL, S., HOUTHOOFD, W., VAN GANSBEKE, R. & BORGONIE, G. (2007). The somatic female gonad of Cephalobidae (Nematoda): cellular architecture and associated function. *Nematology* 9, 285-297.

References

ANDERSON, R.V. & DARLING, H. M. (1964). Embryology and reproduction of *Ditylenchus destructor* Thorne, with emphasis on gonad development. *Proceedings of the Helminthological Society of Washington* 31, 240-256.

ANDRÁSSY, I. (1976). Evolution as a basis for the systematization of nematodes. London, San Francisco & Melbourne, Pitman Publishing, pp 287.

BAUGH, L.R., HILL, A.A., CLAGGETT, J.M., HILL-HARFE, K., WEN, J.C., SLONIM, D.K., BROWN, E.L. & HUNTER, C.P. (2005). The homeodomain protein PAL-1 specifies a lineage-specific regulatory network in the *Caenorhabditis elegans* embryo. *Development* 132, 1843-1854.

BEI, Y.X., HOGAN, J., BERKOWITZ, L. A., SOTO, M., ROCHELEAU, C. E., PANG, K.M., COLLINS, J. & MELLO, C. C. (2002). SRC-1 and Wnt signaling act together to specify endoderm and to control cleavage orientation in early *Caenorhabditis elegans* embryos. *Developmental Cell* 3, 113-125.

BELL, G. (1989). A comparative method. *American Naturalist* 133, 553-571.

BERKOWITZ, L.A. & STROME, S. (2000). MES-1, a protein required for unequal divisions of the germline in early *Caenorhabditis elegans* embryos, resembles receptor tyrosine kinases and is localized to the boundary between the germline and gut cells. *Development* 127, 4419-4431.

BERT, W. & BORGONIE, G. (2006). Suborder Tylenchina. In: Eyualem, A., Andrássy I. & Traunspurger W. (Eds.) Freshwater Nematodes: Ecology and Taxonomy. Wallingford, UK, CABI Publishing, 648-695.

BERT, W., DE LEY, I., VAN DRIESSCHE, R., SEGERS, H. & DE LEY, P. (2003). *Baujardia mirabilis* gen. n., sp. n. from pitcher plants and its phylogenetic position within Panagrolaimidae (Nematoda: Rhabditida). *Nematology* 5, 405-420.

BERT, W., LELIAERT, F., VIERSTRAETE, A.R., VANFLETEREN, J.R. & BORGONIE, G. (2008). Molecular phylogeny of the Tylenchina and evolution of the female gonoduct (Nematoda: Rhabditida). *Molecular Phylogenetics and Evolution* (in press).

BERT, W., VANGESTEL, S., HOUTHOOFD, W., VAN GANSBEKE, R. & BORGONIE, G. (2007). The somatic female gonad of *Cephalobidae* (Nematoda): cellular architecture and associated function. *Nematology* 9, 285-297.

BIRD, G.W., GOODMAN, R.M. & MAI, W.F. (1968). Observations on the embryogenesis of *Trichodorus christiei* (Nematodea: Diphterophoroidea). *Canadian journal of Zoology* 46, 292-293.

BIRD, G.W. (1972). The influence of temperature on embryogenesis of Meloidogyne javanica. Journal of Nematology 4:206-213.

BIRD, A. F. & BIRD, J. (1991). *The Structure of Nematodes*. Academic Press, San Diego.

BIRD, G.W., DE LEY, P; & BIRD, J. (1993). Morphology, oviposition and embryogenesis in an Australian population of *Acrobeloides nanus. Journal of Nematology* 25, 607-615.

BISCHOFF, M. & SCHNABEL, R. (2006a). Global cell sorting is mediated by local cell-cell interactions in the *C-elegans* embryo. *Developmental Biology* 294, 432-444.

BISCHOFF, M. & SCHNABEL, R. (2006b). A posterior centre establishes and maintains polarity of the *Caenorhabditis elegans* embryo by a Wnt-dependent relay mechanism. *PLoS Biology* 4, 2262-2273.

BLAXTER, M.L., DE LEY, P., LIU, L.X., SCHELDEMAN, P., VIERSTRAETE, A., VANFLETEREN, J.R., MACKEY, L.Y., DORRIS, M., FRISSE, L.M., VIDA, J.T. & THOMAS, K. (1998). A molecular evolutionary framework for the phylum Nematoda. *Nature* 392, 71-75.

BLUNDEN, A.S., KHALIL, L.F. & WEBBON, P.M. (1987). *Halicephalobus deletrix* infection in a horse. *Equine Veterinary Journal* 19, 255-260.

BORGONIE, G., JACOBSEN, K. & COOMANS A. (2000). Embryonic lineage evolution within nematodes. *Nematology* 2, 65-69.

BOSSINGER, O. & SCHIERENBERG, E. (1992). Cell-Cell Communication in the embryo of *Caenorhabditis elegans*. *Developmental Biology* 151, 401-409.

BOSSINGER, O. & SCHIERENBERG, E. (1996a). Cell-cell communication in nematode embryos: Differences between *Cephalobus spec* and *Caenorhabditis elegans*. *Development Genes and Evolution* 206, 25-34.

BOSSINGER, O. & SCHIERENBERG, E. (1996b). The use of fluorescent marker dyes for studying intercellular communication in nematode embryos. *International Journal of Developmental Biology* 40, 431-439.

BOSSINGER, O., WIEGNER, O. & SCHIERENBERG, E. (1996). Embryonic gut differentiation in nematodes: Endocytosis of macromolecules and its experimental inhibition. *Roux's Archives of Developmental Biology* 205, 494-497.

BOVERI, T. (1887). Über die Differenzierung der Zellkerne während der Furchung des Eies von *Ascaris megalocephala. Anatomischer Anzeiger* (*Annals of Anatomy)* 2, 668-693.

BOVERI, T. (1892). Ueber die entstehung des Gegensatzes zwischen den Geschlechtszellen und den somatischen Zellen bei *Ascaris megalocephala*. Sitzungsberichte der Gesellschaft für Morphologie und Physiologie in München 8, 114-125.

BOVERI, T. (1899). Die Entwicklung von *Ascaris megalocephala* mit besonderer Rücksicht auf die Kernverhältnisse. *Festschrift für C. von Kupffer*, 383-430. Fischer, Jena.

BOVERI, T. (1910). Die Potenzen der *Ascaris*-Blastomeren bei abgeänderter Furchung. *Festschrift zum sechzigsten Geburtstag Richard Hertwigs* III, 133-213. Fischer, Jena.

BOWERMAN, B., EATON, B.A. & PRIESS, J.R. (1992). *skn-1*, a maternally expressed gene required to specify the fate of ventral blastomeres in the early *C. elegans* embryo. *Cell* 68, 1061-1075.

BOWERMAN, B., (1998). Maternal control of pattern formation in early *Caenorhabditis elegans* embryos. *Current Topics in Developmental Biology* 39, 73-117.

BRENNER, S. (1974). The genetics of *Caenorhabditis elegans*. *Genetics* 77, 71-94.

BRIGANDT, I. (2003). Homology in comparative, molecular, and evolutionary developmental biology: the radiation of a concept. *Journal of Experimental Zoology (Molecular and Developmental Evolution)* 299, 9-17.

BRUN, J. & CAYROL, J.C. (1970). Le développement embryonnaire du nematode mycophage *Ditylenchus myceliophagus* Goodey, 1958 (Nematode-Tylenchida). *Nematologica* 16, 523-531.

CAENORHABDITIS ELEGANS SEQUENCING CONSORTIUM (1998). Genome sequence of the nematode *Caenorhabditis elegans*: a platform for investigating biology. *Science* 282, 2012-2018.

CALVO, D., VICTOR, M., GAY, F., SUI, G., LUKE, M.P., DUFOURCQ, P., WEN, G., MADURO, M., ROTHMAN, J. & SHI, Y. (2001). A POP-1 repressor complex restricts inappropriate cell type-specific gene transcription during *Caenorhabditis elegans* embryogenesis. *EMBO Journal* 20, 7197-7208.

CHENG, N.N., KIRBY, C.M. & KEMPHUES K.J. (1995). Control of cleavage spindle orientation in *Caenorhabditis elegans:* The role of the genes *par-2* and *par-3. Genetics* 139, 549-559.

CHITWOOD, B.G. (1937). A revised classification of the Nematoda. In *Papers on helminthology, 30 year jubileum K.J. Skrjabin,* edited by Anon, 67-79. Moscow: All-Union Lenin Academy of Agricultural Sciences.

CHITWOOD, B.G. (1958). The designation of official names for higher taxa of invertebrates. *Bulletin of Zoological Nomenclature* 15, 860-895.

CHUANG, S.H. (1962). The embryonic and post-embryonic development of *Rhabditis teres*. *Nematologica* 7, 317-330.

CLARK, S.A. (1967). The development and life history of the false root-knot nematode, *Nacobbus serendipiticus*. *Nematologica* 13, 91-101.

COOMANS, A. (2000). Nematode systematics: past, present and future. *Nematology* 2, 3-7.

COWAN, C.R. & HYMAN, A.A. (2004). Asymmetric cell division in *Caenorhabditis elegans: c*ortical polarity and spindle positioning. *Annual Review of Cell and Developmental Biology* 20*, 427-453.*

COWAN, A.E. & MCINTOSH, J.R. (1985). Mapping the distribution of differentiation potential for intestine, muscle, and hypodermis during early development in *Caenorhabditis elegans. Cell* 41, 923-932.

DASGUPTA, D.R. & RASKI, D.J. (1968). The biology of *Rotylenchulus parvus. Nematologica* 14, 429-440.

DE LEY, P. & BLAXTER, M.L. (2002). Systematic position and phylogeny. In: Lee, D.L. (Ed.). *The biology of nematodes*. London, UK, Taylor & Francis, pp. 1-30.

DE LEY, P. (1992). The nematode community of a marginal soil at Camberene, Senegal, withspecial attention to functional morphology and niche partitioning in the family Cephalobidae. *Mededelingen van de Koninklijke Academie voor Wetenschapen, Letteren en Schone Kunsten van Belgie - Klasse der Wetenschappen* 53, 107-153.

DEPPE, U., SCHIERENBERG, E., COLE, T., KRIEG, C., SCHMITT, D., YODER , B. & VON EHRENSTEIN, G. (1978). Cell Lineages of the embryo of the nematode *Caenorhabditis elegans. Proceedings of the National Academy of Sciences of the United States of America* 75, 376-380.

DOBZHANSKY, T. (1964). Biology, Molecular and Organismic. *American Zoologist* 4, 443-452.

DOLINSKI, C., BALDWIN, J.G. & THOMAS, W.K. (2001). Comparative survey of early embryogenesis of Secernentea (Nematoda), with phylogenetic implications. *Canadian Journal of Zoology* 79, 82-94.

DORRIS, M., DE LEY, P. & BLAXTER, M.L. (1999). Molecular Analysis of Nematode Diversity and the Evolution of Parasitism. *Parasitology Today* 15, 188-193.

DORRIS, M., VINEY, M. E. & BLAXTER, M. L. (2002). Molecular phylogenetic analysis of the genus *Strongyloides* and related nematodes. *International Journal of Parasitology* 32, 1507-1517.

DRAPER, B.W., MELLO, C.C., BOWERMAN, B.A., HARDIN, J.D. & PRIESS, J.R. (1996). MEX-3 is a KH domain protein that regulates blastomere identity in early *Caenorhabditis elegans* embryos. *Cell* 87, 205-16.

DROZDOVSKY, E.M. (1967). The use of embryonic development in nematode taxonomy. *Transactions of the Helminthological Laboratory of the Academy of Sciences of the U.S.S.R.* 18, 22-29.

DROZDOVSKY, E. M. (1978). The structure and formation of the preblastula as an indication of the phylogenetic relationships and taxonomic position of various groups of nematodes. *In Fitgel' minthologicheskiye Issiedovaniya (*Phytohelminthological research). Edited by K.M. Ryzhikov. Nauka [Science], Moscow 14-32.

DUNN, C.W., HEJNOL, A., MATUS D.Q., PANG, K., BROWNE, W.E., SMITH S.A., SEAVER, E., ROUSE, G.W., OBST, M., EDGECOMBE, G.D., SØRENSEN, M.V., HADDOCK, S.H.D., SCHMIDT-RHAESA, A., OKUSU, A., KRISTENSEN, R.M, WHEELER, W.C., MARTINDALE, M.Q. & GIRIBET, G. (2008). Broad phylogenomic sampling improves resolution of the animal tree of life. *Nature* 452, 745-749.

EDGAR, L.G. & MCGHEE, J.D. (1986). Embryonic expression of a gut-specific esterase in *Caenorhabditis elegans. Developmental Biology* 114, 109-118.

EDGAR, L.G., CARR, S.H., WANG, H. & WOOD, W.B. (2001). Zygotic expression of the caudal homolog pal-1 is required for posterior patterning in *Caenorhabditis elegans* embryogenesis. *Developmental Biology* 229, 71-88.

EDGAR, L.G., WOLF, N. & WOOD, W.B. (1994). Early transcription in *Caenorhabditis elegans. Development* 120, 443-451.

EISENMANN, D. M. (2005).Wnt signaling, In: The *Caenorhabditis elegans* Research Community (Eds.), WormBook, http://www.wormbook.org.

EIZINGER, A., JUNGBLUT, B. & SOMMER, R.J. (1999). Evolutionary change in the functional specificity of genes. *Trends in Genetics* 15, 197-202.

EVANS, T.C., CRITTENDEN, S.L., KODOYIANNI, V., & KIMBLE, J. (1994). Translational control of maternal *glp-1* mRNA establishes an asymmetry in the *Caenorhabditis elegans* embryo. Cell 77, 183-194.

EXTAVOUR, C. & AKAM, M.E. (2003). Mechanisms of germ cell specification across the metazoans: epigenesis and preformation. *Development* 130, 5869-5884.

FASSULIOTIS, G. (1962). Life history of *Hemicriconemoides chitwoodi* Esser. *Nematologica* 8, 110-116.

FASSULIOTIS, G. (1975). Feeding, egg-laying, and embryology of the Columbia lance nematode, *Hoplolaimus columbus. Journal of Nematology* 7, 152-158.

FÉLIX, M.A., HILL, R.J., SCHWARZ, H., STERNBERG, P.W., SUDHAUS, W. & SOMMER, R.J. (1999). *Pristionchus pacificus*, a nematode with only three juvenile stages, displays major heterochronic changes relative to *Caenorhabditis elegans*. *Proceedings of the Royal Society Biological Sciences* 266, 1617-1621.

FLEGG, J.J.M. (1968). Embryogenetic studies on some *Xiphinema* and *Longidorus* species. *Nematologica*14, 137-145.

FÜRST VON LIEVEN, A. (2002). The sister group of the Diplogastrina (Nematoda). *Russian Journal of Nematology* 10, 127-137.

FÜRST VON LIEVEN, A. & SUDHAUS, W. (2000). Comparative and functional morphology of the buccal cavity of Diplogastrina (Nematoda) and a first outline of the phylogeny of this taxon. *Journal of Zoological Systematics and Evolutionary Research* 38, 37-63.

FUKUSHIGE, T, HAWKINS, M.G. & MCGHEE, J.D. (1998). The GATA-factor elt-2 is essential for formation of the *Caenorhabditis elegans* intestine. *Developmental Biology* 198, 286-302.

GARDINER, C.H., KOH, D.S. & CARDELLA, T.A. (1981). *Micronema* in man: third fatal infection. *American Journal of Medicine and Hygiene* 30, 586-589.

GILBERT, S.F. (2006). Developmental Biology, 8th edition. Sinauer Associates, Sunderland, Massachusetts, USA, 817 pp.

GILBERT, S.F. & BOLKER, J.A. (2001). Homologies of process and modular elements of embryonic construction. *Journal of experimental Zoology, part B Molecular Developmental Evolution* 291, 1-12.

GILBERT, S.F., OPITZ, J.M. & RAFF, R.A. (1996). Resynthesizing evolutionary and developmental biology. *Developmental Biology* 173, 357-372.

GINARTE, A.C. & MIJARES, S.A. (1994). Fecundity and embryonal development of *Romanomermis culicivorax*. *Revista Cubana de Medicina Tropical* 46, 159-163.

GITTLEMAN, J.L. & LUH, H.-K. (1992). On comparing comparative methods. *Annual Review of ecological systems* 23, 283-404.

GOLDSTEIN, B. (1992). Induction of gut in *Caenorhabditis elegans* embryos. *Nature* 35, 255-257.

GOLDSTEIN, B. (1993). Establishment of gut fate in the E lineage of *Caenorhabditis elegans:* The roles of lineage-dependent mechanisms and cell interactions. *Development* 118, 1267-1277.

GOLDSTEIN, B. (1995). An analysis of the response to gut induction in the *Caenorhabditis elegans* embryo. *Development* 121, 1227-1236.

GOLDSTEIN, B. (2001). On the evolution of early development in the Nematoda. *Philosophical Transactions of the Royal Society Biological Sciences* 356, 1521-1531.

GOLDSTEIN, B. & HIRD, S.N. (1996). Specification of the anteroposterior axis in *Caenorhabditis elegans*. *Development* 122, 1467-1474.

GOLDSTEIN, B., FRISSE, L.M. & THOMAS, W.K. (1998). Embryonic axis specification in nematodes: evolution of the first step in development. *Current Biology* 8, 157-160.

GOULD, S.J. (1977). Ontogeny and Phylogeny. Belknap Harvard, Cambridge, MA, USA.

GREENWALD, I. (2005). LIN-12/Notch signaling in *Caenorhabditis elegans*. In: The *Caenorhabditis elegans* Research Community (Eds.), WormBook, http://www.wormbook.org.

GURALNICK, R.P. & LINDBERG, D.R. (2001). Reconnecting cell and animal lineages: what do cell lineages tell us about the evolution and development of *Spiralia*? *Evolution* 5, 1501-1519.

HASEGAWA, K., FUTAI, K., MIWA, S. & MIWA, J. (2004). Early embryogenesis of the pinewood nematode *Bursaphelenchus xylophilus. Development, Growth & Differentiation* 46, 153-161.

HAWKINS, M.G. & MCGHEE, J.D. (1995). elt-2, a second GATA factor from the nematode *Caenorhabditis elegans* . *Journal of Biological Chemistry* 270, 14666-14671.

HEJNOL, A., SCHNABEL, R. & SCHOLTZ, G. (2006). A 4D-microscopic analysis of the germ band in the isopod crustacean *Porcellio scaber* (Malacostraca, Peracarida)-developmental and phylogenetic implications. *Development, Genes and Evolution* 216, 755-767.

HENNIG, W. (1966). Phylogenetic systematics. University of Illinois press. Urbana, XIV + 263 pp.

HERRMANN, M., MAYER, W.E. & SOMMER, R.J. (2006). Nematodes of the genus *Pristionchus* are closely associated with scarab beetles and the Colorado potato beetle in Western Europe. *Zoology* 109, 96-108.

HIRD, S.N. & WHITE, J.G. (1993). Cortical and cytoplasmic flow polarity in early embryonic-cells of *Caenorhabditis elegans*. *Journal of Cell Biology* 121, 1343-1355.

HIRD, S.N., PAULSEN, J.E. & STROME, S. (1996). Segregation of germ granules in living *Caenorhabditis elegans* embryos: type-specific mechanisms for cytoplasmic localization. *Development* 122, 1303-1312.

HOLTERMAN, M., VAN DER WURFF, A., VAN DEN ELSEN, S., VAN MEGEN, H., BONGERS, T., HOLOVACHOV, O., BAKKER, J. & HELDER, J. (2006). Phylum-wide analysis of SSU rDNA reveals deep phylogenetic relationships among nematodes and accelerated evolution toward crown clades. *Molecular Biology and Evolution* 23, 1792-1800.

HOLTERMAN, M., HOLOVACHOV, O., VAN DEN ELSEN, S., VAN MEGEN, H., BONGERS, T., BAKKER, J. & HELDER, J. (2008). Small subunit ribosomal DNA-based phylogeny of basal Chromadoria (Nematoda) suggests that transitions from marine to terrestrial habitats (and vice versa) require relatively simple adaptations. *Molecular Phylogenetics and Evolution*

HOUTHOOFD, W. & BORGONIE, G. (2007). The embryonic cell lineage of the nematode *Halicephalobus gingivalis* (Nematoda: Cephalobina: Panagrolaimoidea). *Nematology* 9, 573-584.

HOUTHOOFD, W., JACOBSEN, K., MERTENS, C., VANGESTEL, S., COOMANS, A. & BORGONIE, G. (2003). Embryonic cell lineage of the marine nematode *Pellioditis marina*. *Developmental Biology* 258, 57-69.

HOUTHOOFD, W., WILLEMS, M., VANGESTEL, S., MERTENS, C., BERT, W. & BORGONIE, G. (2006). Different roads to form the same gut in nematodes. *Evolution & Development* 8, 362-369.

HOUTHOOFD, W., WILLEMS, M., JACOBSEN, K., COOMANS, A. & BORGONIE, G. (2008). The embryonic cell lineage of the nematode *Rhabditophanes* sp. *Nematology* (in press).

HUANG, N.N., MOOTZ, D.E., VIDAL, M., HUNTER, C.P. & WALHOUT, A.J. (2002). MEX-3 interacting proteins link cell polarity to asymmetric gene expression in *Caenorhabditis elegans. Development* 129, 747-759.

HUANG, S., SHETTY, P., ROBERTSON S.M. & LIN R. (2007). Binary cell fate specification during *Caenorhabditis elegans* embryogenesis driven by reiterated reciprocal asymmetry of TCF POP-1 and its coactivator ß-catenin SYS-1. *Development* 134, 2685-2695.

HUNG, C.-L. & JENKINS, W.R. (1969). Oogenesis and embryology of two plant-parasitic nematodes, *Pratylenchus penetrans* and *P. zeae*. *Journal of Nematology* 1, 352-356.

HUNTER, C.P. & KENYON, C.J. (1996). Spatial and temporal controls target pal-1 blastomere-specification activity to a single blastomere lineage in *Caenorhabditis elegans* embryos. *Cell* 87, 217-26.

HUTTER, H. & SCHNABEL, R. (1994). Glp-1 and inductions establishing embryonic axes in *Caenorhabditis elegans*. *Development* 120, 2051-2064.

HUTTER, H. & SCHNABEL, R. (1995a). Specification of anterior-posterior differences within the AB lineage in the *Caenorhabditis elegans* embryo: a polarising induction. *Development* 121, 1559-1568.

HUTTER, H. & SCHNABEL, R. (1995b). Establishment of left-right asymmetry in the *Caenorhabditis elegans* embryo: a multistep process involving a series of inductive events. *Development* 121, 3417-3424.

HYMAN, A.A. & WHITE, J.G. (1987). Determination of cell division axes in the early embryogenesis of *Caenorhabditis elegans*. *The Journal of Cell Biology* 105, 2123-2135.

JONES, C.C., ROSEN, T. & GREENBERG, C. (1991). Cutaneous larva migrans due to *Pelodera strongyloides*. *Cutis* 48, 123-126.

JUNKERSDORF, B. & SCHIERENBERG, E. (1992). Embryogenesis in *Caenorhabditis elegans* after elimination of individual blastomeres or induced alteration of the cell-division order. *Roux's Archives of Developmental Biology* 202, 17-22.

KALETTA, T., SCHNABEL, H. & SCHNABEL, R. (1997). Binary specification of the embryonic lineage in *Caenorhabditis elegans. Nature* 390, 294-298.

KEMPHUES, K.J. (1989). *Caenorhabditis*. In: D.M. Glover & E.D. Hames (Eds). Frontiers in molecular biology: Genes and embryos ,IRL Press, London, pp. 95-126.

KEMPHUES, K.J., PRIESS, J.R., MORTON, D.G. & CHENG, N. (1988). Identification of genes required for cytoplasmic localization in early *Caenorhabditis elegans* embryos. *Cell* 52, 311-320.

KIONTKE, K., BARRIÈRE, A., KOLOTUEV, I., PODBILEWICZ, B., SOMMER, R., FITCH, D.H.A. & FÉLIX, M.A. (2007). Trends, stasis, and drift in the evolution of nematode vulva development. *Current Biology* 17, 1925-1937.

KIRBY, C., KUSCH, M. & KEMPHUES, K. (1990). Mutations in the *par* genes of *Caenorhabditis elegans* affect cytoplasmic reorganization during the first cell cycle. *Developmental Biology* 142, 203-215.

KORSWAGEN, H.C., (2002). Canonical and non-canonical Wnt signaling pathways in *Caenorhabditis elegans*: variations on a common signaling theme. *BioEssays* 24, 801-810.

KORSWAGEN, H.C., HERMAN, M.A. & CLEVERS, H.C. (2000). Distinct betacatenins mediate adhesion and signalling functions in *Caenorhabditis elegans. Nature* 406, 527-532.

LAHL, V. (2007). Vergleichende und experimentelle Untersuchungen zur Embryonalentwicklung von freilebenden und parasitären Nematoden., Ph.D. thesis, University of Köln, Germany.

LAHL, V., HALAMA, C. & SCHIERENBERG, E. (2003). Comparative and experimental embryogenesis of Plectidae (Nematoda). *Development Genes and Evolution* 213, 18-27.

LAHL, V., SADLER, B. & SCHIERENBERG, E. (2006). Egg development in parthenogenetic nematodes: variations in meiosis and axis formation. *International journal of developmental Biology* 213, 18-27.

LAUFER, J.S., BAZZICALUPO, P. & WOOD, W.B. (1980). Segregation of developmental potential in early embryos of *Caenorhabditis elegans*. *Cell* 19, 569-577.

LAUGSCH, M. & SCHIERENBERG, E. (2004). Differences in maternal supply and early development of closely related nematode species. *International Journal of Developmental Biology* 48, 655-662.

LEE, J.-Y. & GOLDSTEIN, B. (2003). Mechanisms of cell positioning during *Caenorhabditis elegans* gastrulation. *Development* 130, 307-320.

LIN, R., HILL, R.J. & PRIESS, J.R. (1998). POP-1 and anterior–posterior fate decisions in *Caenorhabditis elegans* embryos. *Cell* 92, 229-239.

LIN, R., THOMPSON, S. & PRIESS, J.R. (1995). Pop-1 encodes an HMG box protein required for the specification of a mesoderm precursor in early *Caenorhabditis elegans* embryos. *Cell* 83, 599-609.

LOCKHART, P.J., STEEL, M.A., HENDY, M.D. & PENNY, D. (1994). Recovering evolutionary trees under a more realistic model of sequence. *Molecular Biology and Evolution* 11, 605-612.

LORENZEN, S. (1981) Entwurf eines phylogenetischen Systems de freilebenden Nematoden. *Veröffentlichungen Des Instituts für Meeresforschung in Bremerhaven*, 7, 1-449.

LORENZEN, S. (1994). The phylogenetic systematics of free-living nematodes. London, The Ray Society, 383 pp.

LUC, M., MAGGENTI, A.R., FORTUNER, R., RASKI, D. J. & GERAERT, E. (1987). A reappraisal of Tylenchina (Nemata). 1: For a new approach of the taxonomy of Tylenchina. *Revue de Nématologie* 10, 127-134.

MABEE, P.M. & TRENDLER, T.A. (1996). Development of the cranium and paired fins in Betta splendens (Teleostei: Percomorpha): Intraspecific variation and interspecific comparisons. *Journal of Morphology* 227, 249-287.

MADDISON, W.P. & MADDISSON, D.R. (2006). Mesquite: a modular system for evolutionary analysis. Version 1.11. (http://mesquiteproject.org).

MADURO, M.F., KASMIR, J.J., ZHU, J.W. & ROTHMAN, J.H. (2005). The Wnt effector POP-1 and the PAL-1/Caudal homeoprotein collaborate with SKN-1 to activate *C-elegans* endoderm development. *Developmental Biology* 285, 510-523.

MADURO, M.F., LIN, R. & ROTHMAN, J.H. (2002). Dynamics of a developmental switch: recursive intracellular and intranuclear redistribution of *Caenorhabditis elegans* POP-1 parallels Wnt-inhibited transcriptional repression. *Developmental Biology* 248, 128-142.

MAGGENTI, A.R. (1961). Morphology and biology of the genus *Plectus* (Nematoda: Plectidae). *Proceedings of the Helminthological Society of Washington* 28, 118-130.

MAGGENTI, A.R. (1963). Comparative morphology in nemic phylogeny. In: Dougherty, E.C. (Ed.). The lower Metazoa, comparative biology and phylogeny. Berkeley, USA, University of California press, 273-282.

MAGGENTI, A.R. (1983). Nematode higher classification as influenced by species and family concepts. In: Stone, A.R., Platt, H.M. & Khalil, L.F. Concepts in Nematode Systematics, Academic Press, New York, 25-40.

MALAKHOV, V.V. (1994). Nematodes. Structure, development, classification and phylogeny. Hope, W.D. (Ed.), Smithsonian Institution Press, Washington and London, 286 pp.

MALAKHOV, V.V. (1998). Embryological and histological pecularities of the order Enoplida, a primitive group of nematodes. *Russian Journal of Nematology* 6, 41-46.

MALAKHOV, V.V. & CHERDANTSEV, V.G. (1975). Embryonic development of free living marine nematode *Pontonema vulgare. Zoologichesky Zhurnal* 54, 165-174.

MALAKHOV, V.V. & SPIRIDONOV, S.E. (1981). Embryonic development of *Gastromermis* (Nematoda, Mermithida). *Zoologicheskii Zhurnal* 60, 1574-1577.

MANGO, S.E, LAMBIE, E.J. & KIMBLE, J. (1994a). The *pha-4* gene is required to generate the pharyngeal primordium of *Caenorhabditis elegans. Development* 120, 3019-3031.

MANGO, S.E., THORPE, C.J., MARTIN, P.R., CHAMBERLAIN, S.H. & BOWERMAN, B. (1994b). Two maternal genes, *apx-1* and *pie-1*, are required to distinguish the fates of equivalent blastomeres in the early *Caenorhabditis elegans* embryo. *Development* 120, 2305-2315.

MARSHALL, S.D.G. & MCGHEE, J.D. (2001). Coordination of ges-1 expression between the *Caenorhabditis* pharynx and intestine. *Developmental Biology* 239, 350-363.

MCGHEE, J.D., BIRCHALL, J.C., CHUNG, M.A., COTTRELL, D.A., EDGAR, L.G., SVENDSEN, P.C. & FERRARI, D.C. (1990). Production of null mutants in the major intestinal esterase gene (ges-1) of the nematode *Caenorhabditis elegans. Genetics* 125, 505-514.

MCGHEE, J.D., SLEUMER, M.C., BILENKY, M., WONG, K., MCKAY, S.J., GOSZCZYNSKI, B., TIAN, H., KRICH, N.D., KHATTRA, J., HOLT, R.A., BAILLIE, D.L., KOHARA, Y., MARRA, M.A., JONES, S.J., MOERMAN, D.G. & ROBERTSON, A.G. (2006). The ELT-2 GATA-factor and the global regulation of transcription in the *Caenorhabditis elegans* intestine. *Developmental Biology* 302, 627-45.

MELDAL, B.H.M., DEBENHAM, N.J., DE LEY, P., DE LEY, I.T., VANFLETEREN, J.R., VIERSTRAETE, A.R., BERT, W., BORGONIE, G., MOENS, T., TYLER, P.A., AUSTEN, M.C., BLAXTER, M.L., ROGERS, A.D. & LAMBSHEAD, P.J.D. (2007). An improved molecular phylogeny of the Nematoda with special emphasis on marine taxa. *Molecular Phylogenetics and Evolution* 42, 622-636.

MELLO, C.C., DRAPER, B.W., M. KRAUSE, M., H. WEINTRAUB, H. & PRIESS, J.R. (1992). The *pie-1* and *mex-1* genes and maternal control of blastomere identity in early *Caenorhabditis elegans* embryos. *Cell* 70, 163-176.

MELLO, C.C., DRAPER, B.W. & PRIESS, J.R. (1994). The maternal genes *apx-1* and *glp-1* and establishment of dorsal-ventral polarity in the early *Caenorhabditis elegans* embryo. *Cell* 77, 95-106.

MENEGHINI, M.D., ISHITANI, T., CARTER, J.C., HISAMOTO, N., NINOMIYA-TSUJI, J., THORPE, C.J., HAMILL, D.R., MATSUMOTO, K. & BOWERMAN, B. (1999). MAP kinase and Wnt pathways converge to downregulate an HMG-domain repressor in *Caenorhabditis elegans. Nature* 399, 793-797.

MICOLETZKY, H. (1922). Die freilebenden Erd-Nematoden mit besonderer Berücksichtigung der Steiermark und der Bukowina, zugleich mit einer Revision sämtlicher nicht mariner, freilebender Nematoden in Form von Genus-Beschreibungen und Bestimmungs-schlüsseln. *Archiv für Naturgeschichte, Abteilung A* 87, 1-650.

MINELLI, A. (2003). The development of animal form: Ontogeny, morphology, and evolution. Cambridge: Cambridge university press. 339 pp.

MORTON, D.G., ROOS, J.M. & KEMPHUES, K.J. (1992). par-4, a gene required for cytoplasmic localization and determination of specific cell types in *Caenorhabditis elegans* embryogenesis. *Genetics* 130, 771-790.

MORTON, D.G., SHAKES, D.C., NUGENT, S., DICHOSO, D., WANG, W., GOLDEN, A. & KEMPHUES, K.J. (2002). The *Caenorhabditis elegans par-5* gene encodes a 14-3-3 protein required for cellular asymmetry in the early embryo. *Developmental Biology* 241, 47-58.

MOSKOWITZ, P., GENDREAU, S.B. & ROTHMAN, J.H. (1994). Combinatorial specification of blastomere identity by *glp-1* -dependant cellular interactions in the nematode *Caenorhabditis elegans. Development* 120, 3325-3338.

MULLER, H. (1903). Beitrag zur Embryonalentwicklung von *Ascaris megalocephala*. *Zoologica* 41, 1-30.

NADLER, S.A., CARRENO, R.A., ADAMS, B.J., KINDE, H., BALDWIN, J.G. & MUNDO-OCAMPO, M. (2003). Molecular genetics and diagnosis of soil and clinical isolates of *Halicephalobus gingivalis* (Nematoda: Cepalobina: Panagrolaimidea), an opportunistic pathogen of horses. *International Journal for Parasitology* 33, 1115-1125.

NADLER, S.A., DE LEY, P., MUNDO-OCAMPO, M., SMYTHE, A.B., STOCK, S.P., BUMBARGER, D., BYRON, J., ADAMS, B.J., TANDINGAN DE LEY, I., HOLOVACHOV, O. & BALDWIN, J.G. (2006). Phylogeny of Cephalobina (Nematoda): Molecular evidence for recurrent evolution of probolae and incongruence with traditional classifications. *Molecular Phylogenetics and Evolution* 40, 696-711.

NANCE, J. & PRIESS, J.R. (2002). Cell polarity and gastrulation in *Caenorhabditis elegans*. *Development* 129, 387-397.

NANCE, J., MUNRO, E.M. & PRIESS, J.R. (2003). *Caenorhabditis elegans* PAR-3 and PAR-6 are required for apicobasal asymmetries associated with cell adhesion and gastrulation. *Development* 130, 5339-5350.

NIELSEN, C. & MEIER R. (2002). What cell lineages tell us about the evolution of *Spiralia* remains to be seen. *Evolution* 56, 2554-2557.

NYLANDER, J.A.A., RONQUIST, F., HUELSENBECK, J.P. & NIEVES-ALDREY, J.L. (2004). Bayesian phylogenetic analysis of combined data. *Systematic Biology* 53, 47-67.

ORION, D., WERGIN, W.P., CHITWOOD, D.J. &. ERBE, E.F. (1994). Low-temperature scanning electron microscope observations of the *Meloidogyne incognita* egg mass: the gelatinous matrix and embryo development. *Journal of Nematology* 26, 402-411.

PARK, F.D. & PRIESS, J.R. (2003). Establishment of POP-1 asymmetry in early *Caenorhabditis elegans* embryos. *Development* 130, 3547-3556.

PATTERSON, P. (1988). Homology in classical and molecular biology. *Molecular Biology and Evolution* 5, 603-625.

PERRY, R.N. & WESEMAEL, W.M.L. (2008). Host plant effects on hatching of root-knot nematodes. *Russian Journal of Nematology* 16, 1-5.

PIRES-DASILVA, A. & SOMMER, R. (2004). Conservation of the global sex determination gene tra-1 in distantly related nematodes. *Genes and Development* 18, 1198-1208.

PRIESS, J. (2005). Notch signaling in the *Caenorhabditis elegans* embryo. In: The *Caenorhabditis elegans* Research Community (Eds.), WormBook, <http://www.wormbook.org>.

PRIESS, J.R. & THOMSON, J.N. (1987). Cellular interactions in early *Caenorhabditis elegans* embryos. *Cell* 48, 241-250.

PRIESS, J. R., SCHNABEL, H. & SCHNABEL, R. (1987). The *glp-1* locus and cellular interactions in early *Caenorhabditis elegans* embryos. *Cell* 51, 601-611.

RASKI, D.J. (1950). The life history and morphology of the sugar-beet nematode, *Heterodera schachtii* Schmidt. *Phytopathology* 40, 135-153.

RICHTER, S. (2005). Homologies in phylogenetic analyses-concept and tests. *Theory in Biosciences* 124, 105-120.

RIEPPEL, O. (1996). Testing homology by congruence: the pectoral girdle of turtles. *Proceedings: Biological Sciences* 263, 1395-1398.

RIEPPEL, O. (2007). The performance of morphological characters in broad-scale phylogenetic analyses. *Biological Journal of the Linnean Society* 92, 297-308.

ROCHELEAU, C.E., DOWNS, W.D., LIN, R., WITTMANN, C., BEI, Y., CHA, Y.H., ALI, M., PRIESS J.R. & MELLO, C.C. (1997). Wnt signaling and an APC-related gene specify endoderm in early *Caenorhabditis elegans* embryos. *Cell* 90, 707-716.

ROMAN, J. & HIRSCHMANN, H. (1969). Embryogenesis and postembryogenesis in species of *Pratylenchus* (Nematoda: Tylenchidae). *Proceedings of the Helminthological Society of Washington* 36, 164-174.

RONQUIST, F. & HUELSENBECK, J.P. (2003). MrBayes 3: Bayesian phylogenetic inference under mixed models. *Bioinformatics* 19, 1572-1574.

RUDEL, D., RIEBESELL, M. & SOMMER, R.J. (2005). Gonadogenesis in *Pristionchus pacificus* and organ evolution: development, adult morphology and cell/cell interactions in the hermaphrodite gonad. *Developmental Biology* 277, 200-221.

SARR, E., COOMANS, A. & LUC, M. (1987). Development and life cycle of *Neodolichodorus rostrulatus* (Siddiqi, 1976), with observations on the copulatory plug (Nematoda: Tylenchina). *Revue de Nématologie* 10, 87-92.

SCHIERENBERG, E. (1987). Reversal of cellular polarity and early cell-cell interaction in the embryos of *Caenorhabditis elegans*. *Developmental Biology* 122, 452-463.

SCHIERENBERG, E. (1988). Localization and segregation of lineage-specific cleavage potential in embryos of *Caenorhabditis elegans. Roux's Archives Of Developmental Biology* 197, 282-293.

SCHIERENBERG, E. (1997). Nematodes, the roundworms. In: Gilbert, S.F. and Raunio, A.M.(eds.). *Embryology: constructing the organism.* Sinauer Associates, Sunderland: pp. 131-148.

SCHIERENBERG, E. (2000). New approaches to a better understanding of nematode phylogeny: molecular and developmental studies. *Journal of Zoological Systematics & Evolutionary Research* 38, 129-132.

SCHIERENBERG, E. (2001). Three sons of fortune: early embryogenesis, evolution and ecology of nematodes. *BioEssays* 23, 841-847.

SCHIERENBERG, E. (2005). Unusual cleavage and gastrulation in a freshwater nematode: developmental and phylogenetic implications. *Development, Genes and Evolution* 215, 103-108.

SCHIERENBERG, E. & JUNKERSDORF, B. (1992). The role of eggshell and underlying vitelline membrane for normal pattern formation in the early *Caenorhabditis elegans* embryo. *Roux's Archives of Developmental Biology* 202, 10-16.

SCHIERENBERG, E. & LAHL, V. (2004). Embryology and phylogeny of nematodes. *Nematology Monographs & Perspectives* 2, 667-679.

SCHNABEL, R. (1991). Cellular interactions involved in the determination of the early *Caenorhabditis elegans* embryo. *Mechanisms of Development* 34, 85-100.

SCHNABEL, R. (1994). Autonomy and nonautonomy in cell fate specification of muscle in the *Caenorhabditis elegans* embryo: A reciprocal induction. *Science* 263, 1449-1452.

SCHNABEL, R. (1995). Duels without obvious sense: Counteracting inductions involved in body wall muscle development in the *Caenorhabditis elegans* embryo. *Development* 121, 2219-2232.

SCHNABEL, R., BISCHOFF, M., HINTZE, A., SCHULZ, A.K., HEJNOL, A., MEINHARDT, H. & HUTTER, H. (2006). Global cell sorting in the *C.elegans* embryo defines a new mechanism for pattern formation. *Developmental Biology* 294, 418-431.

SCHNABEL, R., HUTTER, H., MOERMAN, D. & SCHNABEL, H. (1997). Assessing normal embryogenesis in *Caenorhabditis elegans* using a 4D microscope: variability of development and regional specification. *Developmental Biology* 184, 234-265.

SCHULMEISTER, S. & WHEELER, W.C. (2004). Comparative and phylogenetic analysis of developmental sequences. *Evolution & Development* 6, 50-57.

SCHULZE, J. & SCHIERENBERG, E. (2008). Cellular pattern formation, establishment of polarity and segregation of colored cytoplasm in embryos of the nematode *Romanomermis culicivorax. Developmental Biology* 315, 426-436.

SESHADRI, A.R. (1965). Investigations on the biology and life cycle of *Criconemoides xenoplax* Raski, 1952 (Nematoda: Criconematidae). *Nematologica* 10, 540-562.

SEYDOUX, G., MELLO, C.C., PETTITT, J., WOOD, W.B., PRIESS, J.R. & FIRE, A. (1996). Repression of gene expression in the embryonic germ lineage of *Caenorhabditis elegans. Nature* 382, 713-716.

SHAFQAT, S., JAIRAJPURI, M.S. & BILGRAMI. A.L. (1991). Developmental biology of *Dorylaimus stagnalis* Dujardin,1845 (Nematoda: Dorylaimida). *Revue de Nématologie* 14, 61-71.

SHAFQAT, S., AHMAD, I. & JAIRAJPURI, M.S. (1996). Early embryonic development patterns in some predacious dorylaims. *Afro-Asian Journal of Nematology* 6, 133-136.

SHAHINA, F. & MAQBOOL, M.A. (1989). Embryonic and postembryonic developmental stages of *Heterodera zeae* Koshy et al., 1971 on *Zea mays*. *Pakistan Journal of Nematology* 7, 3-16.

SHETTY, P., LO, M.C., SCOTT, M., ROBERTSON, S.M. & LIN, R. (2005). *Caenorhabditis elegans* TCF protein, POP-1, converts from repressor to activator as a result of Wnt-induced lowering of nuclear levels. *Developmental Biology* 285 , 584-592.

SIDDIQI, M.R. (2000). Tylenchida parasites of plants and insects, 2nd Edition. Wallingford, UK, CABI Publishing, 864 pp.

SIGRIST, C.B. & SOMMER, R.J. (1999). Vulva formation in *Pristionchus pacificus* relies on continuous gonadal induction. *Development Genes and Evolution* 209, 451-459.

SIJMONS, P.C., GRUNDLER, F.M.W., VON MENDE, N., BURROWS, P.R. & WYSS, U. (1991). *Arabidopsis thaliana* as a new model host for plant-parasitic nematodes. *The Plant Journal* 1, 245-254.

SKIBA, F. & SCHIERENBERG, E. (1992). Cell lineages, developmental timing and spatial pattern formation in embryos of free-living soil nematodes. *Developmental Biology* 151, 597-610.

SMITH, K.K. (1996). Integration of craniofacial structures during development in mammals. *American Zoologist* 36, 70-79.

SMITH, K.K. (1997). Comparative patterns of craniofacial development in eutherian and metatherian mammals. *Evolution* 51, 1663-1678.

SMITH, K.K. (2001). Heterochrony revisited: the evolution of developmental sequences. *Biological Journal of the Linnean Society* 73, 169-186.

SOMMER, R.J. (2000). Evolution of nematode development. *Current Opinion in Genetics and Development* 10, 443-448.

SOMMER, R.J. (2005). Evolution of development in nematodes related to *Caenorhabditis elegans.* In: The *Caenorhabditis elegans* Research Community (Eds.), WormBook,http://www.wormbook.org.

SOMMER, R.J. & STERNBERG, P.W. (1994). Changes of induction and competence during the evolution of vulva development in nematodes. *Science* 5168, 114-118.

SOMMER, R.J. & STERNBERG, P.W. (1996). Evolution of nematode vulval fate patterning. *Developmental Biology* 17, 396-407.

SPIELER, M. & SCHIERENBERG, E. (1995). On the development of the alternating free-living and parasitic generations of the nematode *Rhabdias bufonis*. *Invertebrate Reproduction and Development* 28, 193-203.

SRINIVASAN, J., SINZ, W., JESSE, T., WIGGERS-PEREBOLTE, L., JANSEN, K., BUNTJER, J., VAN DER MEULEN, M. & SOMMER, R.J. (2003). An integrated physical and genetic map of the nematode *Pristionchus pacificus*. *Molecular Genetics and Genomics* 269, 715-722.

SRINIVASAN, J., SINZ, W., LANZ, C., BRAND, A., NANDAKUMAR, R., RADDATZ, G., WITTE, H., KELLER, H., KIPPING, I., PIRES-DASILVA, A., JESSE, T., MILLARE, J., DE BOTH, M., SCHUSTER, S.C. & SOMMER, R.J. (2002). A BAC-based genetic linkage map of the nematode *Pristionchus pacificus*. *Genetics* 162, 129-134.

STENT, G.S. & WEISBLAT, D.A. (1982). The development of a simple nervous system. *Scientific American* 246, 100-110.

STROME, S. (1993). Determination of cleavage planes. *Cell* 72, 3-6.

STROME, S. (2005). Specification of the germ line. In: The *Caenorhabditis elegans* Research Community (Eds.), WormBook, http://www.wormbook.org.

STROME, S. & WOOD, W.B. (1983). Generation of asymmetry and segregation of germ-line granules in early *Caenorhabditis elegans* embryos. *Cell* 35, 15-25.

SUDHAUS, W. & FITCH, D. (2001). Comparative studies on the phylogeny and systematics of the Rhabditidae (Nematoda). *Journal of Nematology* 33, 1-72.

SUDHAUS, W. & FÜRST VON LIEVEN, A. (2003). A phylogenetic classification and catalogue of the Diplogastridae (Secernentea, Nematoda). *Journal of Nematode Morphology and Systematics 6*, 43-90.

SUDHAUS, W. & SCHULTE, F. (1988). *Rhabditis (Pelodera) strongyloides* (Nematoda) als Verursacher von Dermatitis, mit systematischen und biologischen Bemerkungen über verwandte Arten. *Zoologische Jahrbücher (Systematik)* 115, 187-205.

SULSTON, J.E. & HORVITZ, H.R. (1977). Post-embryonic cell lineages of the nematode, *Caenorhabditis elegans. Developmental Biology* 56, 110-156.

SULSTON, J.E., SCHIERENBERG, E., WHITE, J.G. & THOMSON, J.N. (1983). The embryonic cell lineage of the nematode *Caenorhabditis elegans*. *Developmental Biology* 100, 64-119.

SWOFFORD, D.L. (2002). PAUP*. Phylogenetic Analysis Using Parsimony (*and Other Methods). Version 4. Sinauer Associates, Sunderland, Massachusetts.

TAHSEEN, Q., AHMAD, I. & JAIRAJPURI, M.S. (1992). Description and developmental biology of *Plectus zelli* n. sp. (Nematoda: Araeolaimida). *Fundamental and Applied Nematology* 15, 503-510.

TAHSEEN, Q., JAIRAJPURI, M.S. & AHMAD, I. (1991). Observations on the embryonic and post-embryonic development of *Diploscapter orientalis* (Nematoda: Rhabditida). *Revue de Nématologie* 14, 251-260.

THOMAS, P.R. (1965). Biology of *Acrobeles complexus* Thorne cultivated on agar. *Nematologica* 11, 395-408.

THOMPSON, J.D., GIBSON, T.J., PLEWNIAK, F., JEANMOUGIN, F. & HIGGINS, D.G. (1997). The ClustalX windows interface: flexible strategies for multiple sequence alignment aided by quality analysis tools. *Nucleic Acids Research* 25, 4876-4882.

THORPE, C.J., SCHLESINGER, A., CARTER, J.C. & BOWERMAN, B. (1997). Wnt signaling polarizes an early *Caenorhabditis elegans* blastomere to distinguish endoderm from mesoderm. *Cell 90,* 695-705.

VAN BENEDEN, E. (1883). Récherches sur la maturation de l'oeuf, la fécondation et la division cellulaire. Archives de Biologie 4, 265-640.

VAN WEERDT, L.G. (1960). Studies on the biology of *Radopholus similis* (Cobb, 1893) Thorne, 1949. *Nematologica* 5, 43-52.

VANCOPPENOLLE, B., BORGONIE, G. & COOMANS, A. (1999). Generation times of some free-living nematodes cultured at three temperatures. *Nematology* 1, 15-18.

VANGESTEL, S., HOUTHOOFD, W., BERT, W. & BORGONIE, G. (2008). The early embryonic development of the satellite organism *Pristionchus pacificus*: differences and similarities with *Caenorhabditis elegans*. *Nematology* 10, 301-312.

VELHAGEN, W.A. (1995). A comparative study of cranial development in thethamnophiine snakes (Serpentes: Colubridae) (unpublished Ph.D. thesis), Duke University, Durham, NC, USA.

VELHAGEN, W.A. (1997). Analyzing Developmental Sequences Using Sequence Units. *Systematic Biology* 46, 204-210.

VON BAER, K.E. (1828). *Entwicklungsgeschichte der Tiere: Beobachtung und Reflexion*. Bornträger, Konigsberg.

VORONOV, D.A. (1999). The Embryonic Development of *Pontonema vulgare* (Enoplida: Oncholaimidae) with a discussion of nematode phylogeny. *Russian Journal of Nematology* 7, 105-114.

VORONOV, D.A. & PANCHIN, Y.V. (1998). Cell lineage in marine nematode *Enoplus brevis*. *Development* 125, 143-150.

VORONOV, D.A., PANCHIN, Y.V. & SPIRIDONOV, S.E. (1998). Nematode phylogeny and embryology. *Nature* 395, 28.

VOVLAS, N. (1977). Osservazioni sullo sviluppo embrionale di *Zygotylenchus guevarai*. *Nematologia Mediterranea* 5, 121-124.

WALSTON, T., TUSKEY, C., EDGAR, L., HAWKINS, N., ELLIS, G., BOWERMAN, B., WOOD, W. & HARDIN, J. (2004). Multiple Wnt signaling pathways converge to orient the mitotic spindle in early *Caenorhabditis elegans* embryos. *Developmental Cell* 7, 831-841.

WANG, L.H. (1971). Embryology and life cycle of *Tylenchorhynchus claytoni* Steiner, 1937 (Nematoda: Tylenchoidea). *Journal of Nematology* 3, 101-110.

WAY, J.C., WANG, L.L., RUN, J.Q. & HUNG, M.-S. (1994). Cell polarity and the mechanism of asymmetric cell division. *Bioessays* 16, 925-931.

WHEELER, W.C. (2003). Search-based optimization. *Cladistics* 19, 348-355.

WIEGNER, O. & SCHIERENBERG, E. (1998). Specification of gut cell fate differs significantly between the nematodes *Acrobeloides nanus* and *Caenorhabditis elegans*. *Developmental Biology* 204, 3-14.

WIEGNER, O. & SCHIERENBERG, E. (1999). Regulative development in a nematode embryo: a hierarchy of cell fate transformations. *Developmental Biology* 215, 1-12.

WILLEMS, M., HOUTHOOFD, W., CLAEYS, M., COUVREUR, M., VAN DRIESSCHE, R., ADRIAENS, D., JACOBSEN, K. & BORGONIE, G. (2005). Unusual intestinal lamellae in

the nematode *Rhabditophanes sp* KR3021 (Nematoda: Alloinematidae). *Journal of Morphology* 264, 223-232.

WOOD, W.B. (1991). Evidence from reversal of handedness in *Caenorhabditis elegans* embryos for early cell interactions determining cell fates. *Nature* 349, 536-538.

WYLIE, C. (1999). Germ cells. *Cell* 96, 165-174.

YUKSEL, H.S. (1960). Observations on the life cycle of Ditylenchus dipsaci on onion seedlings. *Nematologica* 5, 289-296.

ZHU, J.W., HILL, R.J., HEID, P.J., FUKUYAMA, M., SUGIMOTO, A., PRIESS, J.R. & ROTHMAN, J.H. (1997). End-1 encodes an apparent GATA factor that specifies the endoderm precursor in *Caenorhabditis elegans* embryos. *Genes and Development* 11, 2883-2896.

ZUR STRASSEN, O. (1959). Neue Beiträge zur Entwicklungsmechanik der Nematoden. Z*oologica* 107, 1-142.

ZUR STRASSEN, O. (1896). Embryonalentwickelung der *Ascaris megalocephala*. *Development Genes and Evolution* 3, 1432-1441

ZUR STRASSEN, O. (1906). Die Geschichte der T-Riesen von *Ascaris megalocephala* als Grundlage zu einer Entwickelungsmechanik dieser Spezies. Stuttgart. E. Schweizerbartsche Verlagsbuchhandlung (E. Nägele).

UNIVERSITEIT GENT

Academiejaar 2008-2009
Faculteit Wetenschappen

Comparative and phylogenetic analysis of the early embryonic development in the phylum Nematoda

Vergelijkende en fylogenetische analyse van de vroege embryonale ontwikkeling in het fylum Nematoda

PART II: TABLES AND FIGURES


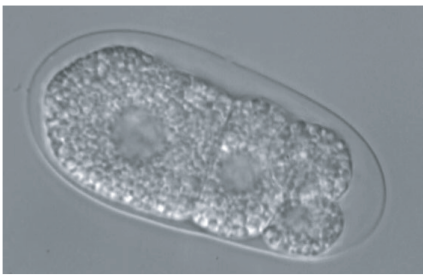


Sandra Vangestel

Promotor: Prof. dr. G. Borgonie

Co-promotors: dr. W. Houthoofd and Prof. dr. T. Artois

Thesis submitted to obtain the degree of Doctor in Sciences (Biology)

Proefschrift voorgelegd tot het bekomen van de graad van Doctor in de Wetenschappen (Biologie)

LIST OF TABLES

LIST OF FIGURES

Figure 1.1 Nomarski photomicrographs showing the early events in the developing *Caenorhabditis elegans embryo*

A Constriction of the membrane near the equator, showing the process of pseudocleavage. **B** The egg pronucleus migrates posteriorly towards the sperm nucleus and they meet in the posterior half of the egg. **C** The first cleavage is asymmetrical with the formation of a larger anterior founder cell AB and a smaller posterior germline cell P1. **D** AB divides in a direction perpendicular to the longitudinal axis. **E** P1 divides in a direction, parallel to the longitudinal axis. **F** After the migration of ABa to the anterior side and ABp to the future dorsal side of the embryo, a rhomboidal configuration is reached. Orientation: anterior to the left, ventral below. Scale bar = 10 μm.

Figure 1.2 Lineage of early cleavages in the *C. elegans* embryo

Establishment of six founder cells AB, MS, E, C, D and P4. Below each founder cell is indicated what type and number of cells that originate from these blastomeres. (adapted from Sulston *et al*., 1983 and Wood, 1991).

Fig. 1.1

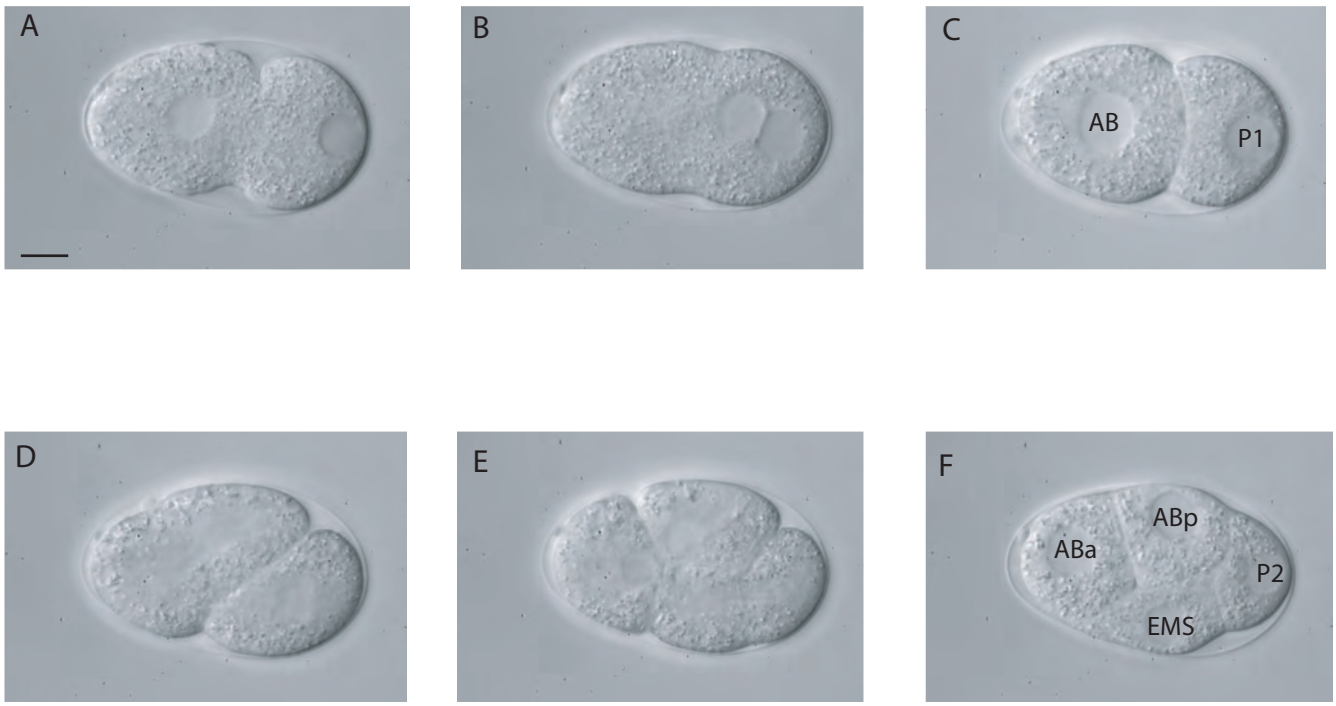
A
B
C
AB
P1
D
E
F
ABp
ABa
P2
EMS

Fig. 1.2

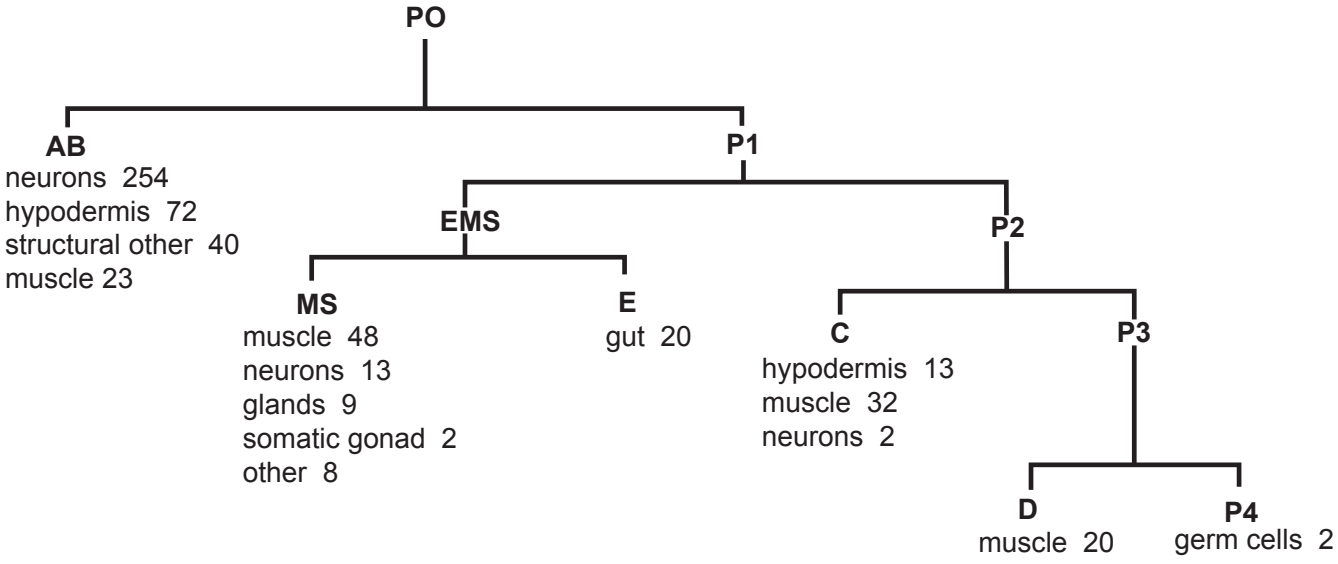
PO
AB
neurons 254
hypodermis 72
structural other 40
muscle 23
P1
EMS
P2
MS
muscle 48
neurons 13
glands 9
somatic gonad 2
other 8
E
gut 20
C
hypodermis 13
muscle 32
neurons 2
P3
D
muscle 20
P4
germ cells 2

Figure 1.3 Spatial configuration of the two-, 4- and 8 cell embryo of *C. elegans*

Orientation: anterior to the left, dorsal to the top.

Figure 1.4 Establishment of different body layers during gastrulation

The figure shows the origin of the three basic layers (endoderm, mesoderm and ectoderm) from the founder cells. **A** Position of founder cells and their descendants at the 26-cell stage, prior to gastrulation. **B** 102-cell stage, after the inward migration of the E, P4 and D descendants. **C** position of the cells at the end of gastrulation. The dotted and dashed lines represent regions from the hypodermis contributed by AB and C, respectively. Blue: ectoderm, red: mesoderm, yellow: endoderm, pink: ectoderm + mesoderm, purple: germline. (Gilbert, 2006 after Schierenberg, 1997).

Fig. 1.3

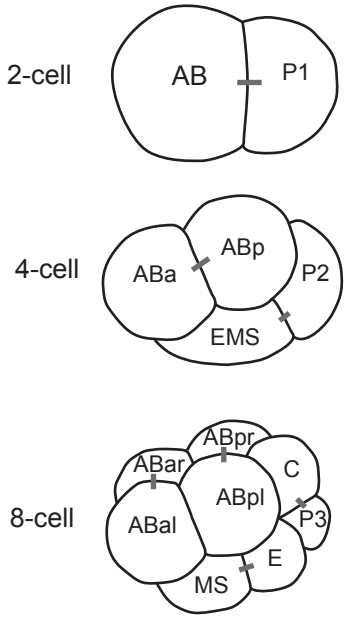

Fig. 1.4

A

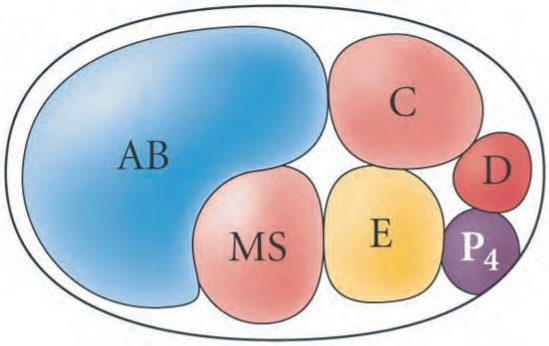

B

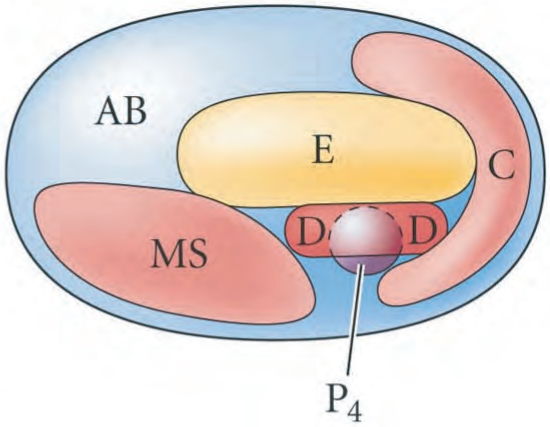

C

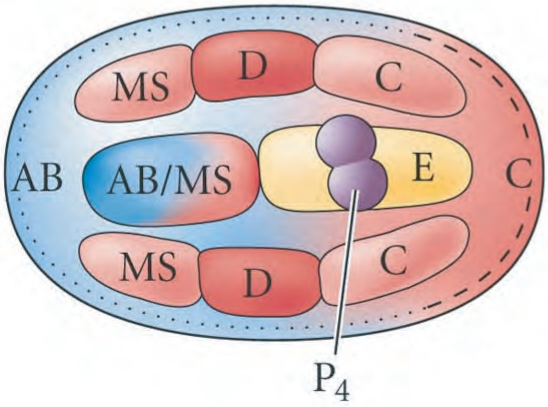

Figure 1.5 The four Notch interactions in the AB lineage

A partial lineage of the AB blastomere is shown in red; for simplicity the vertical axis is not scaled accurately with respect to time. A subset of descendants of ABa and ABp that express GLP-1 or LIN-12 contact various ligand-expressing cells (blue) and activate Notch signalling. Expression of the REF-1 family members occurs about 25 minutes after an interaction (bold black lines).

1 = first induction from P2 to ABp
2 = second induction from MS to ABalp and ABara
3 = third induction from ABalapp to ABplaaa
4 = fourth induction fom MSap to ABplpapp
(Priess, 2005)

Fig. 1.5

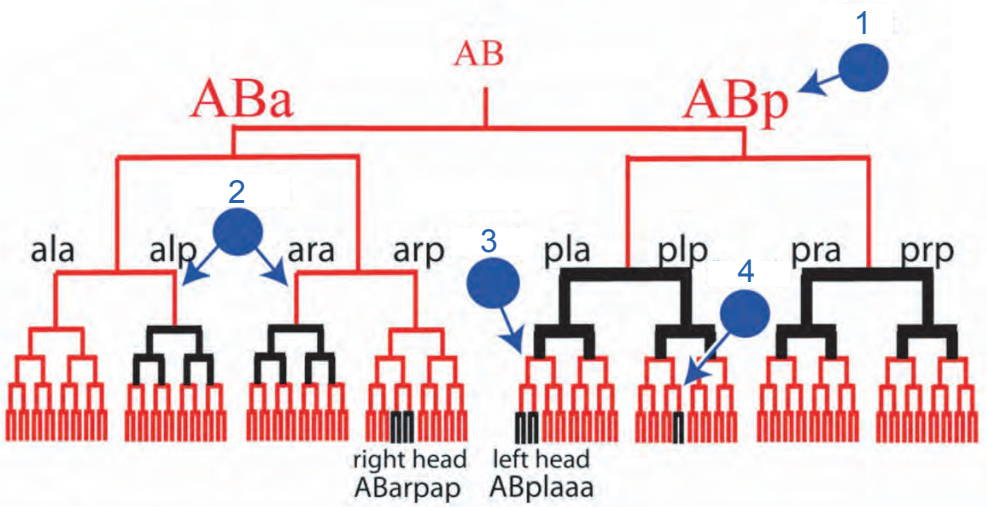
AB
ABa
ABp
1
2
3
4
ala
alp
ara
arp
pla
plp
pra
prp
right head
ABarpap
left head
ABplaaa

Table 1.1 Literature overview of nematodes, which embryonic development has been studied

The nematodes are grouped per clade. Taxa names are given as in the original publication.

Table 1.1

clade	taxon	Species	Reference
1	**Enoplida**	*Enoplus brevis*	Voronov and Panchin (1998), Voronov (1999)
		Enoplus demanei	Malakhov (1994), Malakhov (1998)
		Pontonema vulgare	Malakhov (1994), Malakhov (1998), Voronov, 1999
	Triplonchida	*Tobrilus diversipapillatus*	Schierenberg (2005)
		Trichodorus christiei	Bird *et al.* (1968)
2	**Dioctophymida**	*Eustrongyloides excisus*	Malakhov (1994)
	Mononchida	*Prionchulus* sp.	Malakhov (1994), Borgonie *et al*. (2000)
	Trichinellida	*Trichocephalus trichurus*	Malakhov and Spiridinov (1981), Malakhov (1994)
		Trichuris muris	Schierenberg and Lahl (2004)
	Mermithida	*Gastromermis hibernalis*	Malakhov (1994)
		Romanomermis culicivorax	Schulze and Schierenberg (2008)
	Dorylaimida	*Dorylaimus sp.*	Schierenberg and Lahl (2004)
		Dorylaimus stagnalis	Shafquat *et al.* (1991)
		Labronemapararapax spp.	Shafquat *et al.* (1996)
		Mesodorylaimus brassicus	Shafquat *et al.* (1996)
		M. vulvastriatus	Shafquat *et al.* (1996)
		Drepanodorylaimus flexus	Shafquat *et al.* (1996)
		Aporcelaimus laevis	Shafquat *et al.* (1996)
		Laimydorus baldus	Shafquat *et al.* (1996)
		Labronema goodeyi	Shafquat *et al.* (1996)
		Dorylaimus afghanicus	Shafquat *et al.* (1996)
		Eudorylaimus chauhani	Shafquat *et al.* (1996)
		Aporcelaimellus heynsi	Shafquat *et al.* (1996)
		Xiphinema diversicaudatum	Flegg (1968)
3	**Chromadorida**	*Hypodontolaimus inaequalis*	Malakhov (1994)
4	**Desmodorida**	*Desmodora serpentulus*	Malakhov (1994)
5	**Monhysterida**	*Daptonema setosum*	Malakhov (1994)
	Araeolaimida	*Axonolaimus paraspinosus*	Malakhov (1994)

Table 1.1 (2) Literature overview of nematodes, which embryonic development has been studied

The nematodes are grouped per clade. Taxa names are given as in the original publication.

Table 1.1 (2)

6	**Plectida**	*Plectus* spp.	Maggenti (1961), Drozdovsky (1978)
		Plectus zelli	Tahseen *et al*. (1992)
		Plectus sp. ES601	Lahl *et al.* (2003), Lahl *et al.* (2006)
		Plectus minimus	Goldstein *et al.* (1998), Lahl *et al.* (2003)
		Plectus aquatilis	Goldstein *et al.* (1998), Schierenberg (2000), Lahl *et al.* (2003)
		Anaplectus sp.	Lahl *et al.* (2003)
		Tylocephalus auriculatus	Lahl *et al.* (2003)
		Plectus acuminatus	Lahl *et al.* (2003)
		Ereptonema arcticum	Lahl *et al.* (2003)
7	**Teratocephalidae**	*Teratocephalus lirellus*	Dolinski *et al.* (2001), Lahl *et al.* (2003)
8	**Ascaridida**	*Parascaris equorum (formerly Ascaris megalocephala)*	Boveri (1887, 1899), zur Strassen (1896, 1906), Muller (1903)
9	**Brevibuccidae**	*Plectonchus* sp.	Dolinski *et al.* (2001)
	Rhabditidae	*Caenorhabditis elegans*	Sulston *et al.* (1983), Skiba and Schierenberg (1992), Goldstein (1995), Goldstein *et al.* (1998), Goldstein (2001), Dolinski *et al.* (2001), Laugsch and Schierenberg (2004), Houthoofd *et al.* (2006)
		Caenorhabditis briggsae	Goldstein *et al.* (1998)
		Caenorhabditis remanei	Goldstein *et al.* (1998)
		Pelodera teres =Rhabditis teres	Chuang (1962)
		Dolichorhabditis dolichura DF5033	Goldstein *et al.* (1998)
		Dolichorhabditis dolichuroides	Goldstein *et al.* (1998)
		Cruznema sp.	Dolinski *et al.* (2001)
		Mesorhabditis longespiculosa	Dolinski *et al.* (2001)
		Pellioditis marina	Houthoofd *et al.* (2003); Houthoofd *et al.* (2006)
		Protorhabditis sp.	Dolinski *et al.* (2001)
		Rhabditella axei	Goldstein *et al.* (1998), Dolinski *et al.* (2001)
		Rhabditis belari	Laugsch and Schierenberg (2004)
		Rhabditis broughtonalcocki	Skiba and Schierenberg (1992), Laugsch and Schierenberg (2004)
		Rhabditis dolichura	Bossinger and Schierenberg (1992), Skiba and Schierenberg (1992), Laugsch and Schierenberg (2004)
		Rhabditis terricola	Skiba and Schierenberg (1992); Schierenberg (2000), Laugsch and Schierenberg (2004)

Table 1.1 (3) Literature overview of nematodes, which embryonic development has been studied

The nematodes are grouped per clade. Taxa names are given as in the original publication.

Table 1.1 (3)

9	**Rhabditidae**	*Rhabditoides regina*	Goldstein *et al.* (1998)
		Rhabditis sp.	Dolinski *et al.* (2001)
		Oscheius myriophila	Goldstein *et al.* (1998)
		Pellioditis sp.	Goldstein *et al.* (1998)
		Pellioditis typica	Goldstein *et al.* (1998)
		Pelodera strongyloides	Goldstein *et al.* (1998)
		Teratorhabditis palmarum	Goldstein *et al.* (1998), Dolinski *et al.* (2001)
	Bunonematidae	*Bunonema* sp.	Dolinski *et al.* (2001)
	Diploscapteridae	*Diploscapter* sp.	Dolinski *et al.* (2001)
		Diploscapter orientalis	Tahseen *et al.* (1991)
		Diploscapter coronatus	Lahl (2007)
	Cylindrocorporidae	*Goodeyus ulmi*	Dolinski *et al.* (2001)
	Trichostrongylidae	*Haemonchus contortus*	Goldstein *et al.* (1998)
	Diplogasteridae	*Aduncospiculum halicti*	Goldstein *et al.* (1998), Dolinski *et al.* (2001)
	Neodiplogasteridae	*Diplenteron* sp.	Dolinski *et al.* (2001)
		Pristionchus sp.	Dolinski *et al.* (2001)
		Pristionchus pacificus	Goldstein *et al.* (1998), Dolinski *et al.*(2001), Vangestel *et al.* (2008)
10	**Panagrolaimidae**	*Halicephalobus gingivalis*	Borgonie *et al.* (2000), Dolinski *et al.* (2001), Houthoofd *et al.* (2003), Houthoofd *et al.* (2006)
		Panagrellus redivivus	Goldstein *et al.* (1998), Dolinski *et al.* (2001), Houthoofd *et al.* (2006)
		Panagrobelus stammeri	Houthoofd *et al.* (2006)
		Panagrolaimus sp.	Skiba and Schierenberg (1992), Schierenberg (2000)
		Panagrolaimus sp.	Goldstein *et al.* (1998)
		Panagrolaimus rigidus	Houthoofd *et al.* (2006)
		Panagrolaimus sp.	Goldstein *et al.* (1998)
		Turbatrix aceti	Sulston *et al.* (1983), Goldstein *et al.* (1998)
	Alloionematidae	*Rhabditophanes sp.*	Borgonie *et al.* (2000), Houthoofd *et al.* (2006), Houthoofd & Borgonie (2007)
	Rhabdiasidae	*Rhabdias bufonis*	Spieler and Schierenberg (1995)
	Aphelenchoididae	*Aphelenchoides sp.*	Dolinski *et al.* (2001)
		Aphelenchoides ritsemabosa	Drozdovsky (1967)
		Aphelenchoides besseyi	Drozdovsky (1967)

Table 1.1 (4) Literature overview of nematodes, which embryonic development has been studied

The nematodes are grouped per clade. Taxa names are given as in the original publication.

Table 1.1 (4)

10	**Aphelenchoididae**	*Aphelenchoides fragariae*	Drozdovsky (1967)
		Aphelenchoides dactylocercus	Rowse (1969)
		Pseudaphelenchoides sp.	Drozdovsky (1978)
		Seinura sp.	Drozdovsky (1967)
		Bursaphelenchus xylophilus	Hasegawa *et al.* (2004)
11	**Cephalobidae**	*Acrobeloides nanus*	Skiba and Schierenberg (1992), Bird *et al.* (1993), Bossinger and Schierenberg (1996), Goldstein *et al.* (1998), Wiegner and Schierenberg (1999), Schierenberg (2000), Dolinski *et al.* (2001), Goldstein (2001), Laugsch and Schierenberg (2004), Lahl *et al.* (2006)
		Acrobeles complexus	Thomas (1965), Dolinski *et al.* (2001)
		Acrobeloides sp.	Dolinski *et al.* (2001)
		Cephalobus cubaensis	Borgonie *et al.* (2000), Dolinski *et al.* (2001), Houthoofd *et al.* (2006)
		Cervidellus alutus	Dolinski *et al.* (2001)
		Chiloplacus sp.	Dolinski *et al.* (2001)
		Eucephalobus sp.	Dolinski *et al.* (2001)
		Pseudoacrobeles sp.	Dolinski *et al.* (2001)
		Nothacrobeles sp.	Dolinski *et al.* (2001)
		Zeldia punctata	Goldstein *et al.* (1998), Dolinski *et al.* (2001)
		Acrobeloides sp. ES501	Goldstein *et al.* (1998)
		Acrobeloides sp. PS1146	Goldstein *et al.* (1998)
		Acrobeloides sp. PS1156	Goldstein *et al.* (1998)
		Cephalobus oryzae	Goldstein *et al.* (1998)
		Cephalobus sp. PS1215	Goldstein *et al*. (1998)
		Chilopacus minimus	Goldstein *et al.* (1998)
12	**Aphelenchidae**	*Aphelenchus* sp.	Dolinski *et al.* (2001)
		Aphelenchus avenae	Drozdovsky (1978)
		Paraphelenchus sp.	Drozdovsky (1978)
	Tylenchidae	*Tylenchus davainei*	Drozdovsky (1978)
		Filenchus sp.	Drozdovsky (1978)
		Aglenchus costatus	Drozdovsky (1978)
		Psilenchus sp.	Drozdovsky (1978)

Table 1.1 (5) Literature overview of nematodes, which embryonic development has been studied

The nematodes are grouped per clade. Taxa names are given as in the original publication.

Table 1.1 (5)

12	**Tylenchidae**	*Boleodorus thylactus*	Drozdovsky (1978)
	Anguinidae	*Ditylenchus* sp.	Drozdovsky (1967)
		Ditylenchus destructor	Anderson and Darling (1964)
		Ditylenchus dipsaci	Yuksel (1960), van Weerdt (1960)
		Ditylenchus myceliophagus	Brun and Cayrol (1970)
		Anguina millefolii	Drozdovsky (1978)
	Criconematidae	*Hemicriconemoides chitwoodi*	Fassuliotis (1962)
		Criconemoides xenoplax	Seshadri (1965)
	Hoplolaimidae	*Rotylenchus parvus*	Dasgupta and Raski (1968)
		Helicotylenchus sp.	Drozdovsky (1978)
		Hoplolaimus columbus	Fassuliotis (1975)
		Hoplolaimus indicus	Dasgupta *et al.* (1970) (in Fassuliotis 1975)
		Neodolichodorus rostrulatus	Sarr *et al.* (1987)
		Rotylenchus sp.	Drozdovsky (1978)
	Belonolaimidae	*Belonolaimus longicaudatus*	Dolinski *et al.* (2001)
	Pratylenchidae	*Pratylenchus brachyurus*	Dolinski *et al.* (2001)
		Pratylenchus scribneri	Roman and Hirschmann (1969)
		Pratylenchus penetrans	Hung and Jenkins (1969)
		Pratylenchus zeae	Hung and Jenkins (1969)
		Nacobbus aberrans	Dolinski *et al.* (2001)
		Nacobbus serendipiticus	Clark (1967)
		Radopholus similis	Van Weerdt (1960)
		Zygotylenchus guevarai	Vovlas (1977)
	Meloidogynidae	*Heterodera schachtii*	Raski (1950), Dolinski *et al.* (2001)
		Heterodera zeae	Shahina en Maqbool (1989)
		Meloidogyne javanica	Bird (1972)
		Meloidogyne incognita	Goldstein *et al.* (1998), Dolinski *et al.* (2001)
	Allantonematidae	*Bradynema rigidum*	zur Strassen (1959), Skiba and Schierenberg (1992)

Figure 1.6 Phylogenetic tree for the phylum Nematoda

Tree based on 18SrDNA, according to Holterman *et al.* (2006). Twelve major clades (Arabic numbers) are identified. The 5 major clades identified by Blaxter *et al*. (1998) (Roman numbers), are shown in colours.

Fig. 1.6

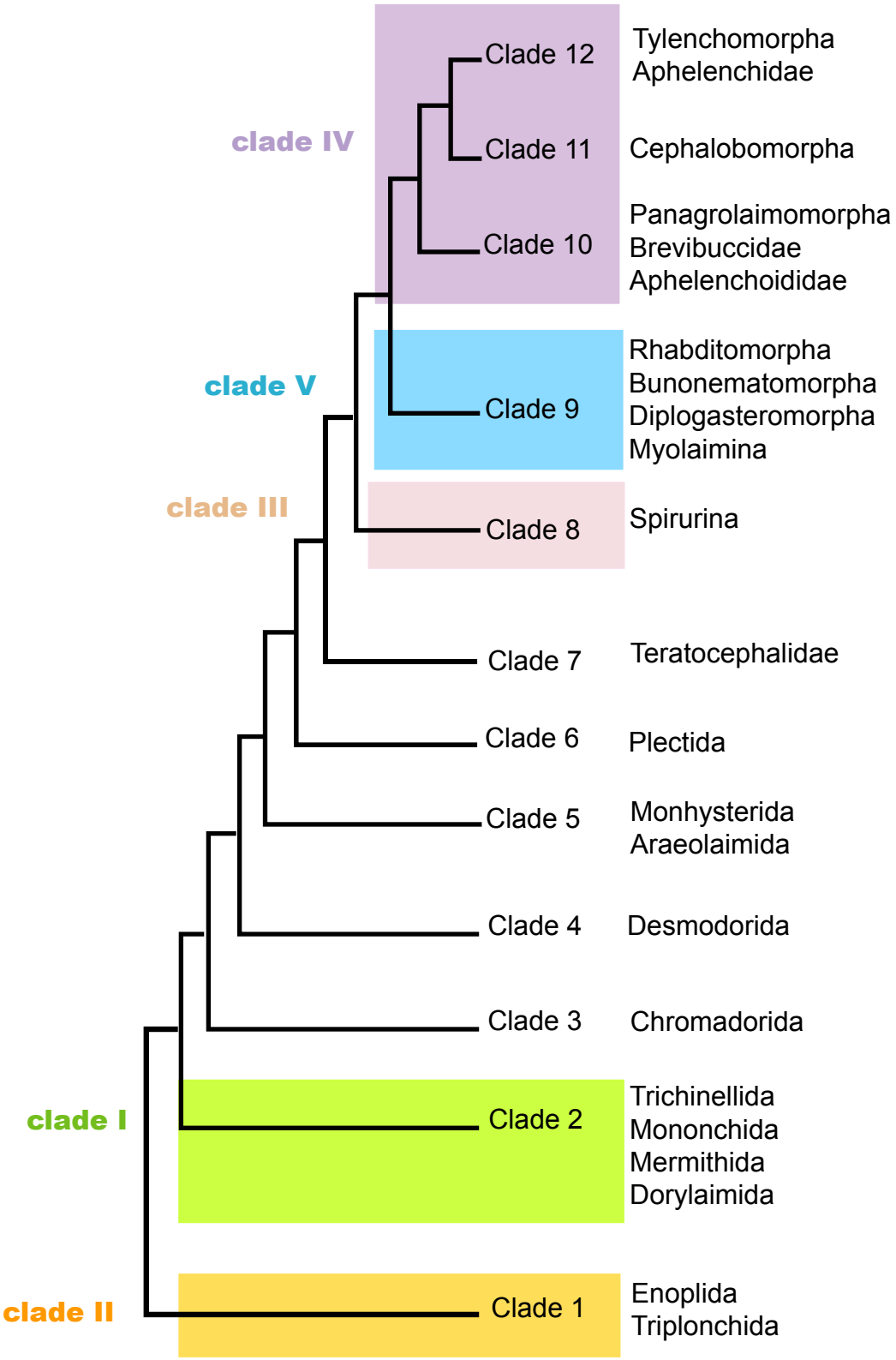
clade IV
clade V
clade III
clade I
clade II
Clade 12
Clade 11
Clade 10
Clade 9
Clade 8
Clade 7
Clade 6
Clade 5
Clade 4
Clade 3
Clade 2
Clade 1
Tylenchomorpha
Aphelenchidae
Cephalobomorpha
Panagrolaimomorpha
Brevibuccidae
Aphelenchoididae
Rhabditomorpha
Bunonematomorpha
Diplogasteromorpha
Myolaimina
Spirurina
Teratocephalidae
Plectida
Monhysterida
Araeolaimida
Desmodorida
Chromadorida
Trichinellida
Mononchida
Mermithida
Dorylaimida
Enoplida
Triplonchida

Figure 2.1 Possible configurations in the four-cell stage

A linear configuration, **B** partially linear configuration, **C** rhomboidal configuration and **D** tetrahedral configuration. (adapted from Dolinski *et al*., 2001).

Figure 2.2 Diagram representing the four possible configurations of the posterior cells

A: no reversal of polarity in germline divisions leading to the configuration C-D-P4. One reversal of polarity in P2, leading to **B:** the configuration C-P4-D or **C:** the configuration P4-D-C (*C. elegans* pattern). **D**: double reversal of polarity in germline divisions, leading to the configuration D-P4-C. Orientation: anterior to the left, dorsal to the top

Fig. 2.1

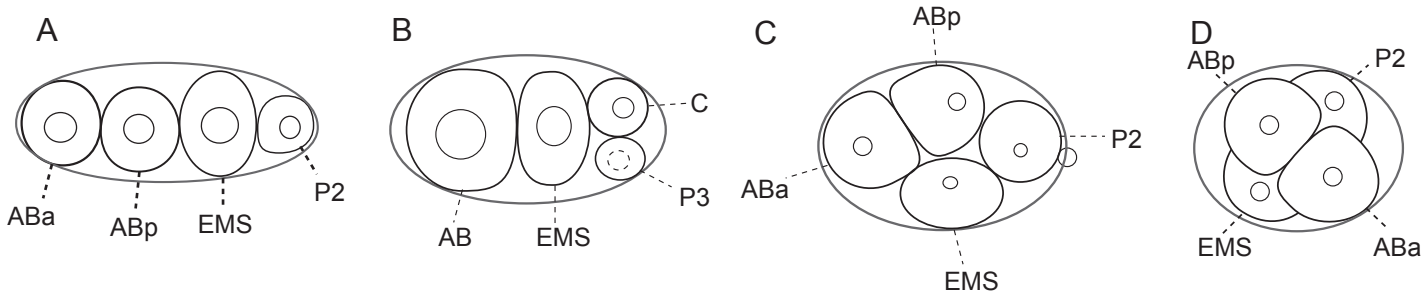
A
ABa
ABp
EMS
P2
B
AB
EMS
C
P3
C
ABp
ABa
P2
EMS
D
ABp
P2
EMS
ABa

Fig. 2.2

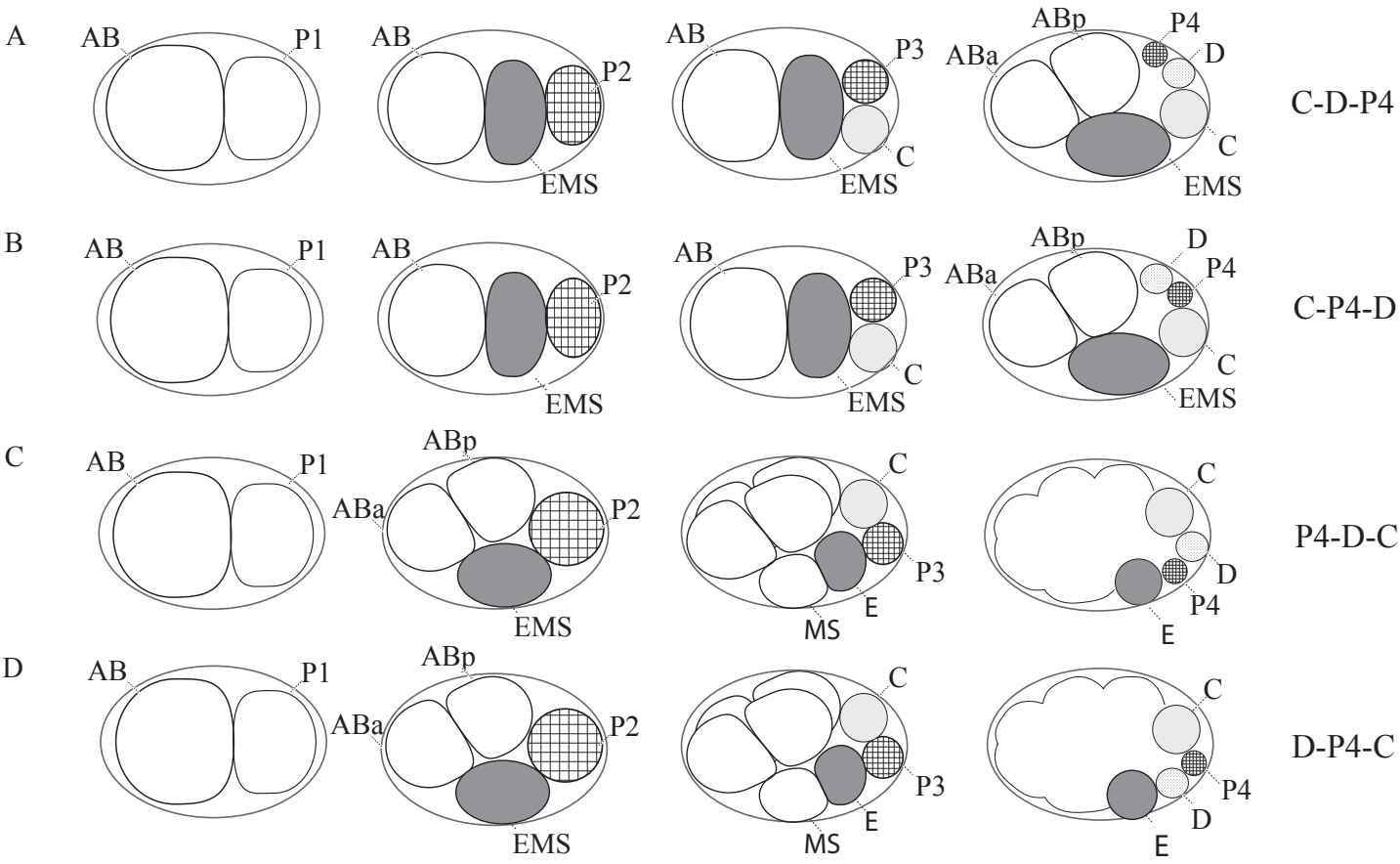
A
AB
P1
AB
P2
EMS
AB
P3
C
EMS
ABp
P4
D
ABa
C
EMS
C-D-P4
B
AB
P1
AB
P2
EMS
AB
P3
C
EMS
ABp
D
P4
ABa
C
EMS
C-P4-D
C
AB
P1
ABp
ABa
P2
EMS
C
P3
E
MS
C
D
P4
E
P4-D-C
D
AB
P1
ABp
ABa
P2
EMS
C
P3
E
MS
C
P4
D
E
D-P4-C

Table 2.1 Overview of the analyzed strains

The number between brackets is the number of lineages which were established for that species. For the calculation of the egg shape index (ESI) sometimes more individuals were examined, but this number will be given in the corresponding table of ESI. [a] Only the 5 examined characters in chapter 4 were examined in these species, [b] CGC = Caenorhabditis Genomics Centre

Table 2.2 Overview of the strains, for which data were obtained from literature

Table 2.1

Clade	Family	Species	Code	Source
2	**Mononchidae**	*Prionchulus punctatus* (n=3)[a]	GB0021	G. Borgonie, Ghent University, Belgium
6	**Plectidae**	*Plectus aquatilis* (n=5)	PDL0018	P. De Ley, University of California, Riverside
9	**Diplogastridae**	*Pristionchus pacificus* (n=12)	PS 312	CGC[b], University of Minnesota
	Rhabditidae	*Caenorhabditis elegans* (n=8)	N2	CGC, University of Minnesota
		Caenorhabditis remanei (n=3)	PB206	CGC, University of Minnesota
		Mesorhabditis longespiculosa (n=3)	DF5017	CGC, University of Minnesota
		Mesorhabditis miotki (n=3)	AF72	CGC, University of Minnesota
		Oscheius dolichuroides (n=3)	DF5018	CGC, University of Minnesota
		Pellioditis marina (n=2)	TM02	T. Moens, University of Ghent, Belgium
		Pelodera strongyloides (n=3)	DF5022	CGC, University of Minnesota
		Rhabditella axei (n=3)	DF5006	CGC, University of Minnesota
		Teratorhabditis palmarum (n=2)	DF5019	CGC, University of Minnesota
10	**Panagrolaimidae**	*Halicephalobus gingivalis* (n=3)	JB128	P. De Ley, University of California, Riverside
		Panagrellus redivivus (n=2)	PS1163	CGC, University of Minnesota
		Panagrolaimus detritophagus (n=3)	BS0008	A. Burnell, National University of Ireland, Maynooth
		Panagrolaimus rigidus (n=3)	AF36	CGC, University of Minnesota
		Procephalobus sp. (n=3)	JU 169	P. De Ley, University of California, Riverside
	Alloionematidae	*Rhabditophanes sp.* (n=2)	PDL0036	P. De Ley, University of California, Riverside
11	**Cephalobidae**	*Acrobeloides butschlii* (n=3)	DWF1107	CGC, University of Minnesota
		Acrobeloides maximus[a] (n=3)	DWF5048	P. De Ley, University of California, Riverside
		Acrobeloides nanus (n=2)	BSS0003	R. Rhode, University of California, Davis
		Acrobeloides thornei (n=3)	DWF1109	CGC, University of Minnesota
		Cephalobus cubaensis (n=3)	PS1197	R. Rhode, University of California, Davis
12	**Meloydoginidae**	*Meloidogyne incognita* (n=3)		G. Gheysen, University of Ghent, Belgium

Table 2.2

Clade	Taxon	Species	Source
1	Enoplida	*Enoplus brevis*	Voronov and Panchin (1998), Voronov (1999)
		Pontonema vulgare	Malakhov (1994), Malakhov (1998), Voronov *et al.* (1999)
	Triplonchida	*Tobrilus diversipappilatus*	Schierenberg (2005)
2	Trichinellida	*Trichocephalus trichurus*	Malakhov and Spiridinov (1981), Malakhov (1994)
	Mermithida	*Romanomermis culicivorax*	Schulze and Schierenberg (2008)
		Gastromermis hibernalis	Malakhov (1994)
3	Chromadorida	*Hypodontolaimus inaequalis*	Malakhov (1994)
4	Desmodorida	*Desmodora serpentulus*	Malakhov (1994)
5	Areolaimida	*Axonolaimus paraspinosus*	Malakhov (1994)
	Monhysterida	*Daptonema setosum*	Malakhov (1994)
6	Plectida	*Tylocephalus auriculatus*	Lahl *et al.* (2003)
		Plectus minimus	Goldstein *et al.* (1998), Lahl *et al.* (2003)
7	Teratocephalidae	*Teratocephalus lirellus*	Dolinski *et al.* (2001), Lahl *et al.* (2003)
8	Ascaridida	*Parascaris equorum (formerly Ascaris megalocephala)*	Boveri (1887, 1899), zur Strassen (1896, 1906), Muller (1903)
9	Rhabditidae	*Rhabditis terricola*	Laugsch and Schierenberg (2004)
		Rhabditis dolichura	Laugsch and Schierenberg (2004)
	Diploscapteridae	*Diploscapter coronatus*	Lahl (2007)
10	Rhabdiasidae	*Rhabdias bufonis*	Spieler and Schierenberg (1995)
	Aphelenchoididae	*Bursaphelenchus xylophilus*	Hasegawa *et al.* (2004)

Figure 3.1 Cell lineage of the first divisions of *Plectus aquatilis*

A-D Lineages of embryos 1-4. The vertical axis indicates time of development and every division is visualised by a horizontal bar. The left branch is always the anterior/left/dorsal sister. Time starts after the division of AB. For reasons of uniformity the P cells are always the posterior branches.

Fig. 3.1

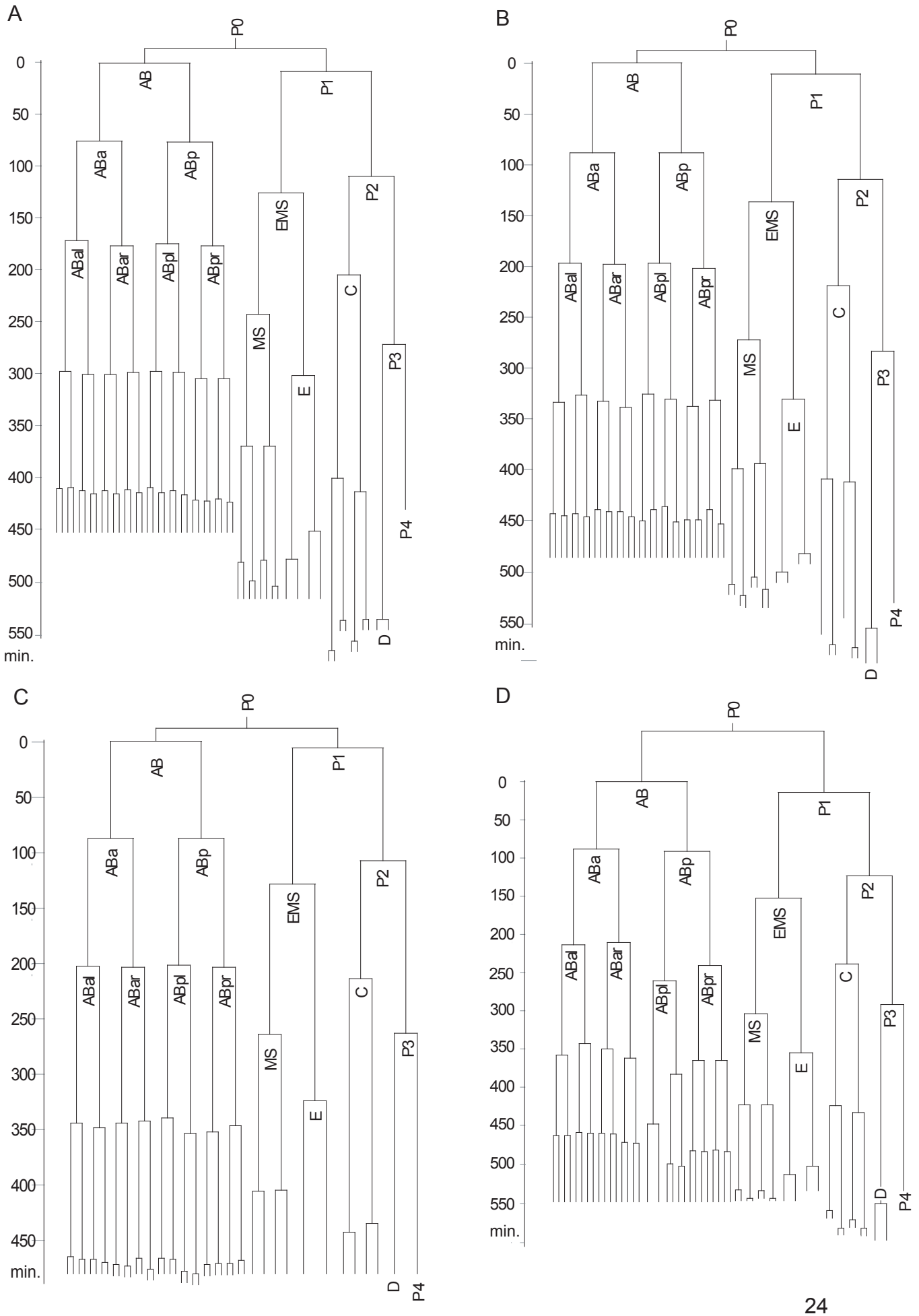
A
B
C
D
P0
AB
P1
ABa
ABp
EMS
P2
ABal
ABar
ABpl
ABpr
MS
E
C
P3
D
P4
0
50
100
150
200
250
300
350
400
450
500
550
min.

Fig. 3.1 (2) Cell lineage of the first divisions of *P. aquatilis*

E Lineage of embryo 5. The vertical axis indicates time of development and every division is visualised by a horizontal bar. The left branch is always the anterior/left/dorsal sister. Time starts after the division of AB.

Figure 3.2 Complex movements of the complete embryo within the eggshell of *P. aquatilis*

A Tetrahedral configuration in the 4-cell stage, which is converted into **B** the rhomboidal configuration as seen in the *C. elegans* embryo. **C** In the 8-cell stage MS comes to lie closest to the anterior pole. **D** In the 12 cell stage the embryo rotated again, placing MS to this side, which was assigned as the dorsal side in the 4-cell stage embryo. **D** The position of the two daughter cells of MS before the division of the 8 AB cells. **E** Rotation of the two daughter cells of MS after the division of the 8 AB cells. **F** Rotation of the embryo after the division of 16AB. Orientation: A-B: lateral view, anterior to the right; C-F ventral view. Dashed line represents the a-p axis of the embryo. Scale bar = 10 µm.

Fig. 3.1

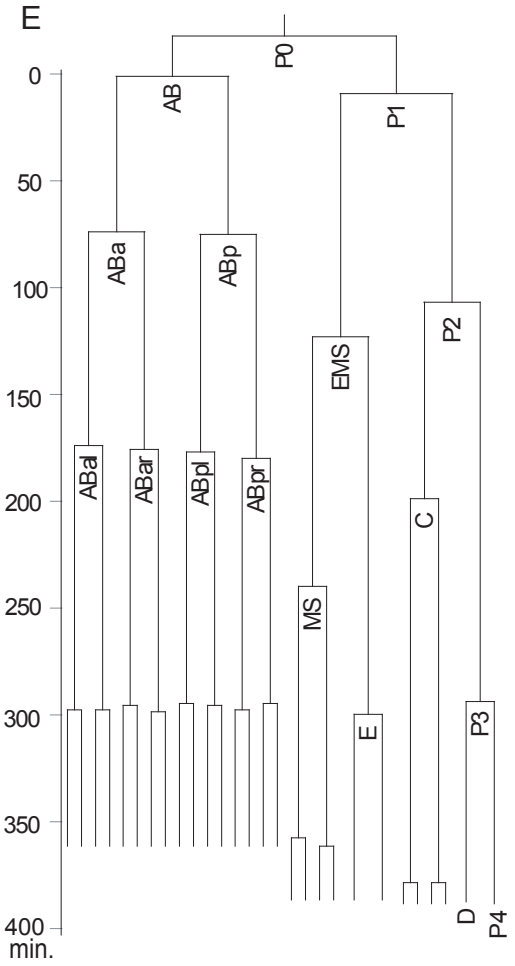
E
0
50
100
150
200
250
300
350
400
min.
P0
AB
P1
ABa
ABp
EMS
P2
ABal
ABar
ABpl
ABpr
MS
E
C
P3
D
P4

Fig. 3.2

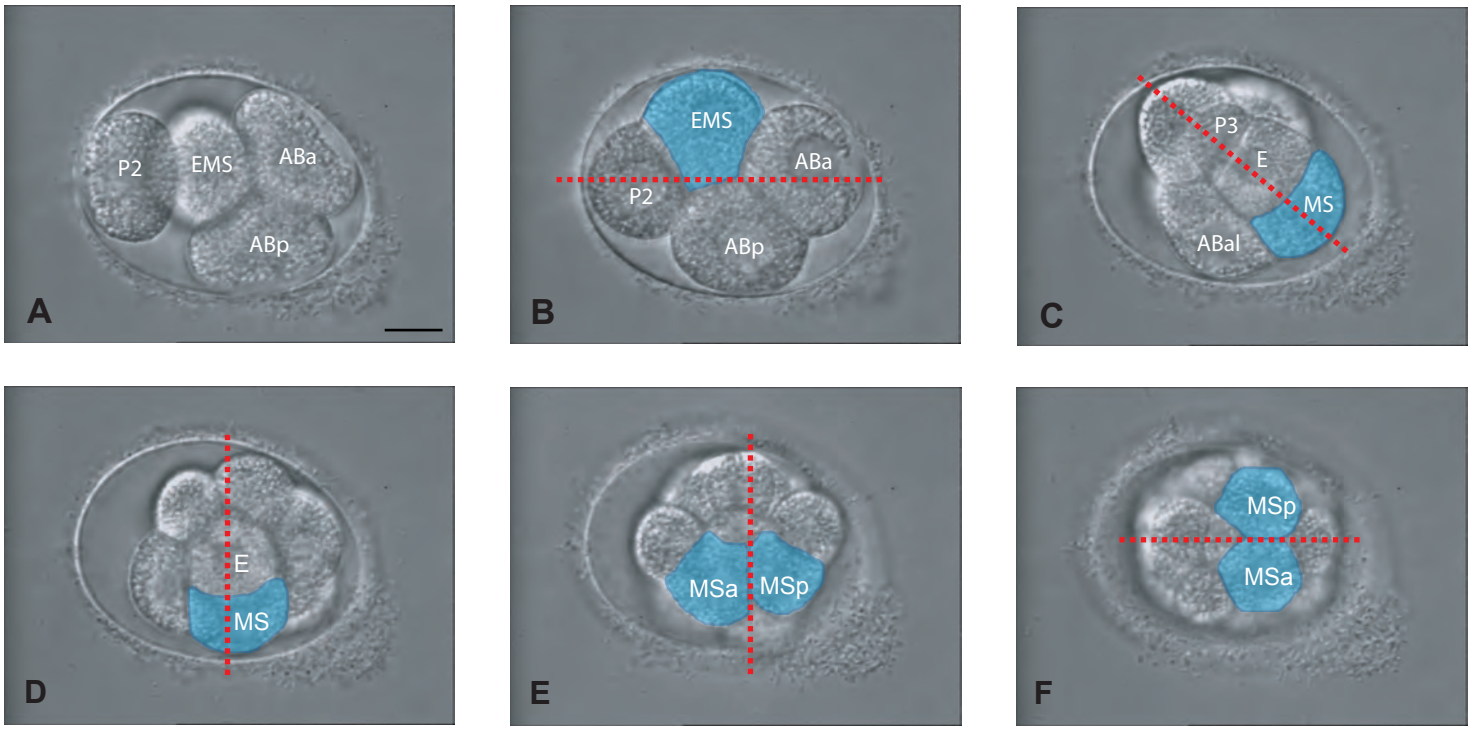
P2
EMS
ABa
ABp
A
EMS
ABa
P2
ABp
B
P3
E
MS
ABal
C
E
MS
D
MSa
MSp
E
MSp
MSa
F

Figure 3.3 Schematic representation of 8-cell embryos of *P. aquatilis* and *C. elegans*

A *C. elegans*; ABpl (not shown) is located behind MS, E and ABpr. **B** *P. aquatilis*; ABal and ABpl (not shown) are located directly behind their right sister cells ABar and ABpr. Orientation: anterior to the right, dorsal to the top.

Table 3.1 Division sequence of the early cell divisions in *P. aquatilis*

The division sequences of embryo 1-3 of *P. aquatilis*, the sequence described in Lahl *et al*. (2003) and the division sequence of *C. elegans*. Germline divisions are marked in bold.

Figure 3.4 Number of cells during embryonic development for *P. aquatilis*, compared to *C. elegans*.

Time (min) starts after the division of AB.

Fig. 3.3

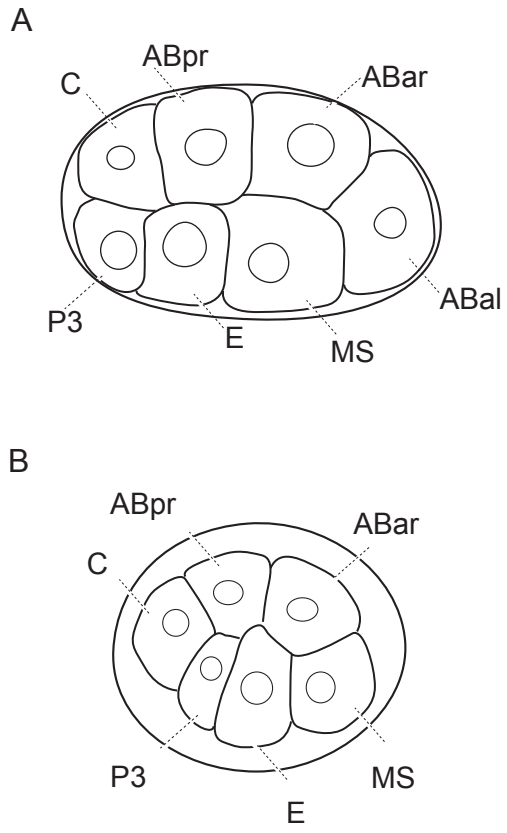

Table 3.1

P. aquatilis				*C. elegans*
embr 1	embr 2	embr 3	Lahl *et al.* (2003)	
AB	AB	AB	AB	AB
P1	**P1**	**P1**	**P1**	**P1**
2AB	2AB	2AB	2AB	2AB
P2	**P2**	**P2**	**P2**	EMS
EMS	EMS	EMS	EMS	**P2**
4AB	4AB	4AB	4AB	4AB
C	C	C	C	MS
MS	**P3**	**P3**	MS	E
P3	MS	MS	**P3**	C
8AB	E	E	8AB	8AB
E	8AB	8AB	E	**P3**
2MS	2MS	2MS	2MS	2MS
2C	2C	2C	2C	2C
16AB	16AB	16AB	16AB	16AB
2E	2E	2E	2E	2E
4MS	4MS	4MS	4MS	4MS
D	D	D	D	D

Fig. 3.4

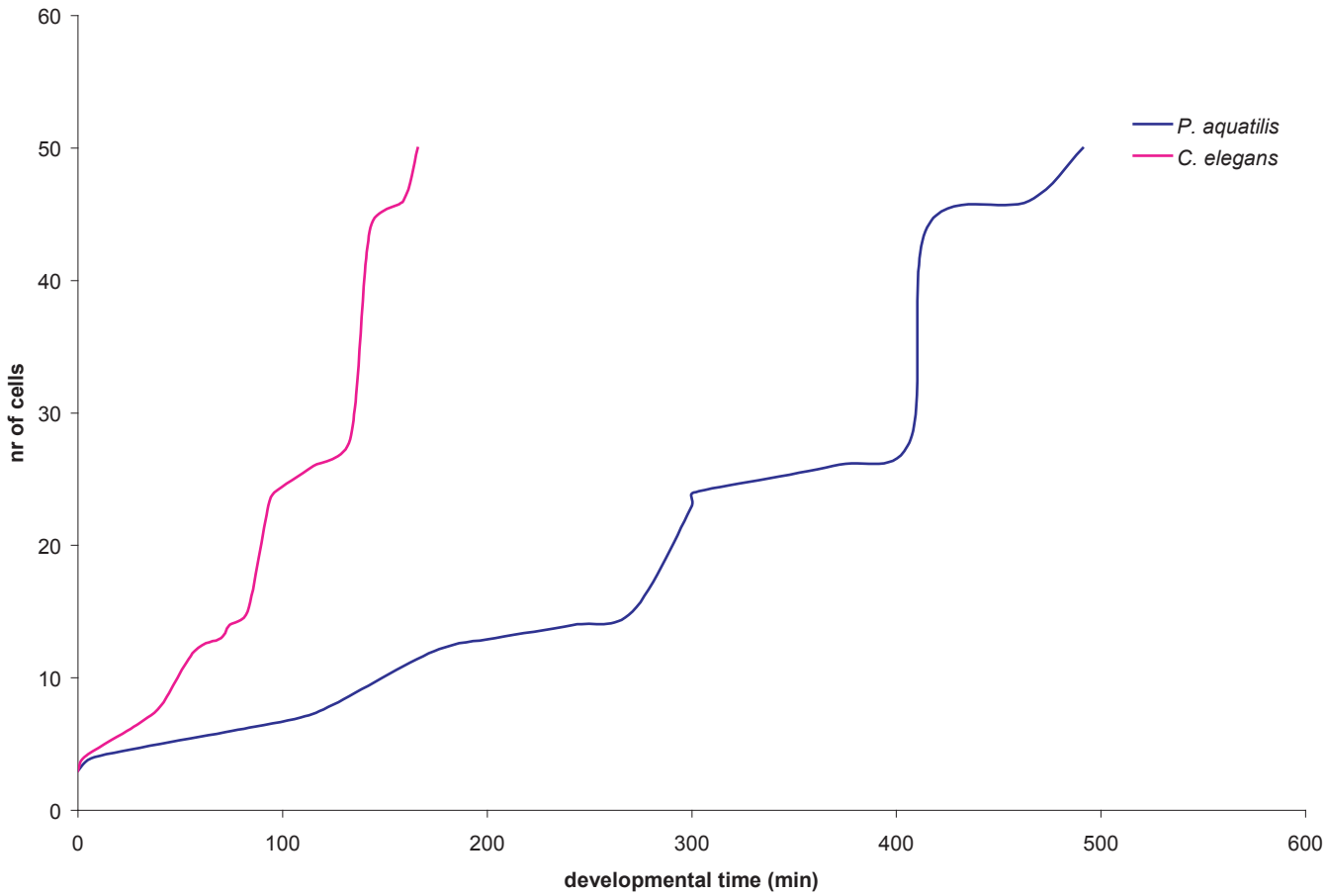

Figure 3.5 Average cell cycle lengths (± SD) of AB generations plotted over time for *P. aquatilis*

The average cell cycle length for each AB stage was calculated based on 3 recordings.

Figure 3.6 Cell division periods in time for three recorded embryos of *P. aquatilis*

Cell division rounds per founder cell in time (min) in *P. aquatilis*, showing differences in cell-cycle times for the six founder cells (for 3 recorded embryos). On each horizontal line the cell division events of one founder cell are given. Each solid black box indicates the time from the division of the first cell to the division of the last cell in a given round of division. Time (min) starts after the division of AB.

Fig. 3.5

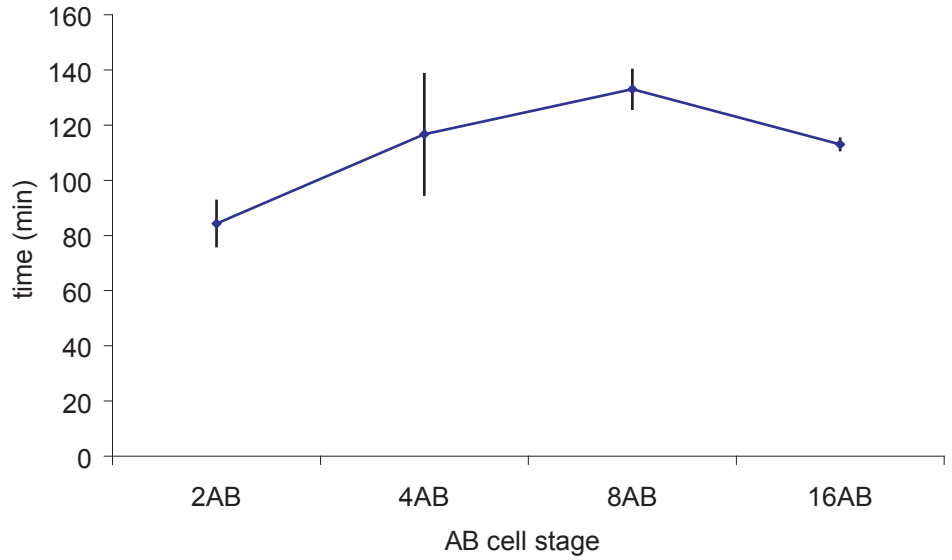
160
140
120
100
80
60
40
20
0
time (min)
2AB
4AB
8AB
16AB
AB cell stage

Fig. 3.6

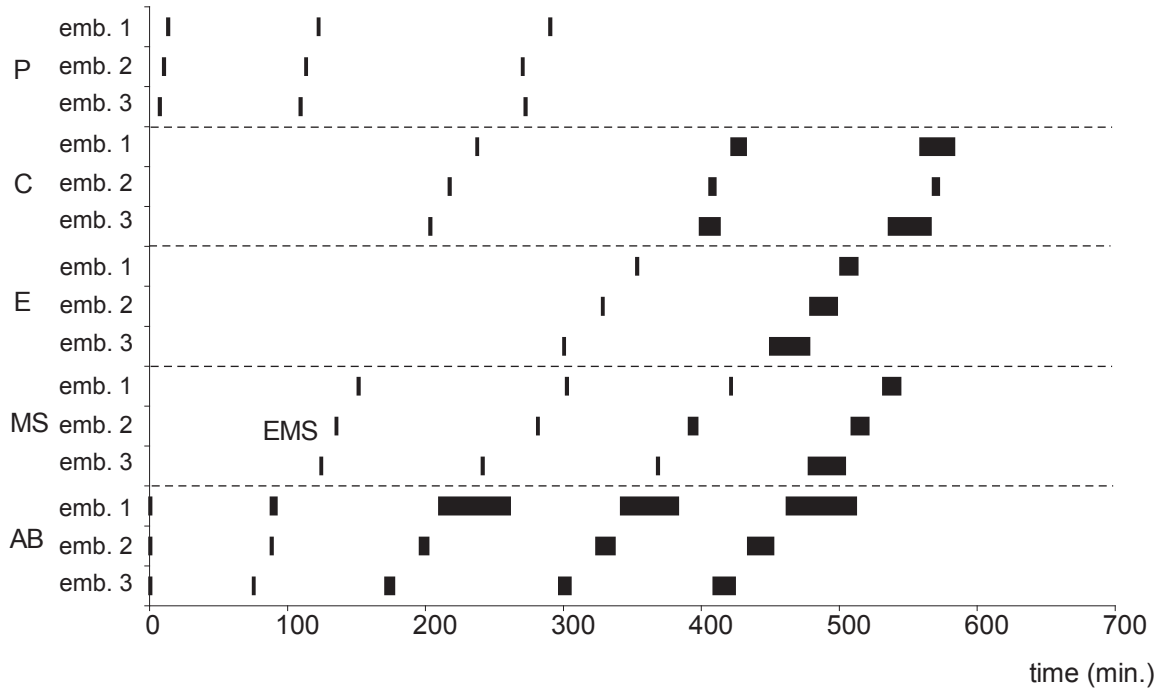
P
C
E
MS
AB
emb. 1
emb. 2
emb. 3
EMS
0
100
200
300
400
500
600
700
time (min.)

Figure 3.7 Gastrulation in *P. aquatilis*

A Only one E cell (marked by a *) migrates to the interior of the embryo. **B** After 80-120 min (24 cell stage) the E cell divides. **C** In the 44 cell stage the two E cells divide again. Orientation: ventral view. Scale bar = 10 µm.

Figure 3.8 Formation of bilateral symmetry in the MS and C lineage in *P. aquatilis*

A 8-cell stage, **B** 13-cell stage, **C** 26-cell stage, **D** 44-cell stage. For better visibility, the AB cells were omitted in D. Orientation: ventral view, anterior to the right.

Fig 3.7


A
B
C

Fig 3.8

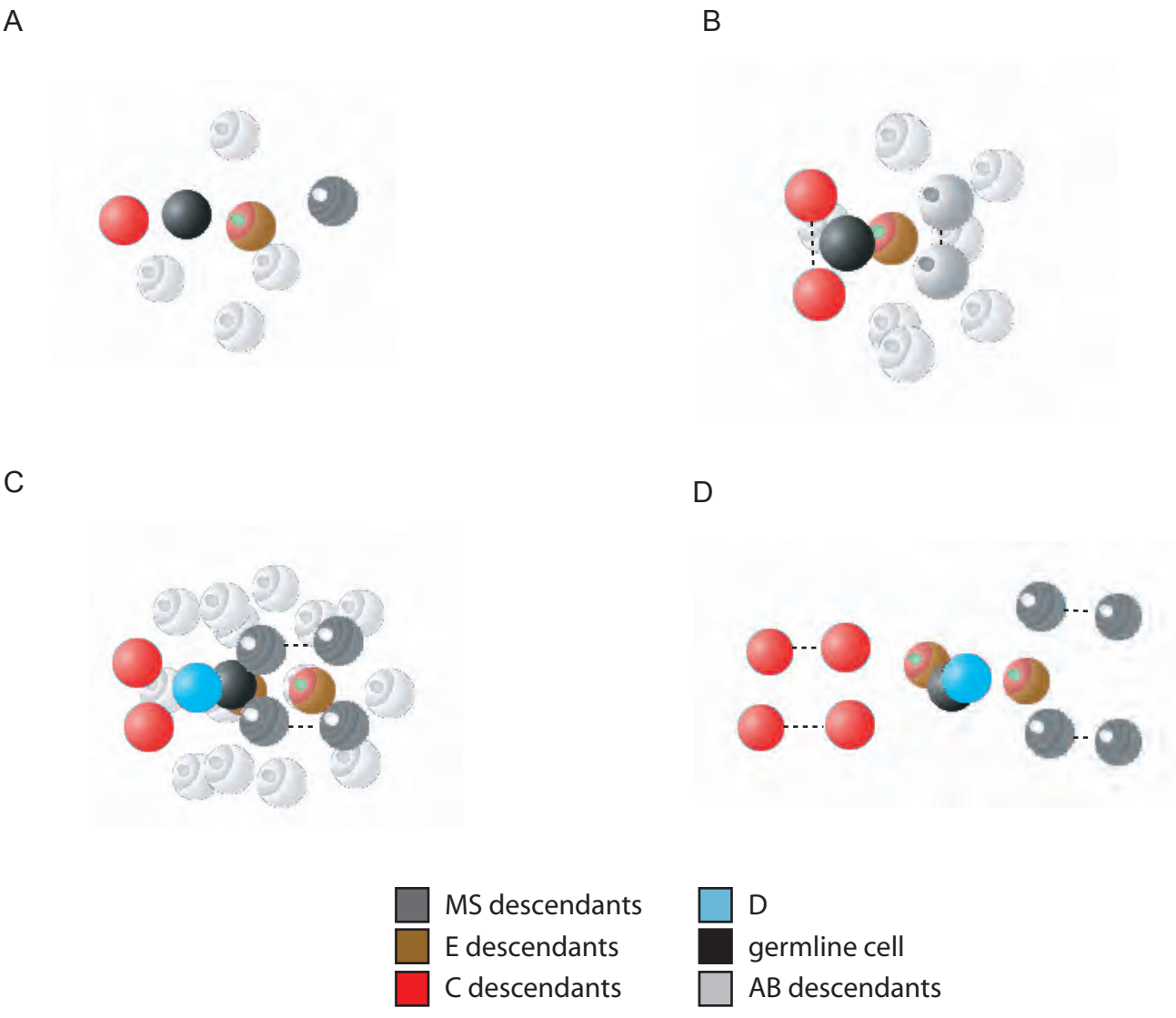
A
B
C
D
MS descendants
E descendants
C descendants
D
germline cell
AB descendants

Figure 3.9 Formation of bilateral symmetry in the AB lineage in *P. aquatilis*

Dashed lines represent mirror image axes. Three different patterns were observed. **A** The mirror image axis is built by the descendants of ABarp and ABplp (2/5 embryos) and ABala-ABara, ABalp-ABprp and ABpla-ABpra descendants form contralateral partners. **B** This axis is built by the descendants of ABpra and ABprp (2/5 embryos) and ABala-ABalp, ABplp-ABarp and ABpla-ABara descendants form contralateral partners. **C** This axis is built by the descendants of ABpla and ABplp and ABara-ABarp, ABalp-ABprp and ABala-ABpra form contralateral partners. Orientation: dorsal view, anterior to the top.

Figure 3.10 The 4AB stage *P. aquatilis*

A The left daughters of the 2AB cells, ABal and ABpl, are skewed into the anterior direction. **B** the right daughters of the 2AB cell stage, ABar and ABpr are shifted to the anterior direction. **C** The division of ABa and ABp does not occur in a left-right direction, positioning ABar and ABpr as the most anterior blastomeres. Daughter cells are connected with a dashed line.

Fig. 3.9

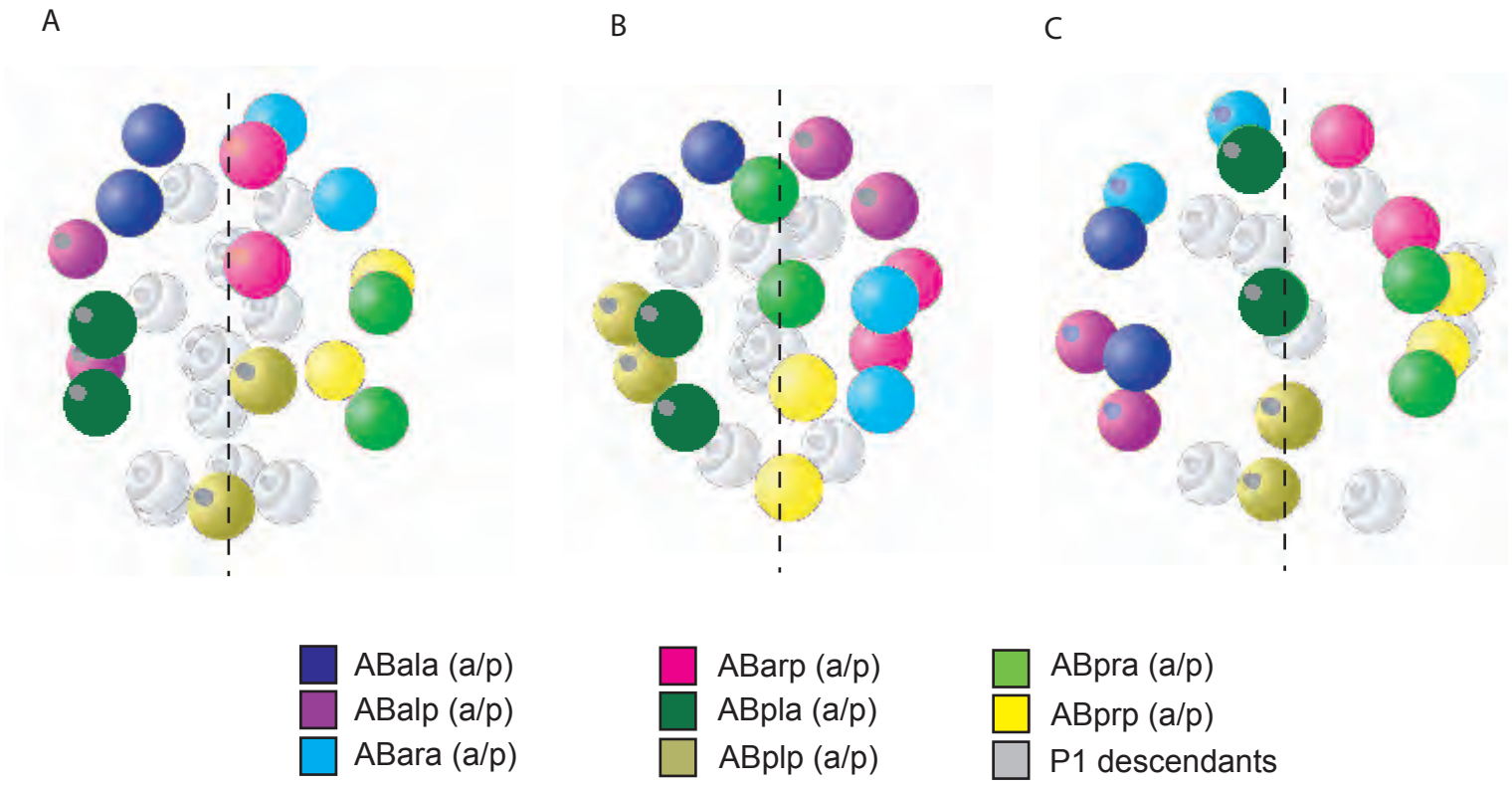

Fig. 3.10

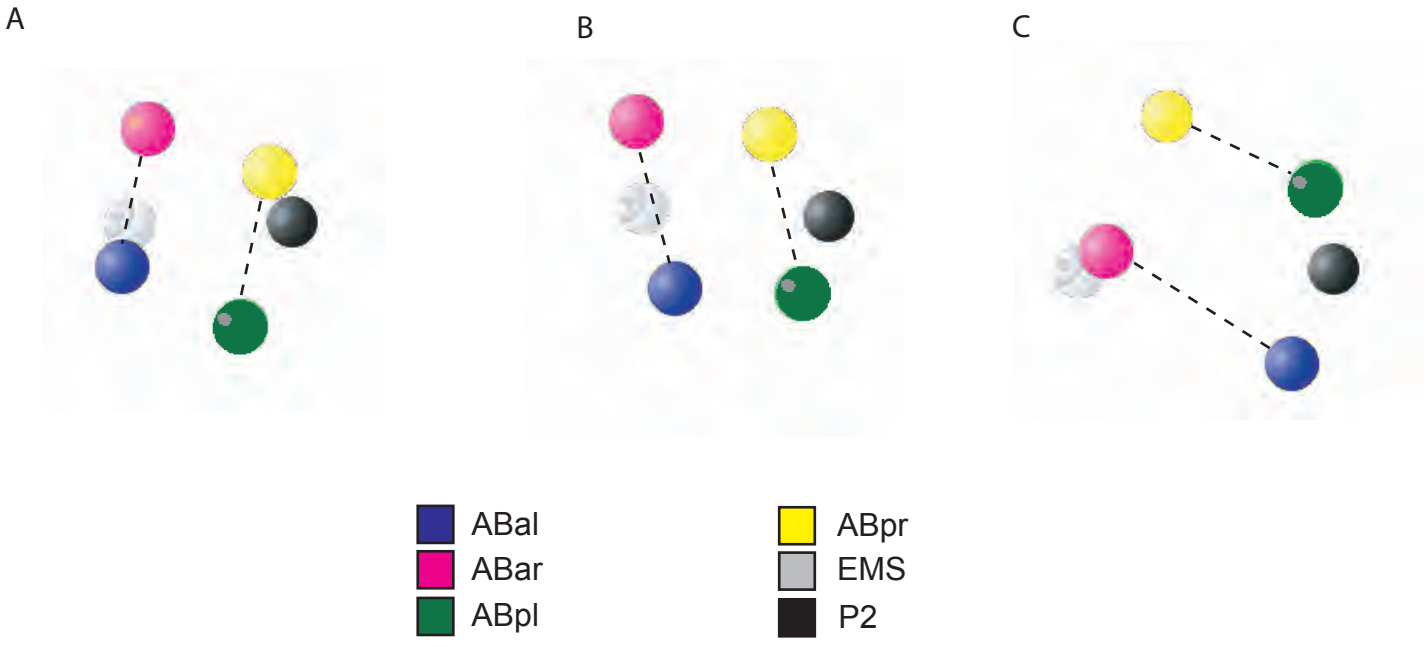

Figure 3.11 Cell lineage of the first divisions of *C. elegans*

A-**D** Lineages of embryos 1-4. The vertical axis indicates time of development and every division is visualised by a horizontal bar. The left branch is always the anterior/left/dorsal sister. Time starts after the division of AB.

Fig. 3.11

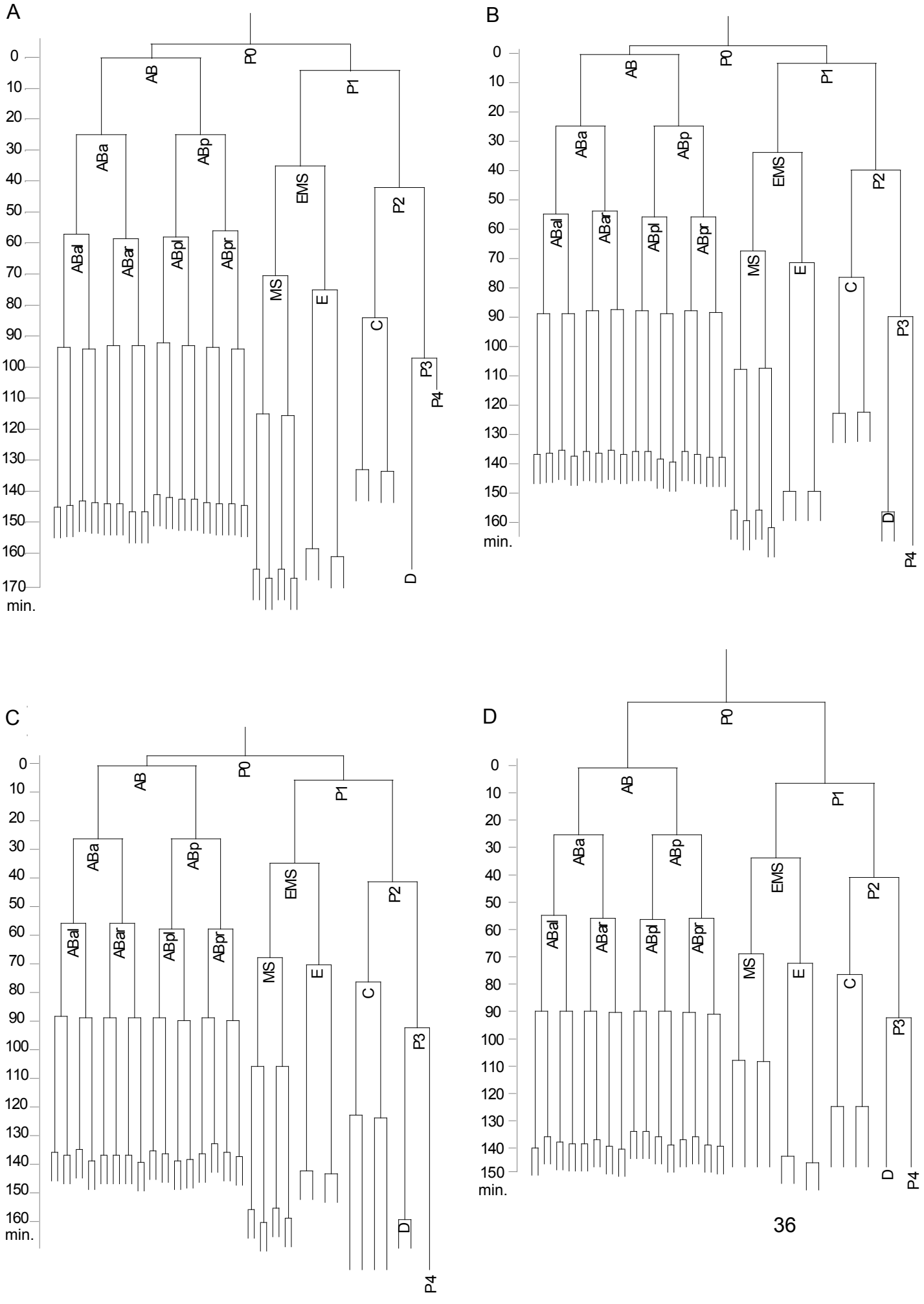
A
B
C
D
0
10
20
30
40
50
60
70
80
90
100
110
120
130
140
150
160
170
min.
P0
AB
P1
ABa
ABp
EMS
P2
ABal
ABar
ABpl
ABpr
MS
E
C
P3
P4
D

Fig. 3.11 (2) Cell lineage of the first divisions of *C. elegans*

E-G Lineages of embryos 5-7. The vertical axis indicates time of development and every division is visualised by a horizontal bar. The left branch is always the anterior/left/dorsal sister. Time starts after the division of AB.

Fig. 3.11 (2)

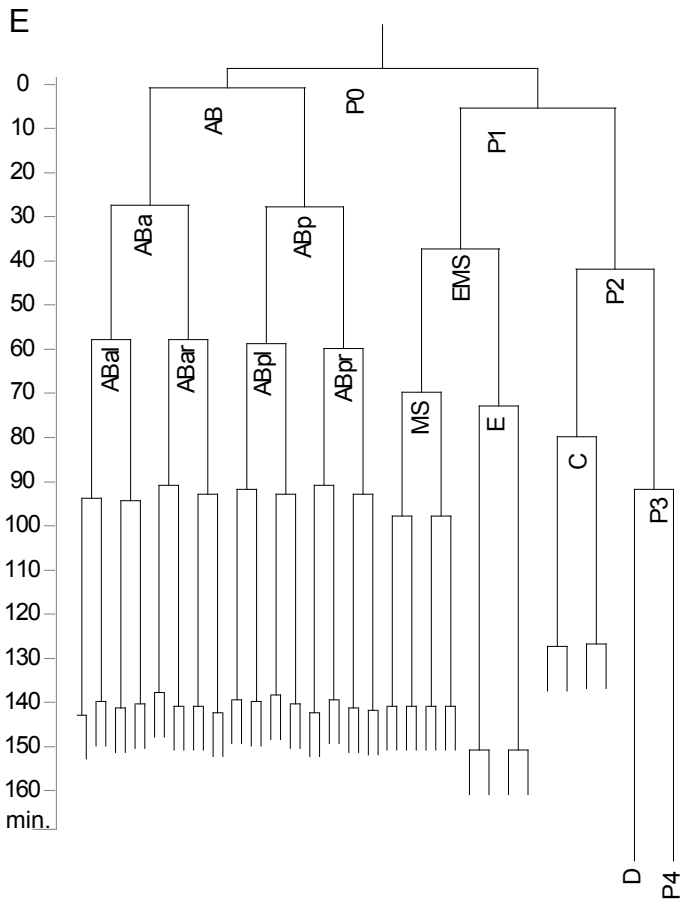
E
0
10
20
30
40
50
60
70
80
90
100
110
120
130
140
150
160
min.
P0
AB
P1
ABa
ABp
EMS
P2
ABal
ABar
ABpl
ABpr
MS
E
C
P3
D
P4

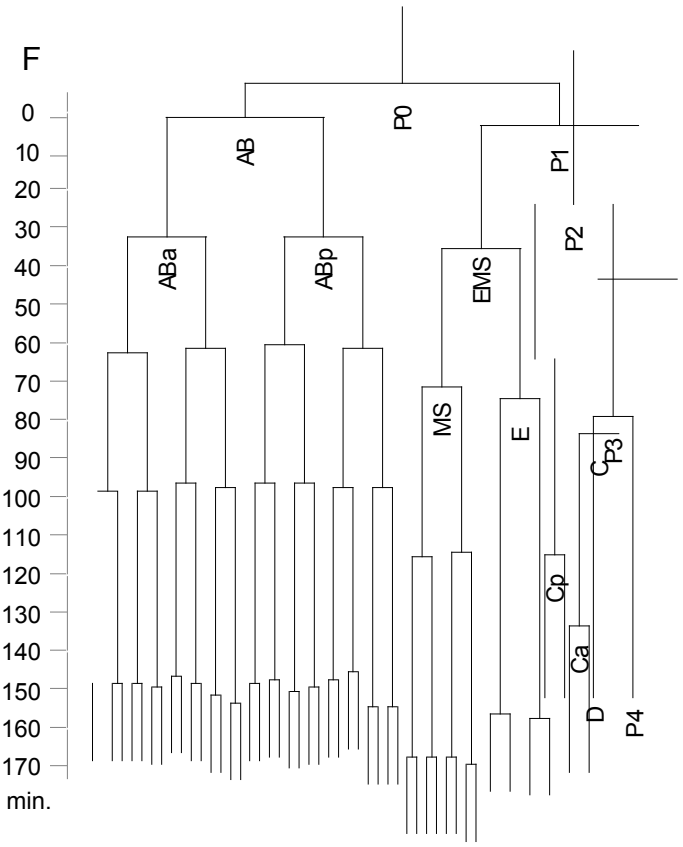
F
0
10
20
30
40
50
60
70
80
90
100
110
120
130
140
150
160
170
min.
P0
AB
P1
P2
ABa
ABp
EMS
MS
E
C
P3
Cp
Ca
D
P4

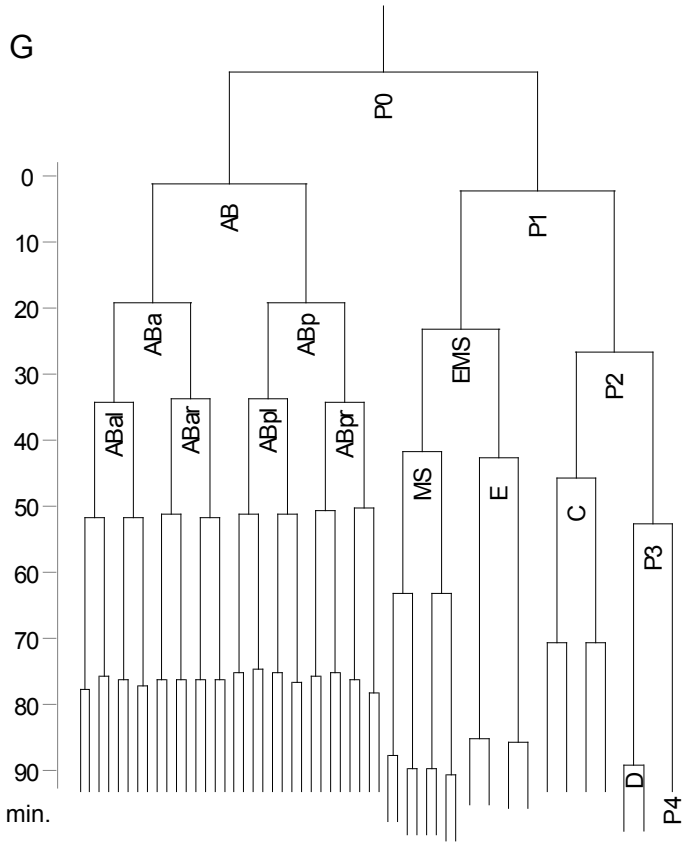
G
0
10
20
30
40
50
60
70
80
90
min.
P0
AB
P1
ABa
ABp
EMS
P2
ABal
ABar
ABpl
ABpr
MS
E
C
P3
D
P4

Figure 3.12 Cell lineage of the first divisions of *Caenorhabditis remanei*

A-C Lineages of embryos 1-3. The vertical axis indicates time of development and every division is visualised by a horizontal bar. The left branch is always the anterior/left/dorsal sister. Time starts after the division of AB.

Fig. 3.12

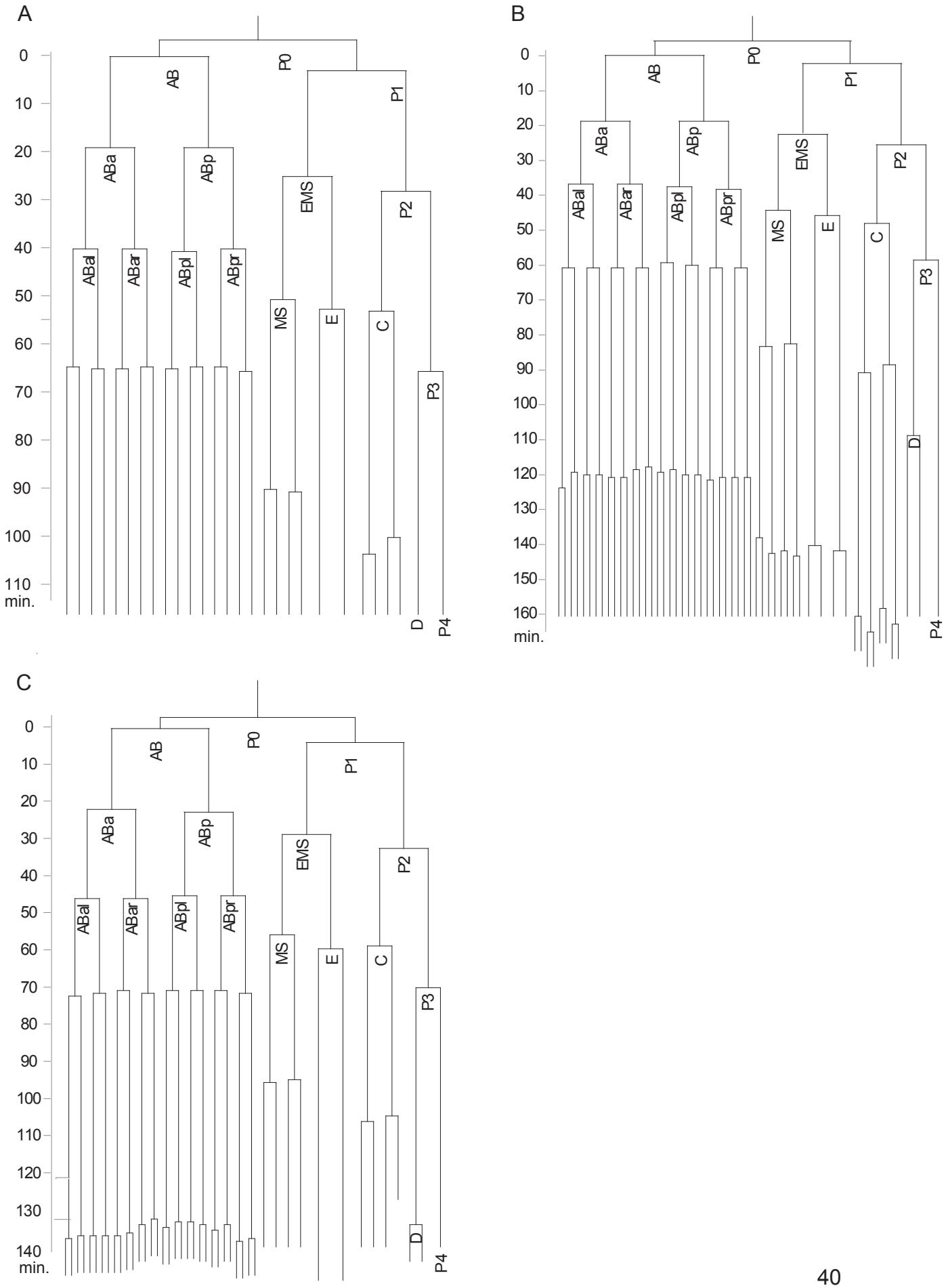
A
0
10
20
30
40
50
60
70
80
90
100
110
min.
AB
P0
P1
ABa
ABp
EMS
P2
ABal
ABar
ABpl
ABpr
MS
E
C
P3
D
P4
B
0
10
20
30
40
50
60
70
80
90
100
110
120
130
140
150
160
min.
AB
P0
P1
ABa
ABp
EMS
P2
ABal
ABar
ABpl
ABpr
MS
E
C
P3
D
P4
C
0
10
20
30
40
50
60
70
80
90
100
110
120
130
140
min.
AB
P0
P1
ABa
ABp
EMS
P2
ABal
ABar
ABpl
ABpr
MS
E
C
P3
D
P4

Figure 3.13 Cell lineage of the first divisions of *Mesorhabditis longespiculosa*

A-C Lineages of embryos 1-3. The vertical axis indicates time of development and every division is visualised by a horizontal bar. The left branch is always the anterior/left/dorsal sister. Time starts after the division of P1.

Fig. 3.13

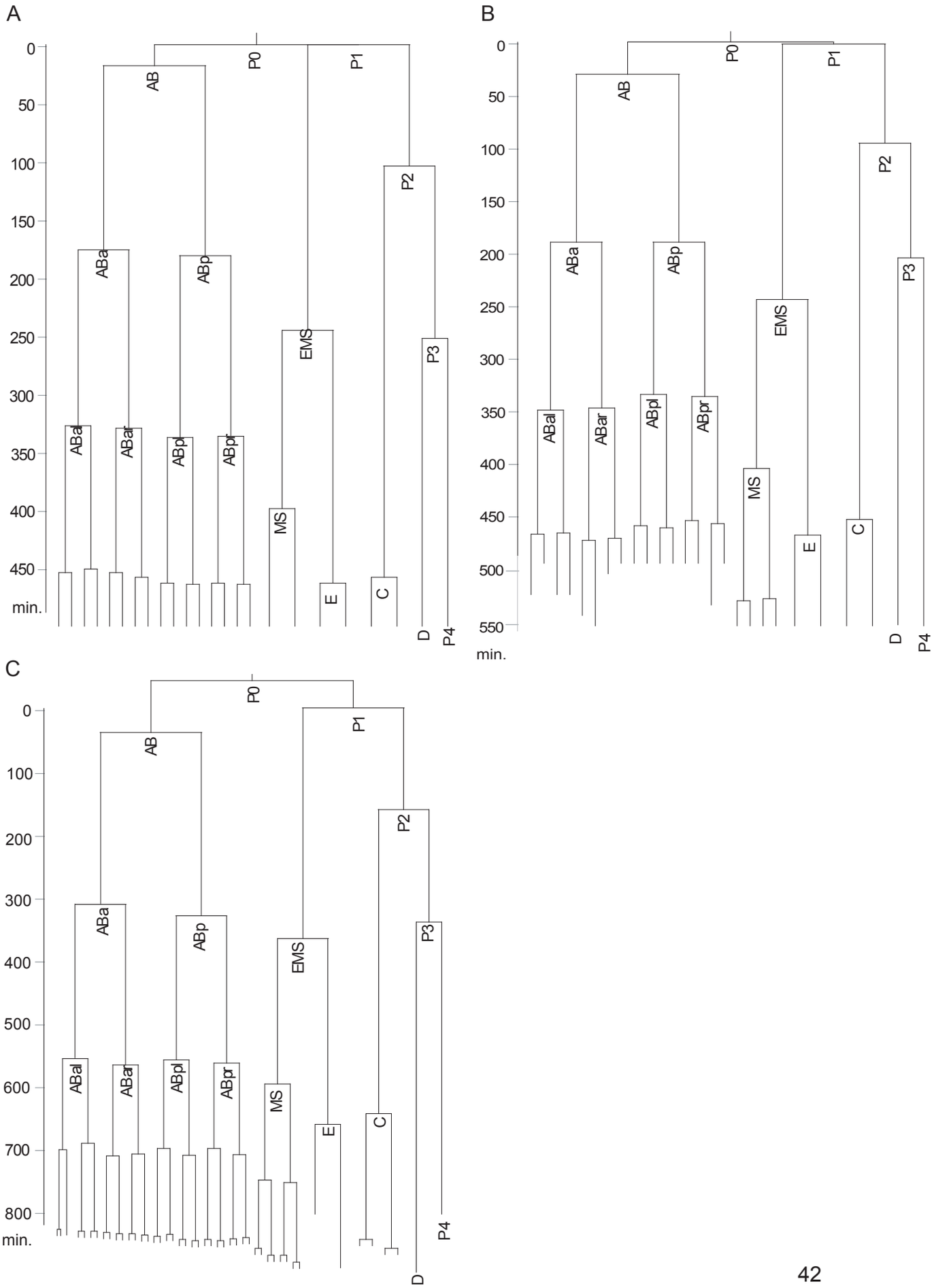
A
0
50
100
150
200
250
300
350
400
450
min.
P0
AB
P1
ABa
ABp
EMS
P2
P3
ABal
ABar
ABpl
ABpr
MS
E
C
D
P4
B
0
50
100
150
200
250
300
350
400
450
500
550
min.
P0
AB
P1
ABa
ABp
EMS
P2
P3
ABal
ABar
ABpl
ABpr
MS
E
C
D
P4
C
0
100
200
300
400
500
600
700
800
min.
P0
AB
P1
ABa
ABp
EMS
P2
P3
ABal
ABar
ABpl
ABpr
MS
E
C
D
P4

Figure 3.14 Cell lineage of the first divisions of *Mesorhabditis miotki*

A-C Lineages of embryos 1-3. The vertical axis indicates time of development and every division is visualised by a horizontal bar. The left branch is always the anterior/left/dorsal sister. Time starts after the division of P1.

Fig. 3.14

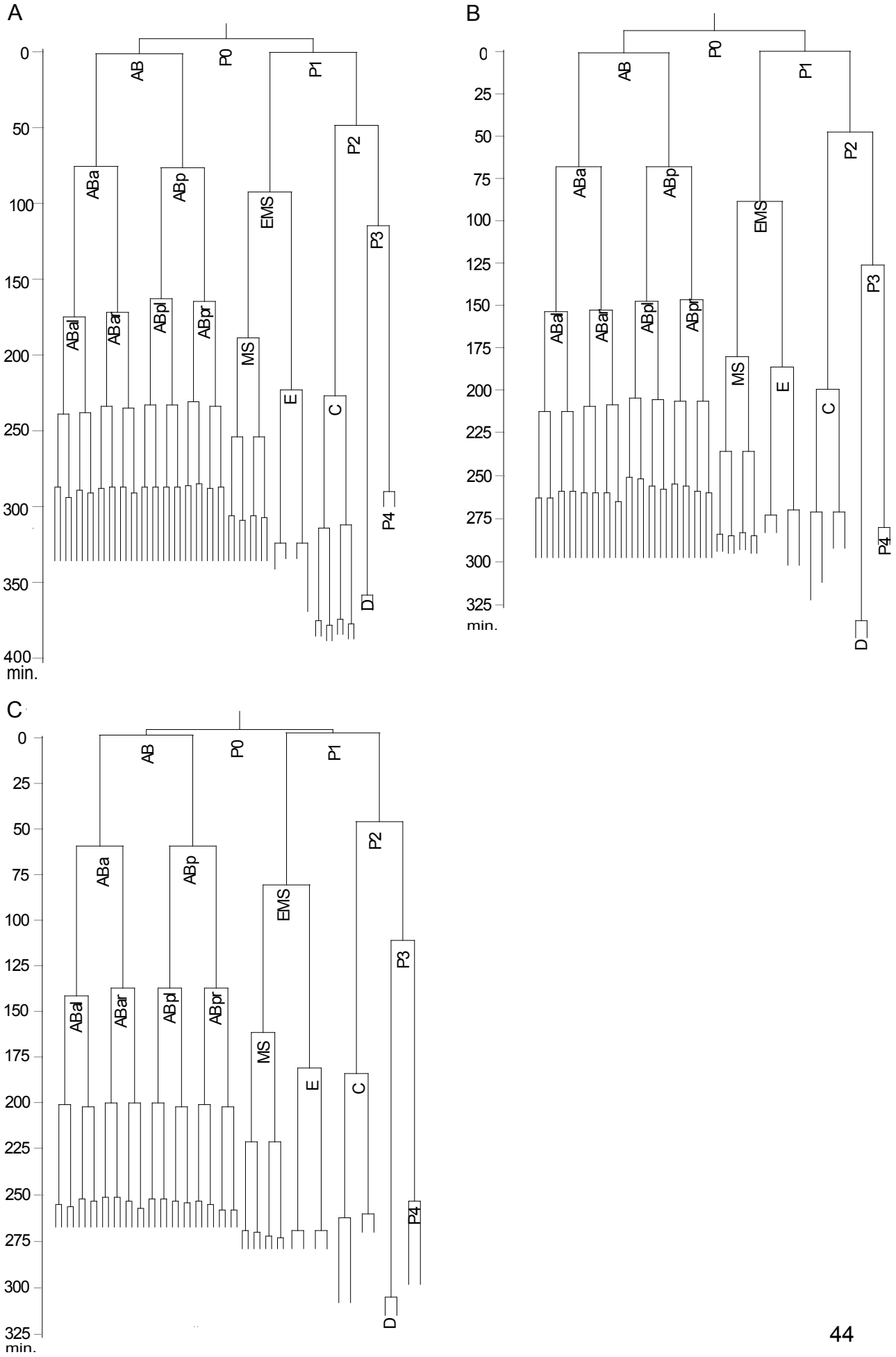
A
0
50
100
150
200
250
300
350
400
min.
AB
P0
P1
P2
P3
P4
ABa
ABp
EMS
ABal
ABar
ABpl
ABpr
MS
E
C
D
B
0
25
50
75
100
125
150
175
200
225
250
275
300
325
min.
C
0
25
50
75
100
125
150
175
200
225
250
275
300
325
min.

Figure 3.15 Cell lineage of the first divisions of *Oscheius dolichuroides*

A-C Lineages of embryos 1-3. The vertical axis indicates time of development and every division is visualised by a horizontal bar. The left branch is always the anterior/left/dorsal sister. Time starts after the division of AB.

Fig. 3.15

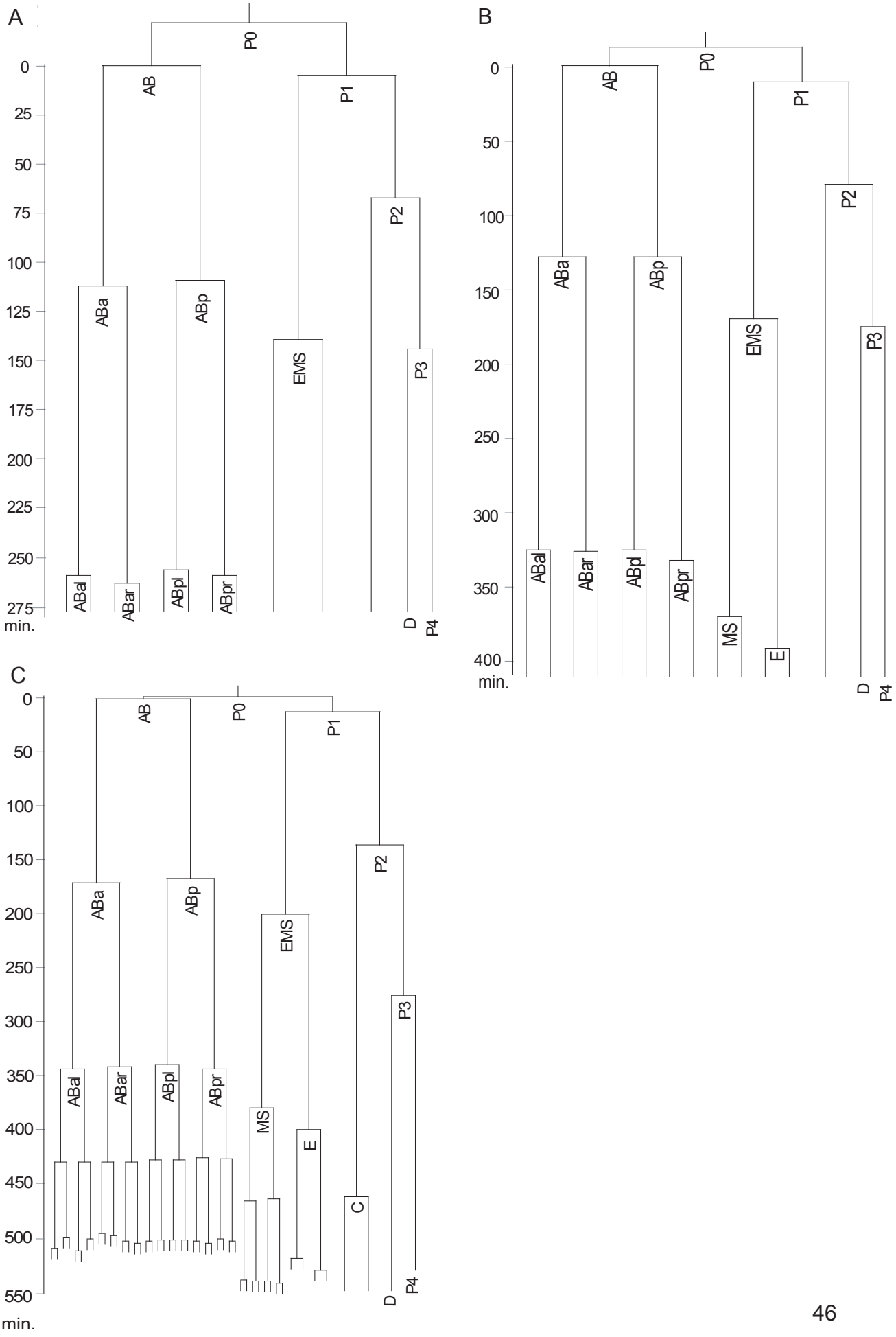
A
0
25
50
75
100
125
150
175
200
225
250
275
min.
P0
AB
P1
P2
P3
ABa
ABp
EMS
ABal
ABar
ABpl
ABpr
D
P4
B
0
50
100
150
200
250
300
350
400
min.
P0
AB
P1
P2
P3
ABa
ABp
EMS
ABal
ABar
ABpl
ABpr
MS
E
D
P4
C
0
50
100
150
200
250
300
350
400
450
500
550
min.
AB
P0
P1
P2
P3
ABa
ABp
EMS
ABal
ABar
ABpl
ABpr
MS
E
C
D
P4

Figure 3.16 Cell lineage of the first divisions of *Pellioditis marina*

A-**B** Lineages of embryos 1-2. The vertical axis indicates time of development and every division is visualised by a horizontal bar. The left branch is always the anterior/left/dorsal sister. Time starts after the division of AB.

Fig. 3.16

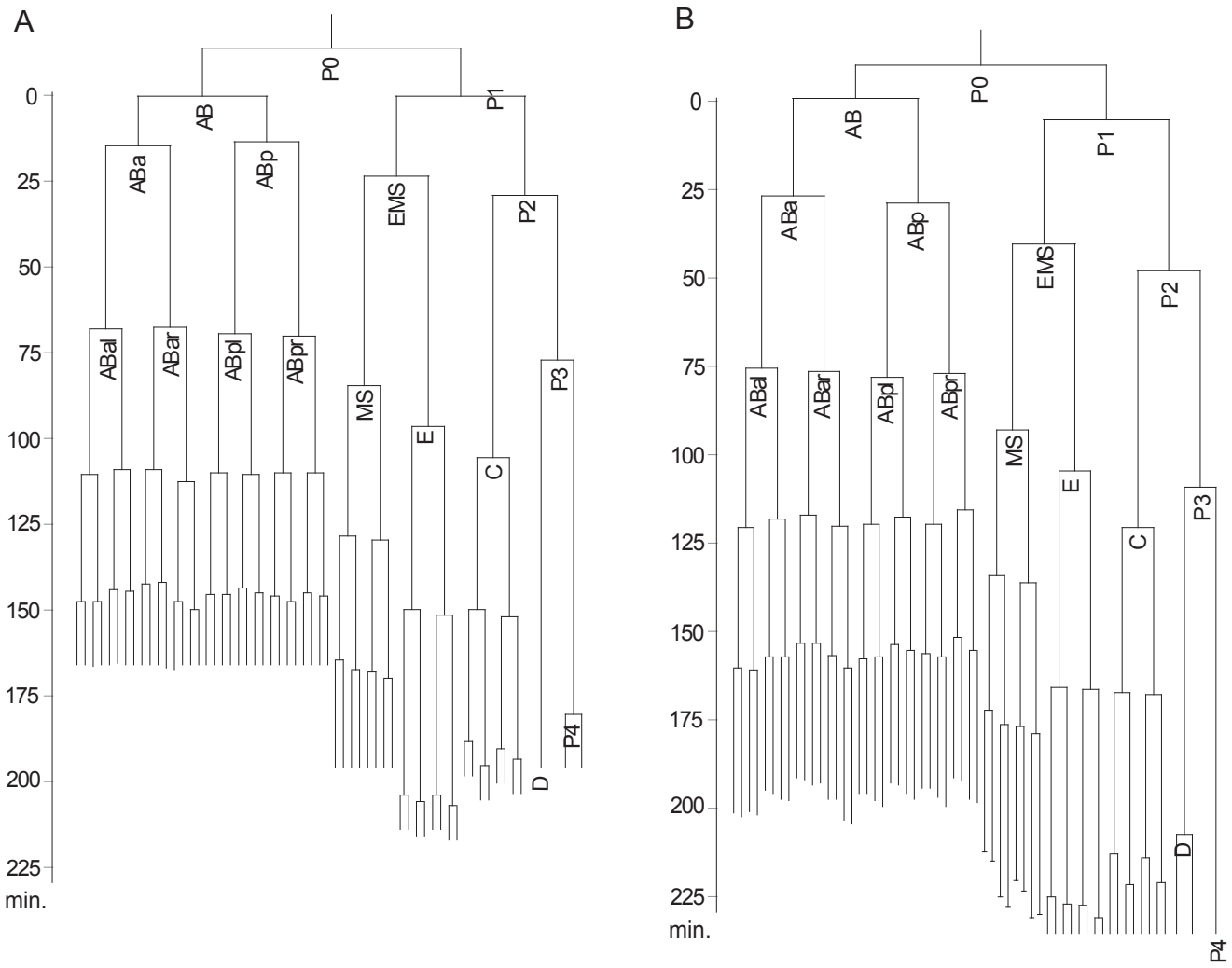
A
B
P0
AB
P1
ABa
ABp
EMS
P2
ABal
ABar
ABpl
ABpr
MS
E
C
P3
D
P4
0
25
50
75
100
125
150
175
200
225
min.

Figure 3.17 Cell lineage of the first divisions of *Pelodera strongyloides*

A-C Lineages of embryos 1-3. The vertical axis indicates time of development and every division is visualised by a horizontal bar. The left branch is always the anterior/left/dorsal sister. Time starts after the division of AB.

Fig. 3.17

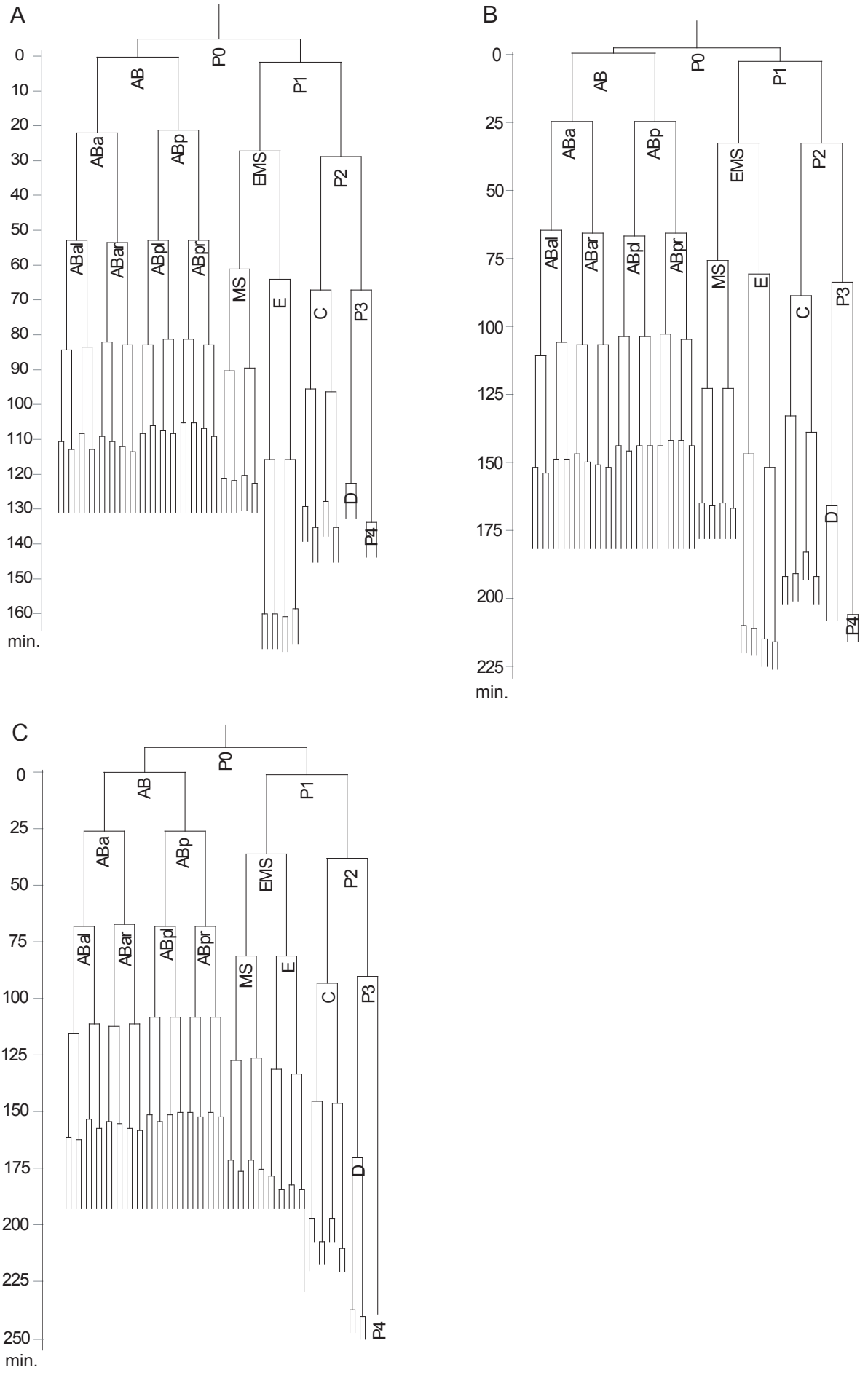
A
0
10
20
30
40
50
60
70
80
90
100
110
120
130
140
150
160
min.
P0
AB
P1
ABa
ABp
EMS
P2
ABal
ABar
ABpl
ABpr
MS
E
C
P3
D
P4
B
0
25
50
75
100
125
150
175
200
225
min.
P0
AB
P1
ABa
ABp
EMS
P2
ABal
ABar
ABpl
ABpr
MS
E
C
P3
D
P4
C
0
25
50
75
100
125
150
175
200
225
250
min.
P0
AB
P1
ABa
ABp
EMS
P2
ABal
ABar
ABpl
ABpr
MS
E
C
P3
D
P4

Figure 3.18 Cell lineage of the first divisions of *Rhabditella axei*

A-C Lineages of embryos 1-3. The vertical axis indicates time of development and every division is visualised by a horizontal bar. The left branch is always the anterior/left/dorsal sister. Time starts after the division of AB.

Fig. 3.18

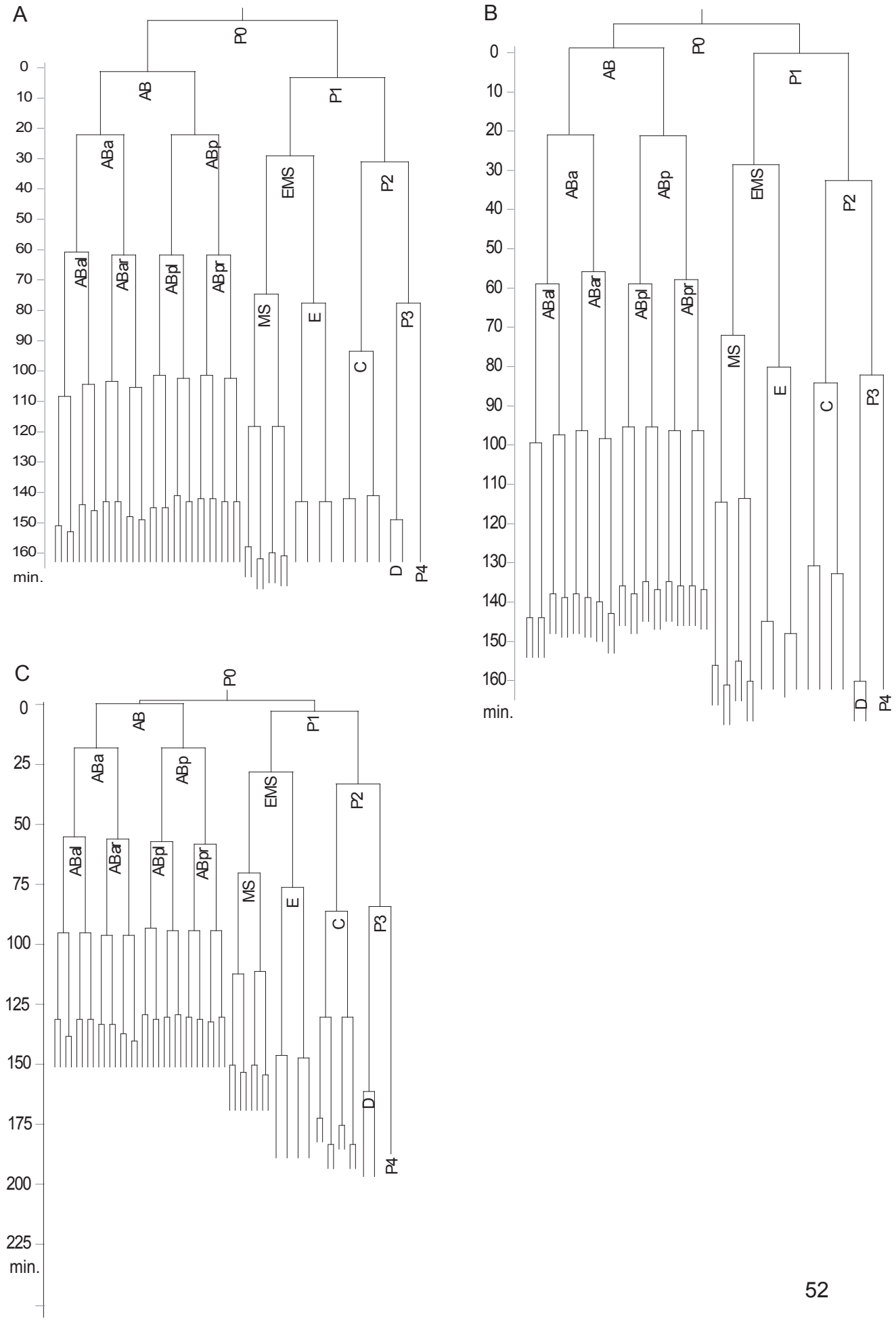
A
P0
AB
P1
ABa
ABp
EMS
P2
ABal
ABar
ABpl
ABpr
MS
E
C
P3
D
P4
0
10
20
30
40
50
60
70
80
90
100
110
120
130
140
150
160
min.
B
P0
AB
P1
ABa
ABp
EMS
P2
ABal
ABar
ABpl
ABpr
MS
E
C
P3
D
P4
0
10
20
30
40
50
60
70
80
90
100
110
120
130
140
150
160
min.
C
P0
AB
P1
ABa
ABp
EMS
P2
ABal
ABar
ABpl
ABpr
MS
E
C
P3
D
P4
0
25
50
75
100
125
150
175
200
225
min.

Figure 3.19 Cell lineage of the first divisions of *Teratorhabdtis palmarum*

A-**B** Lineages of embryos 1-2. The vertical axis indicates time of development and every division is visualised by a horizontal bar. The left branch is always the anterior/left/dorsal sister. Time starts after the division of AB.

Table 3.2 Egg Shape Index for all studied species of Rhabditidae

The average ESI ±SE and number of analyzed embryos

Fig. 3.19

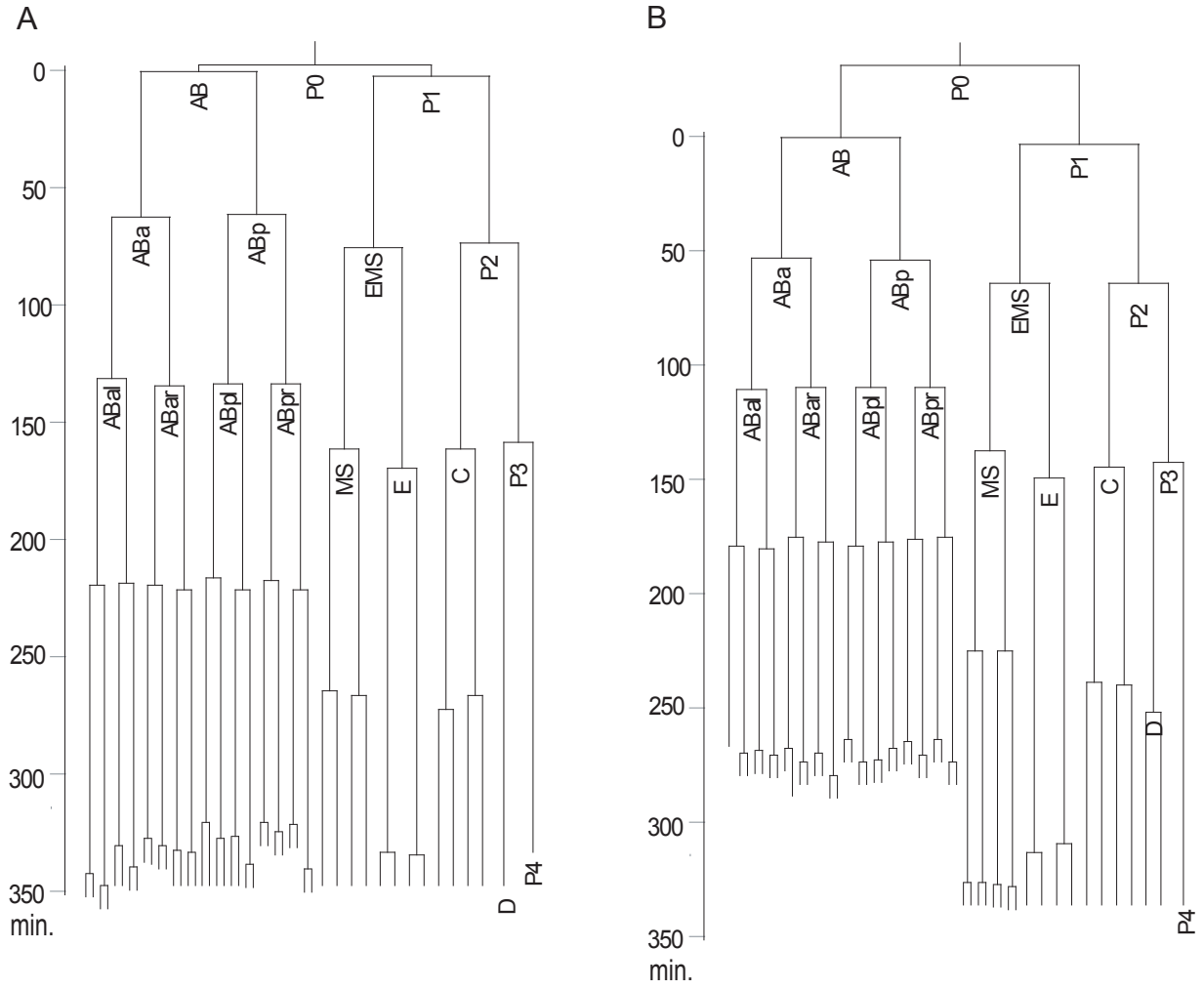

Table 3.2

species	ESI	SE	n
C. elegans	59	2	9
C. remanei	63	1	3
M. longespiculosa	59	3	4
M. miotki	53	2	6
O. dolichuroides	61	2	6
P. marina	84	5	2
P. strongyloides	56	5	3
R. axei	63	3	3
T. palmarum	59	6	3

Table 3.3 Division sequence of the early cell divisions in species of Rhabditidae

Comparison of the division sequence of the early divisions of the founder cells between *C. elegans, C. remanei, M. longespiculosa, M. miotki, O. dolichuroides, P. marina, P. strongyloides, R. axei and T. palmarum.* The germline cells are marked in bold.

Table 3.3

Caenorhabditis elegans	embr1	P0	AB	**P1**	2AB	EMS	**P2**	4AB	MS	E	C	8AB	**P3**	2MS	2C	16AB	2E	4MS				
	embr2	P0	AB	**P1**	2AB	EMS	**P2**	4AB	MS	E	C	8AB	**P3**	2MS	2C	16AB	2E	D	4MS			
	embr3	P0	AB	**P1**	2AB	EMS	**P2**	4AB	MS	E	C	8AB	**P3**	2MS	2C	16AB	2E	D	4MS			
	embr4	P0	AB	**P1**	2AB	EMS	**P2**	4AB	MS	E	C	8AB	**P3**	2MS	2C	16AB	2E					
	embr5	P0	AB	**P1**	2AB	EMS	**P2**	4AB	MS	E	C	**P3**	8AB	2MS	2C	16AB	2E	4MS				
	embr6	P0	AB	**P1**	2AB	EMS	**P2**	4AB	MS	E	C	8AB	**P3**	2MS	2C	16AB	2E	4MS				
	embr7	P0	AB	**P1**	2AB	EMS	**P2**	4AB	MS	E	C	8AB	**P3**	2MS	2C	16AB	2E	D	4MS			
Caenorhabditis remanei	embr1	P0	AB	**P1**	2AB	EMS	**P2**	4AB	MS	E	C	8AB	**P3**	2MS	2C							
	embr2	P0	AB	**P1**	2AB	EMS	**P2**	4AB	MS	E	C	**P3**	8AB	2MS	2C	D	16AB	2E	4MS			
	embr3	P0	AB	**P1**	2AB	EMS	**P2**	4AB	MS	C	E	**P3**	8AB	2MS	2C	D	16AB					
Mesorhabditis longespiculosa	embr1	P0	**P1**	AB	**P2**	2AB	EMS	**P3**	4AB	MS	C	8AB	E									
	embr2	P0	**P1**	AB	**P2**	2AB	**P3**	EMS	4AB	MS	C	8AB	E	2MS								
	embr3	P0	**P1**	AB	**P2**	2AB	**P3**	EMS	4AB	MS	C	8AB	E	2MS	16AB	2C	4MS					
Mesorhabditis miotki	embr1	P0	**P1/**	AB	P2	2AB	EMS	**P3**	4AB	MS	E	C	8AB	2MS	16AB	**P4**	4MS	2C	2E	D		
	embr2	P0	**P1/**	AB	P2	2AB	EMS	**P3**	4AB	MS	E	C	8AB	2MS	16AB	2C	2E	**P4**	4MS	D		
	embr3	P0	**P1/**	AB	P2	2AB	EMS	**P3**	4AB	MS	E	C	8AB	2MS	16AB	**P4**	2C	2E	4MS	D		
Oscheius dolichuroides	embr1	P0	AB	**P1**	**P2**	2AB	EMS	**P3**	4AB	MS	E											
	embr2	P0	AB	**P1**	**P2**	2AB	EMS	**P3**	4AB	MS	E											
	embr3	P0	AB	**P1**	**P2**	2AB	EMS	**P3**	4AB	MS	E	8AB	C	2MS	16AB	2E	4MS					
Pellioditis marina	embr1	P0	AB	**P1**	2AB	EMS	**P2**	4AB	**P3**	MS	E	C	8AB	2MS	16AB	2E	2C	4MS				
	embr2	P0	AB	**P1**	2AB	EMS	**P2**	4AB	MS	E	**P3**	8AB	C	2MS	16AB	2E	2C	4MS				
Pelodera strongyloides	embr1	P0	AB	**P1**	2AB	EMS	**P2**	4AB	MS	E	**P3**	C	8AB	2MS	2C	16AB	2E	4MS	D	4C	P4	4E
	embr2	P0	AB	**P1**	2AB	EMS/	**P2**	4AB	MS	E	**P3**	C	8AB	2MS	2C	16AB	2E	4MS	D	4C	P4	4E
	embr3	P0	AB	**P1**	2AB	EMS/	**P2**	4AB	MS	E	**P3**	C	8AB	2MS	2E	2C	16AB	D	4MS	4E	4C	2D
Rhabditella axei	embr1	P0	AB	**P1**	2AB	EMS	**P2**	4AB	MS	E	**P3**	C	8AB	2MS	2C	2E	16AB	D	4MS			
	embr2	P0	AB	**P1**	2AB	EMS	**P2**	4AB	MS	E	**P3**	C	8AB	2MS	2C	16AB	2E	4MS	D			
	embr3	P0	AB	**P1**	2AB	EMS	**P2**	4AB	MS	E	**P3**	C	8AB	2MS	2C	16AB	2E	4MS	D			
Teratorhabditis palmarum	embr1	P0	AB	**P1**	2AB	**P2**	EMS	4AB	**P3**	MS	C	E	8AB	2MS	2C	16AB	2E					
	embr2	P0	AB	**P1**	2AB	**P2**	EMS	4AB	MS	**P3**	C	E	8AB	2MS	2C	D	16AB	2E				

Table 3.4 The cell stage when P4 is present for all examined species of Rhabditidae

Table 3.5 Relative developmental tempo of the examined species of Rhabditidae

The relative early developmental tempo, measured as the time between the division of AB (*C. elegans, C. remanei, O. dolichuroides, P. marina, P. strongyloides, R. axei and T. palmarum)* or P1 (*M. longespiculosa and M. miotki*) and the division of E and normalized to the tempo of *C. elegans*.

Figure 3.20 Number of cells during embryonic development in species of Rhabditidae

Time starts after the division of AB (*C. elegans, C. remanei, O. dolichuroides, P. marina, P. strongyloides, R. axei and T. palmarum)* or P1 (*M. longespiculosa and M. miotki*).

Table 3.4

species	cell stage
C. elegans	16 or 24
C. remanei	16 or 24
M. longespiculosa	8 or 9
M. miotki	9
O. dolichuroides	9
P. marina	13 or 15
P. strongyloides	15
R. axei	15
T. palmarum	13 or 14

Table 3.5

species	rel tempo
C. elegans	1
C. remanei	0.7
M. longespiculosa	7.2
M. miotki	2.7
O. dolichuroides	5.6
P. marina	2.5
P. strongyloides	1
R. axei	1.1
T. palmarum	2.2

Fig. 3.20

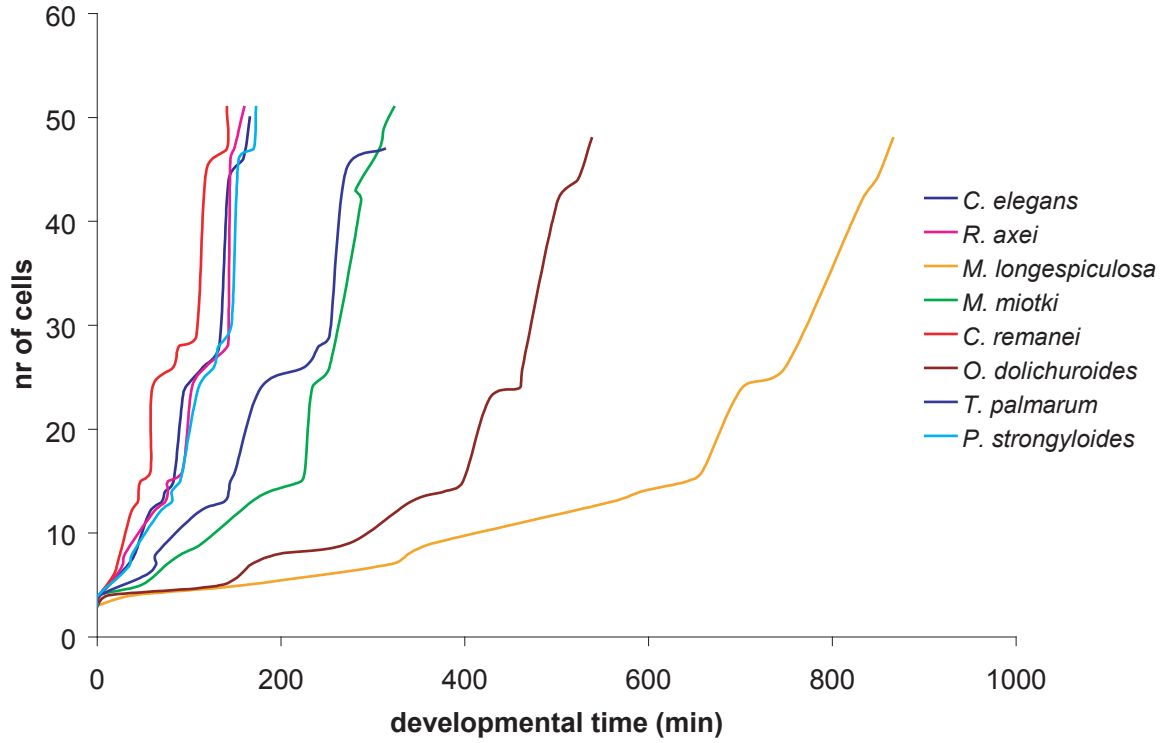

Figure 3.21 Cell cycle length of AB generations in species of Rhabditidae

The average cell cycle length (± SD) of AB in each generation is plotted in time for **A** *C. elegans*, **B** *C. remanei*, **C** *M. longespiculosa*, **D** *M. miotki*, **E** *O. dolichuroides* and **F** *P. marina*. The average cell cycle length for each AB stage was calculated based on 3 recordings, except for *P. marina* (2 recordings).

Fig. 3.21

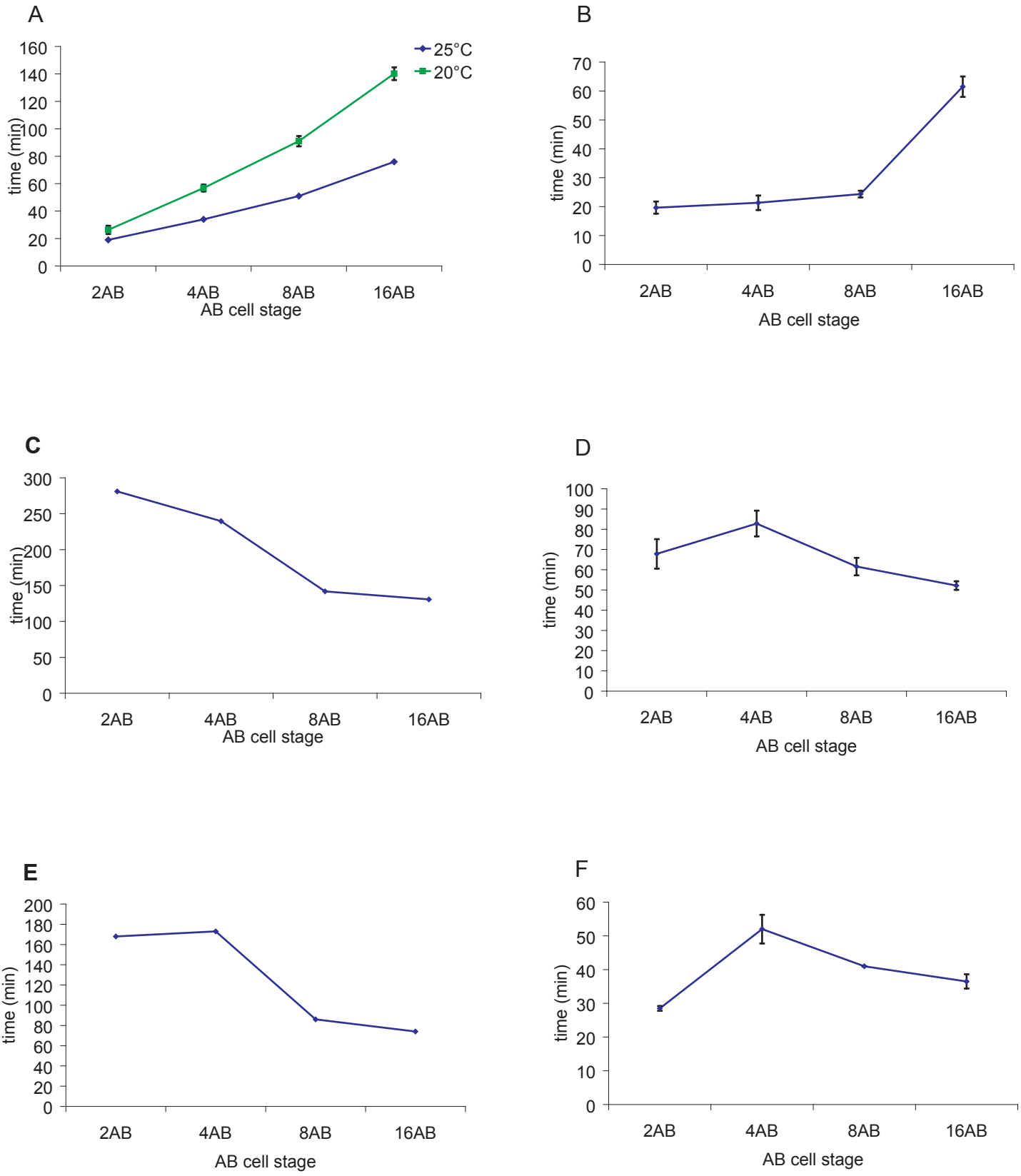
A
160
140
120
100
80
60
40
20
0
time (min)
25°C
20°C
2AB
4AB
8AB
16AB
AB cell stage
B
70
60
50
40
30
20
10
0
time (min)
2AB
4AB
8AB
16AB
AB cell stage
C
300
250
200
150
100
50
0
time (min)
2AB
4AB
8AB
16AB
AB cell stage
D
100
90
80
70
60
50
40
30
20
10
0
time (min)
2AB
4AB
8AB
16AB
AB cell stage
E
200
180
160
140
120
100
80
60
40
20
0
time (min)
2AB
4AB
8AB
16AB
AB cell stage
F
60
50
40
30
20
10
0
time (min)
2AB
4AB
8AB
16AB
AB cell stage

Fig. 3.21(2) Cell cycle length of AB generations in species of Rhabditidae

The average cell cycle length of AB (± SD) in each generation is plotted in time for **G** *P. strongyloides,* **H** *R. axei and* **I** *T. palmarum.*

Figure 3.22 Cell division periods per founder cell in species of Rhabditidae

Cell division rounds per founder cell in time (min) for **A** *C. elegans* at 20°C and 25°C, showing differences in cell-cycle times for the six founder cells. On each horizontal line the cell division events of one founder cell are given. Each solid black box indicates the time from the division of the first cell to the division of the last cell in a given round of division. Time (min) starts after the division of AB.

Fig. 3.21 (2)

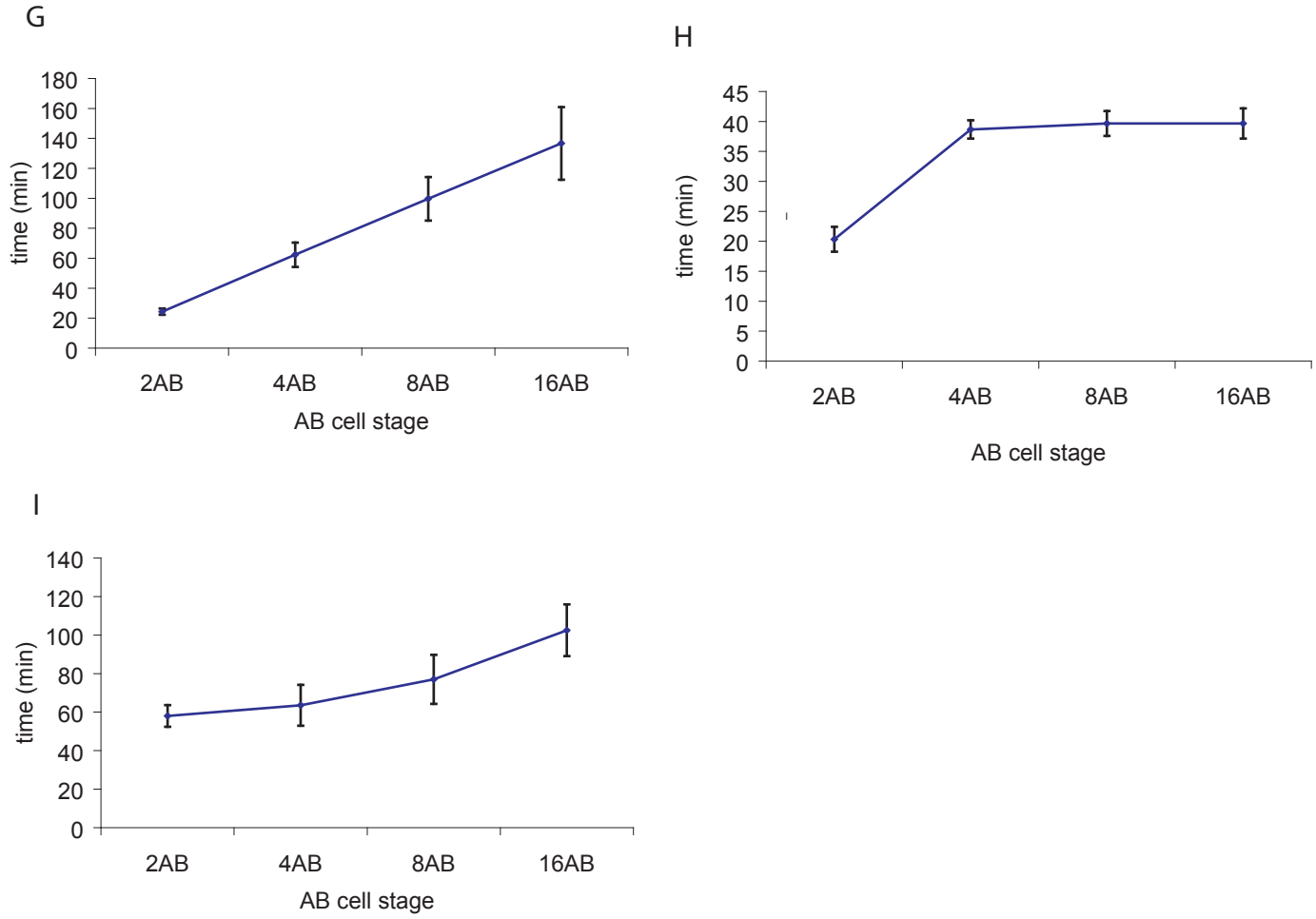

Fig. 3.22

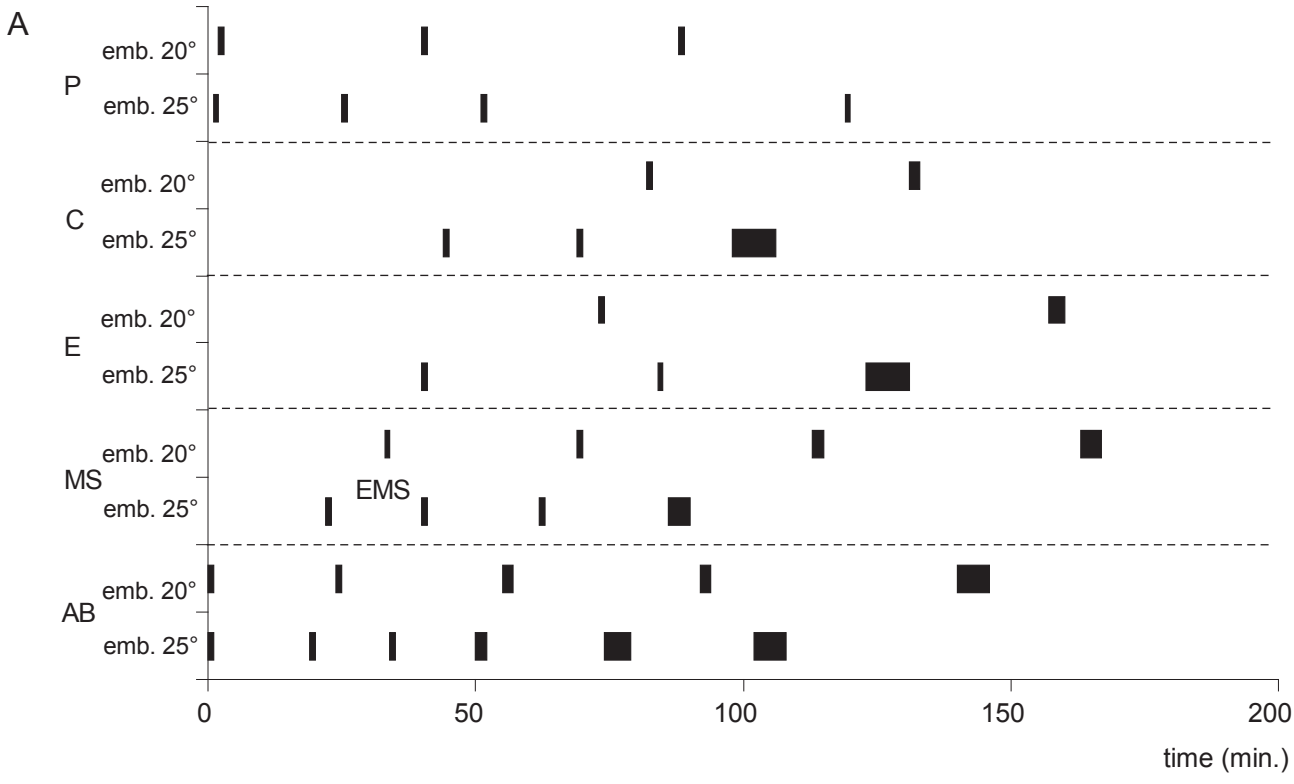

Fig. 3.22 (2) Cell division periods per founder cell in species of Rhabditidae

Cell division rounds per founder cell in time (min) for **B** *C. remanei* (3 recordings), **C** *M. longespiculosa* (3 recordings) and **D** *M. miotki* (3 recordings), showing differences in cell-cycle times for the six founder cells. On each horizontal line the cell division events of one founder cell are given. Each solid black box indicates the time from the division of the first cell to the division of the last cell in a given round of division. Time (min) starts after the division of AB, except for *M. longespiculosa* and *M. miotki*, where time starts after the division of P1.

Fig. 3.22 (2)

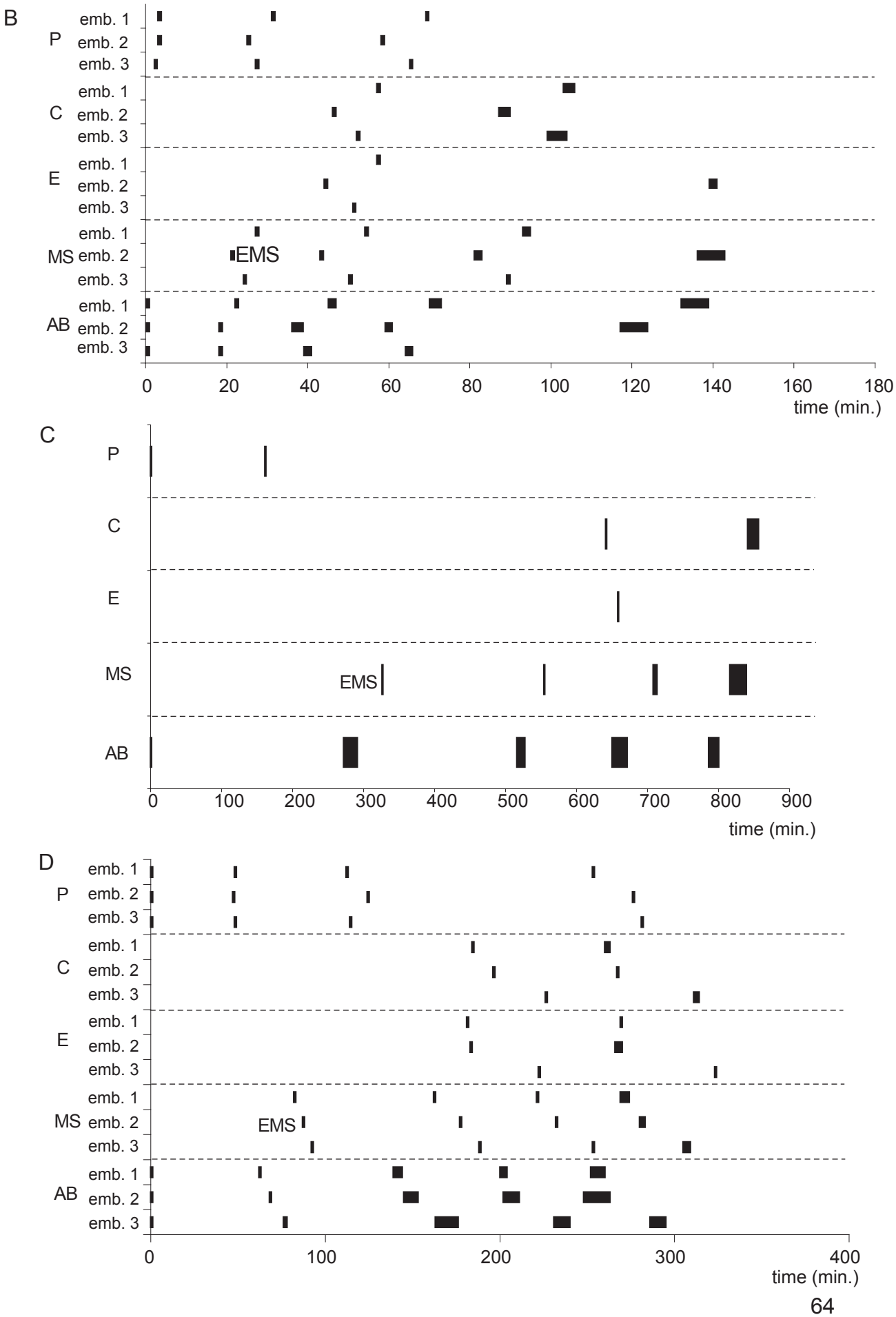
B
P
C
E
MS
AB
emb. 1
emb. 2
emb. 3
EMS
0
20
40
60
80
100
120
140
160
180
time (min.)
C
P
C
E
MS
AB
EMS
0
100
200
300
400
500
600
700
800
900
time (min.)
D
P
C
E
MS
AB
emb. 1
emb. 2
emb. 3
EMS
0
100
200
300
400
time (min.)

Fig. 3.22 (3) Cell division periods per founder cell in species of Rhabditidae

Cell division rounds per founder cell in time (min) for **E** *O. dolichuroides* (3 recordings), **F** *P. marina* (3 recordings) and **G** *P. strongyloides* (3 recordings), showing differences in cell-cycle times for the six founder cells. On each horizontal line the cell division events of one founder cell are given. Each solid black box indicates the time from the division of the first cell to the division of the last cell in a given round of division. Time (min) starts after the division of AB.

Fig. 3.22 (3)

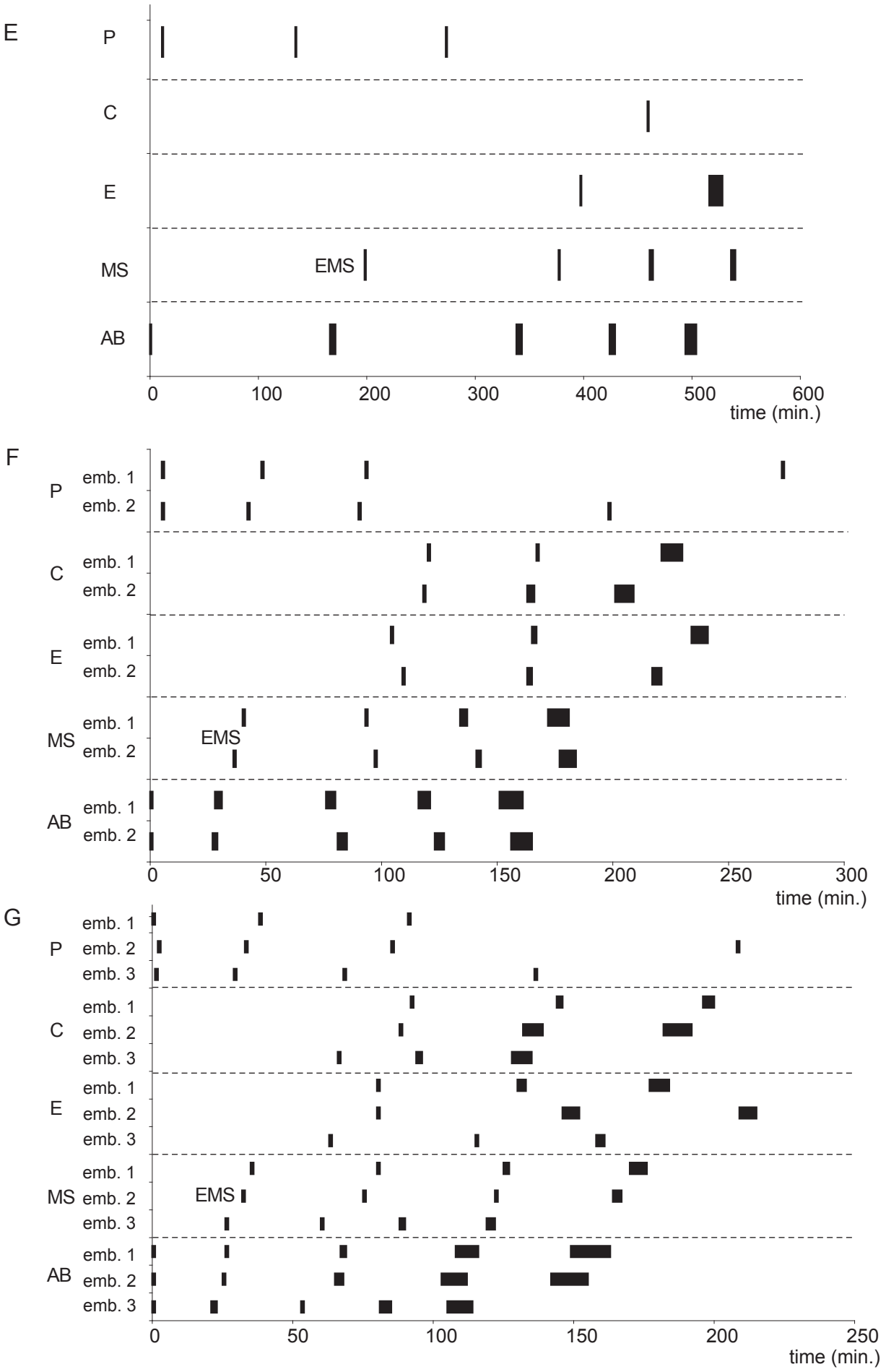
E
P
C
E
MS
EMS
AB
0
100
200
300
400
500
600
time (min.)
F
P
C
E
MS
EMS
AB
emb. 1
emb. 2
0
50
100
150
200
250
300
time (min.)
G
P
C
E
MS
EMS
AB
emb. 1
emb. 2
emb. 3
0
50
100
150
200
250
time (min.)

Fig. 3.22 (4) Cell division periods per founder cell in species of Rhabditidae

Cell division rounds per founder cell in time (min) for **H** *R. axei* (3 recordings) and **I** *T. palmarum* (2 recordings), showing differences in cell-cycle times for the six founder cells. On each horizontal line the cell division events of one founder cell are given. Each solid black box indicates the time from the division of the first cell to the division of the last cell in a given round of division. Time (min) starts after the division of AB.

Fig. 3.22 (4)

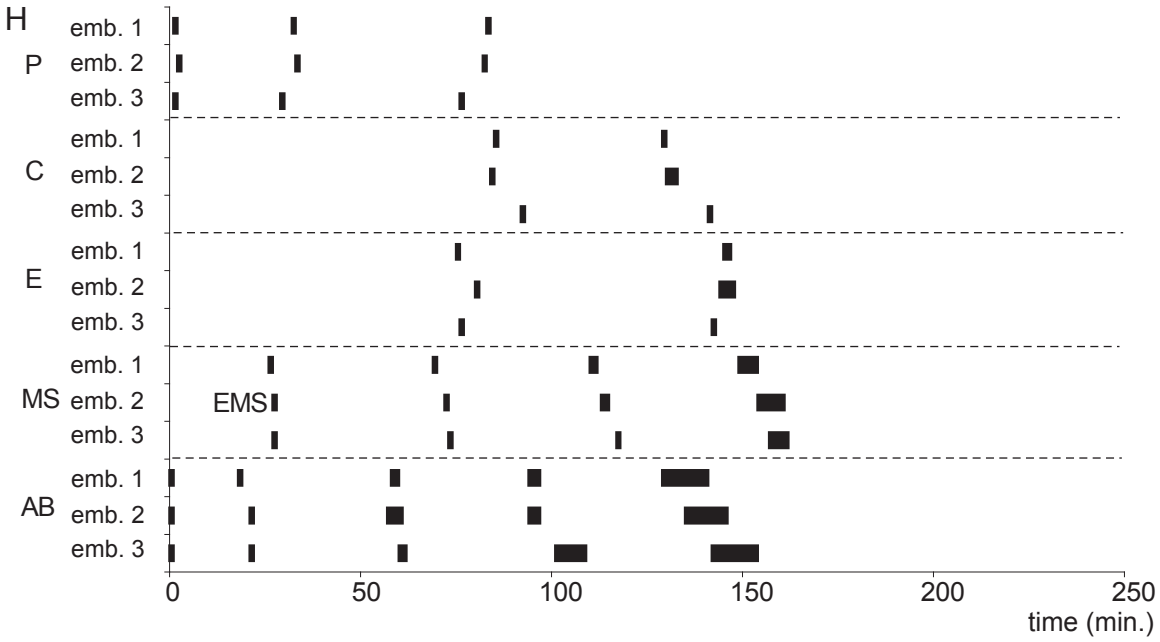
H
P
C
E
MS
AB
emb. 1
emb. 2
emb. 3
EMS
0
50
100
150
200
250
time (min.)

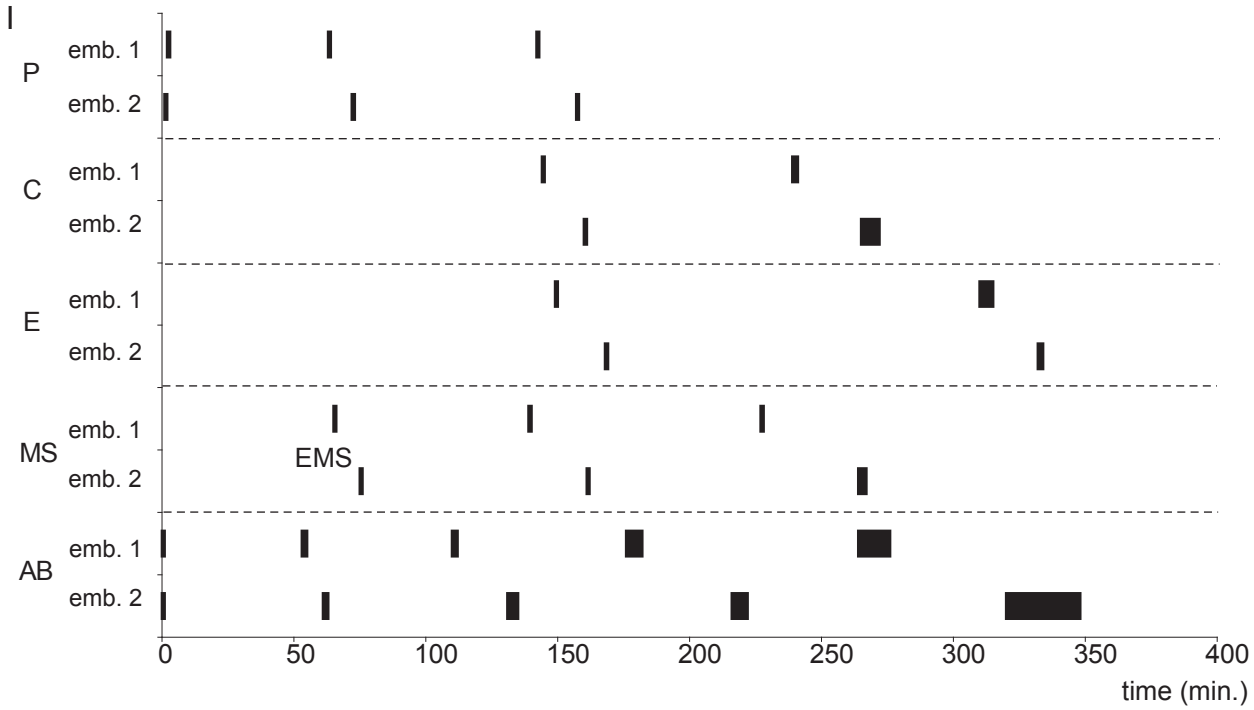
I
P
C
E
MS
AB
emb. 1
emb. 2
EMS
0
50
100
150
200
250
300
350
400
time (min.)

Figure 3.23 Cell-cell contacts at the 8AB cell stage in species of Rhabditidae

A *C. elegans*, a, our analysis; b data from Hutter and Schnabel (1994, 1995), **B** *C. remanei*, **C** *M. longespiculosa*, **D** *M. miotki* and **E** *O. dolichuroides*, (1 = contact is present, 0 = contact is absent). Variable contacts are marked by a yellow square; for *C. elegans* the number of cases is indicated, for other species this is not included due to the low number of recordings (2 or 3).

Fig. 3.23

A a

	ala	alp	ara	arp	pla	plp	pra	prp	MS	E	C	P3
ala		1	1	0	1	1 on 8	0	0	0	0	0	0
alp			1	0	6 on 8	1	0	0	1	0	0	0
ara				1	1	4 on 8	1	2 on 8	1	0	0	0
arp					1	1	1		0	0	0	0
pla						1	0	0	0	0	0	0
plp							0	0	1	0	0	0
pra								1	5 on 8	0	1	0
prp									1	1	1	1
MS										1	3 on 8	0
E											1	1
C												1
P3												

b

	ala	alp	ara	arp	pla	plp	pra	prp	MS
ala		1	1	0	1	5 on 13	0	0	0
alp			1	0	8 on 13	1	0	0	1
ara				1	1	8 on 13	1	7 on 13	1
arp					1	1	1	5 on 13	0
pla						1	0	0	0
plp							0	0	1
pra								1	6 on 13
prp									1
MS									

B

	ala	alp	ara	arp	pla	plp	pra	prp	MS	E	C	P3
ala		1	1		1	0	0	0	0	0	0	0
alp			1	0		1	0	0	1	0	0	0
ara				1	0	0	1	1	1	0	0	0
arp					1	1	1		0	0	1	0
pla						1	0	0	0	0	1	0
plp							0	0	1	1	1	0
pra								1	1	0	1	0
prp									1	1	1	1
MS										1	0	0
E											1	1
C												1
P3												

C

	ala	alp	ara	arp	pla	plp	pra	prp	MS	E	C	D	P4
ala		1	1	0	1	0	0	0	0	0	0	0	0
alp			1	1	1		0	0	1	0	0	0	0
ara				1	1	0	0	0	1	0	0	0	0
arp					1	0	1	0	1	0	0	0	0
pla						1	1	0	1	0	0	0	0
plp							1	1	1	1	1	0	0
pra								1	1	1	0	0	0
prp									0	1	1	1	0
MS										1		0	0
E											1		1
C												1	1
D													1
P4													

D

	ala	alp	ara	arp	pla	plp	pra	prp	MS	E	C	D	P4
ala		1	1	0	1	0	0	0	0	0	0	0	0
alp			1	1	1		0	0	1	0	0	0	0
ara				1	1	0		0	1	0	0	0	0
arp					1	0	1	1	1	0	0	0	0
pla						1	1	0	1		1		0
plp							0	0	1	1	1	1	
pra								1	1	0	1	0	0
prp									1	1	1	1	
MS										1	1	0	0
E											1	1	1
C												1	1
D													1
P4													

E

	ala	alp	ara	arp	pla	plp	pra	prp	MS	E	C	D	P4
ala		1	1	1	1	0	0	0	0	0	0	0	0
alp			1	0	1	1	0	0	1	0	0	0	0
ara				1	1	1	1	0	1	0	0	0	0
arp					1		1	0	0	0	1	0	0
pla						1	0	0	0	0	0	0	0
plp								0	1	1	1	0	0
pra								1	1	0	1	1	0
prp									1		1	1	
MS										1	0	0	0
E											1	1	1
C												1	1
D													1
P4													

Fig. 3.23 (2) Cell-cell contacts at the 8AB cell-stage in species of Rhabditidae

F *P. marina,* **G** *P. strongyloides,* **H** *R. axei and* **I** *T. palmarum.* (1 = contact is present, 0 = contact is absent). Variable contacts are marked by a yellow square.

Figure 3.24 Spatial configuration of the 12 cell-embryo of *T. palmarum*

In *T. palmarum* MS is located more anterior compared to *C. elegans* and other species within Rhabditidae. Lateral right view, anterior to the left. Scale bar = 10 μm. Note that this leads to other cell –cell contacts compared to *C. elegans*.

Fig. 3.23 (2)

F

	ala	alp	ara	arp	pla	plp	pra	prp	MS	E	C	P3
ala		1	1	1	1	0	0	0	0	0	0	0
alp			1	0	1	1	0	0	1	0	0	0
ara				1	0	0	1	0	1	0	0	0
arp					1	0	1	0	0	0	1	0
pla						1	0	0		0	1	0
plp							0	0	1	1	1	1
pra								1	1	0	1	0
prp									1	1		1
MS										1	1	0
E											0	1
C												1
P3												

G

	ala	alp	ara	arp	pla	plp	pra	prp	MS	E	C	P3
ala		1	1	0	1	0	0	0	0	0	0	0
alp			1	0	1	0	0	0	1	0	0	0
ara				1		0	1	0	1	0	0	0
arp					1	1	1	0	0	0	1	0
pla						1	0	0	1	0	0	0
plp							0	0	1	1	1	0
pra								1	1	0	0	0
prp									1	1		1
MS										1	1	0
E											1	1
C												1
P3												

H

	ala	alp	ara	arp	pla	plp	pra	prp	MS	E	C	P3
ala		1	1	1	1	0	0	0	0	0	0	0
alp			1	0	1	1	0	0	1	0	0	0
ara				1			1	1	1	0		0
arp					1		1	0	0	0	1	0
pla						1	0	0	0	0	1	0
plp							0	0	1		1	0
pra								1	0	0	1	
prp									1	1	0	1
MS										1		0
E											1	1
C												1
P3												

I

	ala	alp	ara	arp	pla	plp	pra	prp	MS	E	C	P3
ala		1	1	1	1	0	0	0	1	0	0	0
alp			1	0	0	0	0	0	1		0	0
ara				1	0	0	1	0	1	1	0	0
arp					1	0	1	0	1	0	0	0
pla						1	1	0	0	1	1	0
plp							0	0	0	1	1	1
pra								1	0	0	1	0
prp									0	1	1	1
MS										1	0	0
E											0	1
C												1
P3												

Fig. 3.24

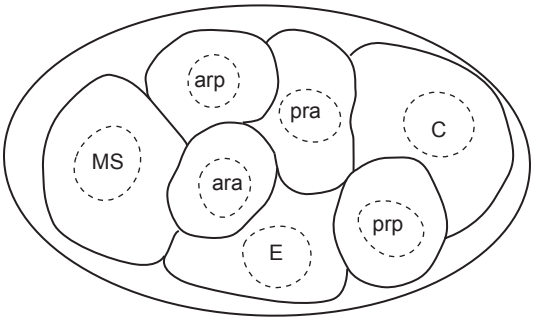

Table 3.6 Cleavage orientation of AB cells in species of Rhabditidae

Division angles (+ SD / SE) are expressed as deviation from the a-p axis in degrees. Divisions which are predominantly oriented along the a-p axis (division angles < 45°) are marked in blue, more skewed divisions (division angles > 45°) are marked in black.

Table 3.6

	C. elegans			*C. remanei*			*M. longespiculosa*			*M. miotki*			*P. strongyloides*			*P. marina*			*R. axei*			*T. palmarum*		
	av	stdev	SE	av	stdev	SE	av	stdev	SE	av	stdev	SE	av	stdev	SE	av	stdev	SE	av	stdev	SE	av	stdev	SE
ABal	68	11	4	56	8	4	61	16	9	31	10	6	50	28	16	60	18	13	72	3	2	70	5	3
ABar	69	9	3	71	15	9	19	14	8	27	19	11	55	16	9	71	7	5	81	9	5	69	9	6
ABpl	39	13	5	37	20	12	24	14	8	57	29	17	35	19	11	36	3	2	45	18	10	58	18	13
ABpr	56	15	5	55	17	10	29	28	16	50	14	8	49	32	19	49	6	4	75	2	1	51	0	0
ABala	63	18	6	43	9	5	47	30	22	37	18	10	37	9	5	31	1	1	38	10	6	20	1	1
ABalp	56	19	7	42	5	3	22	8	6	37	6	3	63	10	6	68	5	3	50	4	2	22	8	6
ABara	20	12	4	27	6	3	15	16	12	24	5	3	51	9	5	68	3	2	40	7	4	26	1	1
ABarp	23	15	5	14	13	7	44	27	19	21	18	10	31	8	4	22	8	5	9	5	3	43	13	9
ABpla	18	13	5	8	6	3	42	16	11	7	5	3	35	7	4	20	8	5	23	22	13	21	25	17
ABplp	19	10	4	28	6	3	21	1	1	6	4	2	22	28	16	8	5	3	21	6	4	30	23	16
ABpra	30	12	4	40	4	2	38	1	1	12	3	2	23	11	6	18	5	4	24	7	4	13	5	3
ABprp	24	12	4	41	17	10	28	8	6	9	5	3	43	7	4	38	9	6	22	6	4	38	15	11

Figure 3.25 Cell lineage of the first divisions of *Pristionchus pacificus*

A-**D** Lineages of embryos 1-4. Recordings are done at 20°C. The vertical axis indicates time of development and every division is visualised by a horizontal bar. Time starts after the division of AB. The left branch is always the anterior/left/dorsal sister.

Fig. 3.25

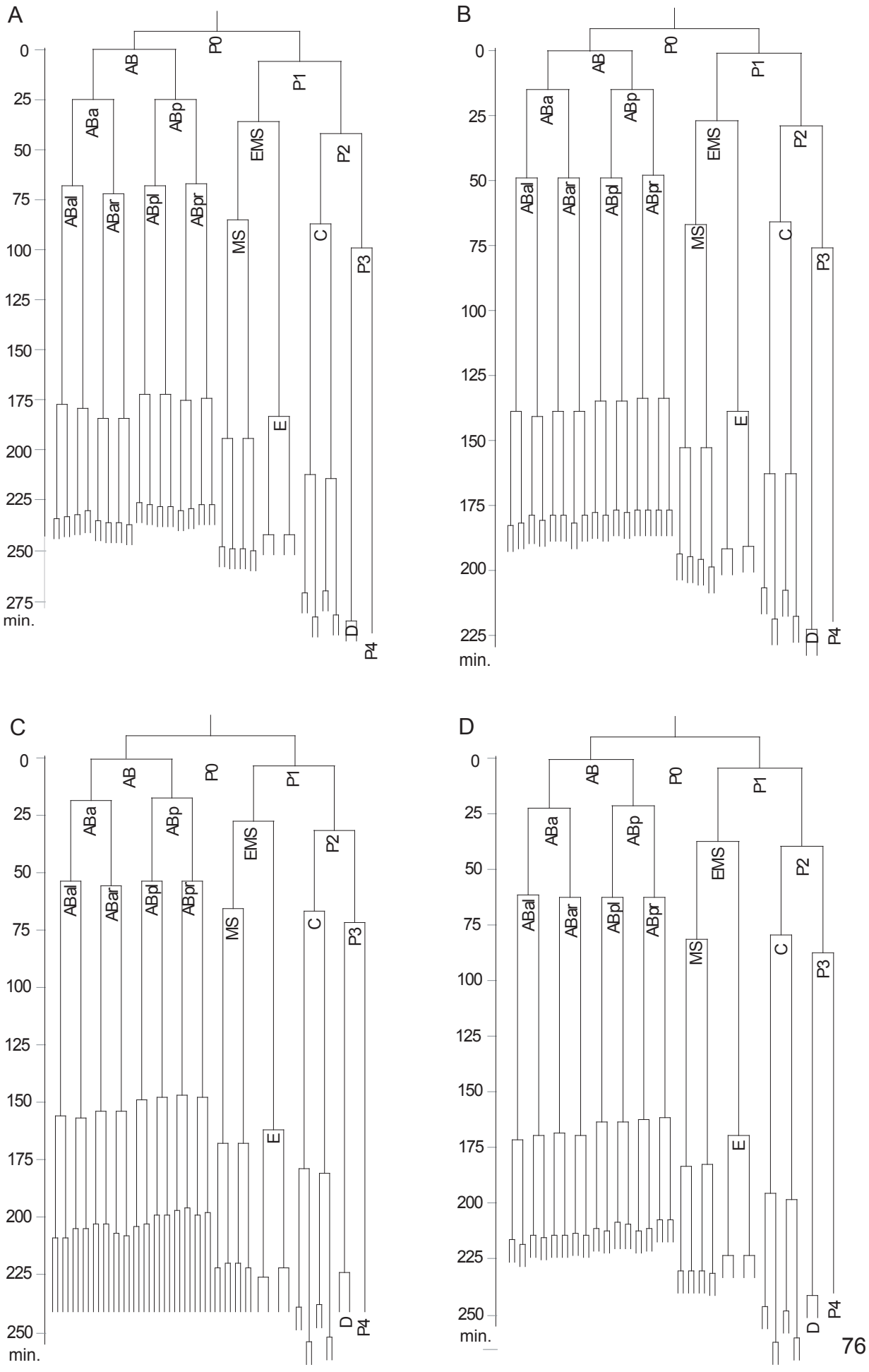
A
B
C
D
0
25
50
75
100
125
150
175
200
225
250
275
min.
P0
AB
P1
ABa
ABp
EMS
P2
ABal
ABar
ABpl
ABpr
MS
E
C
P3
D
P4

Fig. 3.25 (2) Cell lineage of the first divisions of *P. pacificus*

E-H Lineages of embryos 5-8. Recordings are done at 20°C. The vertical axis indicates time of development and every division is visualised by a horizontal bar. Time starts after the division of AB. The left branch is always the anterior/left/dorsal sister.

Fig. 3.25 (2)

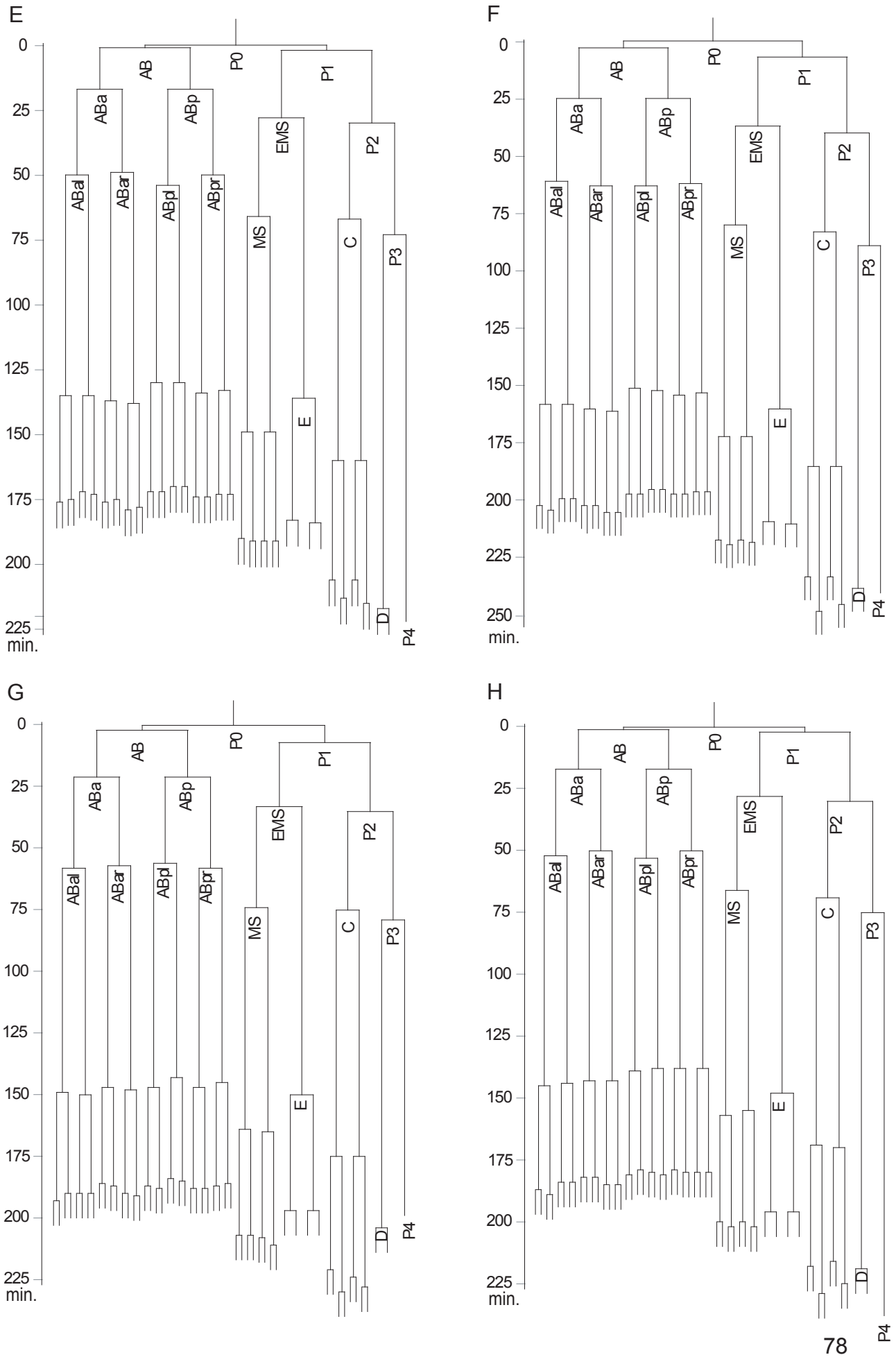
E
F
G
H
0
25
50
75
100
125
150
175
200
225
250
min.
P0
AB
P1
ABa
ABp
EMS
P2
ABal
ABar
ABpl
ABpr
MS
E
C
P3
D
P4

Fig. 3.25 (3) Cell lineage of the first divisions of *P. pacificus*

I-J Lineages of embryos 9-10. Recordings are done at 20°C. **K** Lineage of embryo 11. Recording is done at 15°C. **L** Lineage of embryo 12. Recording is done at 15°C. The vertical axis indicates time of development and every division is visualised by a horizontal bar. Time starts after the division of AB. The left branch is always the anterior/left/dorsal sister.

Fig. 3.25 (3)

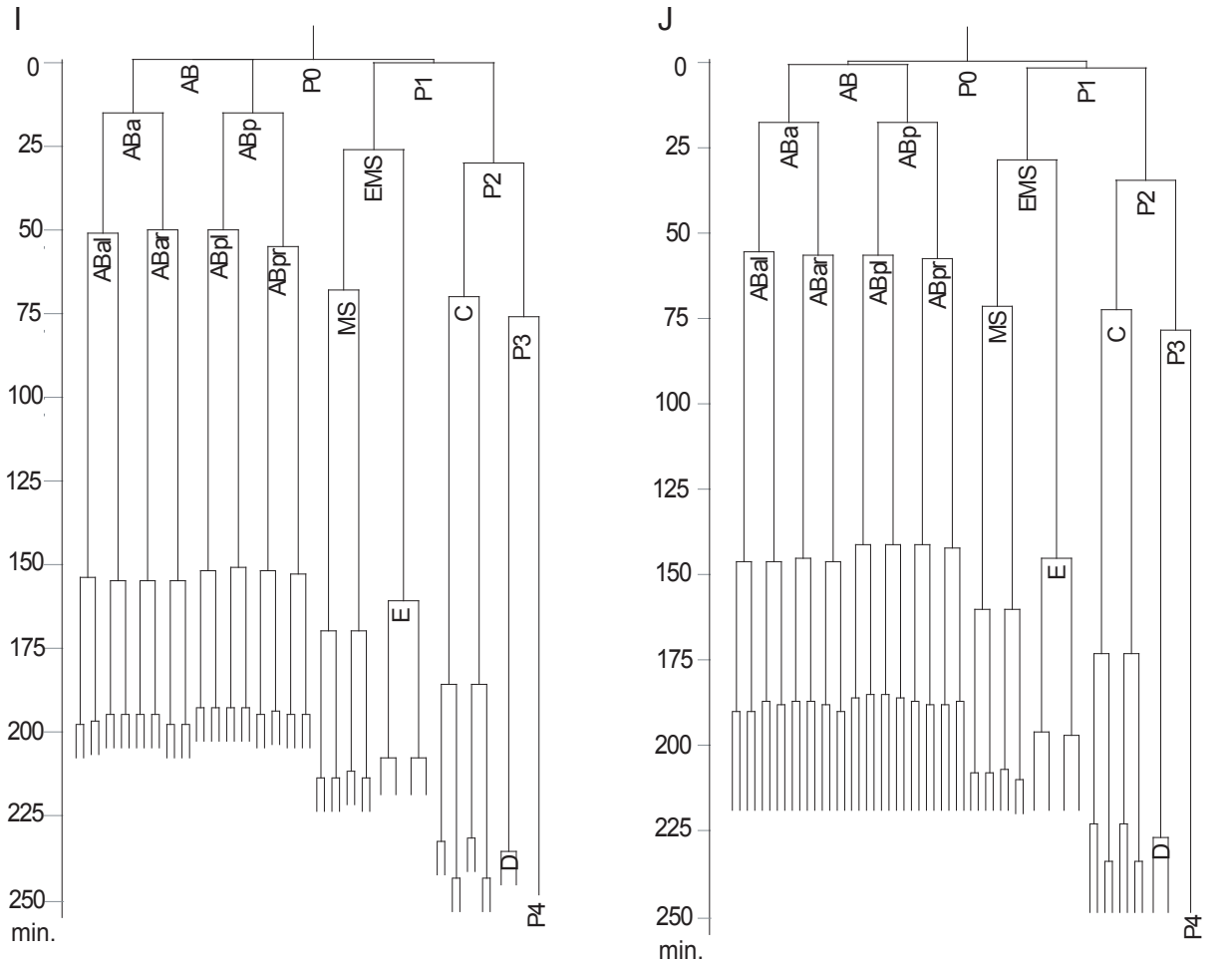
I
J
0
25
50
75
100
125
150
175
200
225
250
min.
AB
P0
P1
ABa
ABp
EMS
P2
ABal
ABar
ABpl
ABpr
MS
C
P3
E
D
P4

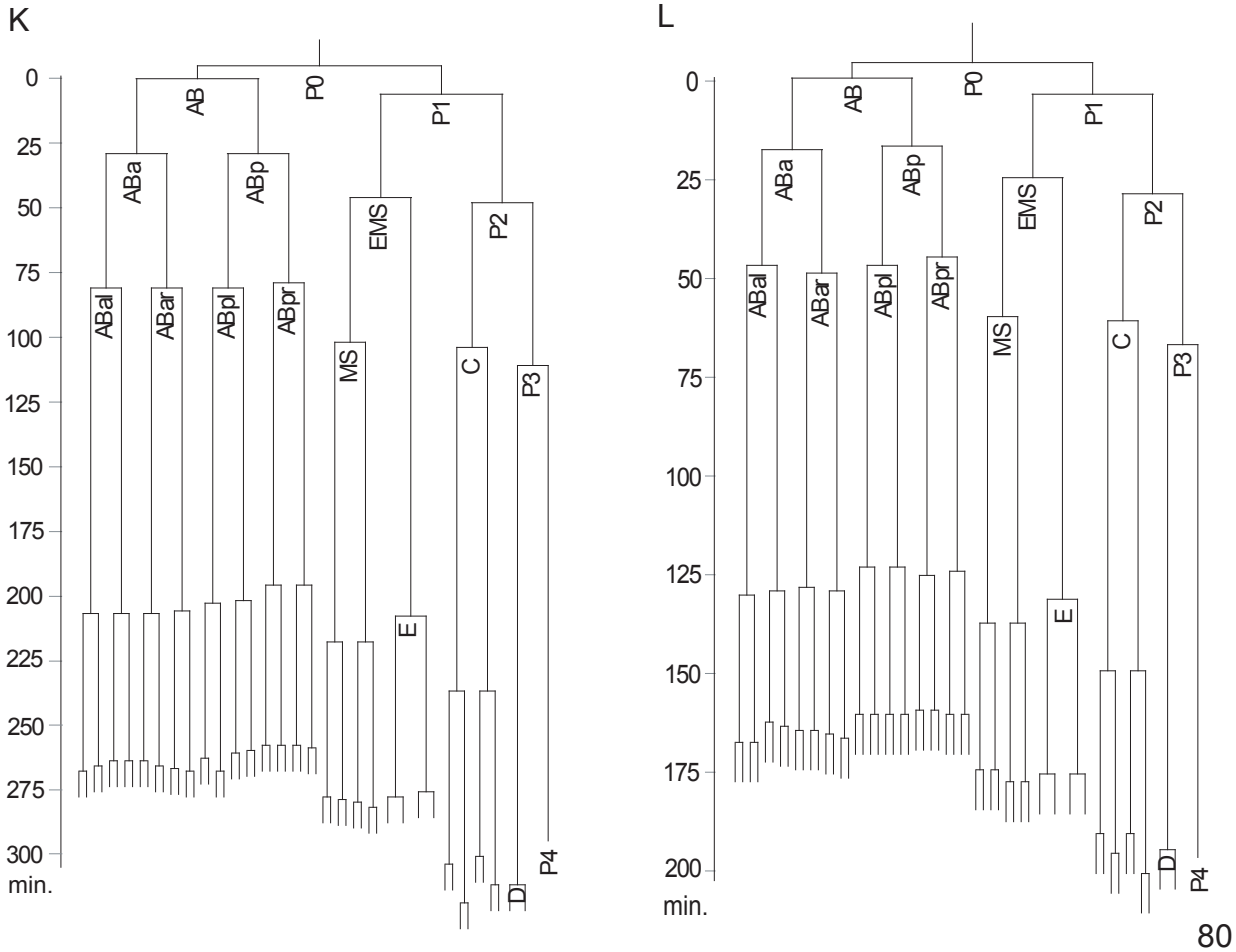
K
L
0
25
50
75
100
125
150
175
200
225
250
275
300
min.
AB
P0
P1
ABa
ABp
EMS
P2
ABal
ABar
ABpl
ABpr
MS
C
P3
E
D
P4

Figure 3.26 Variability of cell division timing in the AB lineage of *P. pacificus*

The figure shows the division pattern of 16AB cells in 4 embryos. **A** Lineage of embryo 4 (20°C), **B** embryo 8 (20°C), **E** embryo 11 (15°) and **F** embryo 12 (25°C). The vertical axis indicates time of development and every division is visualised by a horizontal bar. The left branch is always the anterior/left/dorsal sister. The pattern of the 16AB cells is extracted below each lineage. **C e**mbryo 4, **D** embryo 8, **G** embryo 11 and **H** embryo 12. The mean time (± SD)of the cell divisions is indicated.

Fig. 3.26

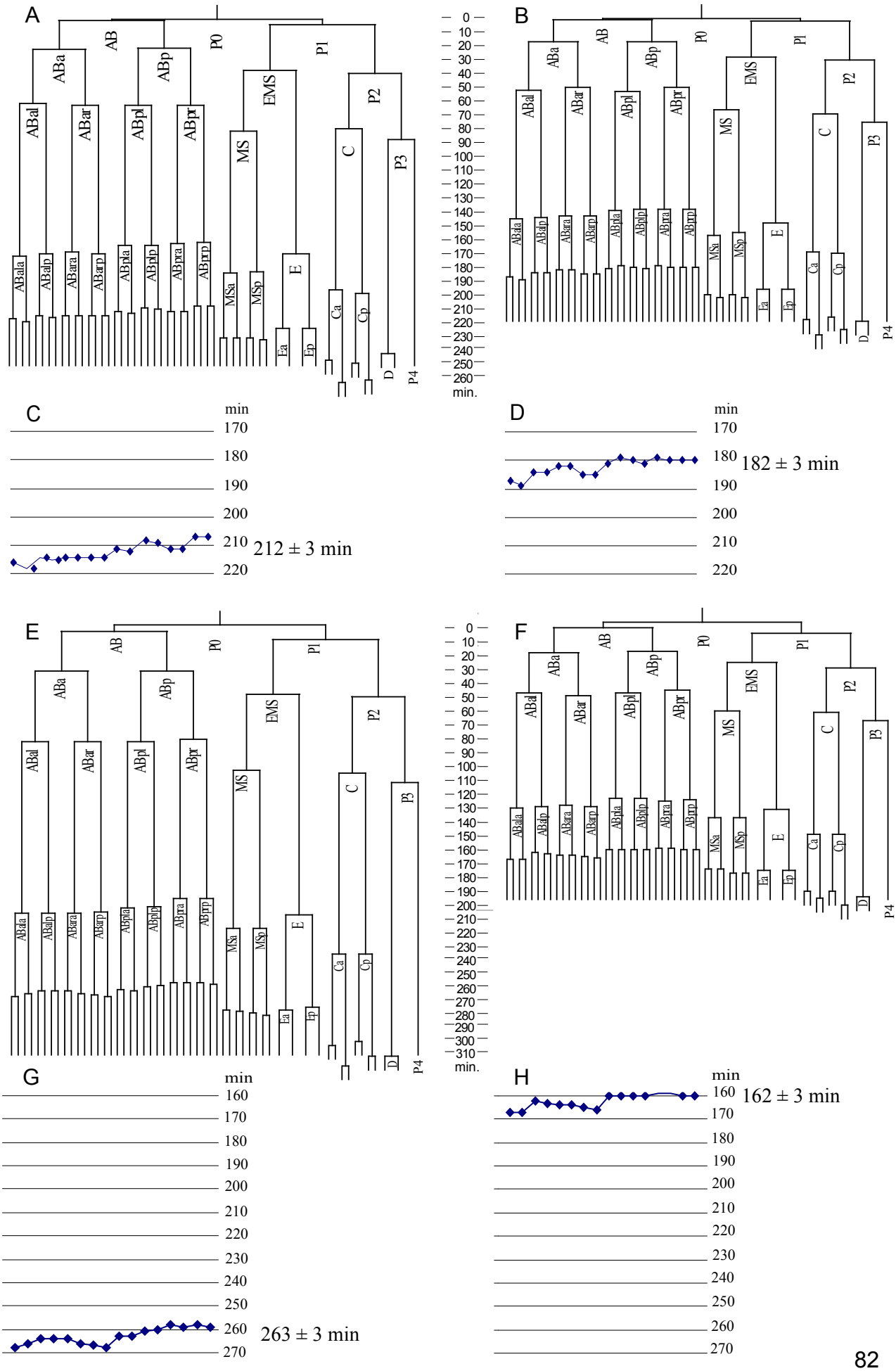
A
B
C
D
E
F
G
H
AB
P0
P1
ABa
ABp
EMS
P2
ABal
ABar
ABpl
ABpr
MS
C
P3
ABala
ABalp
ABara
ABarp
ABpla
ABplp
ABpra
ABprp
MSa
MSp
E
Ea
Ep
Ca
Cp
D
P4
0 10 20 30 40 50 60 70 80 90 100 110 120 130 140 150 160 170 180 190 200 210 220 230 240 250 260
min.
min
170
180
190
200
210
220
212 ± 3 min
182 ± 3 min
0 10 20 30 40 50 60 70 80 90 100 110 120 130 140 150 160 170 180 190 200 210 220 230 240 250 260 270 280 290 300 310
min.
160
170
180
190
200
210
220
230
240
250
260
270
263 ± 3 min
162 ± 3 min

Table 3.7 Division sequence of early cell divisions for 12 recordings *of P. pacificus*

The germline cells are marked in bold.

Figure 3.27 Number of cells during embryonic development in *P. pacificus*

Time starts after the division of AB.

Figure 3.28 Cell cycle length of AB generations in *P. pacificus* at different temperatures

The average cell cycle length of each AB generation is plotted in time for *P. pacificus* recordings at 15°C, 20°C and at 25°C. The average (± SD) of 20°C is based on 10 recordings.

Table 3.7

Embryo/Division	1	2	3	4	5	6	7	8	9	10	11	12	13	14	15	16	17	18	19
Embryo 1	P0	AB	P1	2AB	EMS	P2	4AB	MS	C	P3	8AB	E	2MS	2C	16AB	2E	4MS	D	4C
Embryo 2	P0	AB	P1	2AB	EMS	P2	4AB	C	MS	P3	8AB	E	2MS	2C	16AB	2E	4MS	4C	D
Embryo 3	P0	AB	P1	2AB	EMS	P2	4AB	MS	C	P3	8AB	E	2MS	2C	16AB	4MS	2E	D	4C
Embryo 4	P0	AB	P1	2AB	EMS	P2	4AB	C	MS	P3	8AB	E	2MS	2C	16AB	2E	4MS	D	4C
Embryo 5	P0	AB	P1	2AB	EMS	P2	4AB	MS	C	P3	8AB	E	2MS	2C	16AB	2E	4MS	4C	D
Embryo 6	P0	AB	P1	2AB	EMS	P2	4AB	MS	C	P3	8AB	E	2MS	2C	16AB	2E	4MS	D	4C
Embryo 7	P0	AB	P1	2AB	EMS	P2	4AB	MS	C	P3	8AB	E	2MS	2C	16AB	2E	D	4MS	4C
Embryo 8	P0	AB	P1	2AB	EMS	P2	4AB	MS	C	P3	8AB	E	2MS	2C	16AB	2E	4MS	D	4C
Embryo 9	P0	AB	P1	2AB	EMS	P2	4AB	MS	C	P3	8AB	E	2MS	2C	16AB	2E	4MS	D	D
Embryo 10	P0	AB	P1	2AB	EMS	P2	4AB	MS	C	P3	8AB	E	2MS	2C	16AB	2E	4MS	D	4C
Embryo 11 (15°C)	P0	AB	P1	2AB	EMS	P2	4AB	MS	C	P3	8AB	E	2MS	2C	16AB	2E	4MS	D	4C
Embryo 12 (25°C)	P0	AB	P1	2AB	EMS	P2	4AB	MS	C	P3	8AB	E	2MS	2C	16AB	2E	4MS	D	4C
C. elegans	P0	AB	P1	2AB	EMS	P2	4AB	MS	E	C	P3	8AB	2MS	2C	16AB	2E	4MS	4C	D

Fig. 3. 27

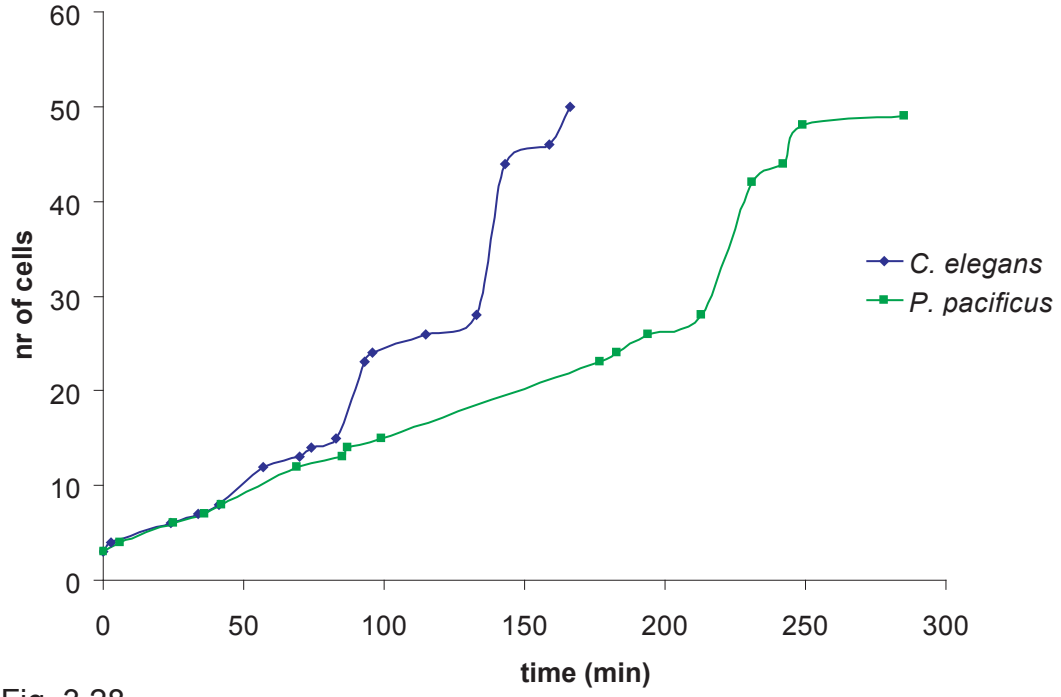

Fig. 3.28

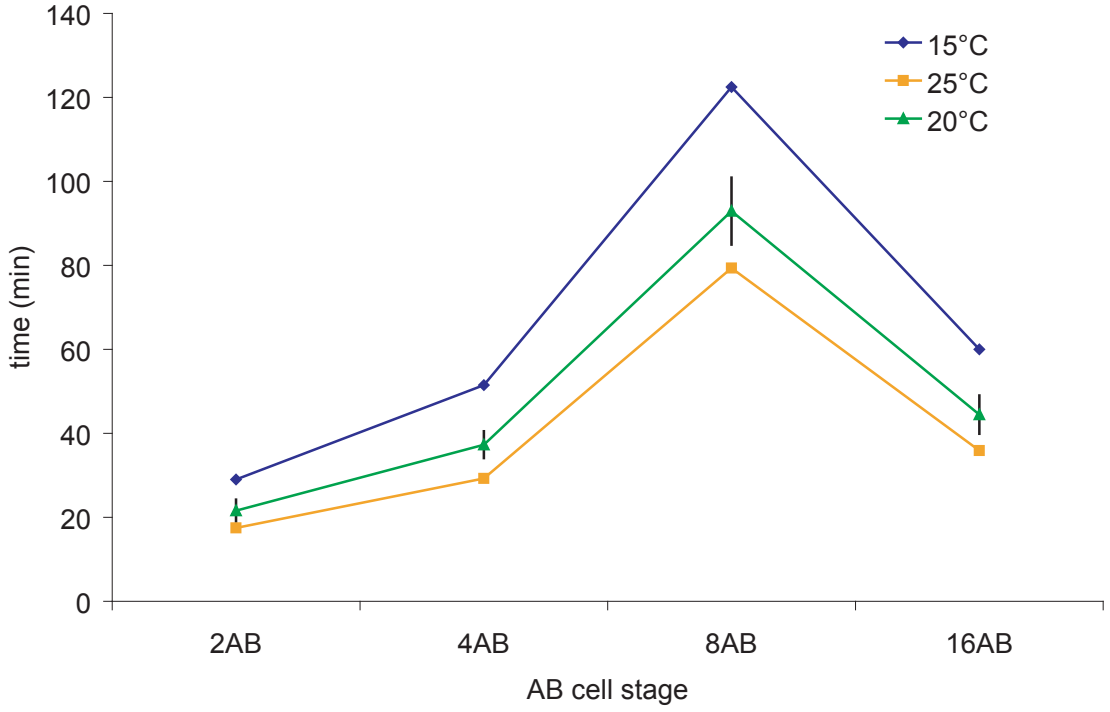

Figure 3.29 Cell division periods of generations of AB cells (until the 16 AB stage) in 12 individuals of *P. pacificus*

Cell division rounds per founder cell in time (min) for12 individuals of *P. pacificus*, showing differences in cell-cycle times for the six founder cells. On each horizontal line the cell division events of one founder cell are given. Each solid black box indicates the time from the division of the first cell to the division of the last cell in a given round of division. Time (min) starts after the division of AB.

Figure 3.30 Cell division periods per founder cell for *P. pacificus*

Cell division rounds per founder cell in time (min) for *P. pacificus* (embryo 1), showing differences in cell-cycle times for the six founder cells. On each horizontal line the cell division events of one founder cell are given. Each solid black box indicates the time from the division of the first cell to the division of the last cell in a given round of division. Time (min) starts after the division of AB.

Fig. 3.29

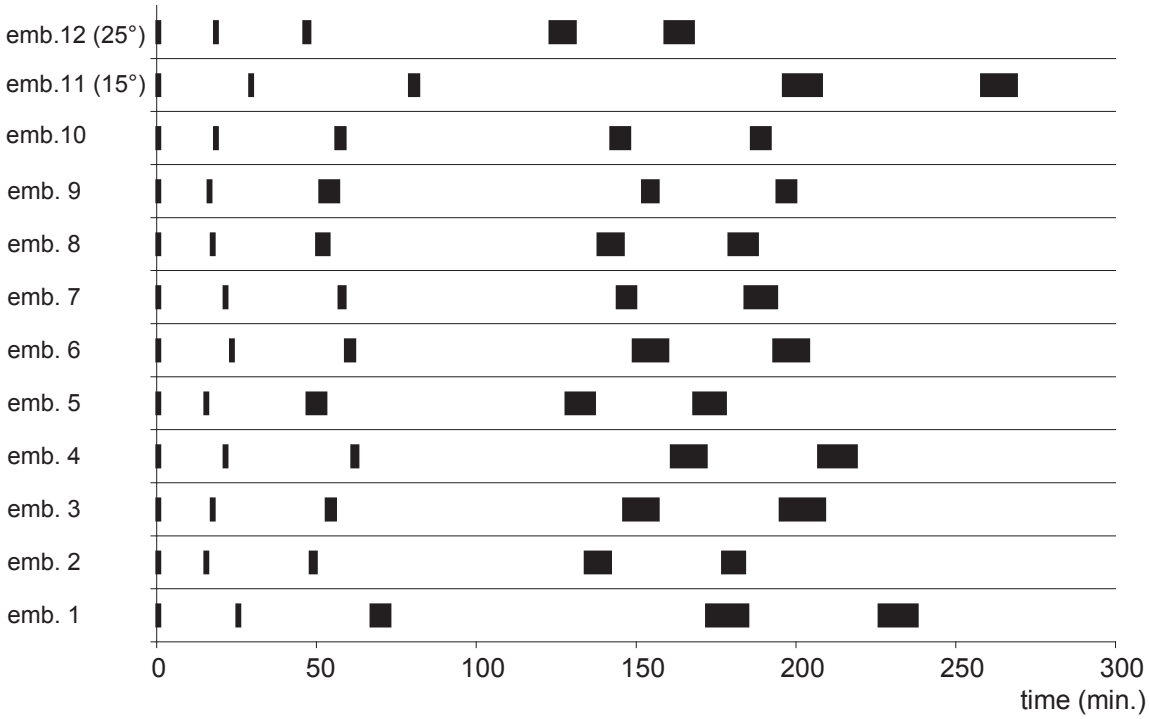

Fig. 3.30

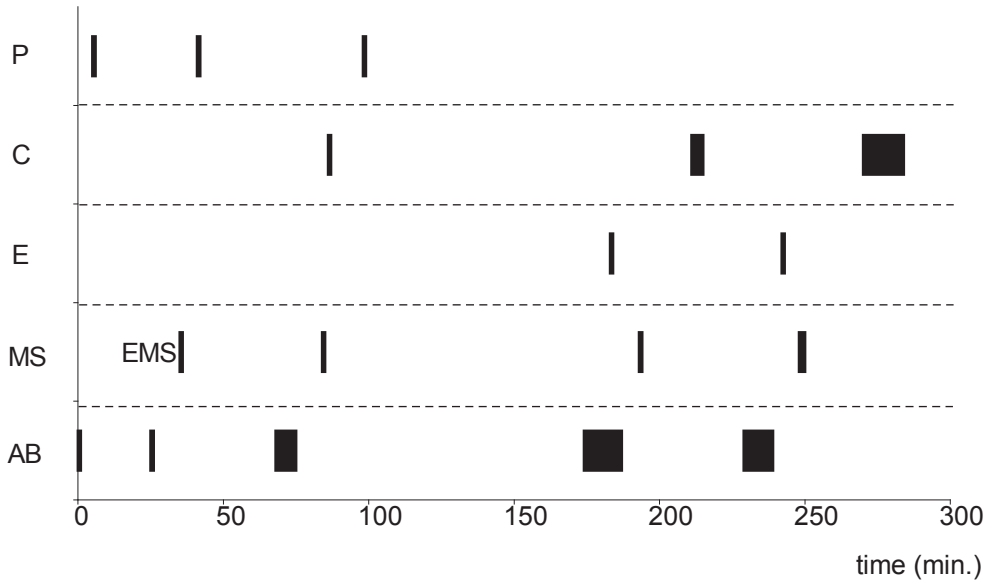

Figure 3.31 Cell-cell contacts at the 8AB cell stage in *P. pacificus*

Cell-cell contacts at the 8 AB cell-stage in *P. pacificus* (upper line) and *C. elegans* (lower line) (1 = contact is present, 0 = contact is absent). Variable contacts are marked by a grey square; numbers indicate the number of cases where contact was present (*P. pacificus*: n=13; *C. elegans*: n = 12). (*C. elegans* data from Hutter and Schnabel, 1994 and Hutter and Schnabel, 1995a).

Figure 3.32 Nomarski pictures and schematic representation of the cell-cell contacts in a 12 cell embryo of *P. pacificus*

A Nomarski pictures of an upper, **B** medial and **C** lower focal plane of embryo 2. **D-F** Drawings corresponding to the pictures A-C. For clarity the AB-prefix in the AB cells was omitted. The contacts ABala-ABarp, ABpla-ABprp exist in *P. pacificus*, but not in *C. elegans*. Right lateral view, anterior to the right.

Fig. 3.31

	ala	alp	ara	arp	pla	plp	pra	prp	MS	E	C	P3
ala		1 1	1 1	1 0	1 1	0 5/13	0 0	0 0	0 0	0	0	0
alp			1 1	0 0	9/12 8/13	1 1	0 0	0 0	1 1	0	0	0
ara				1 1	1 1	5/12 8/13	1 1	1 7/13	1 1	0	0	0
arp					1 1	7/12 1	1 1	4/12 5/13	0 0	0	1	0
pla						1 1	0 0	1 0	3/12 0	0	1	0
plp							0 0	4/12 0	1 1	1	1	0
pra								1 1	0 6/13	3/12	1	0
prp									1 1	1	1	0
MS										1	0	0
E											1	1
C												1
P3												

Fig. 3.32

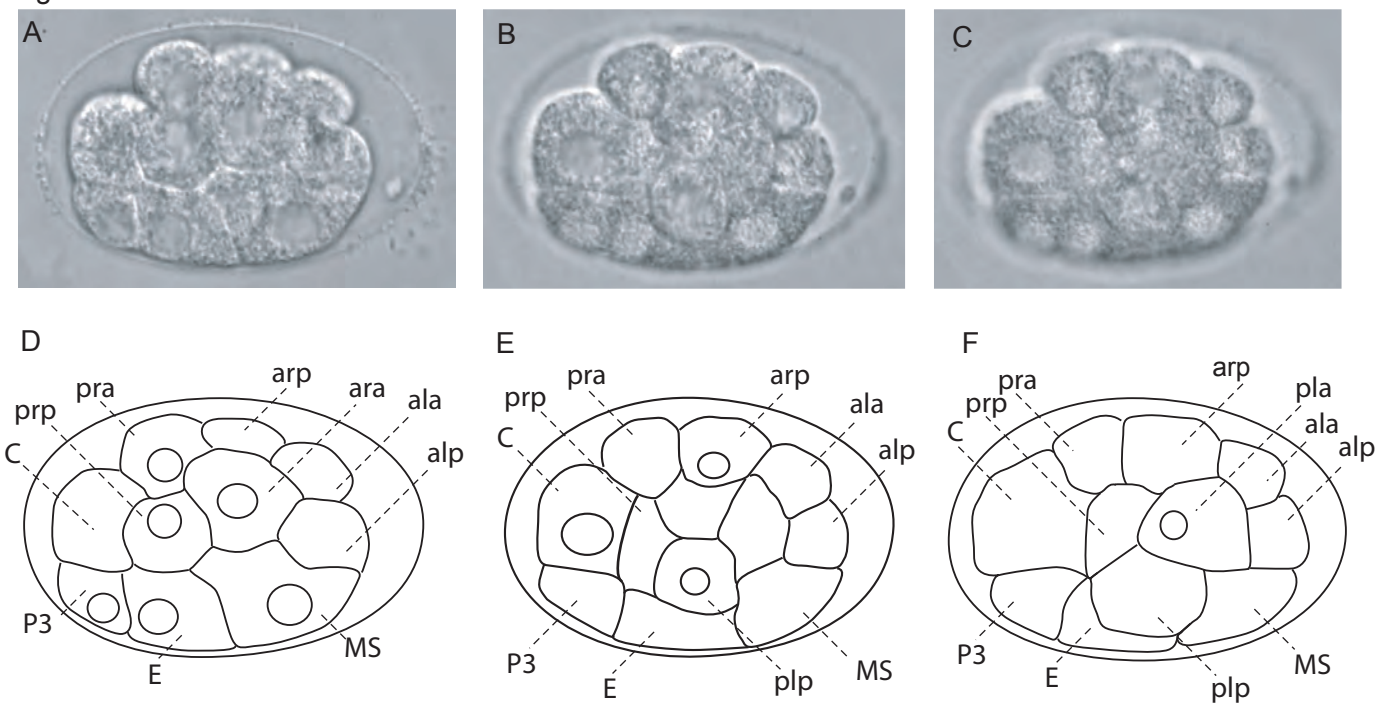

Table 3.8 Cleavage orientation of AB cells in *P. pacificus*.

Division angles (+ SD / SE) are expressed as deviation from the a-p axis in degrees. Divisions which are predominantly oriented along the a-p axis (division angles < 45°) are marked in blue, more skewed divisions (division angles > 45°) are marked in black.

Table 3.8

cell	av	stdev	SE
ABal	83	5	1
Abar	85	3	1
ABpl	57	17	5
ABpr	80	9	3
ABala	44	11	3
ABalp	65	12	3
ABara	37	17	5
ABarp	8	6	2
ABpla	16	12	3
ABplp	39	12	4
ABpra	19	12	4
ABprp	31	20	6

Figure 3.33 Cell lineage of the first divisions of *Halicephalobus gingivalis*

A-C Lineages of embryos 1-3.The vertical axis indicates time of development and every division is visualised by a horizontal bar. Time starts after the division of P1. The left branch is always the anterior/left/dorsal sister.

Fig. 3.33

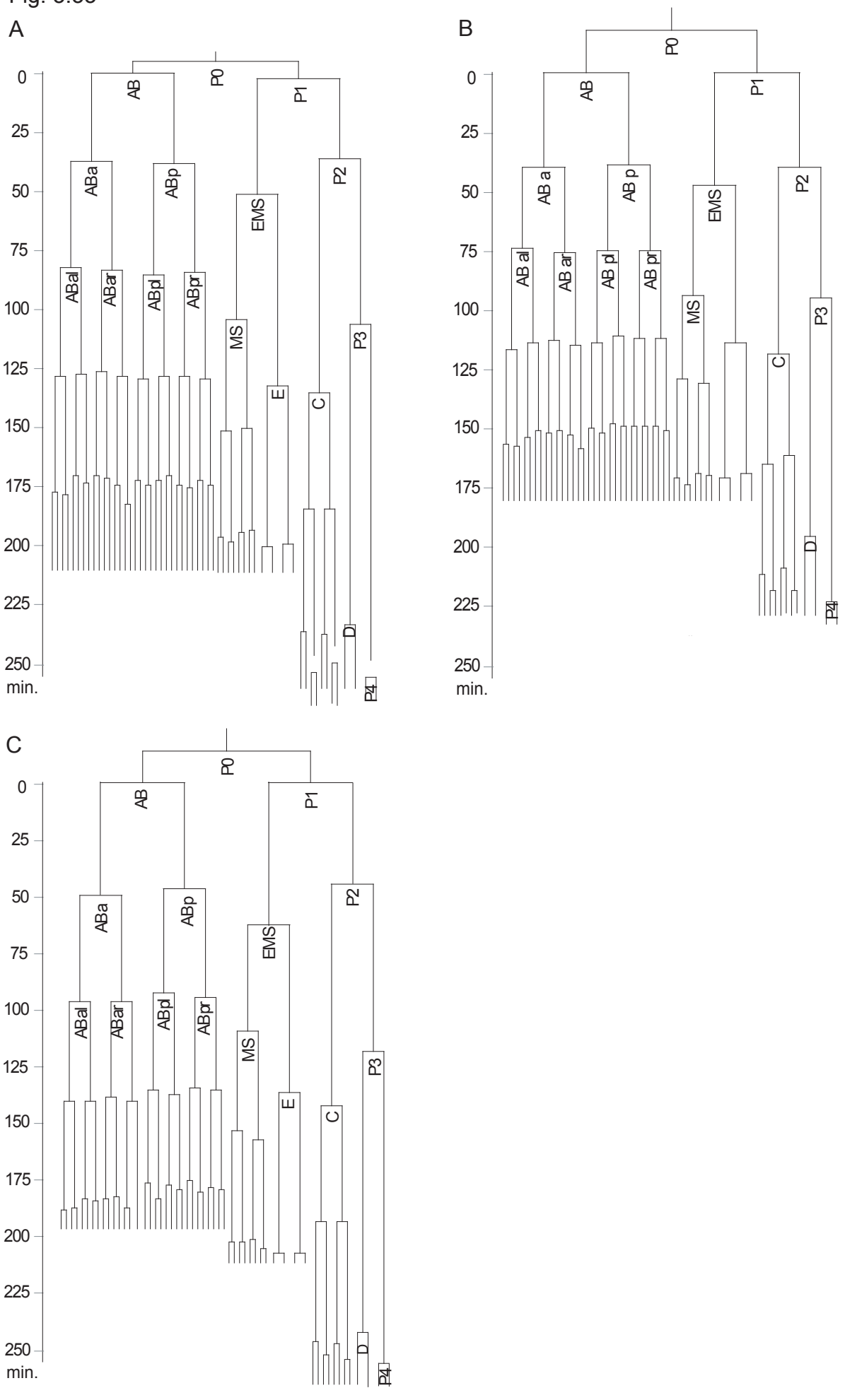
A
0
25
50
75
100
125
150
175
200
225
250
min.
AB
P0
P1
ABa
ABp
EMS
P2
ABal
ABar
ABpl
ABpr
MS
E
C
P3
D
P4
B
AB a
AB p
AB al
AB ar
AB pl
AB pr
C
P3
D
P4
C

Figure 3.34 Cell lineage of the first divisions of *Panagrellus redivivus*

A-**B** Lineages of embryos 1-2.The vertical axis indicates time of development and every division is visualised by a horizontal bar. Time starts after the division of AB. The left branch is always the anterior/left/dorsal sister.

Fig. 3.34

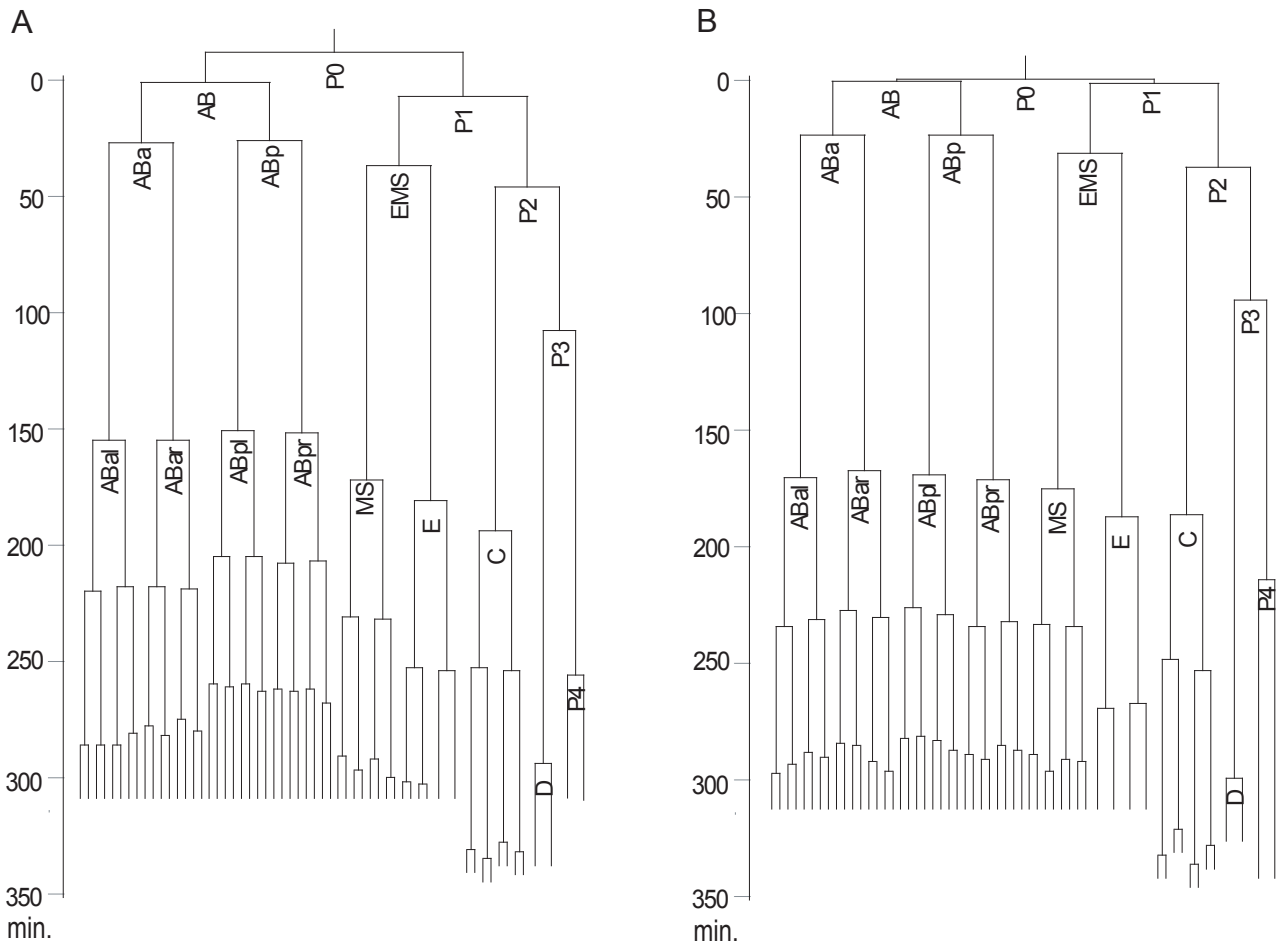
A
B
0
50
100
150
200
250
300
350
min.
P0
AB
P1
ABa
ABp
EMS
P2
P3
ABal
ABar
ABpl
ABpr
MS
E
C
D
P4

Figure 3.35 Cell lineage of the first divisions of *Panagrolaimus detritophagus*

A-C Lineages of embryos 1-3.The vertical axis indicates time of development and every division is visualised by a horizontal bar. Time starts after the division of P1. The left branch is always the anterior/left/dorsal sister.

Fig. 3.35

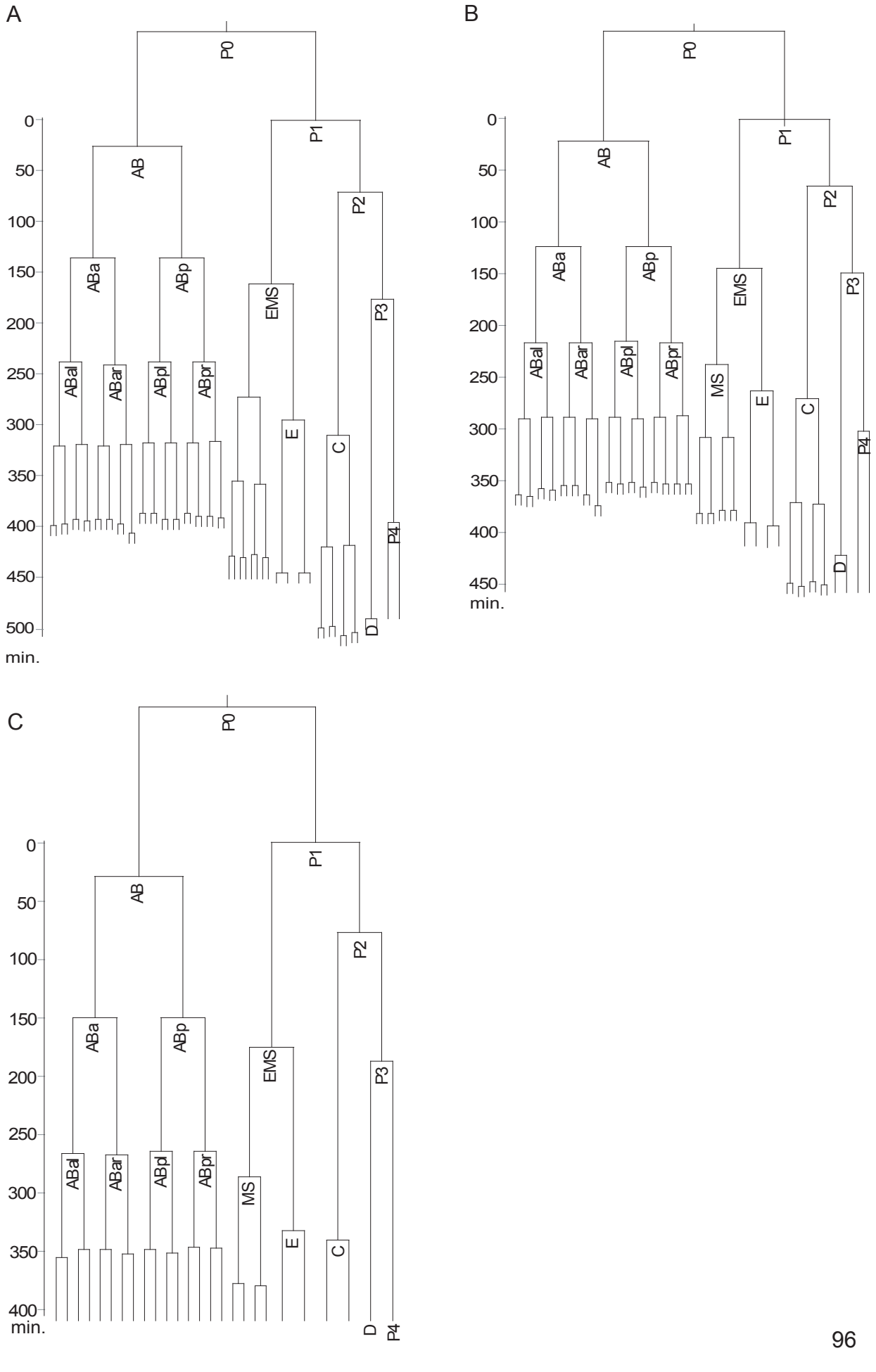
A
P0
P1
AB
P2
ABa
ABp
EMS
P3
ABal
ABar
ABpl
ABpr
E
C
P4
D
0
50
100
150
200
250
300
350
400
450
500
min.
B
P0
P1
AB
P2
ABa
ABp
EMS
P3
ABal
ABar
ABpl
ABpr
MS
E
C
P4
D
0
50
100
150
200
250
300
350
400
450
min.
C
P0
P1
AB
P2
ABa
ABp
EMS
P3
ABal
ABar
ABpl
ABpr
MS
E
C
D
P4
0
50
100
150
200
250
300
350
400
min.

Figure 3.36 Cell lineage of the first divisions of *Panagrolaimus rigidus*

A-C Lineages of embryos 1-3.The vertical axis indicates time of development and every division is visualised by a horizontal bar. Time starts after the division of AB. The left branch is always the anterior/left/dorsal sister.

Fig. 3.36

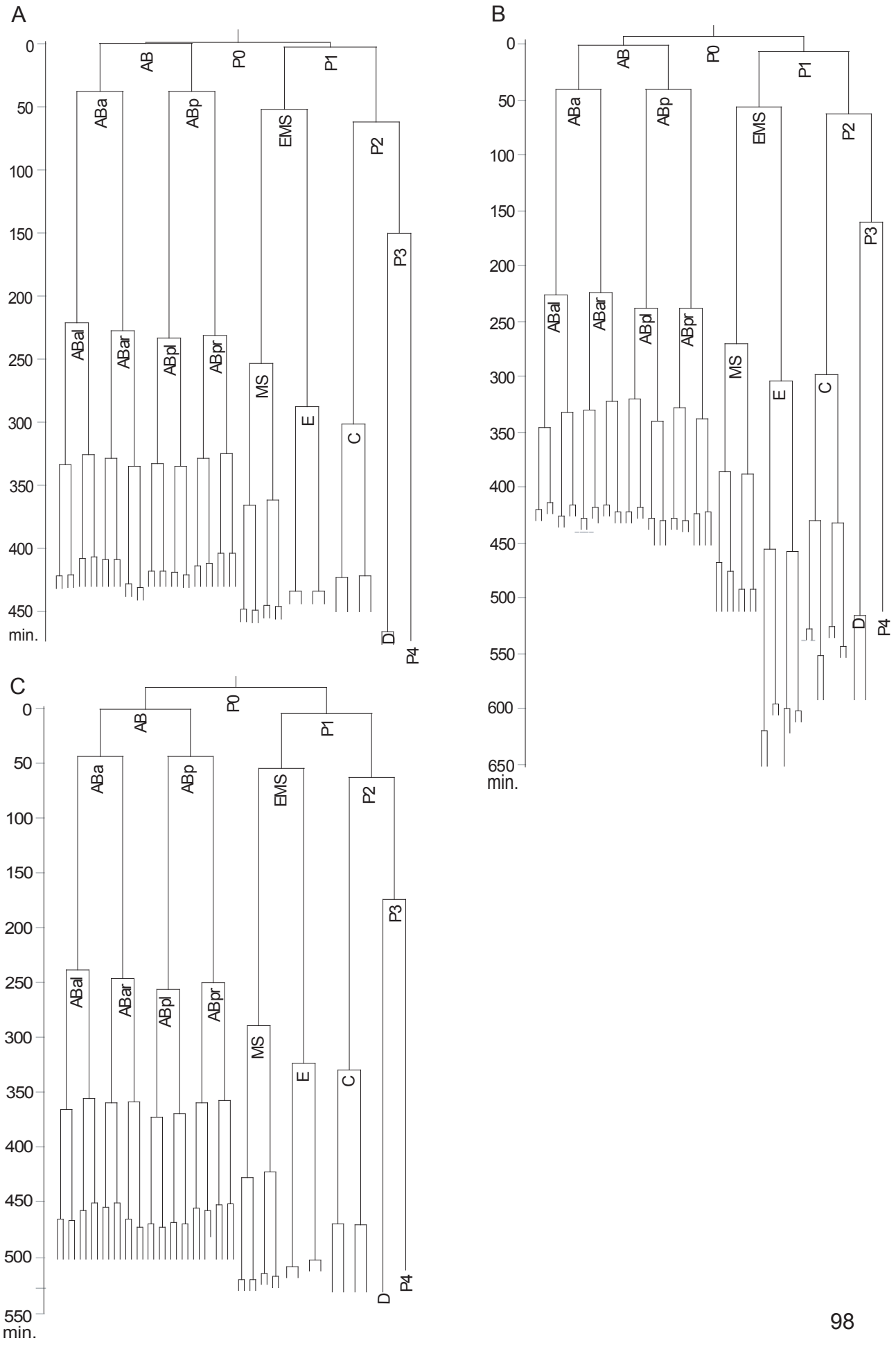
A
B
C
0
50
100
150
200
250
300
350
400
450
500
550
600
650
min.
AB
P0
P1
ABa
ABp
EMS
P2
P3
ABal
ABar
ABpl
ABpr
MS
E
C
D
P4

Figure 3.37 Cell lineage of the first divisions of *Procephalobus* sp.

A-C Lineages of embryos 1-3.The vertical axis indicates time of development and every division is visualised by a horizontal bar. Time starts after the division of P1. The left branch is always the anterior/left/dorsal sister.

Fig. 3.37

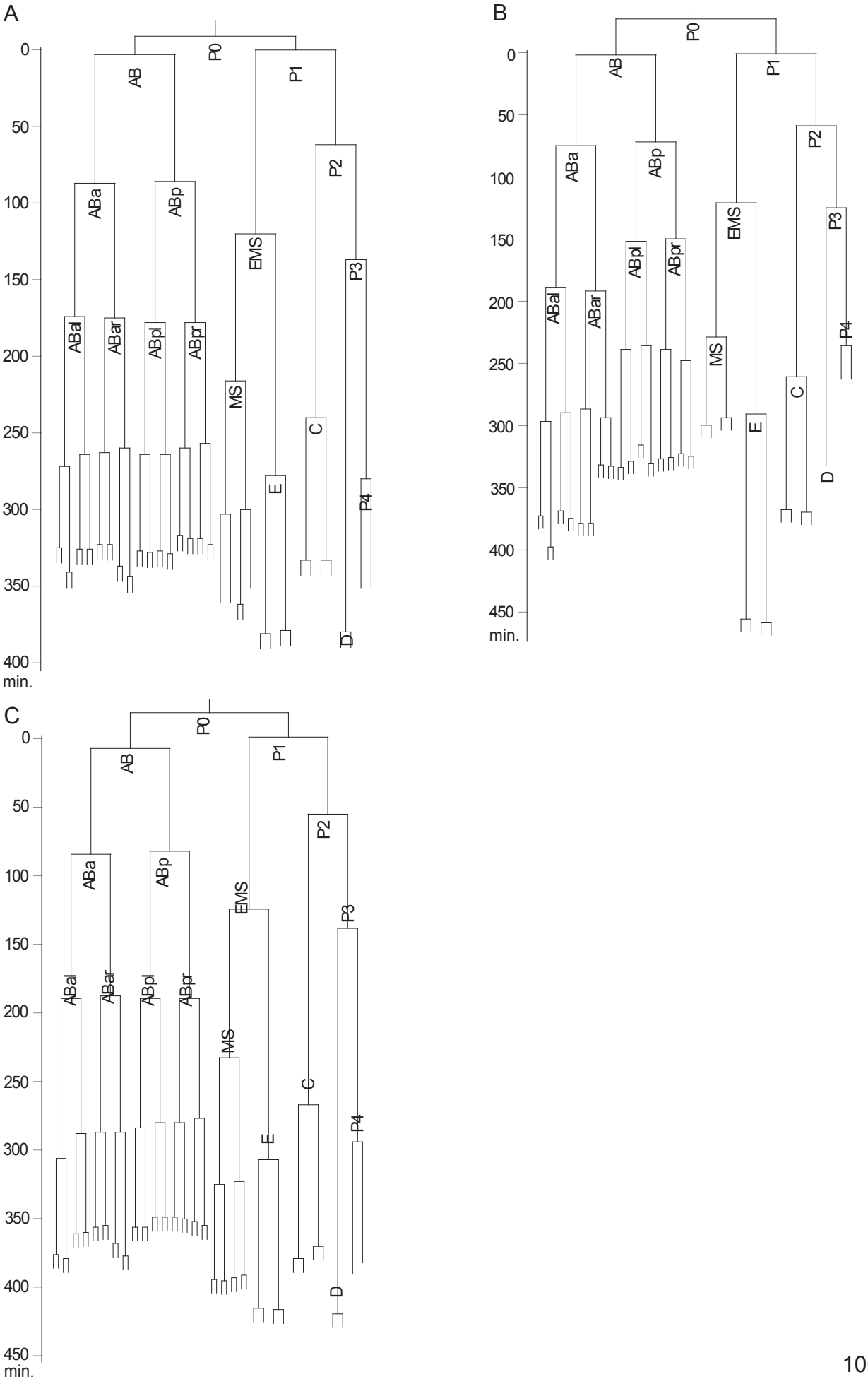
A
B
C
P0
AB
P1
ABa
ABp
EMS
P2
P3
ABal
ABar
ABpl
ABpr
MS
C
E
P4
D
0
50
100
150
200
250
300
350
400
450
min.

Table 3.9 Egg Shape Index calculated for all examined species of Panagrolaimidae

The average ESI ± SE and number of analyzed embryos for all examined species.

Figure 3.38 Nomarski image of the divisions of AB and P1 in *Procephalobus* sp.

Early four cell stage. The division axes of AB and P1 are perpendicular to each other, resulting in a transient T-shape, that converts to the rhomboid configuration when the anterior daughter cell of AB migrated to the anterior side (ABa) and the other AB daughter cell migrated to the future dorsal side of the embryo (ABp). Scale-bar = 10 µm

Table 3.9

species	ESI	SE	n
H. gingivalis	56	2	3
P. redivivus	65	4	2
P. detritophagus	58	1	3
P. rigidus	59	2	3
Procephalobus sp.	47	4	3

Fig. 3.38

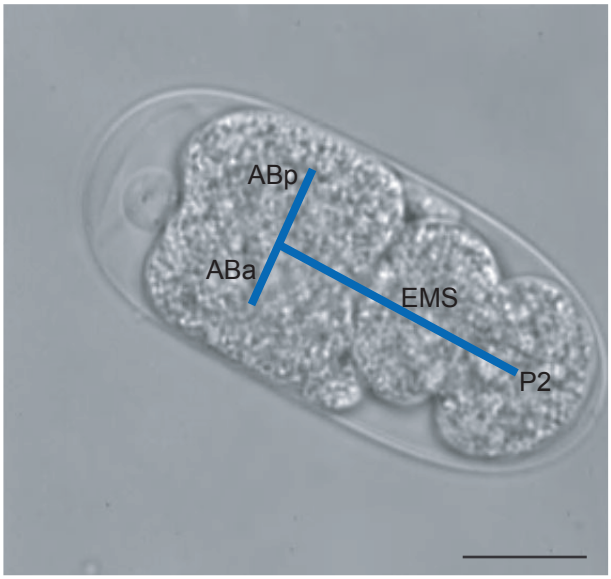

Table 3.10 Division sequence of early cell divisions in species of Panagrolaimidae

The germline cells are marked in bold.

Table 3.10

species	recording	sequence																	
H. gingivalis	embr1	**P1**	AB	**P2**	2AB	EMS	4AB	MS	**P3**	8AB	E	C	2MS	16AB	2C	4MS	2E	D	4C	**P4**
	embr2	**P1**	AB	2AB	**P2**	EMS	4AB	MS	**P3**	8AB	E	C	2MS	16AB	2C	2E	4MS	D	4C	**P4**
	embr3	**P1**	AB	**P2**	2AB	EMS	4AB	MS	**P3**	8AB	E	C	2MS	16AB	2C	4MS	2E	D	4C	**P4**
P. redivivus	embr1	AB	**P1**	2AB	EMS	**P2**	**P3**	4AB	MS	E	C	8AB	2MS	2C	2E	**P4**	16AB	D	4MS	4C
	embr2	AB	**P1**	2AB	EMS	**P2**	**P3**	4AB	MS	C	E	**P4**	8AB	2MS	2C	2E	16AB	4MS	D	4C
P. detritophagus	embr1	**P1**	AB	**P2**	2AB	EMS	**P3**	4AB	MS	E	C	8AB	2MS	16AB	**P4**	4MS	2E	D	4C	
	embr2	**P1**	AB	**P2**	2AB	EMS	**P3**	4AB	MS	E	C	8AB	**P4**	2MS	16AB	4MS	2E	D	4C	
	embr3	**P1**	AB	**P2**	2AB	EMS	**P3**	4AB	MS	E	C	8AB	2MS							
P. rigidus	embr1	AB	**P1**	2AB	EMS	**P2**	**P3**	4AB	MS	E	C	8AB	2MS	16AB	2C	2E	4MS	D		
	embr2	AB	**P1**	2AB	EMS	**P2**	**P3**	4AB	MS	C	E	8AB	2MS	16AB	2C	2E	4MS	D		
	embr3	AB	**P1**	2AB	EMS	**P2**	**P3**	4AB	MS	E	C	8AB	2MS	16AB	2C	2E	4MS			
Procephalobus sp.	embr1	**P1**	AB	**P2**	2AB	EMS	**P3**	4AB	MS	C	8AB	E	**P4**	2MS	16AB	2C	2E	D		
	embr2	**P1**	AB	**P2**	2AB	EMS	**P3**	4AB	MS	**P4**	C	8AB	E	2MS	2C	16AB	2E			
	embr3	**P1**	AB	**P2**	2AB	EMS	**P3**	4AB	MS	C	8AB	**P4**	2E	2MS	16AB	2C	2E			

Table 3.11 The relative early developmental tempo of the examined species of Panagrolaimidae

The relative early developmental tempo was measured as the time between the division of AB (*P. rigidus* and *P. redivivus*) or P1 (*H. gingivalis, P. detritophagus* and Proce*phalobus* sp.) and the division of E and normalized to the tempo of *C. elegans*.

Figure 3.39 Number of cells during embryonic development in species of Panagrolaimidae

Time starts after the division of AB (*P. rigidus* and *P. redivivus*) or P1 (*P. detritophagus* and Proce*phalobus* sp.). *H. gingivalis* is not included in the figure, since this recording was done at 25°C.

Table 3.11

species	rel tempo
H. gingivaluis	3.1
P. redivivus	2.6
P. detritophagus	4.6
P. rigidus	4.2
Procephalobus sp.	4.1

Fig. 3.39

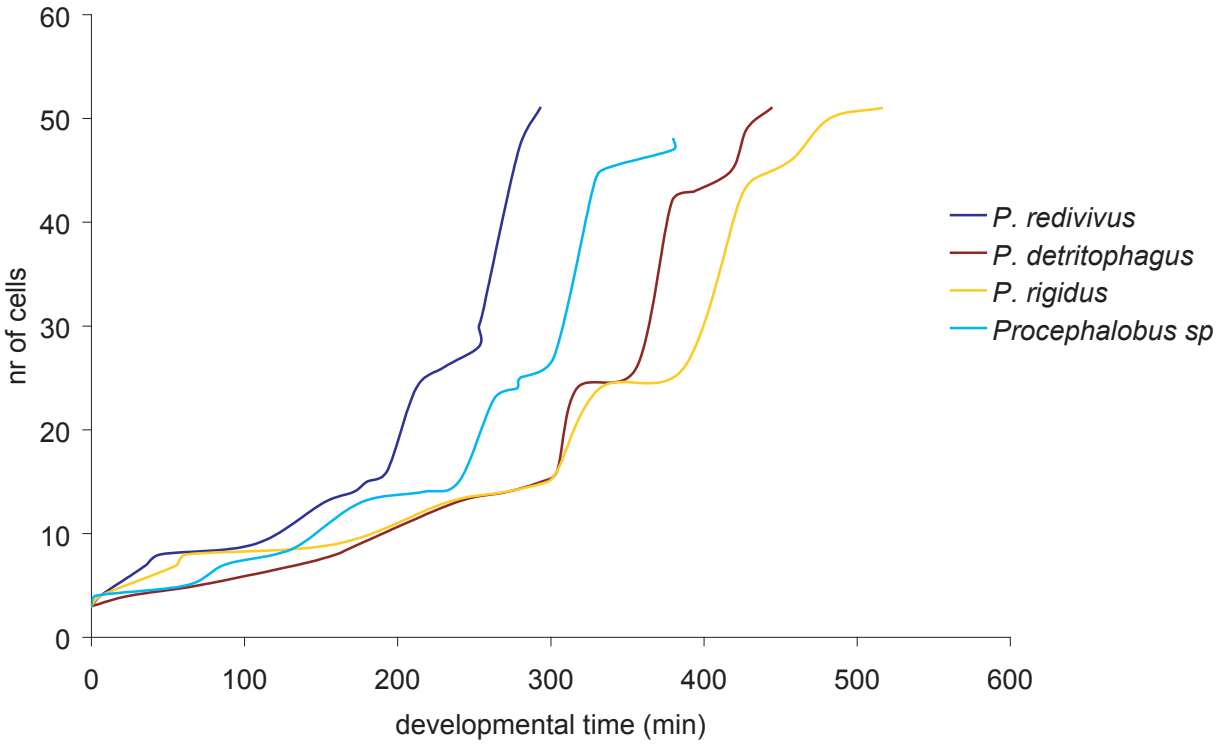

Figure 3.40 Cell cycle length of AB generations in species of Panagrolaimidae

The average cell cycle length (± SD) of AB in each generation is plotted in time for **A** *H. gingivalis*, **B** *P. redivivus*, **C** *P. detritophagus*, **D** *P. rigidus*, **E** *Procephalobus* sp. The average cell cycle length for each AB stage was based on 3 recordings, except for *P. redivivus* (2 recordings).

Fig. 3.40

A

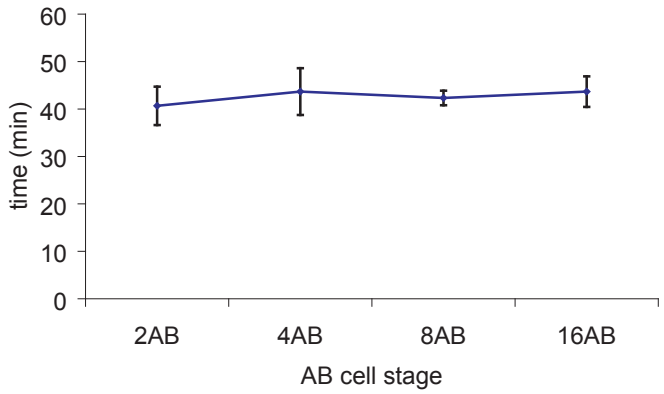

B

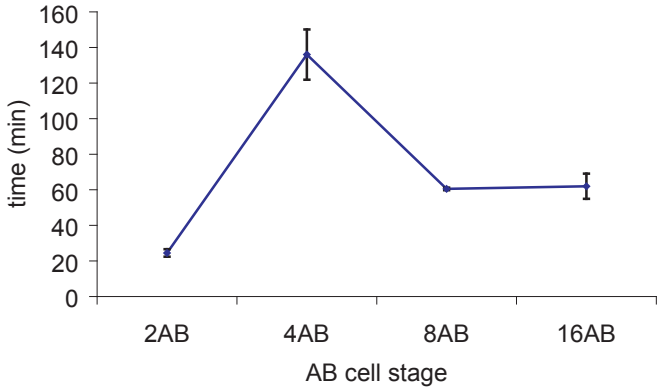

C

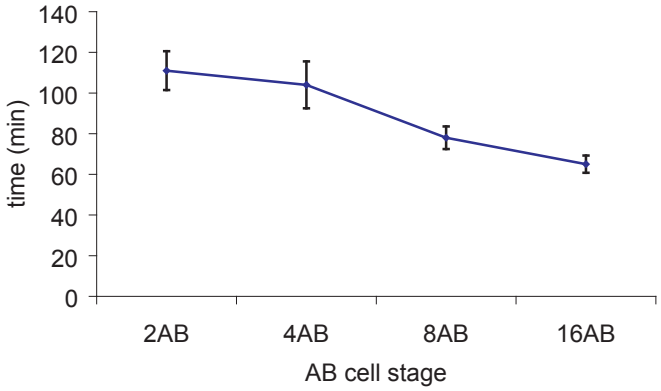

D

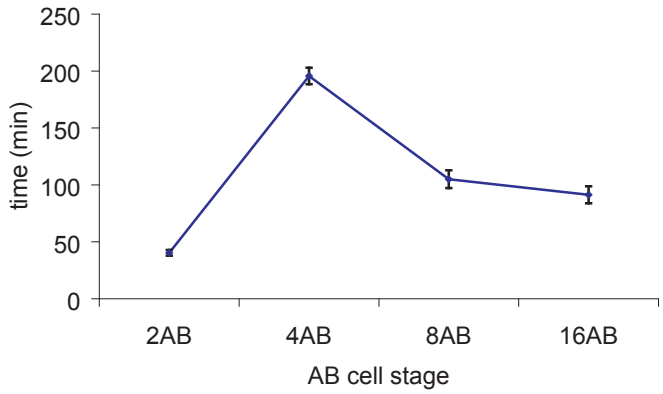

E

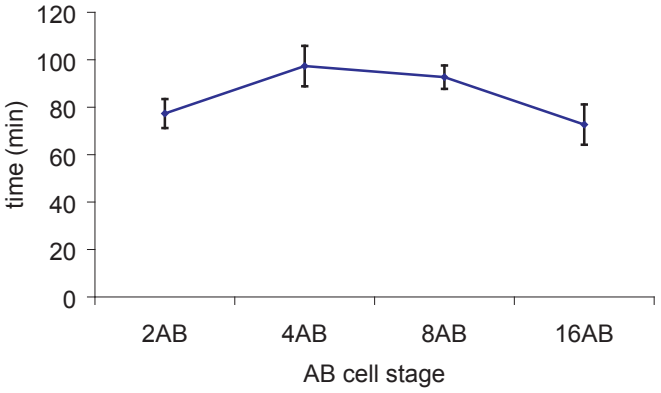

Figure 3.41 Cell division periods per founder cell in species of Panagrolaimidae

Cell division rounds per founder cell in time (min) for **A** *H. gingivalis* (3 recordings), **B** *P. redivivus* (2 recordings) and **C** *P. detritophagus* (3 recordings), showing differences in cell-cycle times for the six founder cells. On each horizontal line the cell division events of one founder cell are given. Each solid black box indicates the time from the division of the first cell to the division of the last cell in a given round of division. Time starts after the division of AB (*P. rigidus* and *P. redivivus*) or P1 (*H. gingivalis, P. detritophagus* and Procep*halobus* sp.).

Fig. 3.41

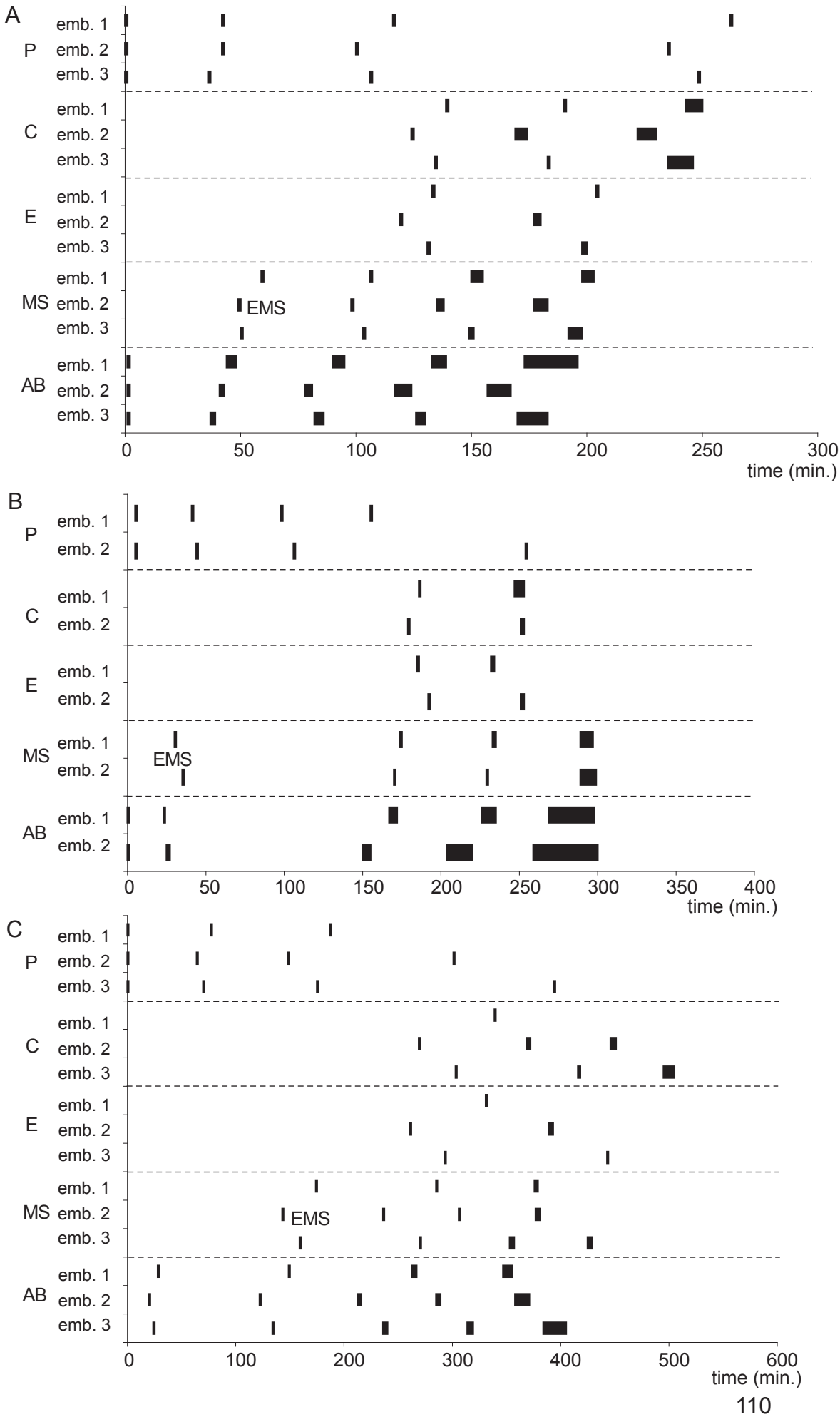
A
P
C
E
MS
AB
emb. 1
emb. 2
emb. 3
EMS
0
50
100
150
200
250
300
time (min.)
B
P
C
E
MS
AB
emb. 1
emb. 2
EMS
0
50
100
150
200
250
300
350
400
time (min.)
C
P
C
E
MS
AB
emb. 1
emb. 2
emb. 3
EMS
0
100
200
300
400
500
600
time (min.)

Fig. 3.41 (2) Cell division periods per founder cell

Cell division rounds per founder cell in time (min) for **D** *P. rigidus* (3 recordings) and **E** *Procephalobus* sp. (3 recordings)., showing differences in cell-cycle times for the six founder cells. On each horizontal line the cell division events of one founder cell are given. Each solid black box indicates the time from the division of the first cell to the division of the last cell in a given round of division. Time starts after the division of AB (*P. rigidus* and *P. redivivus*) or P1 (*H. gingivalis, P. detritophagus* and Proce*phalobus* sp.).

Fig. 3.41 (2)

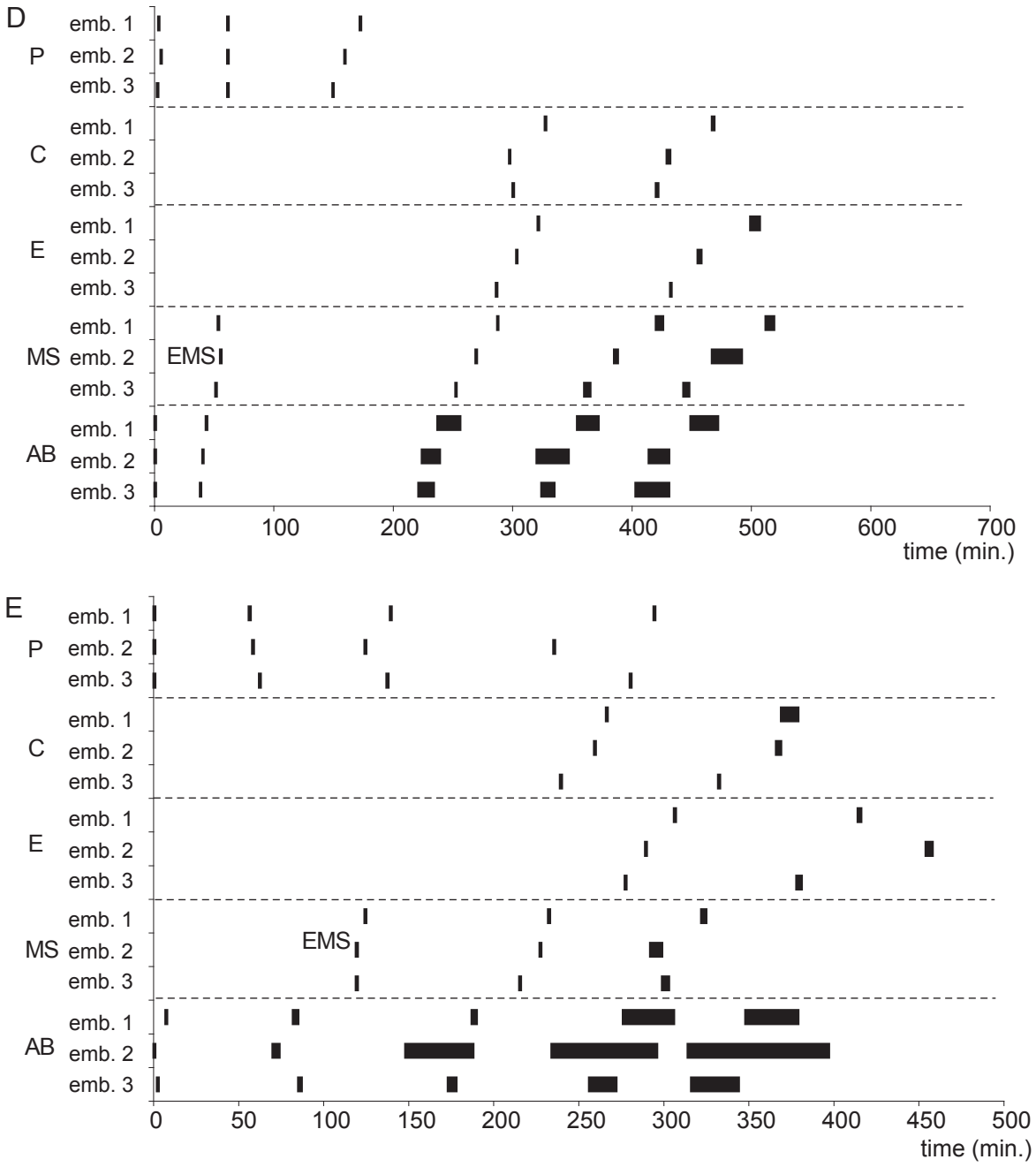
D
P
C
E
MS
AB
emb. 1
emb. 2
emb. 3
EMS
0
100
200
300
400
500
600
700
time (min.)
E
P
C
E
MS
AB
emb. 1
emb. 2
emb. 3
EMS
0
50
100
150
200
250
300
350
400
450
500
time (min.)

Figure 3.42 Cell-cell contacts at the 8AB cell stage in species of Panagrolaimidae

A *H. gingivalis*, **B** *P. redivivus*, **C** *P. detritophagus*, **D** *P. rigidus* and **E** *Procephalobus* sp. (1 = contact is present, 0 = contact is absent). Variable contacts are marked by a yellow square.

Fig. 3.42

A

	ala	alp	ara	arp	pla	plp	pra	prp	MS	E	C	P3
ala		1	1	1	1	0	0	0	0	0	0	0
alp			1	0	1	0	0	0	1	0	0	0
ara				1	0	0	1	0	1	0	0	0
arp					1	0	1	0	0	0	1	0
pla						1	0	0	1	0	1	0
plp								1	1	1	1	0
pra								1	1	0	1	0
prp									1	1	1	
MS										1	0	0
E											1	1
C												1
P3												

B

	ala	alp	ara	arp	pla	plp	pra	prp	MS	E	C	D	P4
ala		1	1	1	1	0	0	0	0	0	0	0	0
alp			1	0	1	1	0	0	1	0	0	0	0
ara				1	1	0	1	0	1	0	0	0	0
arp					1	0	1	0	0	0	1	0	0
pla						1	0	0	0	0	1	0	0
plp							0	0	1	1	1	0	0
pra								1	1	0	1	0	0
prp									1	1	1	1	1
MS										1	1	0	0
E											1	1	1
C												1	0
D													1
P4													

C

	ala	alp	ara	arp	pla	plp	pra	prp	MS	E	C	D	P4
ala		1	1	1	1	0	0	0	0	0	0		0
alp			1	0	1	0	0	0	1	0	0	0	0
ara				1	0	0	1	0	1	0	0	0	0
arp					1	0	1	0	0	0	1	0	0
pla						1	0	0		0		0	0
plp							0	0	1	1	1	0	0
pra								1	1	0	1	0	0
prp									1	1	1		0
MS										1	0	0	0
E											1	1	1
C												1	0
D													1
P4													

D

	ala	alp	ara	arp	pla	plp	pra	prp	MS	E	C	D	P4
ala		1	1	1	1	0	0	0	0	0	0	0	0
alp			1	0	1	1	0	0	1	0	0	0	0
ara				1	0	0	1		1	0	0	0	0
arp					1		1	0	0	0	1	0	0
pla						1	0	0	0	0		0	0
plp							0	0	1	1	1	0	0
pra								1		0	1	0	0
prp									1	1	1	1	
MS										1	0	0	0
E											1	1	1
C												1	
D													1
P4													

E

	ala	alp	ara	arp	pla	plp	pra	prp	MS	E	C	D	P4
ala		1	1	1	1	0	0	0	0	0	0	0	0
alp			1	0	1		0	0	1	0	0	0	0
ara				1	0	0	1	0	1	0	0	0	0
arp					1		1	0	0	0	0	0	0
pla						1	0	0	1	0	0	0	0
plp							0		1	1	1	0	0
pra								1	1	0	1	0	0
prp									1	1	1		
MS										1		0	0
E											1	1	1
C												1	0
D													1
P4													

Table 3.12 Cleavage orientation of AB cells for all examined species of Panagrolaimidae

Cleavage orientations for *H. gingivalis*, *P. redivivus*, *P. detritophagus*, *P. rigidus*, and *Procephalobus* sp. Division angles (+ SD / SE) are expressed as deviation from the a-p axis in degrees. Divisions which are predominantly oriented along the a-p axis (division angles < 45°) are marked in blue, more skewed divisions (division angles > 45°) are marked in black.

Table 3.12

	H. gingivalis			*P. redivivus*			*P. detritophagus*			*P. rigidus*			*Procephalobus* sp.		
	av	stdev	SE	av	stdev	SE	av	stdev	SE	av	stdev	SE	av	stdev	SE
ABal	78	7	4	37	18	13	56	9	5	68	8	5	74	14	8
Abar	83	9	5	87	4	3	86	3	2	77	6	3	74	1	1
ABpl	43	6	3	32	16	11	26	7	4	44	5	3	31	28	16
ABpr	46	7	4	31	9	6	35	9	5	62	12	7	45	22	13
ABala	65	17	10	71	4	3	76	13	7	52	12	7	31	8	5
ABalp	72	8	4	52	28	20	76	3	2	76	6	3	70	9	5
ABara	59	3	2	54	19	14	74	7	4	32	13	8	49	10	6
ABarp	11	8	5	18	17	12	27	8	4	34	17	10	16	12	7
ABpla	13	6	4	24	9	6	16	6	3	52	33	19	26	14	8
ABplp	37	11	6	16	3	2	27	4	2	19	18	10	40	17	10
ABpra	40	1	0	19	1	1	34	5	3	50	9	5	21	14	8
ABprp	71	17	10	31	1	1	31	16	9	48	9	5	54	34	19

Figure 3.43 Cell lineage of the first divisions of *Rhabditophanes* sp.

A-B lineages of embryos 1-2**.**The vertical axis indicates time of development and every division is visualised by a horizontal bar. Time starts after the division of AB. The left branch is always the anterior/left/dorsal sister.

Table 3.13 Division sequence of early cell divisions of *Rhabditophanes* sp.

The germline cells are marked in bold.

Figure 3.44 Number of cells during embryonic development of *Rhabditophanes* sp.

Time starts after the division of AB.

Fig. 3.43

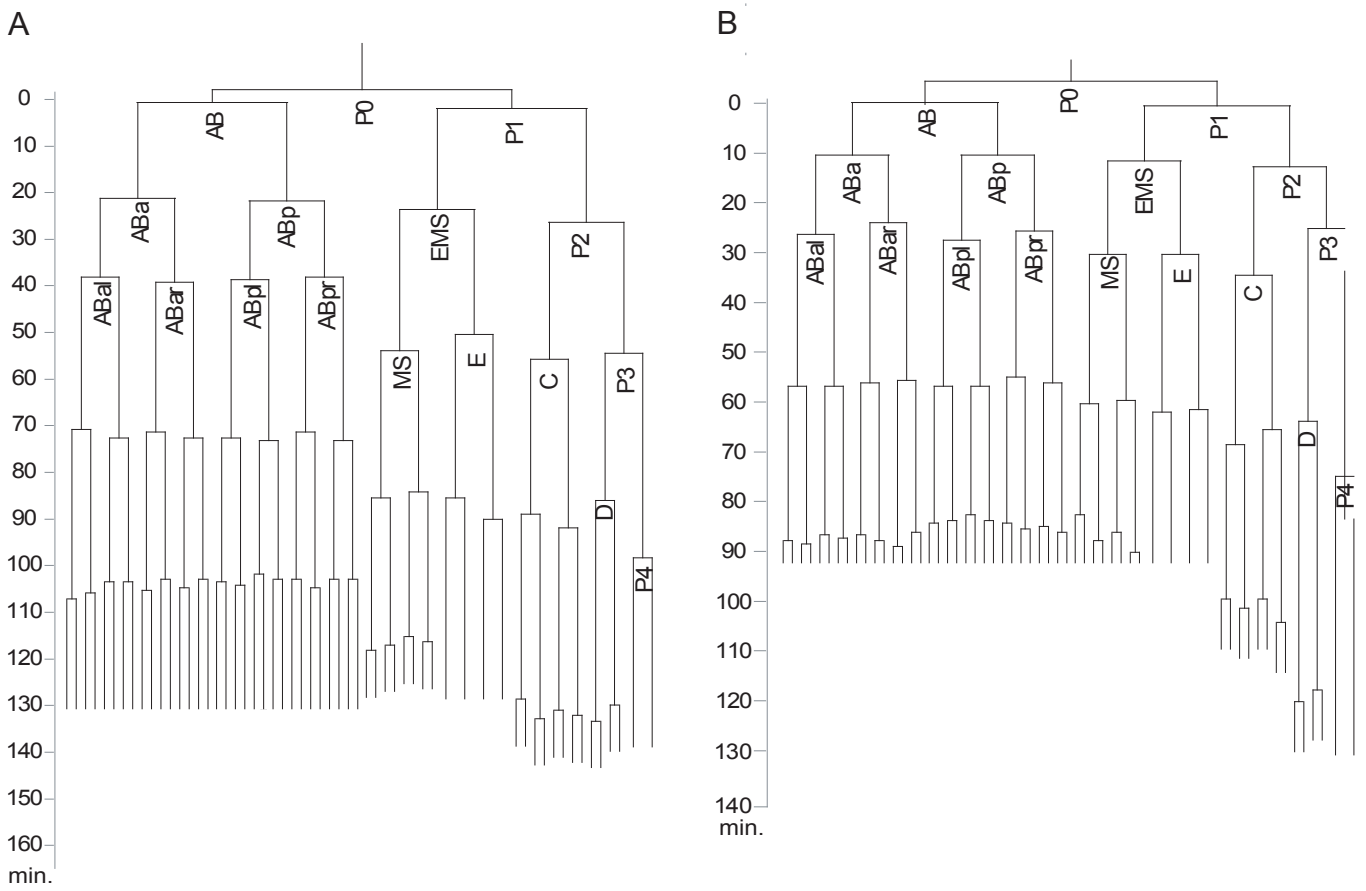

Table 3.13

embr 1	AB	**P1**	2AB	EMS	**P2**	4AB	E	MS	**P3**	C	8AB	2MS	D	2E	2C	P4	16AB	4MS	4C
embr 2	AB	**P1**	2AB	EMS	**P2**	**P3**	4AB	MS	E	C	8AB	2MS	2E	D	2C	P4	16AB	4MS	4C

Fig. 3.44

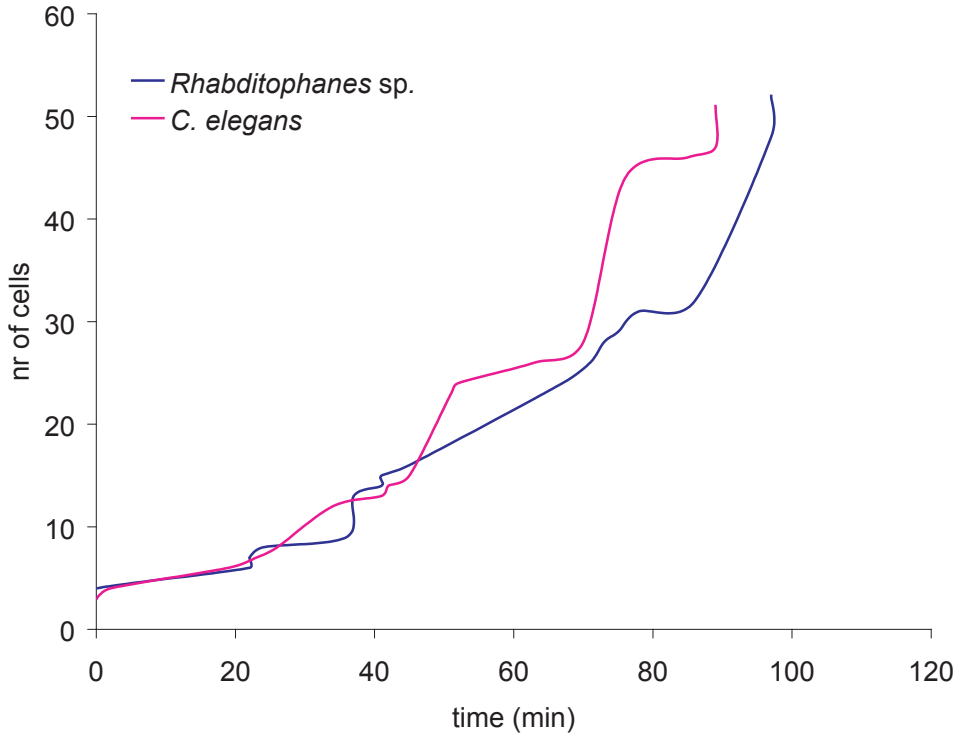

Figure 3.45 Cell cycle length of AB generations in *Rhabditophanes* sp.

The average cell cycle length (± SD) of each AB generation is plotted in time.

Figure 3.46 Cell division periods per founder cell of *Rhabditophanes* sp.

Cell division rounds per founder cell in time (min) for *Rhabditophanes* sp**.** (2 recordings), showing differences in cell-cycle times for the six founder cells. On each horizontal line the cell division events of one founder cell are given. Each solid black box indicates the time from the division of the first cell to the division of the last cell in a given round of division. Time starts after the division of AB.

Figure 3.47 Cell-cell contacts at the 8AB cell stage in *Rhabditophanes* sp.

1 = contact is present, 0 = contact is absent. Variable contacts are marked by a yellow square.

Table 3.14 Cleavage orientation of AB cells in *Rhabditophanes* sp.

Division angles (+ SD / SE) are expressed as deviation from the a-p axis in degrees. Divisions which are predominantly oriented along the a-p axis (division angles < 45°) are marked in blue, more skewed divisions (division angles > 45°) are marked in black.

Fig. 3.45

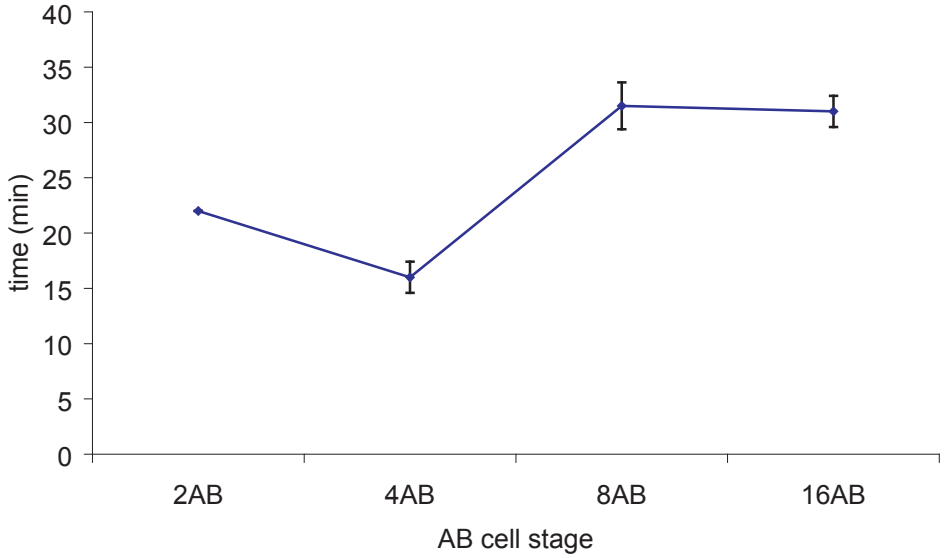

Fig. 3.46

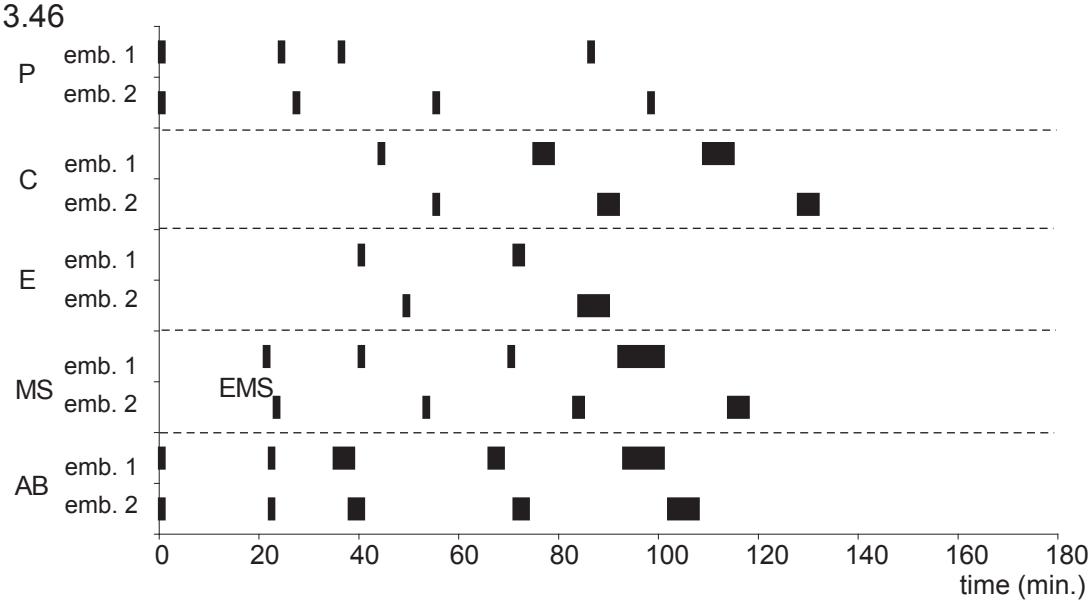

Fig. 3.47

	ala	alp	ara	arp	pla	plp	pra	prp	MS	E	C	P3
ala		1	1	1	1	0	0	0	0	0	0	0
alp			1	0	1	0	0	0	1	0	0	0
ara				1	0	0	1	0	1	0	0	0
arp					1	0	1	0	1	0	1	0
pla						1	0	0	1	0	1	0
plp							0	0		1	1	0
pra								1	0	0	1	0
prp									1	1	1	1
MS										1	1	0
E											1	1
C												1
P3												

Table 3.14

cell	av	stdev	SE
ABal	78	3	2
Abar	78	7	5
ABpl	4	4	3
ABpr	43	29	21
ABala	51	5	3
ABalp	60	11	8
ABara	41	5	3
ABarp	3	4	3
ABpla	11	10	7
ABplp	54	25	18
ABpra	14	2	1
ABprp	39	2	2

Figure 3.48 Cell lineage of the first divisions of *Acrobeloides butschlii*

A-C Lineages of embryos 1-3. The vertical axis indicates time of development and every division is visualised by a horizontal bar. Time starts after the division of P1. The left branch is always the anterior/left/dorsal sister.

Fig. 3.48

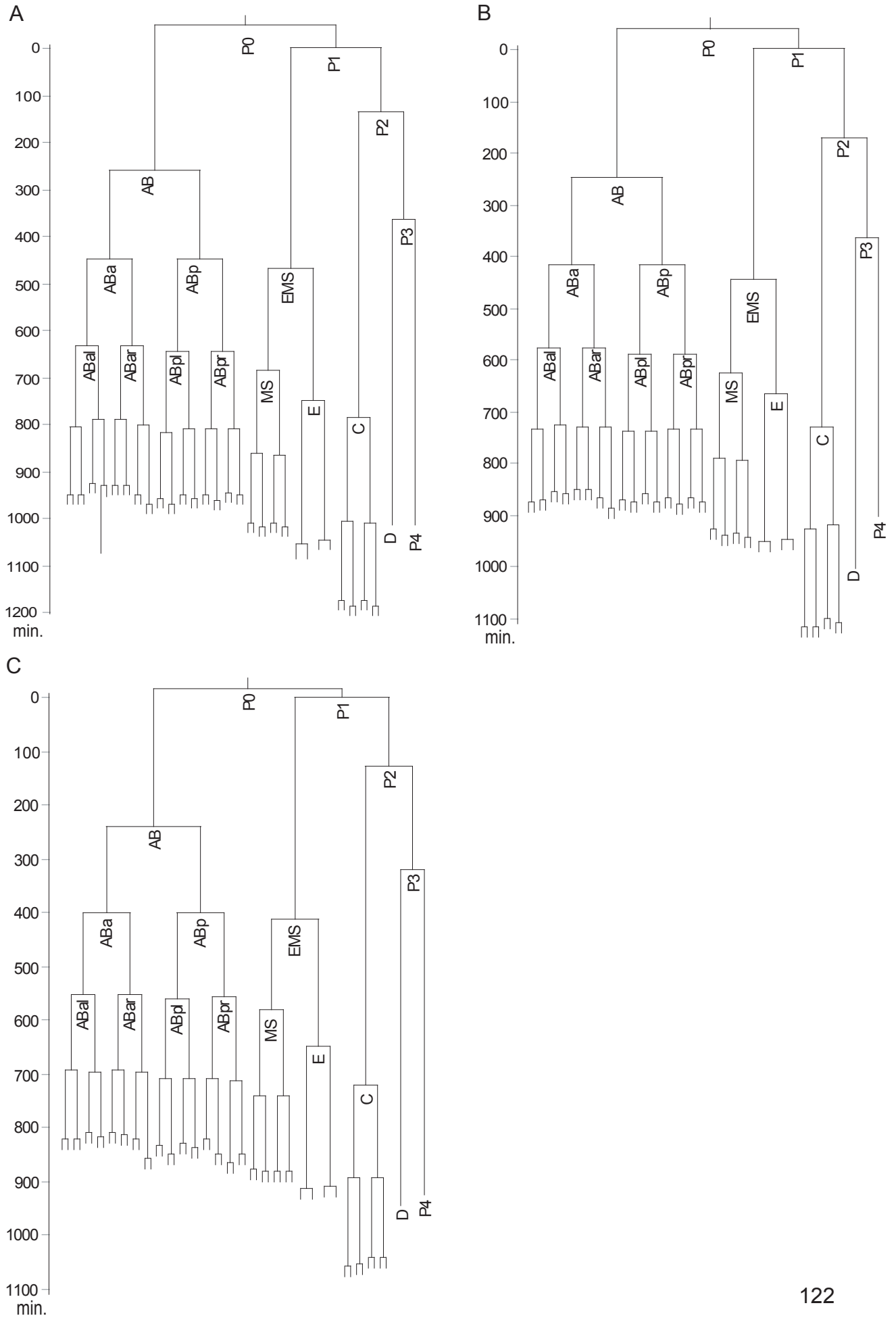
A
0
100
200
300
400
500
600
700
800
900
1000
1100
1200
min.
P0
P1
P2
P3
P4
AB
ABa
ABp
EMS
ABal
ABar
ABpl
ABpr
MS
E
C
D
B
0
100
200
300
400
500
600
700
800
900
1000
1100
min.
P0
P1
P2
P3
P4
AB
ABa
ABp
EMS
ABal
ABar
ABpl
ABpr
MS
E
C
D
C
0
100
200
300
400
500
600
700
800
900
1000
1100
min.
P0
P1
P2
P3
P4
AB
ABa
ABp
EMS
ABal
ABar
ABpl
ABpr
MS
E
C
D

Figure 3.49 Cell lineage of the first divisions of A*crobeloides nanus*

A-**B** Lineages of embryos 1-2. The vertical axis indicates time of development and every division is visualised by a horizontal bar. Time starts after the division of P1. The left branch is always the anterior/left/dorsal sister.

Fig. 3.49

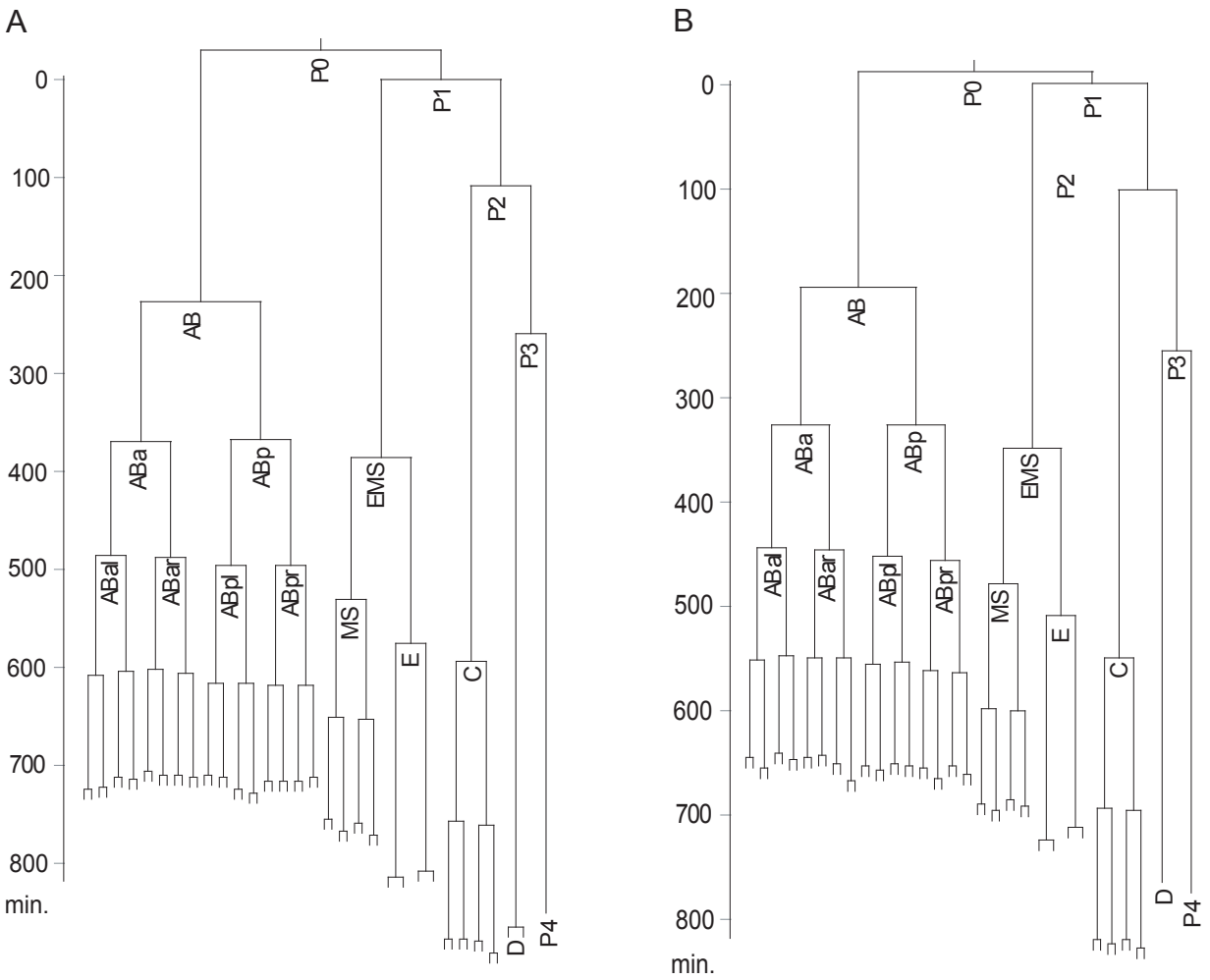
A
0
100
200
300
400
500
600
700
800
min.
P0
P1
P2
P3
AB
ABa
ABp
EMS
ABal
ABar
ABpl
ABpr
MS
E
C
D
P4
B
0
100
200
300
400
500
600
700
800
min.
P0
P1
P2
P3
AB
ABa
ABp
EMS
ABal
ABar
ABpl
ABpr
MS
E
C
D
P4

Figure 3.50 Cell lineage of the first divisions of *Acrobeloides thornei*

A-C Lineages of embryos 1-3. The vertical axis indicates time of development and every division is visualised by a horizontal bar. Time starts after the division of P1. The left branch is always the anterior/left/dorsal sister.

Fig. 3.50

A

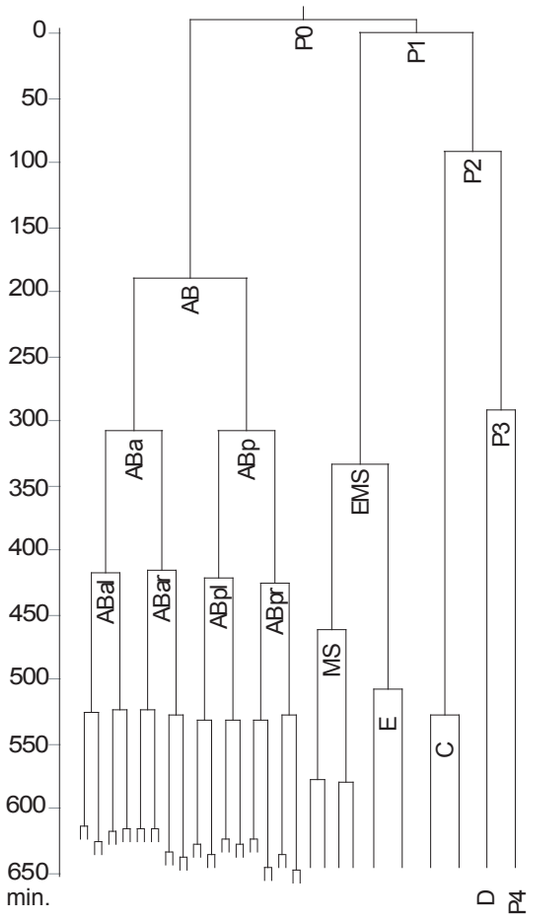
0
50
100
150
200
250
300
350
400
450
500
550
600
650
min.
P0
P1
P2
P3
AB
ABa
ABp
EMS
ABal
ABar
ABpl
ABpr
MS
E
C
D
P4

B

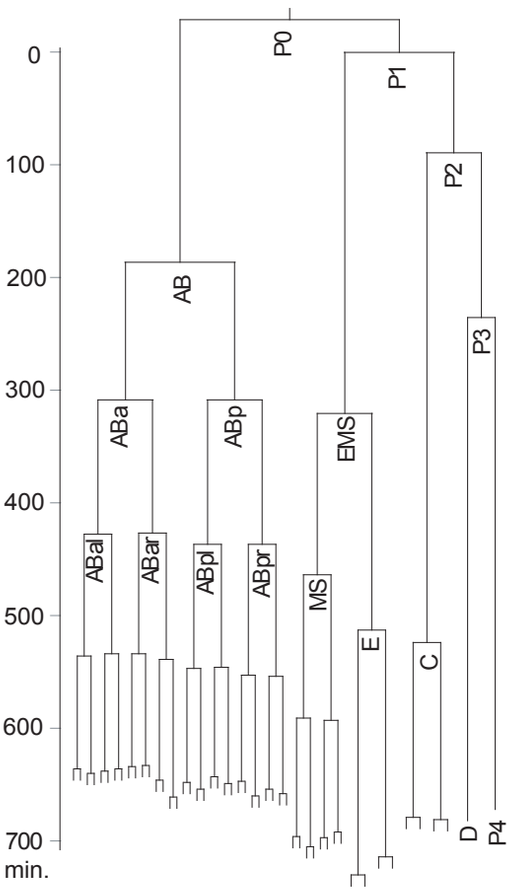
0
100
200
300
400
500
600
700
min.
P0
P1
P2
P3
AB
ABa
ABp
EMS
ABal
ABar
ABpl
ABpr
MS
E
C
D
P4

C

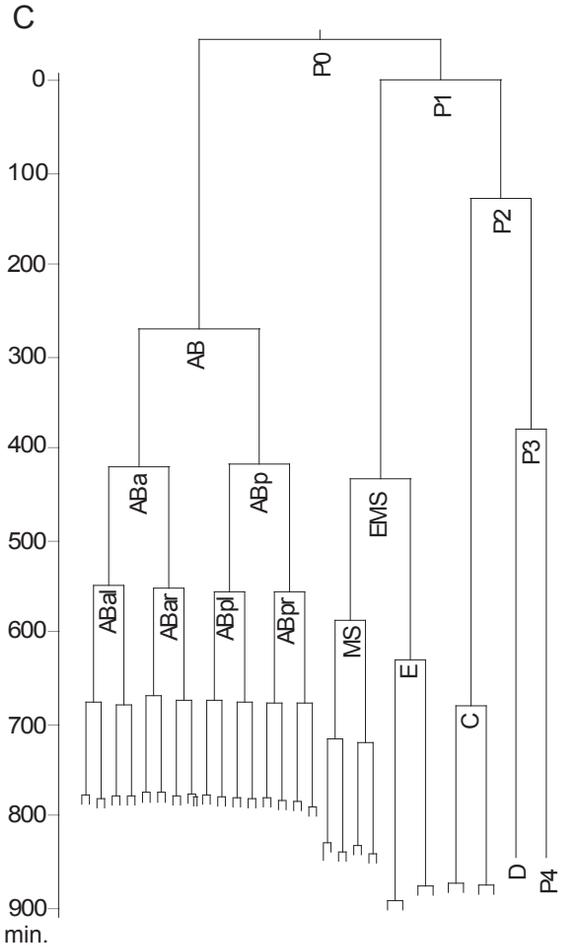
0
100
200
300
400
500
600
700
800
900
min.
P0
P1
P2
P3
AB
ABa
ABp
EMS
ABal
ABar
ABpl
ABpr
MS
E
C
D
P4

Figure 3.51 Cell lineage of the first divisions of *Cephalobus cubaensis*

A-C Lineages of embryos 1-3. The vertical axis indicates time of development and every division is visualised by a horizontal bar. Time starts after the division of P1. The left branch is always the anterior/left/dorsal sister.

Table 3.15 Egg Shape Index for all species of Cephalobidae

The average ESI ± SE and number of analyzed embryos for all examined species.

Fig. 3.51

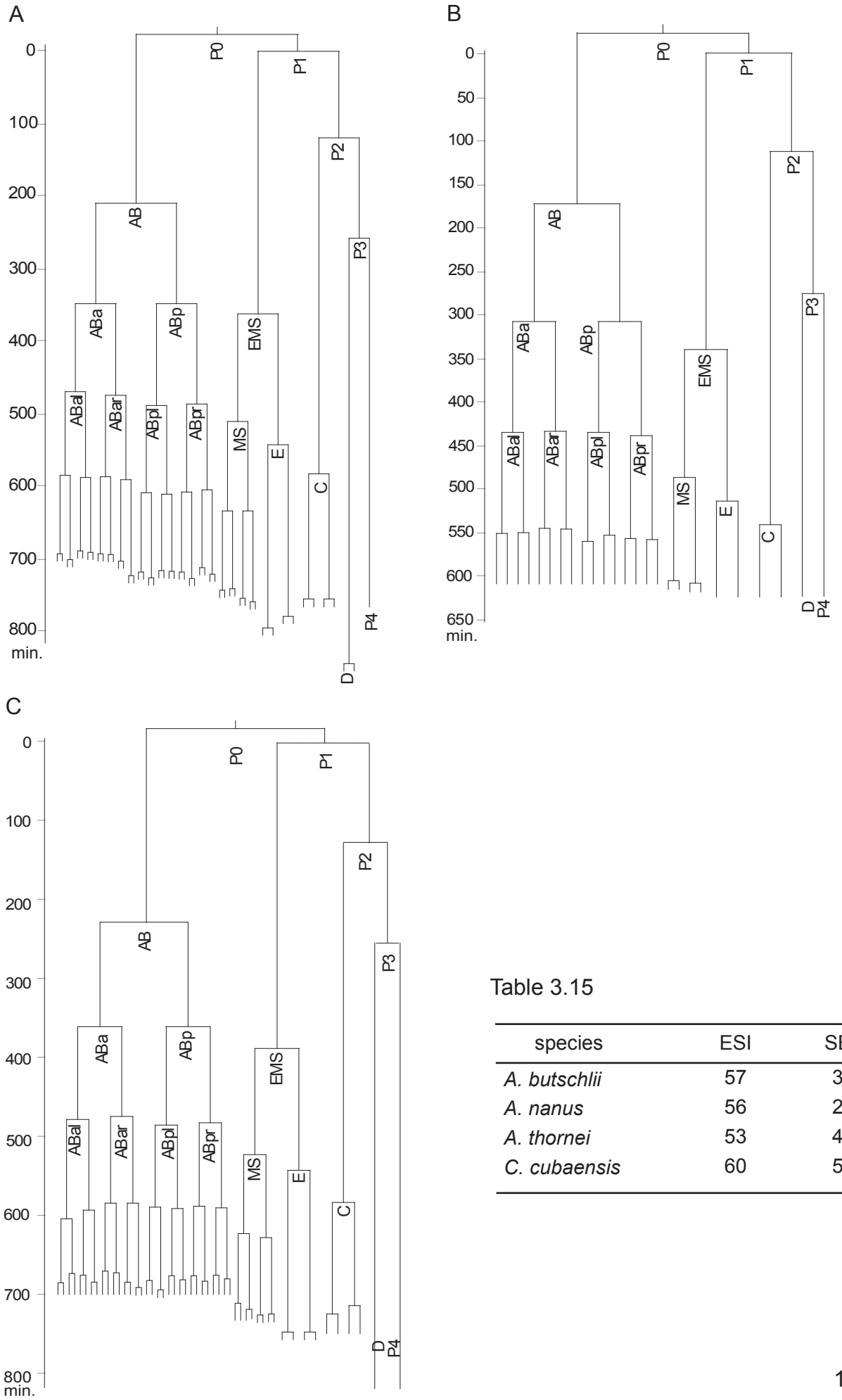

Table 3.15

species	ESI	SE	n
A. butschlii	57	3	3
A. nanus	56	2	3
A. thornei	53	4	5
C. cubaensis	60	5	3

Table 3.16 Division sequence of the early cell divisions of species of Cephalobidae

The germline cells are marked in bold.

Table 3.16

species	recording	sequence															
A. butschlii	embr1	**P1**	**P2**	AB	**P3**	2AB	EMS	4AB	MS	E	C	8AB	2MS	16AB	2C	4MS	2E	
	embr2	**P1**	**P2**	AB	**P3**	2AB	EMS	4AB	MS	E	C	8AB	2MS	16AB	2C	4MS	2E	
	embr3	**P1**	**P2**	AB	**P3**	2AB	EMS	4AB	MS	E	8AB	C	2MS	16AB	4MS	2C	2E	
A. nanus	embr1	**P1**	**P2**	AB	**P3**	2AB	EMS	4AB	MS	E	C	8AB	2MS	16AB	2C	4MS	2E	
	embr2	**P1**	**P2**	AB	**P3**	2AB	EMS	4AB	MS	E	C	8AB	2MS	16AB	4MS	2C	2E	
A. thornei	embr1	**P1**	**P2**	AB	**P3**	2AB	EMS	4AB	MS	E	C	8AB	2MS	16AB				
	embr2	**P1**	**P2**	AB	**P3**	2AB	EMS	4AB	MS	E	C	8AB	2MS	16AB	2C	4MS	2E	
	embr3	**P1**	**P2**	AB	**P3**	2AB	EMS	4AB	MS	E	C	8AB	2MS	16AB	4MS	2C	2E	
C. cubaensis	embr1	**P1**	**P2**	AB	**P3**	2AB	EMS	4AB	MS	E	C	8AB	2MS	16AB	4MS	2C	2E	D
	embr2	**P1**	**P2**	AB	**P3**	2AB	EMS	4AB	MS	E	C	8AB	2MS					
	embr3	**P1**	**P2**	AB	**P3**	2AB	EMS	4AB	MS	E	C	8AB	2MS	16AB	4MS	2C	2E	D

Figure 3.52 Schematic representation of 5-cell stage embryos of species of Cephalobidae

Possible configurations in the 5-cell stage embryo for **A** *A. butschlii,* **B** *A. nanus,* **C** *A. thornei* and **D** *C. cubaensis.* Orientation: anterior to the left, dorsal to the top.

Figure 3.53 Number of cells during embryonic development in species of Cephalobidae

Time (min) starts after the division of P1

Fig 3.52

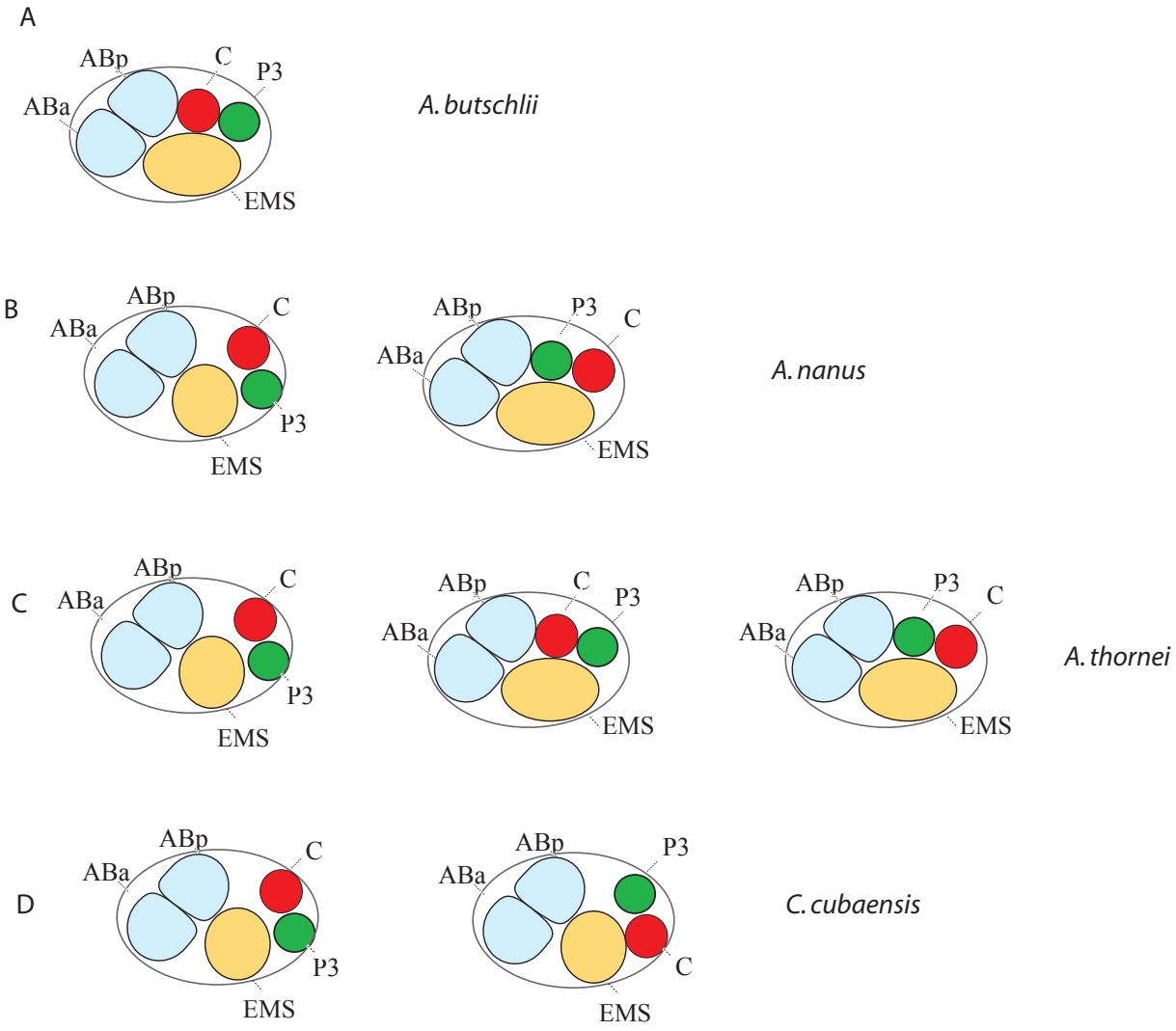

Fig 3.53

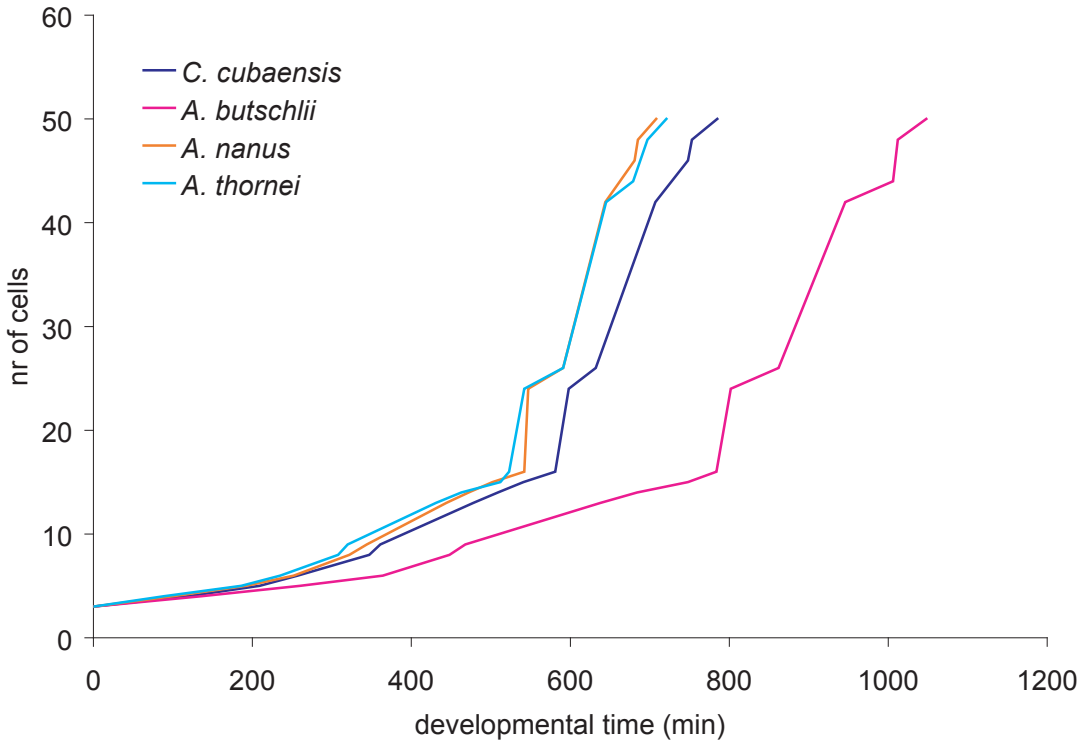

Table 3.17 The relative early developmental tempo of species of Cephalobidae

The relative early developmental tempo was measured as the time between the division of P1 and the division of E and normalized to the tempo of *C. elegans*.

Figure 3.54 Cell cycle length of AB generations in species of Cephalobidae

The average cell cycle length (± SD) of each AB generation is plotted in time for **A** *A. butschlii*, **B** *A. nanus*, **C** *A. thornei* and **D** *C. cubaensis*. The average cell cycle length for each AB stage was based on 3 recordings, except for *A. nanus* (2 recordings).

Table 3.17

species	rel tempo
A. butschlii	9.5
A. nanus	7.4
A. thornei	7.1
C. cubaensis	7.5

Fig. 3. 54

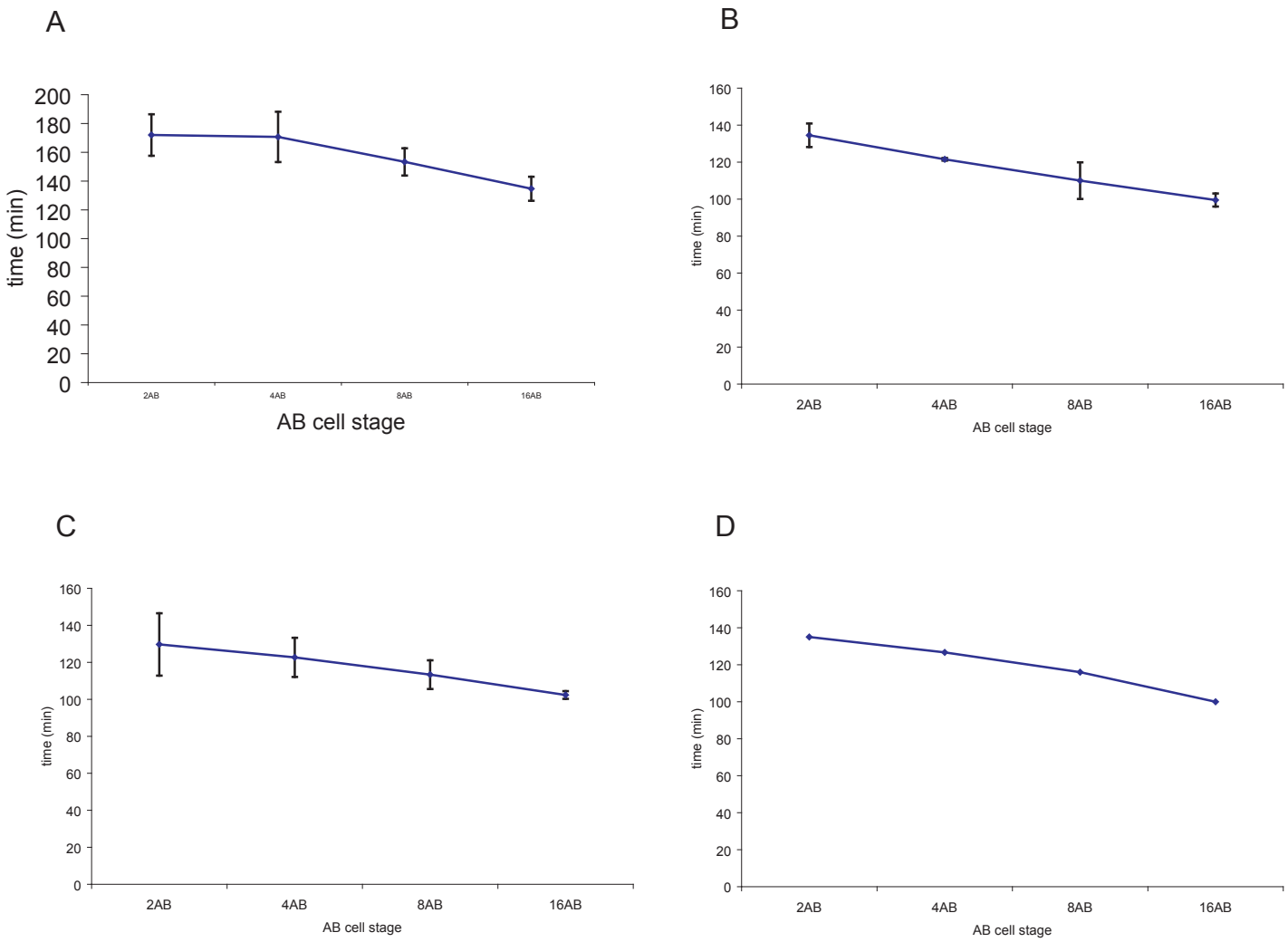

Figure 3.55 Cell division periods per founder cell in species of Cephalobidae

Cell division rounds per founder cell in time (min) for **A** *A. butschlii* (3 recordings), **B** *A. nanus* (2 recordings) and **C** *A. thornei* (3 recordings), showing differences in cell-cycle times for the six founder cells. On each horizontal line the cell division events of one founder cell are given. Each solid black box indicates the time from the division of the first cell to the division of the last cell in a given round of division. Time starts after the division of P1.

Fig. 3.55

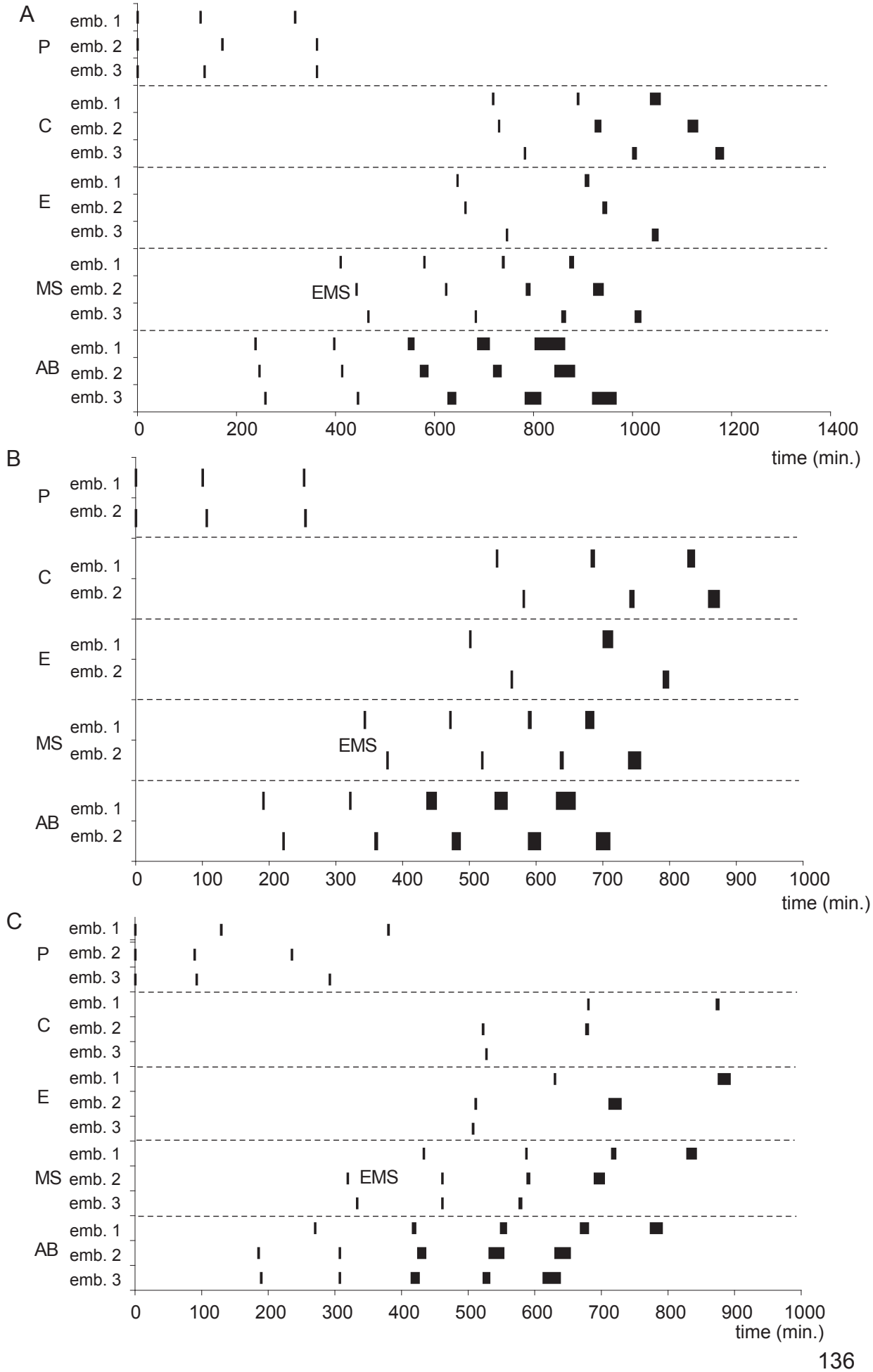
A
P
C
E
MS
AB
emb. 1
emb. 2
emb. 3
EMS
0
200
400
600
800
1000
1200
1400
time (min.)
B
0
100
200
300
400
500
600
700
800
900
1000
time (min.)
C

Figure 3.55 (2) Cell division periods per founder cell in species of Cephalobidae

Cell division rounds per founder cell in time (min) for **D** *C. cubaensis*(3 recordings), showing differences in cell-cycle times for the six founder cells. On each horizontal line the cell division events of one founder cell are given. Each solid black box indicates the time from the division of the first cell to the division of the last cell in a given round of division. Time starts after the division of P1.

Figure 3.56 Compensatory migrations of the C cell in *A. thorneii*

Nomarski images of early stages in the embryonic development of *A. thornei* showing compensatory migrations of the C cell. **A** Six-cell stage, left lateral view. No reversal of polarity is observed; P3 has divided into a dorsal P4 cell and a ventral D cell, leading to the configuration C-D-P4. **B** P4 and D switch places: P4 moves over the left side, while D is moving over the right side (not visible). **C** After the division of EMS, C starts to migrate dorsally. **D** Cells have reached their final position (P4-D-C). Orientation: anterior to the left, dorsal to the top.Scale bar = 10.µm.

Fig. 3.55 (2)

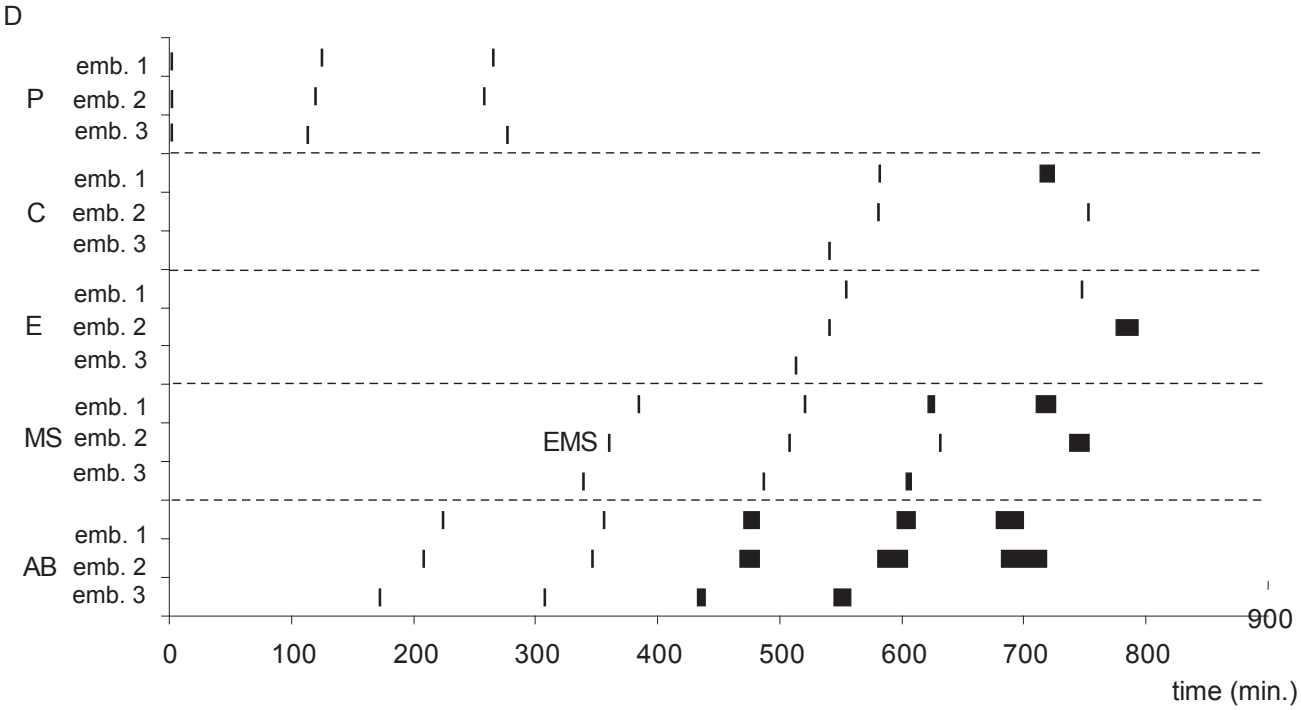

Fig 3.56

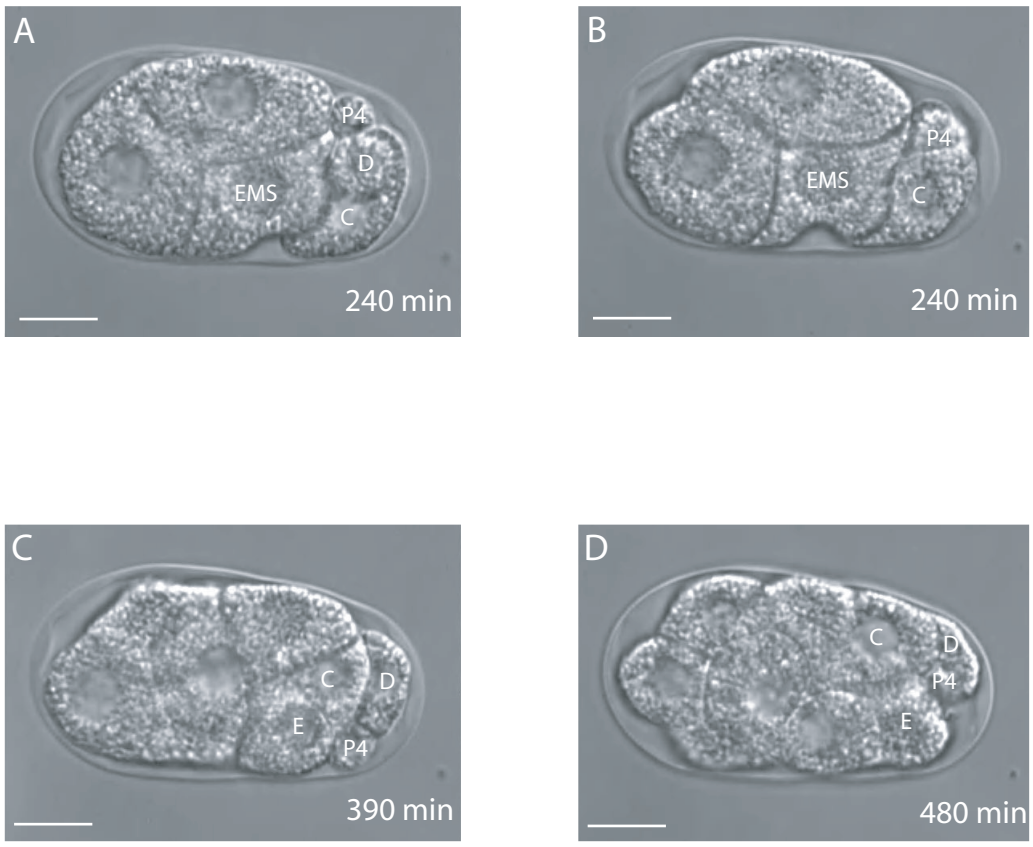

Figure 3.57 Cell-cell contacts in the 8AB cell stage of species of Cephalobidae

A A. butschlii, **B** *A. nanus*, **C** *A. thornei* and **D** *C. cubaensis.*
(1 = contact is present, 0 = contact is absent). Variable contacts are marked by a yellow square.

Table 3.18 Cleavage orientation of AB cells of species of Cephalobidae

A A. *butschlii*, **B** *A. nanus*, **C** *A. thornei* and **D** *C. cubaensis.* Division angles (+ SD / SE) are expressed as deviation from the a-p axis in degrees. Divisions which are predominantly oriented along the a-p axis (division angles < 45°) are marked in blue, more skewed divisions (division angles > 45°) are marked in black.

Fig. 3.57

A

	ala	alp	ara	arp	pla	plp	pra	prp	MS	E	C	D	P4
ala		1	1	1	1	0	0	0	0	0	0	0	0
alp			1	0	1	0	0	0	1	0	0	0	0
ara				1	0	0	1	0	1	0	0	0	0
arp					1	0	1	0	0	0	1	0	0
pla						1	0	0	0	0	1	0	0
plp							0	1	1	1	1	0	0
pra								1	1	0	1	0	0
prp									1	1	1	1	
MS										1	1	0	0
E											1	1	1
C												1	1
D													1
P4													

B

	ala	alp	ara	arp	pla	plp	pra	prp	MS	E	C	D	P4
ala		1	1	1	1	0	0	0	0	0	0	0	0
alp			1	0	1	0	0	0	1	0	0	0	0
ara				1	0	0	1	0	1	0	0	0	0
arp					1	0	1	0	0	0	0	0	0
pla						1	0	0	0	0	1	0	0
plp							0		1	1	1	0	0
pra								1	1	0	1	0	0
prp									1	1	1	1	0
MS										1	1	0	0
E											1	1	1
C												1	1
D													1
P4													

C

	ala	alp	ara	arp	pla	plp	pra	prp	MS	E	C	D	P4
ala		1	1	1	1	0	0	0	0	0	0	0	0
alp			1	0	1		0	0	1	0	0	0	0
ara				1	1	0	1		1	0	0	0	0
arp					1	0	1	0	0	0	1	0	0
pla						1	0	0	0	0	1	0	0
plp							0	1	1	1	1	0	0
pra								1		0	1	0	0
prp									1	1	1	1	
MS										1	1	0	0
E											1	1	1
C												1	1
D													1
P4													

D

	ala	alp	ara	arp	pla	plp	pra	prp	MS	E	C	D	P4
ala		1	1	1	1	0	0	0	0	0	0	0	0
alp			1		1	0	0	0	1	0	0	0	0
ara				1	1	0	1	0	1	0	0	0	0
arp					1	0	1	0	0	0	0	0	0
pla						1	0	0	1	0	1	0	0
plp							0		1	1	1	0	0
pra								1	1	0	1	0	0
prp									1	1	1	0	0
MS										1	0	0	0
E											1	1	1
C												1	1
D													1
P4													

Table 3.18

	A. butschlii			*A. thornei*			*A. nanus*			*C. cubaensis*		
	av	stdev	SE	av	stdev	SE	av	stdev	SE	av	stdev	SE
ABal	68	7	4	77	6	4	86	1	0	66	16	9
Abar	86	1	0	85	2	1	85	5	4	83	14	8
ABpl	34	15	9	54	13	8	59	3	2	45	14	8
ABpr	41	2	1	63	8	5	53	6	5	32	15	9
ABala	63	1	0	59	21	12	65	2	1	68	18	11
ABalp	77	5	3	72	11	7	54	20	14	75	10	6
ABara	69	2	1	60	9	5	68	22	15	56	39	22
ABarp	32	7	4	37	23	14	7	0	0	38	35	20
ABpla	6	4	2	14	10	6	24	20	14	13	6	4
ABplp	21	7	4	15	11	6	33	45	32	14	7	4
ABpra	12	4	2	19	10	6	24	9	7	27	9	5
ABprp	29	12	7	40	15	8	15	17	12	29	16	9

Figure 3.58 Cell lineage of the first divisions of *Meloidogyne incognita*

The vertical axis indicates time of development (hours) and every division is visualised by a horizontal bar. Time starts after the division of P1. The left branch is always the anterior/left/dorsal sister.

Fig. 3.58

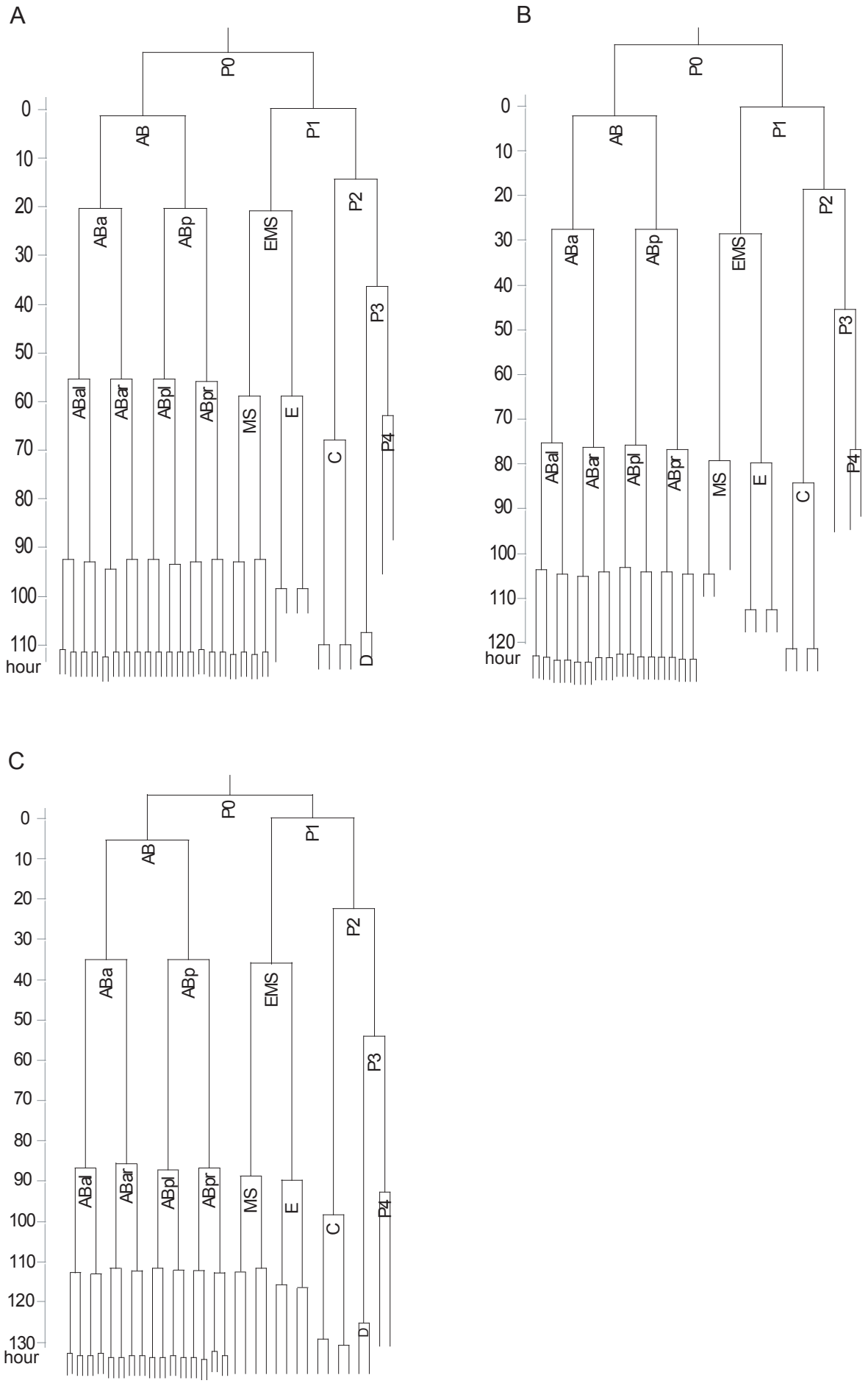
A
P0
AB
P1
ABa
ABp
EMS
P2
P3
ABal
ABar
ABpl
ABpr
MS
E
C
P4
D
0
10
20
30
40
50
60
70
80
90
100
110
hour
B
P0
AB
P1
ABa
ABp
EMS
P2
P3
ABal
ABar
ABpl
ABpr
MS
E
C
P4
0
10
20
30
40
50
60
70
80
90
100
110
120
hour
C
P0
AB
P1
ABa
ABp
EMS
P2
P3
ABal
ABar
ABpl
ABpr
MS
E
C
D
P4
0
10
20
30
40
50
60
70
80
90
100
110
120
130
hour

Figure 3.59 Characteristic stages in the embryonic development of *M. incognita*

The embryos are oriented with the posterior pole to the right. A timescale in days after the first cell division is given at the bottom. The different time points corresponding to the pictures are indicated. **A** single-cell stage; **B** 2-cell stage; **C** 4-cell stage with cells shifting from a linear towards a rhomboid pattern; **D** 8-cell stage prior to the division of the P3 cell; **E** embryo at the onset of gastrulation, both E-cells start to migrate inwards; **F-G** multiple cell stage showing clear differences between large endoderm cells surrounded by smaller ectoderm cells; **H-I** Multiple cell stage showing clear difference between the light anterior pharynx part and a more dense granulated posterior part of the embryo; **J** elongation stage on the onset of bending in the eggshell; **K** 2-fold stage; **L** 3-fold (pretzel) stage. Orientation: anterior, left. Bar = 25µm
(pictures taken by Bartel Vanholme)

Figure 3.60 Schematic representation of the two different spatial arrangements within the 5 cell embryo of *M. incognita*

After the division of P2, P3 could either be **A** in ventral (n=2) or **B** in dorsal position (n=3). Orientation: anterior to the left, dorsal to the top.

Table 3.19 Division sequence of early cell divisions of *M. incognita*

The germline cells are marked in bold.

Fig. 3. 59

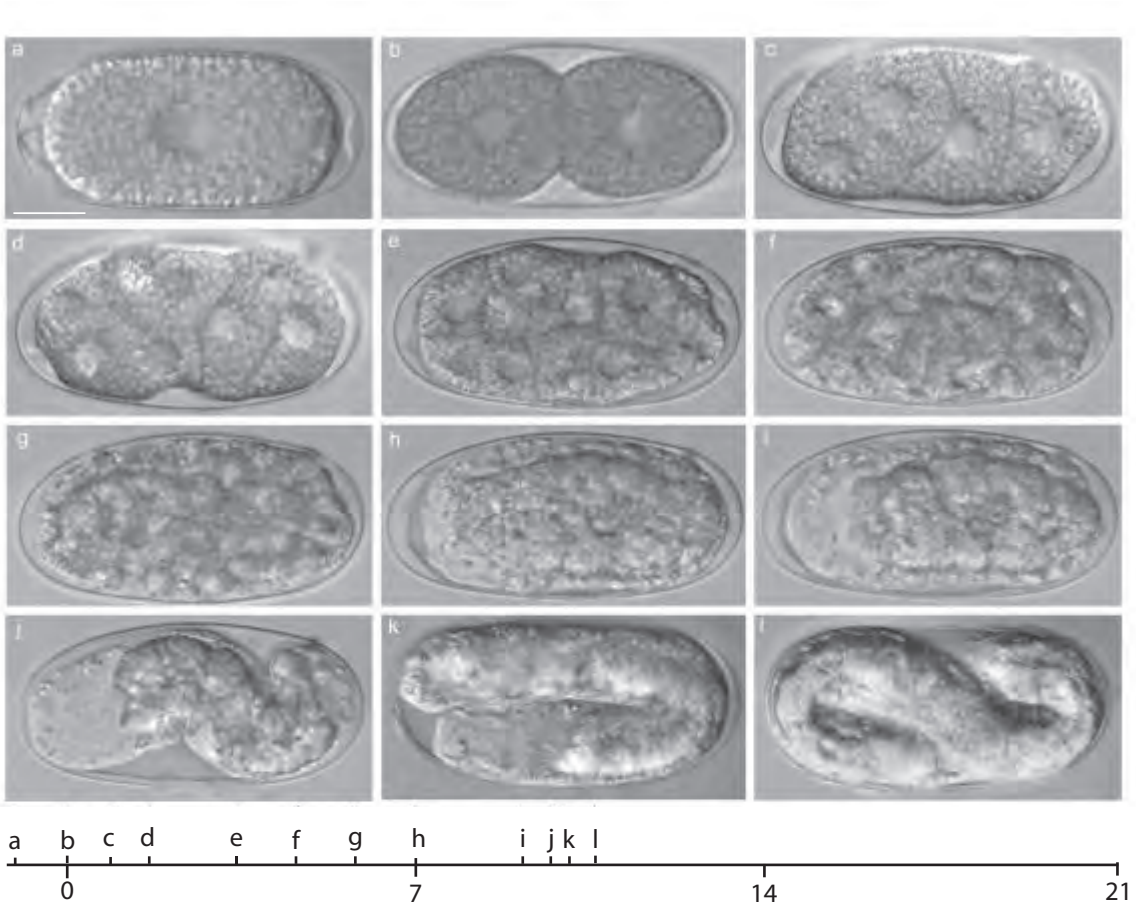

Fig.3.60

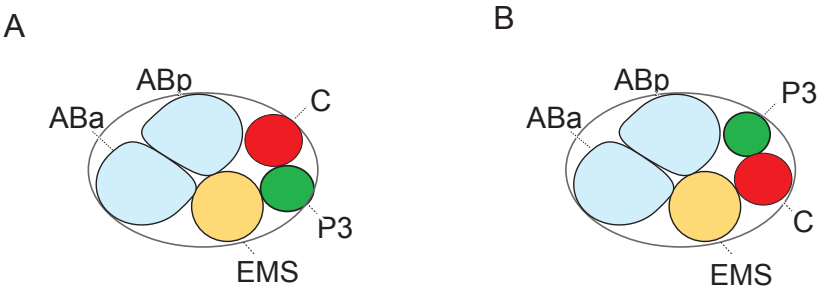

Table 3.19

embr 1	**P1**	AB	**P2**	2AB	EMS	**P3**	4AB	MS	E	**P4**	C	2MS	8AB	2E	D	2C	16AB
embr 2	**P1**	AB	**P2**	2AB	EMS	**P3**	4AB	**P4**	MS	E	C	2MS	8AB	2E			
embr 3	**P1**	AB	**P2**	2AB	EMS	**P3**	4AB	MS	E	**P4**	C	2MS	8AB	2E	D	2C	16AB

Figure 3.61 Cell cycle length of AB generations of *M. incognita*

The average cell cycle length of AB in each generation is plotted in time (hours).

Figure 3.62 Cell division periods per founder cell for *M. incognita*

Cell division rounds per founder cell in time (min) for *M. incognita* (3 recordings), showing differences in cell-cycle times for the six founder cells. On each horizontal line the cell division events of one founder cell are given. Each solid black box indicates the time from the division of the first cell to the division of the last cell in a given round of division. Time starts after the division of P1.

Figure 3.63 Cell-cell contacts in the 8AB cell stage of *M. incognita*

(1 = contact is present, 0 = contact is absent). Variable contacts are marked by a yellow square.

Fig. 3.61

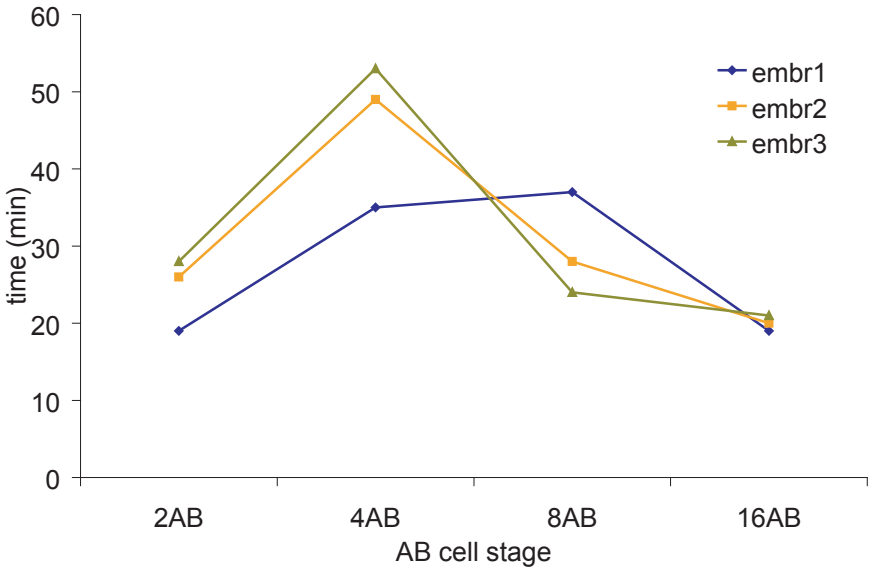

Fig. 3.62

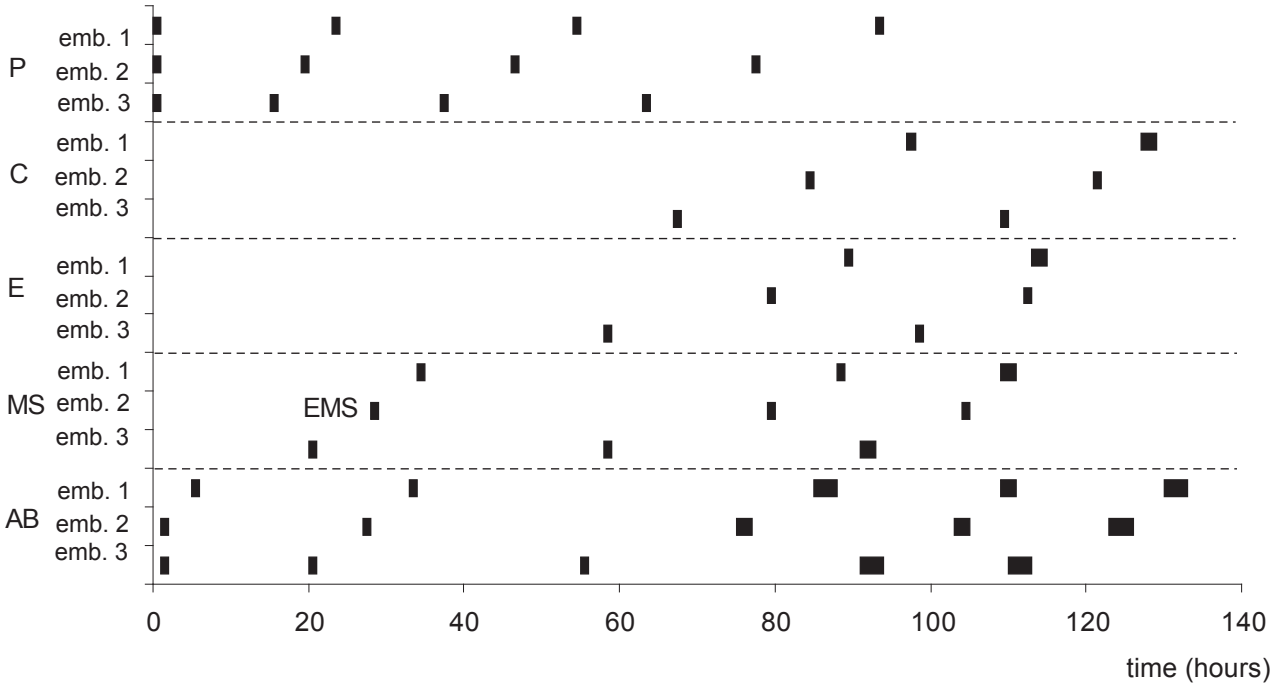

Fig. 3.63

	ala	alp	ara	arp	pla	plp	pra	prp	MS	E	C	D	P4
ala		1	1	1	1	0	0	0	0	0	0	0	0
alp			1	0	1	0	0	0	1	0	0	0	0
ara				1	1	0		0	1	0	0	0	0
arp					1		1	0	0	0	0	0	0
pla						1		0	1		0	0	0
plp							0	1	0	1	0	0	0
pra								1	1	1	0	0	0
prp									0	1	1	0	0
MS										1	0	0	0
E											1		
C												1	1
D													1
P4													

Figure 3.64 Cell cycle patterns in terms of available gene products

Four different patterns in cell cycle lengths of the AB cells were observed. Pattern **a** was found in *C. elegans*, *C. remanei*, *P. strongyloides* and *T. palmarum*. Pattern **b** was found in *A. nanus*, *C. cubaensis*, *A. thornei* and *A butschlii*, *M. longespiculosa* and *P. detritophagus*. Pattern **c** was observed in *M. miotki*, *O. dolichuroides*, *P. marina*, *P. aquatilis*, *M. incognita* and *Procephalobus sp*., in *P. pacificus*, *P. redivivus* and *P. rigidus*. Pattern **d** was only observed in *R. axei* and *H. gingivalis*. **A-D** Proposed decrease of maternal and increase of zygotic products. (Figure from Laugsch and Schierenberg, 2004, with inclusion of the fourth pattern; for details, see text).

Fig. 3.64

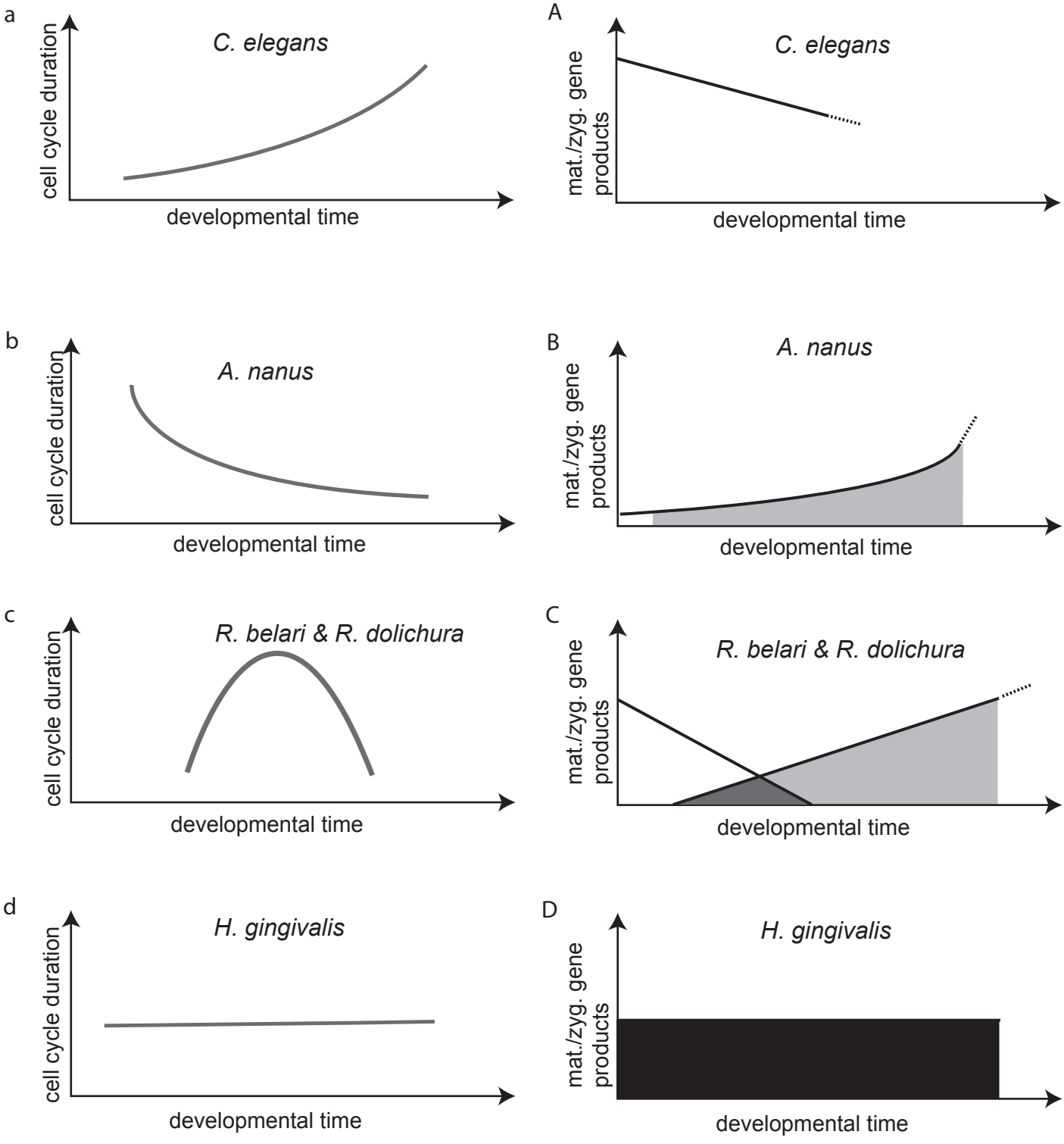

(adapted from Laugsch and Schierenberg, 2004)

Figure 3.65 Relation between the observed cell cycle pattern and relative developmental tempo

Relative early developmental tempo of all analyzed species, expressed as number of times slower than *C. elegans*. (time from of the zygote's second division until the division of the endodermal precursor cell E). The cell cycle patterns were visualized as follows: brown = *C. elegans* pattern, blue = *A. nanus* pattern, green = *R. belari* + *R. dolichura* pattern and yellow= *H. gingivalis pattern*

Figure 3.66 Relation between the time when P4 is established and the relative developmental tempo

X-axis represents the cell stage when P4 is established, Y-axis is relative developmental tempo expressed as number of times slower than *C. elegans*. (time from of the zygote's second division until the division of the endodermal precursor cell E).

Fig. 3.65

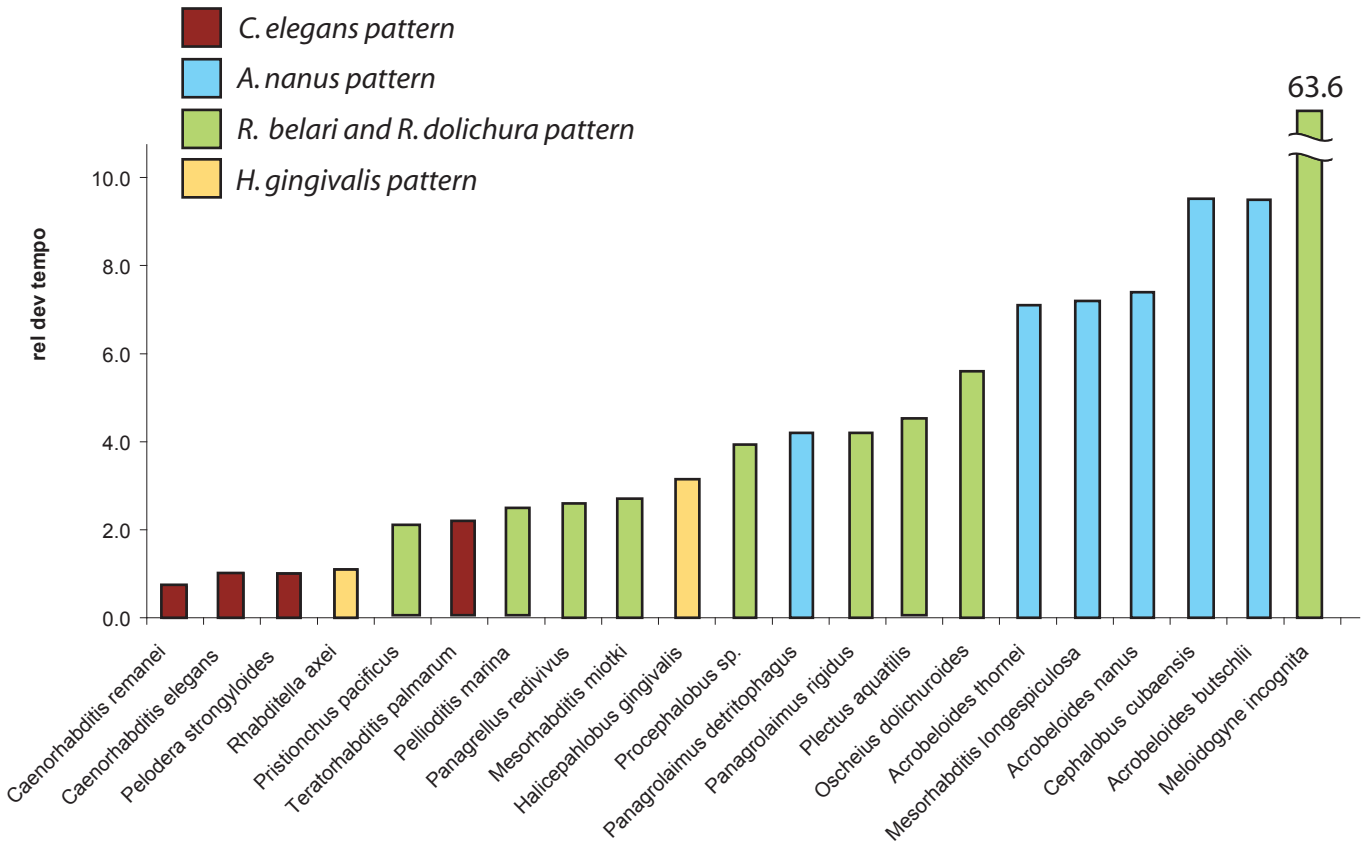

Fig. 3.66

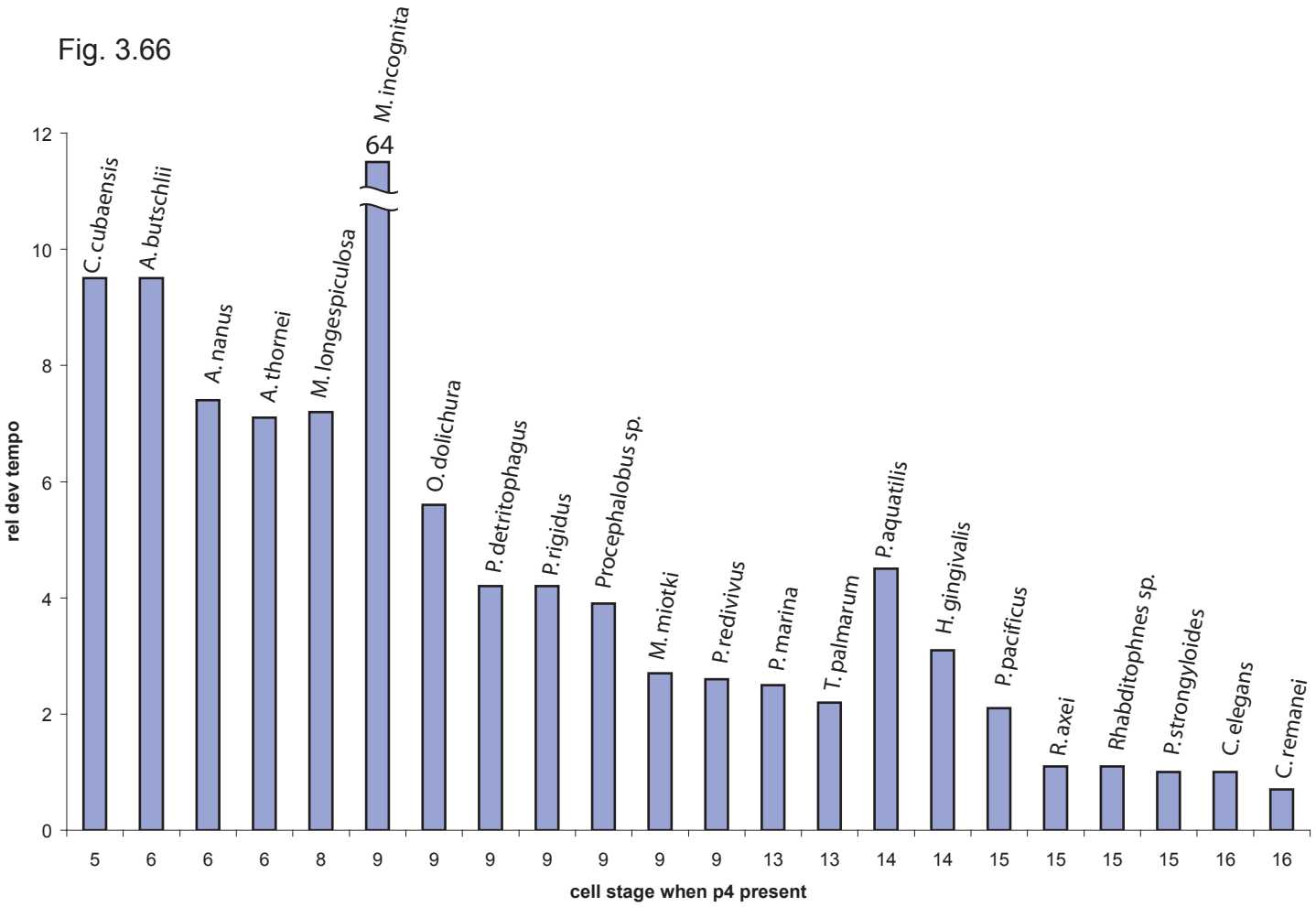

Table 3.20 p-values for the comparison of developmental tempo between the observed cell cycle patterns

For each pairwise comparison of character states the p-value from the Mann-Whitney test is given. Values were adjusted using a sequential Bonferoni method (values between brackets).

Figure 3.67 Cell cell contacts in the 24-cell stage

A In the 24-cell stage contact between MSap and ABplpa was observed in *C. cubaensis*. In *C. elegans* this induction from MSap leads to the production of the excretory cell by a descendant of ABplpa. **B** In the 24-cell stage cell cell contacts between the ABalap and ABplaa blastomeres were observed in *A.butschlii*. In *C. elegans* this contact is required to establish left-right asymmetry in the ABpla/pra lineage. Scale-bar = 10 µm.

Table 3.20

	p
patt 1 - patt 2	**0.0095** (**0.0475**)
patt 1 - patt 3	**0.0056** (**0.0336**)
patt 1 - patt 4	0.2667
patt 2 - patt 3	**0.027** (0.108)
patt 2 - patt 4	0.0714
patt 3 - patt 4	0.3273

Fig. 3.67

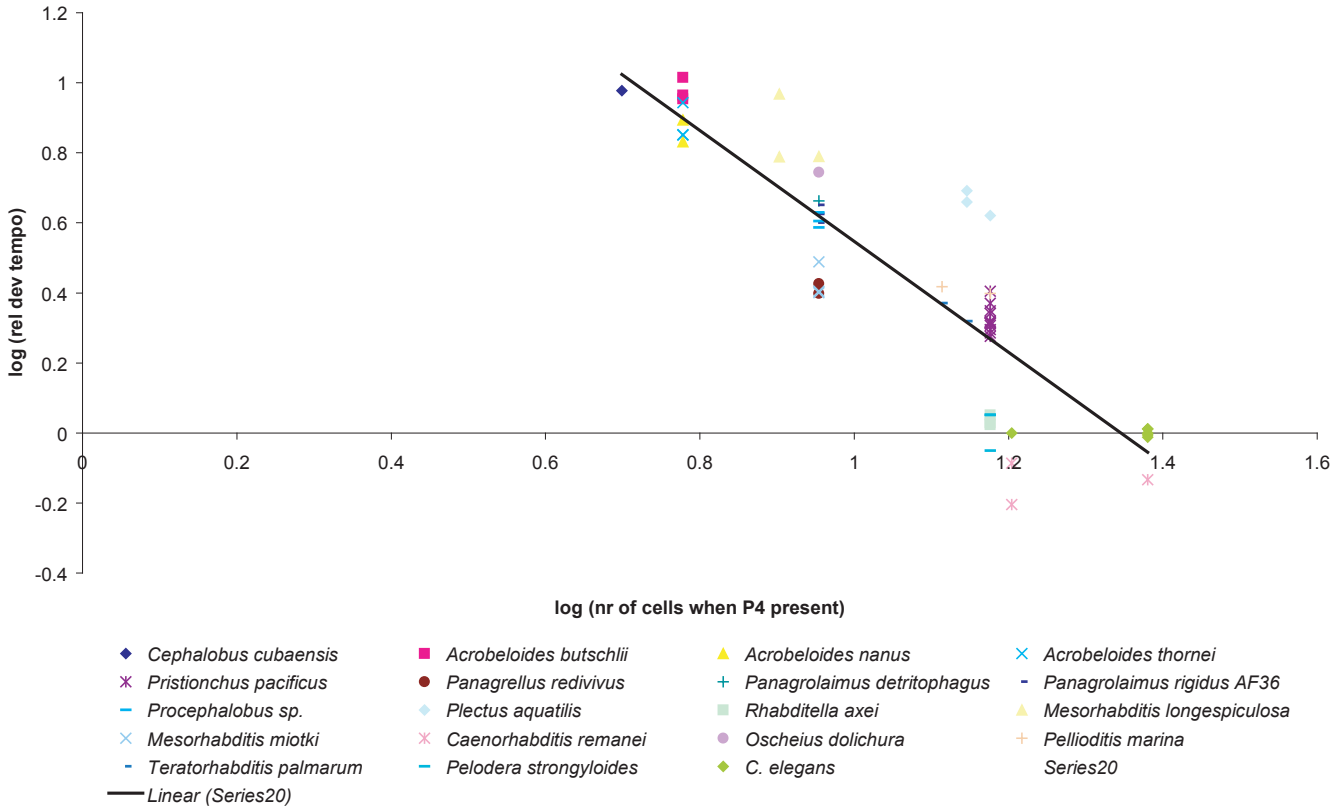

Fig. 3.68

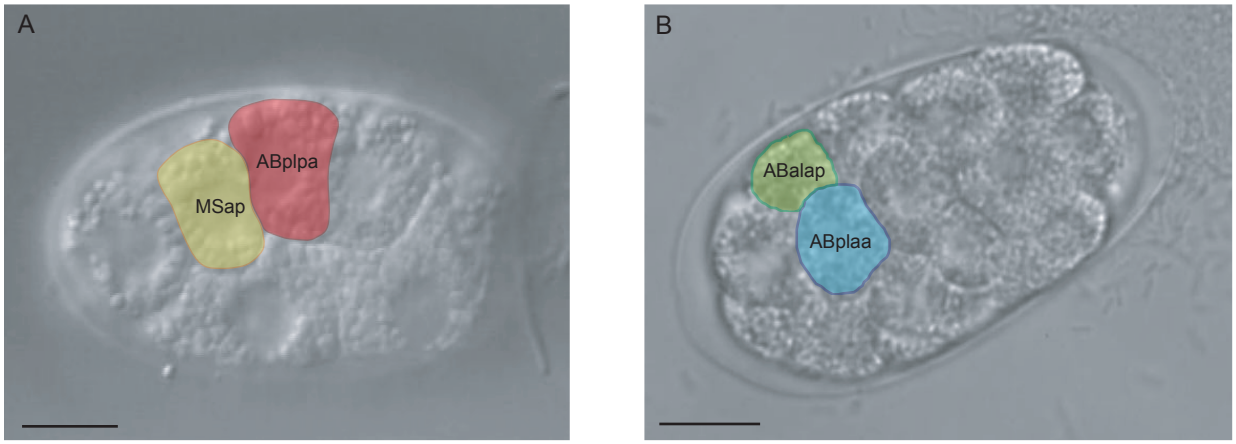

Table 4.1 Data-matrix of the examined characters

The data-matrix contains 43 taxa (rows) and 5 characters (columns). **Character 1** = developmental rate (asynchronous versus synchronous rate); character states: 1 = synchronous development, 2 = asynchronous development. **Character 2** = division sequence of the first 3 divisions with the character states: 1 = AB-P1-2AB, 2 = AB-P1-P2, 3 = P1/AB-EMS/ABa, 4 = P1-P2-AB, 5 = P1-AB-P2, 6 = P1/AB-P2. **Character 3** = number of endodermal cells that gastrulate with the character states: 1 = one endodermal cell, 2 = two endodermal cells, 3 = 4 endodermal cells and 4 = a large group of endodermal cells. **Character 4** = spatial configuration of the four-cell embryo with the character states: 1 = tetrahedral, 2 = rhomboidal, 3 = partially linear and 4 = linear. **Character 5** is the configuration of the posterior cells with the following character states: 1 = P4-D-C, 2 = C-D-P4, 3 = D-P4-C and 4 = C-P4-D.

Table 4.1

Clade	Species	1	2	3	4	5
1	*Pontonema vulgare*	1	?	2	1&2	-
	Enoplus brevis	1	?	2	1&2	-
	Tobrilus diversipapilatus	1	?	5	1&2	-
2	*Prionchulus punctatus*	1	3	2	2	-
	Gastromermis hibernalis	1	?	3	2	-
	Romanomermis culicivorax	1	3	?	2	-
	Trichocephalus trichurus	?	?	1	1	-
3	*Desmodora serpentulus*	1	?	1	2	1
4	*Hypodontolaimus inaequalis*	1	?	1	1&2	1
5	*Daptonema setosum*	1	?	?	1	1
	Axonolaimus paraspinosus	1	?	?	1	1
6	*Plectus aquatilis*	1	1	1	1&2	1
	Plectus minimus	1	1	1	?	1
	Tylocephalus auriculatus	1	1	1	?	1
7	*Teratocephalus lirellus*	1	2	2	2	1
8	*Parascaris equorum*	1	?	2	2	1
9	*Pristionchus pacificus*	1	1	2	2	1
	Caenorhabditis elegans	1	1	2	2	1
	Caenorhabditis remanei	1	1	2	2	1
	Rhabditella axei	1	1	2	2	1
	Oscheius dolichuroides	1	2	2	2	1
	Pellioditis marina	1	1	2	2	1
	Teratorhabditis palmarum	1	1	2	2	1
	Mesorhabditis miotki	1	6	2	2	1
	Mesorhabditis longespiculosa	1	5	2	2	1
	Pelodera strongyloides	1	1	2	2	1
	Rhabditis terricola	1	1	?	2*	?
	Rhabditis dolichura	1	2	?	2	?
	Diploscapter coronatus	1	?	2	4	1&2&3&4
10	*Bursaphelenchus xylophilus*	1	1	2	2	1
	Halicephalobus gingivalis	1	5	2	2	3
	Panagrolaimus detritophagus	1	5	3	2	1
	Panagrolaimus rigidus	1	1	2	2	1
	Procephalobus sp.	1	5	2	2	1
	Pangrellus ridivivus	1	1	2	2	1
	Rhabditophanes sp.	1	1	3	2	1
	Rhabdias bufonis	1	1	3	2	1
11	*Acrobeloides butschlii*	2	4	2	3	1&3
	Acrobeloides thornei	2	4	2	3	1&2&4
	Acrobeloides maximus	2	4	2	3	1&2
	Acrobeloides nanus	2	4	2	3	1&2
	Cephalobus cubaensis	2	4	2	3	2&3&4
12	*Meloidogyne incognita*	1	5	2	4	1&2

Figure 4.1 Molecular phylogeny within Rhabditidae

This consensus tree was based on Bayesian inference and LogDet-transformed distance analyses. Consensus trees were built from the outcome of analyses based on a pronounced conservative approach; conflicts from both analyses and/or branches with lower than a 95 Bayesian posterior probability were presented as unresolved. Three major sub-clades can be distinguished. Sub-clade 1 comprises the Neodiplogasteridae; Sub-clade 2, “Pleiorhabditis’ comprises the *Mesorhabditis*-group and *Pelodera*. Sub-clade 3 “Eurhabditis” includes the genus *Caenorhabditis*, *Diploscapter* and nematodes belonging to the *Rhabditis*-group.

Fig. 4.1

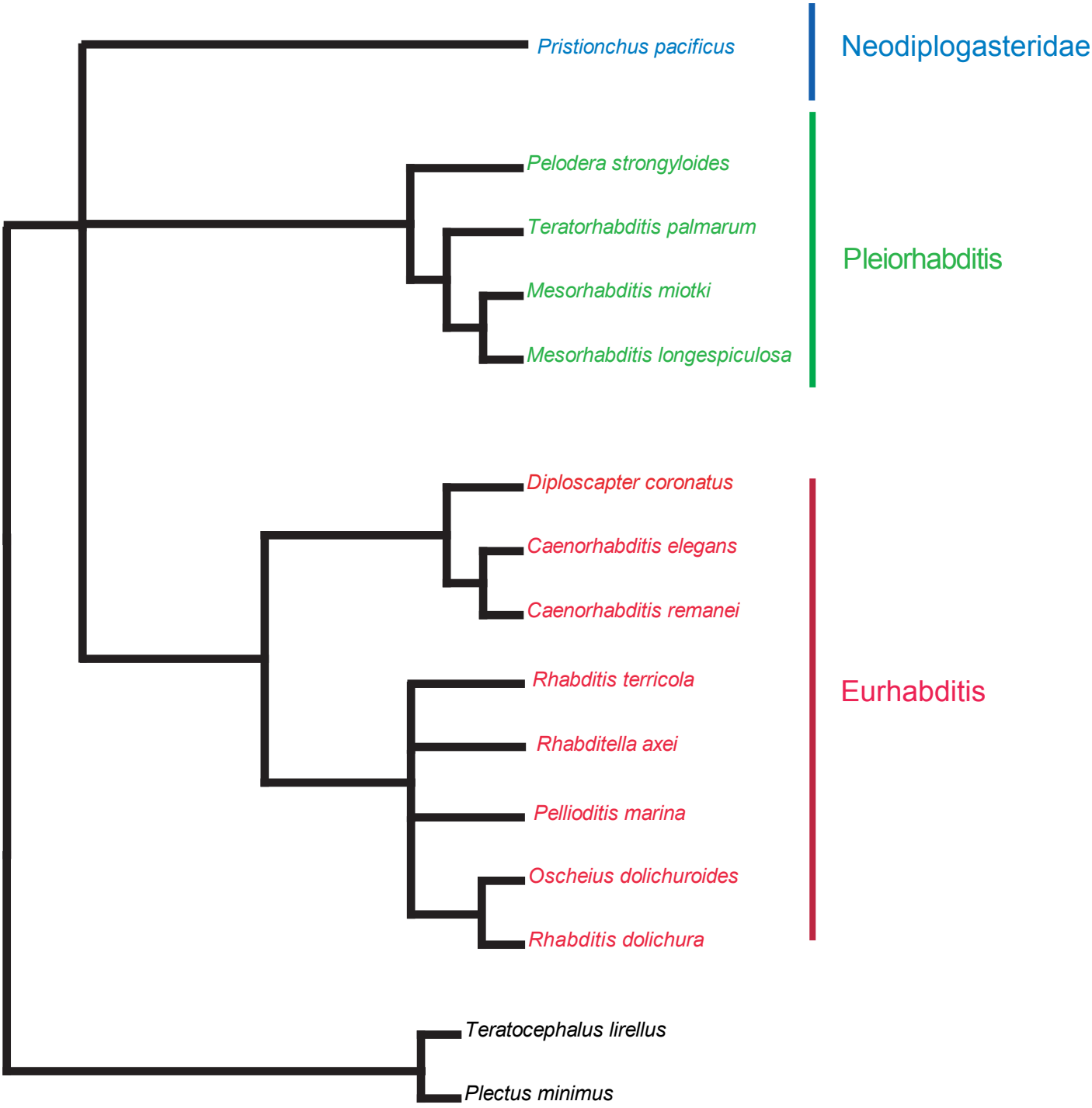
Pristionchus pacificus
Neodiplogasteridae
Pelodera strongyloides
Teratorhabditis palmarum
Mesorhabditis miotki
Mesorhabditis longespiculosa
Pleiorhabditis
Diploscapter coronatus
Caenorhabditis elegans
Caenorhabditis remanei
Rhabditis terricola
Rhabditella axei
Pellioditis marina
Oscheius dolichuroides
Rhabditis dolichura
Eurhabditis
Teratocephalus lirellus
Plectus minimus

Figure 4.2 Parsimonious reconstruction of the developmental rate (asynchronous versus synchronous rate) onto the phylogenetic tree

This tree is a combination of the nematode phylogeny presented by Holterman *et al.* (2006) and newly obtained consensus phylogenies based on SSU rDNA data of clades 9, 10 and 11. Newly obtained SSU rDNA sequences are marked with an asterisk. Data obtained from literature are marked in blue (for references of *E. brevis*: Voronov and Panchin (1998), Voronov (1999); *P. vulgare*: Malakhov (1994), Malakhov (1998), Voronov *et al.* (1999); *Tobrilus diversipappilatus*, Schierenberg (2005); *Romanomermis culicivorax*, Schulze and Schierenberg (2008); *Gastromermis hibernalis*, Malakhov (1994); *Desmodora serpentulus*, Malakhov (1994); *Hypodontolaimus inaequalis*, Malakhov (1994); *Axonolaimus paraspinosus*, Malakhov (1994); *Daptonema setosum*; Malakhov (1994); *Tylocephalus auriculatus*, Lahl *et al.* (2003); *Plectus minimus*, Lahl *et al.* (2003); *Teratocephalus lirellus*, Dolinski *et al.* (2001), Lahl *et al.* (2003); *Parascaris equorum*, Boveri (1888, 1899), zur Strassen (1896, 1906), Muller (1903); *Rhabditis terricola*, Laugsch and Schierenberg (2004); *Rhabditis dolichura*, Laugsch and Schierenberg (2004); *Diploscpater coronatus*, Lahl (2007); *Rhabdias bufonis*, Spieler and Schierenberg (1995); *Bursaphelenchus xylophilus*, Hasegawa *et al.* (2004). When data from literature was not available, the species are shown in grey. The numbering of the clades (1-12) refers to the phylogeny of Holterman *et al.* (2006).

Fig. 4.2

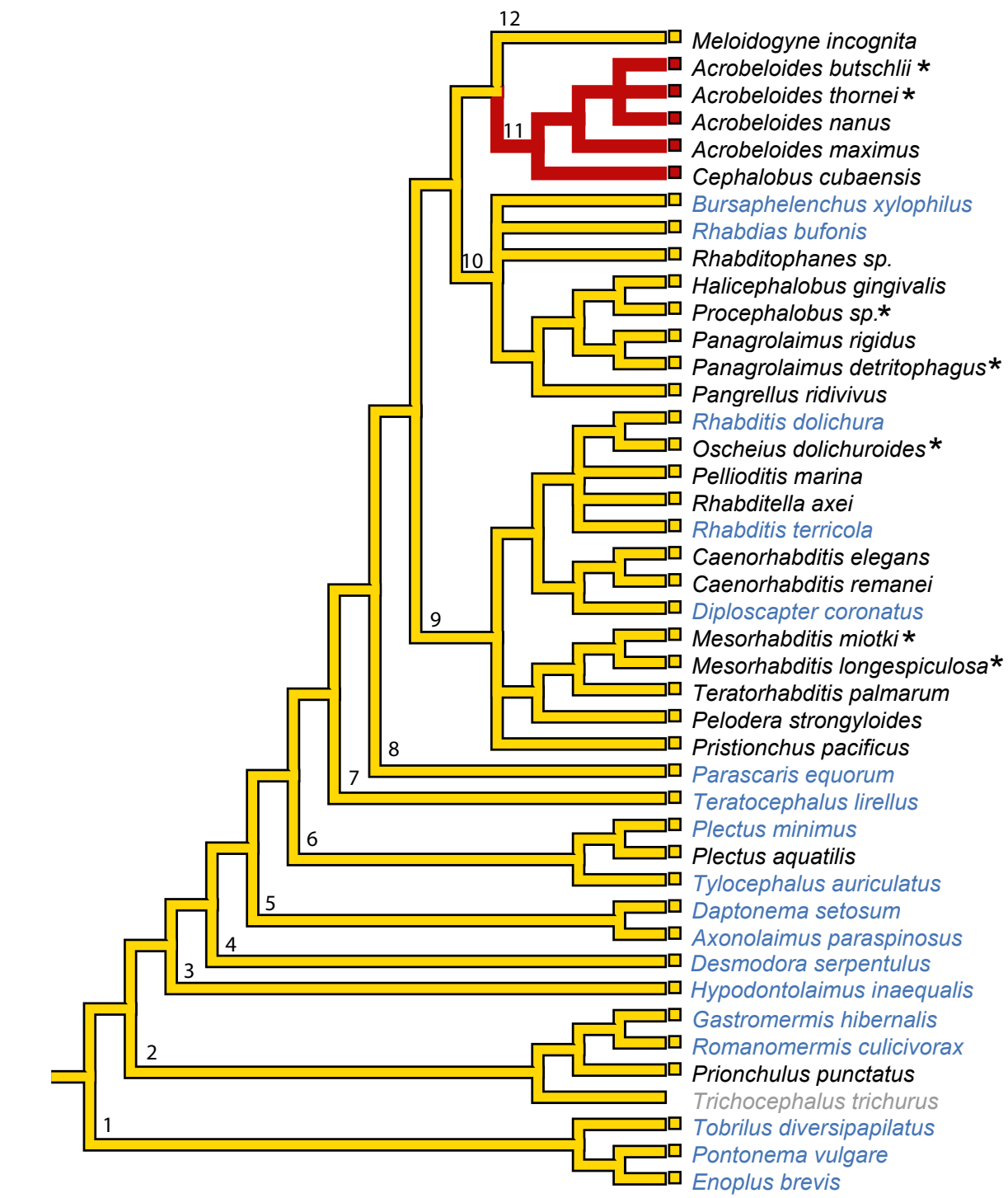
synchronous development
asynchronous development
12
11
10
9
8
7
6
5
4
3
2
1
Meloidogyne incognita
Acrobeloides butschlii *
Acrobeloides thornei *
Acrobeloides nanus
Acrobeloides maximus
Cephalobus cubaensis
Bursaphelenchus xylophilus
Rhabdias bufonis
Rhabditophanes sp.
Halicephalobus gingivalis
Procephalobus sp.*
Panagrolaimus rigidus
Panagrolaimus detritophagus*
Pangrellus ridivivus
Rhabditis dolichura
Oscheius dolichuroides*
Pellioditis marina
Rhabditella axei
Rhabditis terricola
Caenorhabditis elegans
Caenorhabditis remanei
Diploscapter coronatus
Mesorhabditis miotki*
Mesorhabditis longespiculosa*
Teratorhabditis palmarum
Pelodera strongyloides
Pristionchus pacificus
Parascaris equorum
Teratocephalus lirellus
Plectus minimus
Plectus aquatilis
Tylocephalus auriculatus
Daptonema setosum
Axonolaimus paraspinosus
Desmodora serpentulus
Hypodontolaimus inaequalis
Gastromermis hibernalis
Romanomermis culicivorax
Prionchulus punctatus
Trichocephalus trichurus
Tobrilus diversipapilatus
Pontonema vulgare
Enoplus brevis

Figure 4.3 Parsimonious reconstruction of the developmental rate (asynchronous versus synchronous rate) onto clades 9-12

Tree according to Holterman *et al*. (2006). Data for Anguinidae, Tylenchidae, Aphelenchidae and Aphelenchoididae are from Dolinski *et al*., 2001

Fig. 4.3

synchronous development

asynchronous development

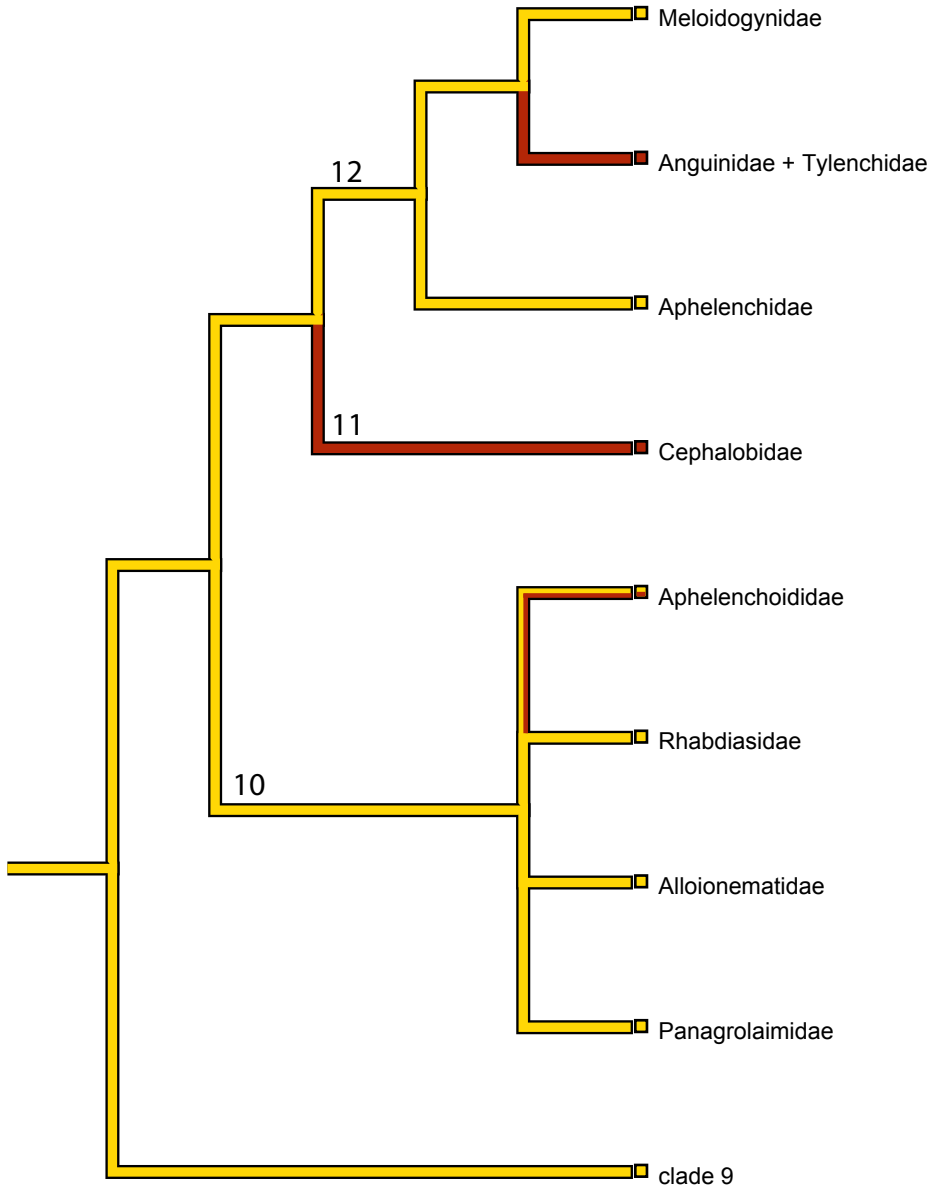

Figure 4.4 Parsimonious reconstruction of the division sequence of the first 3 divisions onto the phylogenetic tree

This tree is a combination of the nematode phylogeny presented by Holterman *et al.* (2006) and newly obtained consensus phylogenies based on SSU rDNA data of clades 9, 10 and 11. Newly obtained SSU rDNA sequences are markedwith an astersk. Data obtained from literature are marked in blue (for references of *Romanomermis culicivorax*, Schulze and Schierenberg (2008); *Tylocephalus auriculatus*, Lahl *et al.* (2003); *Plectus minimus*, Lahl *et al.* (2003); *Teratocephalus lirellus*, Dolinski *et al.* (2001), Lahl *et al.* (2003); *Rhabditis terricola*, Laugsch and Schierenberg (2004); *Rhabditis dolichura*, Laugsch and Schierenberg (2004); *Rhabdias bufonis*, Spieler and Schierenberg (1995); *Bursaphelenchus xylophilus*, Hasegawa *et al.* (2004). When data from literature was not available, the species are shown in grey. The numbering of the clades (1-12) refers to the phylogeny of Holterman *et al.* (2006).

Fig. 4.4

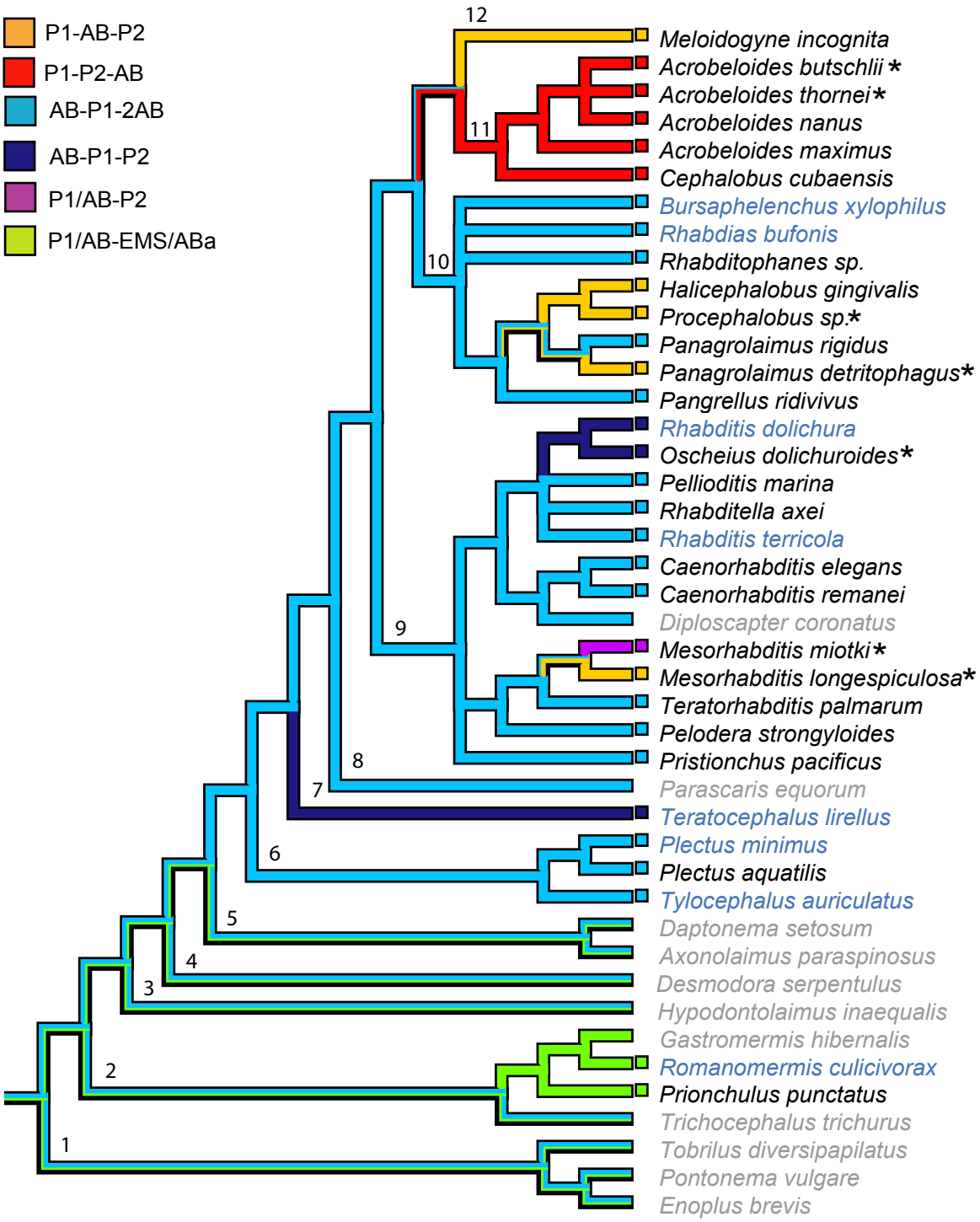
P1-AB-P2
P1-P2-AB
AB-P1-2AB
AB-P1-P2
P1/AB-P2
P1/AB-EMS/ABa
12
11
10
9
8
7
6
5
4
3
2
1
Meloidogyne incognita
Acrobeloides butschlii*
Acrobeloides thornei*
Acrobeloides nanus
Acrobeloides maximus
Cephalobus cubaensis
Bursaphelenchus xylophilus
Rhabdias bufonis
Rhabditophanes sp.
Halicephalobus gingivalis
Procephalobus sp.*
Panagrolaimus rigidus
Panagrolaimus detritophagus*
Pangrellus ridivivus
Rhabditis dolichura
Oscheius dolichuroides*
Pellioditis marina
Rhabditella axei
Rhabditis terricola
Caenorhabditis elegans
Caenorhabditis remanei
Diploscapter coronatus
Mesorhabditis miotki*
Mesorhabditis longespiculosa*
Teratorhabditis palmarum
Pelodera strongyloides
Pristionchus pacificus
Parascaris equorum
Teratocephalus lirellus
Plectus minimus
Plectus aquatilis
Tylocephalus auriculatus
Daptonema setosum
Axonolaimus paraspinosus
Desmodora serpentulus
Hypodontolaimus inaequalis
Gastromermis hibernalis
Romanomermis culicivorax
Prionchulus punctatus
Trichocephalus trichurus
Tobrilus diversipapilatus
Pontonema vulgare
Enoplus brevis

Figure 4.5 Parsimonious reconstruction of the number of endodermal precursor cells involved in gastrulation onto the phylogenetic tree

This tree is a combination of the nematode phylogeny presented by Holterman *et al.* (2006) and newly obtained consensus phylogenies based on SSU rDNA data of clades 9, 10 and 11. Newly obtained SSU rDNA sequences are marked with an asterisk. Data obtained from literature are marked in blue (for references of *E. brevis*: Voronov and Panchin (1998), Voronov (1999); *P. vulgare*: Malakhov (1994), Malakhov (1998), Voronov *et al.* (1999); *Tobrilus diversipappilatus*, Schierenberg (2005); *Trichocephalus trichurus*, Malakhov and Spiridinov (1981), Malakhov (1994); *Gastromermis hibernalis*, Malakhov (1994); *Desmodora serpentulus*, Malakhov (1994); *Hypodontolaimus inaequalis*, Malakhov (1994); *Tylocephalus auriculatus*, Lahl *et al.* (2003); *Plectus minimus*, Lahl *et al.* (2003); *Teratocephalus lirellus*, Dolinski *et al.* (2001), *Parascaris* equorum, Müller, 1903; Lahl *et al.* (2003); *Diploscpater coronatus*, Lahl (2007); *Rhabdias bufonis*, Spieler and Schierenberg (1995); *Bursaphelenchus xylophilus*, Hasegawa *et al.* (2004). When data from literature was not available, the species are shown in grey. The numbering of the clades (1-12) refers to the phylogeny of Holterman *et al.* (2006).

Fig. 4.5

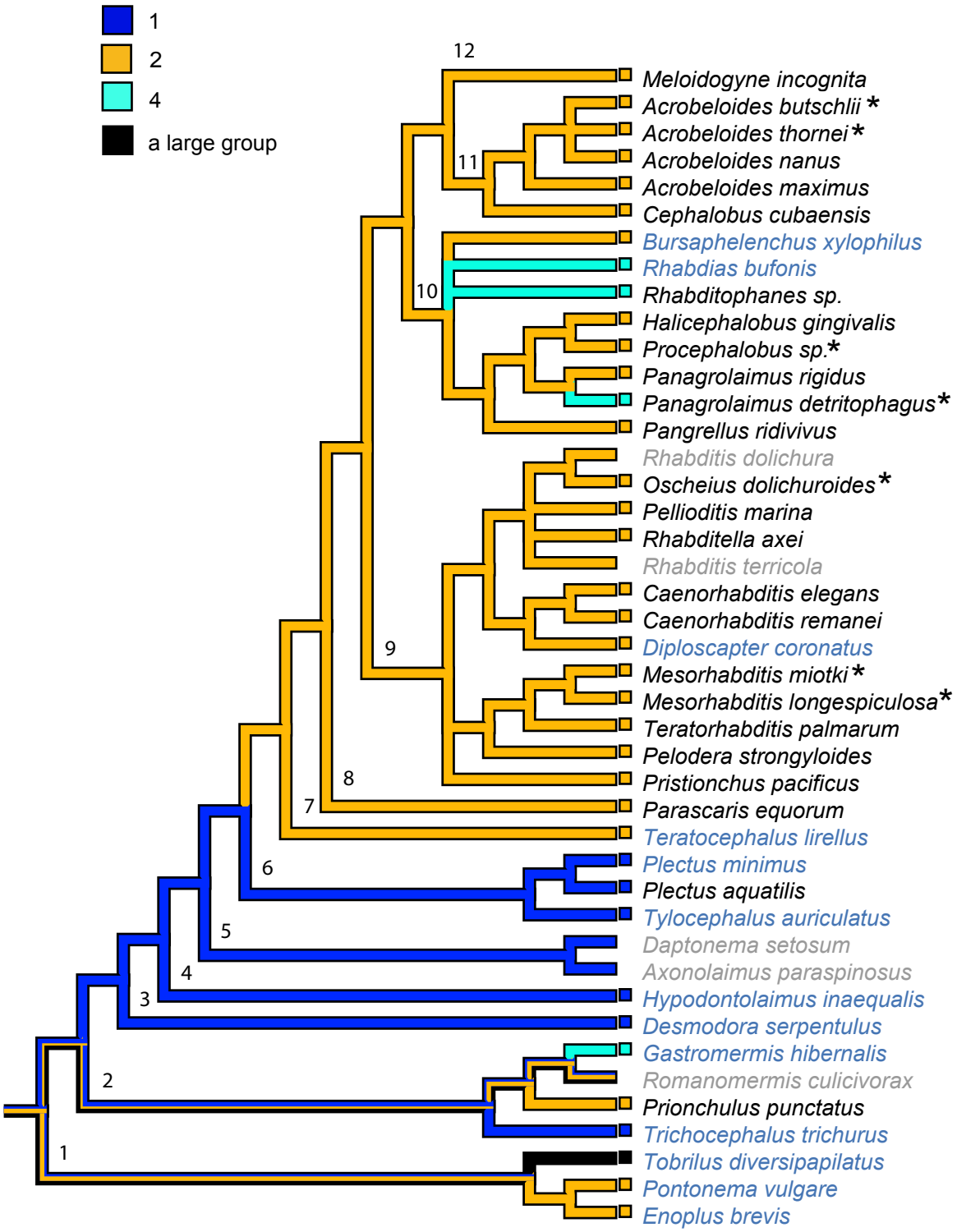
1
2
4
a large group
12
11
10
9
8
7
6
5
4
3
2
1
Meloidogyne incognita
Acrobeloides butschlii *
Acrobeloides thornei *
Acrobeloides nanus
Acrobeloides maximus
Cephalobus cubaensis
Bursaphelenchus xylophilus
Rhabdias bufonis
Rhabditophanes sp.
Halicephalobus gingivalis
Procephalobus sp.*
Panagrolaimus rigidus
Panagrolaimus detritophagus*
Pangrellus ridivivus
Rhabditis dolichura
Oscheius dolichuroides*
Pellioditis marina
Rhabditella axei
Rhabditis terricola
Caenorhabditis elegans
Caenorhabditis remanei
Diploscapter coronatus
Mesorhabditis miotki*
Mesorhabditis longespiculosa*
Teratorhabditis palmarum
Pelodera strongyloides
Pristionchus pacificus
Parascaris equorum
Teratocephalus lirellus
Plectus minimus
Plectus aquatilis
Tylocephalus auriculatus
Daptonema setosum
Axonolaimus paraspinosus
Hypodontolaimus inaequalis
Desmodora serpentulus
Gastromermis hibernalis
Romanomermis culicivorax
Prionchulus punctatus
Trichocephalus trichurus
Tobrilus diversipapilatus
Pontonema vulgare
Enoplus brevis

Table 4.2 Data-matrix for the cell-cell contacts in the 8AB cell stage

Here, each recording was considered a taxon. The data-matrix contains 72 taxa and 90 characters (0 = absent, 1 = present, - = not applicable).

character		character		character		character	
1	ala-alp	26	ara-arp	51	pla-E	76	prp-P4
2	ala-ara	27	ara-pla	52	pla-C	77	MS-E
3	ala-arp	28	ara-plp	53	pla-P3	78	MS-C
4	ala-pla	29	ara-pra	54	pla-D	79	MS-P3
5	ala-plp	30	ara-prp	55	pla-P4	80	MS-D
6	ala-pra	31	ara-MS	56	plp-pra	81	MS-P4
7	ala-prp	32	ara-E	57	plp-prp	82	E-C
8	ala-MS	33	ara-C	58	plp-MS	83	E-P3
9	ala-E	34	ara-P3	59	plp-E	84	E-D
10	ala-C	35	ara-D	60	plp-C	85	E-P4
11	ala-P3	36	ara-P4	61	plp-P3	86	C-P3
12	ala-D	37	arp-pla	62	plp-D	87	C-D
13	ala-P4	38	arp-plp	63	plp-P4	88	C-P4
14	alp-ara	39	arp-pra	64	pra-prp	89	D-P4
15	alp-arp	40	arp-prp	65	pra-MS	90	P3 gedeeld
16	alp-pla	41	arp-MS	66	pra-E		
17	alp-plp	42	arp-E	67	pra-C		
18	alp-pra	43	arp-C	68	pra-P3		
19	alp-prp	44	arp-P3	69	pra-D		
20	alp-MS	45	arp-D	70	pra-P4		
21	alp-E	46	arp-P4	71	prp-MS		
22	alp-C	47	pla-plp	72	prp-E		
23	alp-P3	48	pla-pra	73	prp-C		
24	alp-D	49	pla-prp	74	prp-P3		
25	alp-P4	50	pla-MS	75	prp-D		

Table 4.2

Taxon \ Character	1	2	3	4	5	6	7	8	9	10	11	12	13	14	15	16	17	18	19	20	21	22	23	24	25
C. elegans embr 1	1	1	0	1	0	0	0	0	0	0	0	-	-	1	0	1	1	0	0	1	0	0	0	-	-
C. elegans embr 2	1	1	0	1	0	0	0	0	0	0	0	-	-	1	0	0	1	0	0	1	0	0	0	-	-
C. elegans embr 3	1	1	0	1	0	0	0	0	0	0	0	-	-	1	0	1	1	0	0	1	0	0	0	-	-
C. elegans embr 4	1	1	0	1	0	0	0	0	0	0	0	-	-	1	0	1	1	0	0	1	0	0	0	-	-
C. elegans embr 5	1	1	0	1	0	0	0	0	0	0	0	-	-	1	0	1	1	0	0	1	0	0	0	-	-
C. elegans embr 6	1	1	0	1	0	0	0	0	0	0	0	-	-	1	0	1	1	0	0	1	0	0	0	-	-
C. elegans embr 7	1	1	0	1	0	0	0	0	0	0	0	-	-	1	0	1	1	0	0	1	0	0	0	-	-
C. elegans embr 8	1	1	0	1	1	0	0	0	0	0	0	-	-	1	0	0	1	0	0	1	0	0	0	-	-
C. remanei embr 1	1	1	1	1	0	0	0	0	0	0	0	-	-	1	0	1	1	0	0	1	0	0	0	-	-
C. remanei embr 2	1	1	1	1	0	0	0	0	0	0	0	-	-	1	0	1	1	0	0	1	0	0	0	-	-
C. remanei embr 3	1	1	0	1	0	0	0	0	0	0	0	-	-	1	0	0	1	0	0	1	0	0	0	-	-
M. longespiculosa embr 1	1	1	0	1	0	0	0	0	0	0	-	0	0	1	1	1	1	0	0	1	0	0	-	0	0
M. longespiculosa embr 2	1	1	0	0	0	0	0	0	0	0	-	0	0	1	1	1	1	0	0	1	0	0	-	0	0
M. longespiculosa embr 3	1	1	0	1	0	0	0	0	0	0	-	0	0	1	1	1	0	0	0	1	0	0	-	0	0
M. miotki embr 1	1	1	0	1	0	0	0	0	0	0	-	0	0	1	1	1	1	0	0	1	0	0	-	0	0
M. miotki embr 2	1	1	0	1	0	0	0	0	0	0	-	0	0	1	1	1	1	0	0	1	0	0	-	0	0
M. miotki embr 3	1	1	0	1	0	0	0	0	0	0	-	0	0	1	1	1	0	0	0	1	0	0	-	0	0
O. dolichuroides embr 1	1	1	1	1	0	0	0	0	0	0	-	0	0	1	0	1	1	0	0	1	0	0	-	0	0
O. dolichuroides embr 2	1	1	1	1	0	0	0	0	0	0	-	0	0	1	0	1	1	0	0	1	0	0	-	0	0
O. dolichuroides embr 3	1	1	1	1	0	0	0	0	0	0	-	0	0	1	0	1	1	0	0	1	0	0	-	0	0
P. marina embr 1	1	1	1	1	0	0	0	0	0	0	0	-	-	1	0	1	1	0	0	1	0	0	0	-	-
P. marina embr 2	1	1	1	1	0	0	0	0	0	0	0	-	-	1	0	1	1	0	0	1	0	0	0	-	-
P. strongyloides embr 1	1	1	0	1	0	0	0	0	0	0	0	-	-	1	0	1	0	0	0	1	0	0	0	-	-
P. strongyloides embr 2	1	1	0	1	0	0	0	0	0	0	0	-	-	1	0	1	0	0	0	1	0	0	0	-	-
P. strongyloides embr 3	1	1	0	1	0	0	0	0	0	0	0	-	-	1	0	1	0	0	0	1	0	0	0	-	-
R. axei embr 1	1	1	1	1	0	0	0	0	0	0	0	-	-	1	0	1	1	0	0	1	0	0	0	-	-
R. axei embr 2	1	1	1	1	0	0	0	0	0	0	0	-	-	1	0	1	1	0	0	1	0	0	0	-	-
R. axei embr 3	1	1	1	1	0	0	0	0	0	0	0	-	-	1	0	1	1	0	0	1	0	0	0	-	-
T. palmarum embr 1	1	0	1	1	0	0	0	1	0	0	0	-	-	0	0	0	0	0	0	1	1	0	0	-	-
T. palmarum embr 2	1	0	1	1	0	0	0	1	0	0	0	-	-	0	0	0	0	0	0	1	0	0	0	-	-
P. pacificus embr 1	1	1	1	1	0	0	0	0	0	0	0	-	-	1	0	1	0	0	0	1	0	0	0	-	-
P. pacificus embr 2	1	1	1	1	0	0	0	0	0	0	0	-	-	1	0	0	0	0	0	1	0	0	0	-	-
P. pacificus embr 3	1	1	1	1	0	0	0	0	0	0	0	-	-	1	0	1	0	0	0	1	0	0	0	-	-
P. pacificus embr 4	1	1	1	1	0	0	0	0	0	0	0	-	-	1	0	1	0	0	0	1	0	0	0	-	-
P. pacificus embr 5	1	1	1	1	0	0	0	0	0	0	0	-	-	1	0	1	1	0	0	1	0	0	0	-	-
P. pacificus embr 6	1	1	1	1	0	0	0	0	0	0	0	-	-	1	0	1	0	0	0	1	0	0	0	-	-
P. pacificus embr 7	1	1	1	1	0	0	0	0	0	0	0	-	-	1	0	1	1	0	0	1	0	0	0	-	-
P. pacificus embr 8	1	1	1	1	0	0	0	0	0	0	0	-	-	1	0	1	1	0	0	1	0	0	0	-	-
P. pacificus embr 9	1	1	1	1	0	0	0	0	0	0	0	-	-	1	0	1	1	0	0	1	0	0	0	-	-
P. pacificus embr 10	1	1	1	1	0	0	0	0	0	0	0	-	-	1	0	0	0	0	0	1	0	0	0	-	-
P. pacificus embr 11	1	1	1	1	0	0	0	0	0	0	0	-	-	1	0	0	0	0	0	1	0	?	0	-	-
P. pacificus embr 12	1	1	1	1	0	0	0	0	0	0	0	-	-	1	0	0	0	0	0	1	0	0	0	-	-
Rhabditophanes sp. embr 1	1	1	1	1	0	0	0	0	0	0	0	-	-	1	0	1	0	0	0	1	0	0	0	-	-
Rhabditophanes sp. embr 2	1	1	1	1	0	0	0	0	0	0	-	0	0	1	0	1	0	0	0	1	0	0	-	0	0
H. gingivalis embr 1	1	1	1	1	0	0	0	0	0	0	0	-	-	1	0	1	0	0	0	1	0	0	0	-	-
H. gingivalis embr 2	1	1	1	1	0	0	0	0	0	0	0	-	-	1	0	1	0	0	0	1	0	0	0	-	-
H. gingivalis embr 3	1	1	1	1	0	0	0	0	0	0	0	-	-	1	0	1	0	0	0	1	0	0	0	-	-
P. redivivus embr 1	1	1	1	1	0	0	0	0	0	0	-	0	0	1	0	1	1	0	0	1	0	0	-	0	0
P. redivivus embrc 2	1	1	1	1	0	0	0	0	0	0	-	0	0	1	0	1	1	0	0	1	0	0	-	0	0
P. detritophagus embr 1	1	1	1	1	0	0	0	0	0	0	-	0	0	1	0	1	1	0	0	1	0	0	-	0	0
P. detritophagus embr 2	1	1	1	1	0	0	0	0	0	0	-	0	0	1	0	1	1	0	0	1	0	0	-	0	0
P. detritophagus embr 3	1	1	1	1	0	0	0	0	0	0	-	0	0	1	0	1	1	0	0	1	0	0	-	0	0
P. rigidus embr 1	1	1	1	1	0	0	0	0	0	0	-	0	0	1	0	1	1	0	0	1	0	0	-	0	0
P. rigidus embr 2	1	1	1	1	0	0	0	0	0	0	-	0	0	1	0	1	1	0	0	1	0	0	-	0	0
P. rigidus embr 3	1	1	1	1	0	0	0	0	0	0	-	0	0	1	0	1	1	0	0	1	0	0	-	0	0
Procephalobus sp. embr 1	1	1	1	1	0	0	0	0	0	0	-	0	0	1	0	1	0	0	0	1	0	0	-	0	0
Procephalobus sp. embr 2	1	1	1	1	0	0	0	0	0	0	-	0	0	1	0	1	1	0	0	1	0	0	-	0	0
Procephalobus sp. embr 3	1	1	1	1	0	0	0	0	0	0	-	0	0	1	0	1	0	0	0	1	0	0	-	0	0
A. butschlii embr 1	1	1	1	1	0	0	0	0	0	0	-	0	0	1	0	1	0	0	0	1	0	0	-	0	0
A. butschlii embr 2	1	1	1	1	0	0	0	0	0	0	-	0	0	1	0	1	0	0	0	1	0	0	-	0	0
A. butschlii embr 3	1	1	1	1	0	0	0	0	0	0	-	0	0	1	0	1	0	0	0	1	0	0	-	0	0
A. nanus embr 1	1	1	1	1	0	0	0	0	0	0	-	0	0	1	0	1	0	0	0	1	0	0	-	0	0
A. nanus embr 2	1	1	1	1	0	0	0	0	0	0	-	0	0	1	0	1	0	0	0	1	0	0	-	0	0
A. thornnei embr 1	1	1	1	1	0	0	0	0	0	0	-	0	0	1	0	1	1	0	0	1	0	0	-	0	0
A. thornei embr 2	1	1	1	1	0	0	0	0	0	0	-	0	0	1	0	1	1	0	0	1	0	0	-	0	0
A. thornei embr 3	1	1	1	1	0	0	0	0	0	0	-	0	0	1	0	1	1	0	0	1	0	0	-	0	0
C. cubaensis embr 1	1	1	1	1	0	0	0	0	0	0	-	0	0	1	1	1	0	0	0	1	0	0	-	0	0
C. cubaensis embr 2	1	1	1	1	0	0	0	0	0	0	-	0	0	1	1	1	0	0	0	1	0	0	-	0	0
C. cubaensis embr 3	1	1	1	1	0	0	0	0	0	0	-	0	0	1	0	1	0	0	0	1	0	0	-	0	0
M. incognita embr 1	1	1	1	1	0	0	0	0	0	0	-	0	0	1	0	1	0	0	0	1	0	0	-	0	0
M. incognita embr 2	1	1	1	1	0	0	0	0	0	0	-	0	0	1	0	1	0	0	0	1	0	0	-	0	0
M. incognita embr 3	1	1	1	1	0	0	0	0	0	0	-	0	0	1	0	1	0	0	0	1	0	0	-	0	0

Table 4.2 (2) Data-matrix for the cell-cell contacts in the 8AB cell stage

Table 4.2 (2)

Taxon \ Character	26	27	28	29	30	31	32	33	34	35	36	37	38	39	40	41	42	43	44	45	46	47	48	49	50
C. elegans embr 1	1	1	0	1	1	1	0	0	0	-	-	1	1	1	0	0	0	0	0	-	-	1	0	0	0
C. elegans embr 2	1	1	1	1	0	1	0	0	0	-	-	1	1	1	0	0	0	0	0	-	-	1	0	0	0
C. elegans embr 3	1	1	0	1	0	1	0	0	0	-	-	1	1	1	0	0	0	0	0	-	-	1	0	0	0
C. elegans embr 4	1	1	1	1	0	1	0	0	0	-	-	1	1	1	0	0	0	0	0	-	-	1	0	0	0
C. elegans embr 5	1	1	1	1	0	1	0	0	0	-	-	1	1	1	0	0	0	0	0	-	-	1	0	0	0
C. elegans embr 6	1	1	0	1	0	1	0	0	0	-	-	1	1	1	0	0	0	0	0	-	-	1	0	0	0
C. elegans embr 7	1	1	1	1	0	1	0	0	0	?	-	1	1	1	0	0	0	0	0	-	-	1	0	0	1
C. elegans embr 8	1	1	0	1	1	1	0	0	0	-	-	1	1	1	0	0	0	0	0	-	-	1	0	0	0
C. remanei embr 1	1	0	0	1	1	1	0	0	0	-	-	1	1	1	0	0	0	1	0	-	-	1	0	0	0
C. remanei embr 2	1	0	0	1	1	1	0	0	0	-	-	1	1	1	1	0	0	1	0	-	-	1	0	0	0
C. remanei embr 3	1	0	0	1	1	1	0	0	0	-	-	1	1	1	1	0	0	1	0	-	-	1	0	0	0
M. longespiculosa embr 1	1	1	0	0	0	1	0	0	-	0	0	1	0	1	0	1	0	0	-	0	0	1	1	0	1
M. longespiculosa embr 2	1	1	0	0	0	1	0	0	-	0	0	1	0	1	0	1	0	0	-	0	0	1	1	0	1
M. longespiculosa embr 3	1	1	0	0	0	1	0	0	-	0	0	1	0	1	0	1	0	0	-	0	0	1	1	0	1
M. miotki embr 1	1	1	0	0	0	1	0	0	-	0	0	1	0	1	1	1	0	0	-	0	0	1	1	0	1
M. miotki embr 2	1	1	0	1	0	1	0	0	-	0	0	1	0	1	1	1	0	0	-	0	0	1	1	0	1
M. miotki embr 3	1	1	0	1	0	1	0	0	-	0	0	1	0	1	1	1	0	0	-	0	0	1	1	0	1
O. dolichuroides embr 1	1	1	1	1	0	1	0	0	-	0	0	1	1	1	0	0	0	1	-	0	0	1	0	0	0
O. dolichuroides embr 2	1	1	1	1	0	1	0	0	-	0	0	1	0	1	0	0	0	1	-	0	0	1	0	0	0
O. dolichuroides embr 3	1	1	1	1	0	1	0	0	-	0	0	1	1	1	0	0	0	1	-	0	0	1	0	0	0
P. marina embr 1	1	0	0	1	0	1	0	0	0	-	-	1	0	1	0	0	0	1	0	-	-	1	0	0	1
P. marina embr 2	1	0	0	1	0	1	0	0	0	-	-	1	0	1	0	0	0	1	0	-	-	1	0	0	0
P. strongyloides embr 1	1	0	0	1	0	1	0	0	0	-	-	1	1	1	0	0	0	1	0	-	-	1	0	0	1
P. strongyloides embr 2	1	1	0	1	0	1	0	0	0	-	-	1	1	1	0	0	0	1	0	-	-	1	0	0	1
P. strongyloides embr 3	1	0	0	1	0	1	0	0	0	-	-	1	1	1	0	0	0	1	0	-	-	1	0	0	0
R. axei embr 1	1	0	0	1	1	1	0	0	0	-	-	1	1	1	0	0	0	1	0	-	-	1	0	0	0
R. axei embr 2	1	1	1	1	1	1	0	1	0	-	-	1	0	1	0	0	0	1	0	-	-	1	0	0	0
R. axei embr 3	1	0	0	1	1	1	0	0	0	-	-	1	1	1	0	0	0	1	0	-	-	1	0	0	0
T. palmarum embr 1	1	0	0	1	0	1	1	0	0	-	-	1	0	1	0	1	0	0	0	-	-	1	1	0	0
T. palmarum embr 2	1	0	0	1	0	1	1	0	0	-	-	1	0	1	0	1	0	0	0	-	-	1	1	0	0
P. pacificus embr 1	1	0	1	1	1	1	1	0	0	-	-	1	0	1	0	0	0	0	0	-	-	1	0	0	0
P. pacificus embr 2	1	0	1	1	1	1	0	0	0	-	-	1	1	1	0	0	0	0	0	-	-	1	0	0	0
P. pacificus embr 3	1	0	0	1	1	1	0	0	0	-	-	1	1	1	0	0	0	1	0	-	-	1	0	0	1
P. pacificus embr 4	1	0	0	1	1	1	0	0	0	-	-	0	0	1	1	0	0	0	0	-	-	1	0	0	1
P. pacificus embr 5	1	0	1	1	1	1	0	0	0	-	-	1	0	1	1	0	0	1	0	-	-	1	0	0	0
P. pacificus embr 6	1	0	0	1	1	1	0	0	0	-	-	1	1	1	0	0	0	1	0	-	-	1	0	0	0
P. pacificus embr 7	1	0	1	1	1	1	0	0	0	-	-	1	1	1	0	0	0	1	0	-	-	1	0	0	0
P. pacificus embr 8	1	0	0	1	1	1	0	0	0	-	-	0	0	1	1	0	0	1	0	-	-	1	0	0	0
P. pacificus embr 9	1	0	0	1	1	1	0	0	0	-	-	1	0	1	0	0	0	1	0	-	-	1	0	0	0
P. pacificus embr 10	1	0	0	1	1	1	0	0	0	-	-	1	1	1	1	0	0	1	0	-	-	1	0	0	0
P. pacificus embr 11	1	0	1	1	1	1	0	0	0	-	-	1	1	1	0	0	0	0	0	-	-	1	0	0	0
P. pacificus embr 12	1	0	0	1	1	1	0	0	0	-	-	1	0	1	0	0	0	0	0	-	-	1	0	0	0
Rhabditophanes sp. embr 1	1	0	0	1	0	1	0	0	0	-	-	1	0	1	0	1	0	1	0	-	-	1	0	0	1
Rhabditophanes sp. embr 2	1	0	0	1	0	1	0	0	-	0	0	1	0	1	0	1	0	1	-	0	0	1	0	0	1
H. gingivalis embr 1	1	0	0	1	0	1	0	0	0	-	-	1	0	1	0	0	0	1	0	-	-	1	0	0	1
H. gingivalis embr 2	1	0	0	1	0	1	0	0	0	-	-	1	0	1	0	0	0	1	0	-	-	1	0	0	1
H. gingivalis embr 3	1	0	0	1	0	1	0	0	0	-	-	1	0	1	0	0	0	1	0	-	-	1	0	0	1
P. redivivus embr 1	1	1	0	1	0	1	0	0	-	0	0	1	0	1	0	0	0	1	-	0	0	1	0	0	0
P. redivivus embrc 2	1	1	0	1	0	1	0	0	-	0	0	1	0	1	0	0	0	1	-	0	0	1	0	0	0
P. detritophagus embr 1	1	1	0	1	0	1	0	0	-	0	0	1	0	1	0	0	0	1	-	0	0	1	0	0	1
P. detritophagus embr 2	1	1	0	1	0	1	0	0	-	0	0	1	0	1	0	0	0	1	-	0	0	1	0	0	0
P. detritophagus embr 3	1	1	0	1	0	1	0	0	-	0	0	1	0	1	0	0	0	1	-	0	0	1	0	0	1
P. rigidus embr 1	1	0	0	1	0	1	0	0	-	0	0	1	0	1	0	0	0	1	-	0	0	1	0	0	0
P. rigidus embr 2	1	0	0	1	0	1	0	0	-	0	0	1	0	1	0	0	0	1	-	0	0	1	0	0	0
P. rigidus embr 3	1	0	0	1	1	1	0	0	-	0	?	1	1	1	0	0	0	1	-	0	0	1	0	0	0
Procephalobus sp. embr 1	1	0	0	1	0	1	0	0	-	0	0	1	0	1	0	0	0	0	-	0	0	1	0	0	1
Procephalobus sp. embr 2	1	0	0	1	0	1	0	0	-	0	0	1	0	1	0	0	0	0	-	0	0	1	0	0	1
Procephalobus sp. embr 3	1	0	0	1	0	1	0	0	-	0	0	1	1	1	0	0	0	0	-	0	0	1	0	0	1
A. butschlii embr 1	1	0	0	1	0	1	0	0	-	0	0	1	0	1	0	0	0	1	-	0	0	1	0	0	0
A. butschlii embr 2	1	0	0	1	0	1	0	0	-	0	0	1	0	1	0	0	0	1	-	0	0	1	0	0	0
A. butschlii embr 3	1	0	0	1	0	1	0	0	-	0	0	1	0	1	0	0	0	1	-	0	0	1	0	0	0
A. nanus embr 1	1	0	0	1	0	1	0	0	-	0	0	1	0	1	0	0	0	0	-	0	0	1	0	0	0
A. nanus embr 2	1	0	0	1	0	1	0	0	-	0	0	1	0	1	0	0	0	0	-	0	0	1	0	0	0
A. thornnei embr 1	1	1	0	1	0	1	0	0	-	0	0	1	0	1	0	0	0	1	-	0	0	1	0	0	0
A. thornei embr 2	1	1	0	1	0	1	0	0	-	0	0	1	0	1	0	0	0	1	-	0	0	1	0	0	0
A. thornei embr 3	1	1	0	1	1	1	0	0	-	0	0	1	0	1	0	0	0	1	-	0	0	1	0	0	0
C. cubaensis embr 1	1	1	0	1	0	1	0	0	-	0	0	1	0	1	0	0	0	0	-	0	0	1	0	0	1
C. cubaensis embr 2	1	1	0	1	0	1	0	0	-	0	0	1	0	1	0	0	0	0	-	0	0	1	0	0	1
C. cubaensis embr 3	1	1	0	1	0	1	0	0	-	0	0	1	0	1	0	0	0	0	-	0	0	1	0	0	1
M. incognita embr 1	1	1	0	0	0	1	0	0	-	0	0	1	0	1	0	0	0	0	-	0	0	1	1	0	1
M. incognita embr 2	1	1	0	1	0	1	0	0	-	0	0	1	1	1	0	0	0	0	-	0	0	1	1	0	1
M. incognita embr 3	1	1	0	1	0	1	0	0	-	0	0	1	1	1	0	0	0	0	-	0	0	1	0	0	1

Table 4.2 (3) Data-matrix for the cell-cell contacts in the 8AB cell stage

Table 4.2 (3)

Taxon \ Character	51	52	53	54	55	56	57	58	59	60	61	62	63	64	65	66	67	68	69	70	71	72	73	74	75
C. elegans embr 1	0	0	0	-	-	0	0	1	0	0	0	-	-	1	0	0	1	0	-	-	1	1	1	1	-
C. elegans embr 2	0	0	0	-	-	0	0	1	0	0	0	-	-	1	0	0	1	0	-	-	1	1	1	1	-
C. elegans embr 3	0	0	0	-	-	0	0	1	0	0	0	-	-	1	1	0	1	0	-	-	1	1	1	1	-
C. elegans embr 4	0	0	0	-	-	0	0	1	0	0	0	-	-	1	1	0	1	0	-	-	1	1	1	1	-
C. elegans embr 5	0	0	0	-	-	0	0	1	0	0	0	-	-	1	1	0	1	0	-	-	1	1	1	1	-
C. elegans embr 6	0	0	0	-	-	0	0	1	0	0	0	-	-	1	1	0	1	0	-	-	1	1	1	1	-
C. elegans embr 7	0	0	0	-	-	0	0	1	0	0	0	-	-	1	1	0	1	0	-	-	1	1	1	1	-
C. elegans embr 8	0	0	0	-	-	0	0	1	0	0	0	-	-	1	0	0	1	0	-	-	1	1	1	1	-
C. remanei embr 1	0	1	0	-	-	0	0	1	1	1	0	-	-	1	1	0	1	0	-	-	1	1	1	1	-
C. remanei embr 2	0	1	0	-	-	0	0	1	1	1	0	-	-	1	1	0	1	0	-	-	1	1	1	1	-
C. remanei embr 3	0	1	0	-	-	0	0	1	1	1	0	-	-	1	1	0	1	0	-	-	1	1	1	1	-
M. longespiculosa embr 1	0	0	-	0	0	1	1	1	1	1	-	0	0	1	1	1	0	-	0	0	0	1	1	-	1
M. longespiculosa embr 2	0	0	-	0	0	1	1	1	1	1	-	0	0	1	1	1	0	-	0	0	0	1	1	-	1
M. longespiculosa embr 3	0	0	-	0	0	1	1	1	1	1	-	0	0	1	1	1	0	-	0	0	0	1	1	-	1
M. miotki embr 1	1	1	-	0	0	0	0	1	1	1	-	1	1	1	1	0	1	-	0	0	1	1	1	-	1
M. miotki embr 2	0	1	-	1	0	0	0	1	1	1	-	1	1	1	1	0	1	-	0	0	1	1	1	-	1
M. miotki embr 3	0	1	-	0	0	0	0	1	1	1	-	1	0	1	1	0	1	-	0	0	1	1	1	-	1
O. dolichuroides embr 1	0	0	-	0	0	1	0	1	1	1	-	0	0	1	1	0	1	-	1	0	1	1	1	-	1
O. dolichuroides embr 2	0	0	-	0	0	0	0	1	1	1	-	0	0	1	1	0	1	-	1	0	1	1	1	-	1
O. dolichuroides embr 3	0	0	-	0	0	1	0	1	1	1	-	0	0	1	1	0	1	-	1	0	1	0	1	-	1
P. marina embr 1	0	1	0	-	-	0	0	1	1	1	1	-	-	1	1	0	1	0	-	-	1	1	1	1	-
P. marina embr 2	0	1	0	-	-	0	0	1	1	1	1	-	-	1	1	0	1	0	-	-	1	1	0	1	-
P. strongyloides embr 1	0	0	0	-	-	0	0	1	1	1	0	-	-	1	1	0	0	0	-	-	1	1	0	1	-
P. strongyloides embr 2	0	0	0	-	-	0	0	1	1	1	0	-	-	1	1	0	0	0	-	-	1	1	1	1	-
P. strongyloides embr 3	0	1	0	-	-	0	0	1	1	1	0	-	-	1	0	1	1	0	-	-	0	1	0	1	-
R. axei embr 1	0	1	0	-	-	0	0	1	1	1	0	-	-	1	0	0	1	0	-	-	1	1	0	1	-
R. axei embr 2	0	1	0	-	-	0	0	1	1	1	0	-	-	1	0	0	1	1	-	-	1	1	0	1	-
R. axei embr 3	0	1	0	-	-	0	0	1	0	1	0	-	-	1	0	0	1	1	-	-	1	1	0	1	-
T. palmarum embr 1	1	1	0	-	-	0	0	0	1	1	1	-	-	1	0	0	1	0	-	-	0	1	1	1	-
T. palmarum embr 2	1	1	0	-	-	0	0	0	1	1	1	-	-	1	0	0	1	0	-	-	0	1	1	1	-
P. pacificus embr 1	0	0	0	-	-	0	1	1	1	0	0	-	-	1	0	0	1	0	-	-	0	1	1	0	-
P. pacificus embr 2	0	0	0	-	-	0	0	1	1	0	0	-	-	1	0	0	1	0	-	-	1	1	1	0	-
P. pacificus embr 3	0	1	0	-	-	0	0	1	1	1	0	-	-	1	0	0	1	0	-	-	1	1	1	0	-
P. pacificus embr 4	0	1	0	-	-	0	0	1	1	1	0	-	-	1	0	0	1	0	-	-	1	1	1	0	-
P. pacificus embr 5	0	1	0	-	-	0	1	1	1	1	0	-	-	1	0	0	1	0	-	-	1	1	1	0	-
P. pacificus embr 6	0	0	0	-	-	0	0	1	1	1	0	-	-	1	0	0	1	0	-	-	1	1	1	0	-
P. pacificus embr 7	0	1	0	-	-	0	0	1	1	1	0	-	-	1	0	0	1	0	-	-	1	1	1	0	-
P. pacificus embr 8	0	0	0	-	-	0	1	1	1	1	0	-	-	1	0	0	1	0	-	-	1	1	1	0	-
P. pacificus embr 9	0	1	0	-	-	0	0	1	1	1	0	-	-	1	0	0	1	0	-	-	1	1	1	0	-
P. pacificus embr 10	0	1	0	-	-	0	1	1	1	1	0	-	-	1	0	0	1	0	-	-	1	1	1	0	-
P. pacificus embr 11	0	0	0	-	-	0	1	1	1	0	0	-	-	1	0	0	1	0	-	-	0	1	1	0	-
P. pacificus embr 12	0	0	0	-	-	0	0	1	1	1	0	-	-	1	0	0	1	0	-	-	1	1	1	0	-
Rhabditophanes sp. embr 1	0	1	0	-	-	0	0	1	1	1	0	-	-	1	0	0	1	0	-	-	1	1	1	1	-
Rhabditophanes sp. embr 2	0	1	-	0	0	0	0	0	1	1	-	1	0	1	0	0	1	-	0	0	1	1	1	-	0
H. gingivalis embr 1	0	1	0	-	-	0	1	1	1	1	0	-	-	1	1	0	1	0	-	-	1	1	1	1	-
H. gingivalis embr 2	0	1	0	-	-	0	1	1	1	1	0	-	-	1	1	0	1	0	-	-	1	1	1	0	-
H. gingivalis embr 3	0	1	0	-	-	1	1	1	1	1	0	-	-	1	1	0	1	0	-	-	1	1	1	1	-
P. redivivus embr 1	0	1	-	0	0	0	0	1	1	1	-	0	0	1	1	0	1	-	0	0	1	1	1	-	1
P. redivivus embrc 2	0	1	-	0	0	0	0	1	1	1	-	0	0	1	1	0	1	-	0	0	1	1	1	-	1
P. detritophagus embr 1	0	1	-	0	0	0	0	1	1	1	-	0	0	1	1	0	1	-	0	0	1	1	1	-	1
P. detritophagus embr 2	0	0	-	0	0	0	0	1	1	1	-	0	0	1	1	0	1	-	0	0	1	1	1	-	0
P. detritophagus embr 3	0	1	-	0	0	0	0	1	1	1	-	0	0	1	1	0	1	-	0	0	1	1	1	-	0
P. rigidus embr 1	0	1	-	0	0	0	0	1	1	1	-	0	0	1	1	0	1	-	0	0	1	1	1	-	1
P. rigidus embr 2	0	1	-	0	0	0	0	1	1	1	-	0	0	1	1	0	1	-	0	0	1	1	1	-	1
P. rigidus embr 3	0	0	-	0	0	0	0	1	1	1	-	0	0	1	0	0	1	-	0	0	1	1	1	-	1
Procephalobus sp. embr 1	0	0	-	0	0	0	1	1	1	1	-	0	0	1	1	0	1	-	0	0	1	1	1	-	1
Procephalobus sp. embr 2	0	0	-	0	0	0	0	1	1	1	-	0	0	1	1	0	1	-	0	0	1	1	1	-	0
Procephalobus sp. embr 3	0	0	-	0	0	0	1	1	1	1	-	0	0	1	1	0	1	-	0	0	1	1	1	-	0
A. butschlii embr 1	0	1	-	0	0	0	1	1	1	1	-	0	0	1	1	0	1	-	0	0	1	1	1	-	1
A. butschlii embr 2	0	1	-	0	0	0	1	1	1	1	-	0	0	1	1	0	1	-	0	0	1	1	1	-	1
A. butschlii embr 3	0	1	-	0	0	0	1	1	1	1	-	0	0	1	1	0	1	-	0	0	1	1	1	-	1
A. nanus embr 1	0	1	-	0	0	0	1	1	1	1	-	0	0	1	1	0	1	-	0	0	1	1	1	-	1
A. nanus embr 2	0	1	-	0	0	0	0	1	1	1	-	0	0	1	1	0	1	-	0	0	1	1	1	-	1
A. thornnei embr 1	0	1	-	0	0	0	1	1	1	1	-	0	0	1	1	0	1	-	0	0	1	1	1	-	1
A. thornei embr 2	0	1	-	0	0	0	1	1	1	1	-	0	0	1	1	0	1	-	0	0	1	1	1	-	1
A. thornei embr 3	0	1	-	0	0	0	1	1	1	1	-	0	0	1	0	0	1	-	0	0	1	1	1	-	1
C. cubaensis embr 1	0	1	-	0	0	0	0	1	1	1	-	0	0	1	1	0	1	-	0	0	1	1	1	-	0
C. cubaensis embr 2	0	1	-	0	0	0	0	1	1	1	-	0	0	1	1	0	1	-	0	0	1	1	1	-	0
C. cubaensis embr 3	0	1	-	0	0	0	1	1	1	1	-	0	0	1	1	0	1	-	0	0	1	1	1	-	0
M. incognita embr 1	0	0	-	0	0	0	1	0	1	0	-	0	0	1	1	1	0	-	0	0	0	1	1	-	0
M. incognita embr 2	1	0	-	0	0	0	1	0	1	0	-	0	0	1	1	1	0	-	0	0	0	1	1	-	0
M. incognita embr 3	0	0	-	0	0	0	1	0	1	0	-	0	0	1	1	1	0	-	0	0	0	1	1	-	0

Table 4.2 (4) Data-matrix for the cell-cell contacts in the 8AB cell stage

Table 4.2 (4)

Taxon \ Character	76	77	78	79	80	81	82	83	84	85	86	87	88	89	90
C. elegans embr 1	-	1	0	0	-	-	1	1	-	-	1	-	-	-	0
C. elegans embr 2	-	1	0	0	-	-	1	1	-	-	1	-	-	-	0
C. elegans embr 3	-	1	1	0	-	-	1	1	-	-	1	-	-	-	0
C. elegans embr 4	-	1	0	0	-	-	1	1	-	-	1	-	-	-	0
C. elegans embr 5	-	1	1	0	-	-	1	1	-	-	1	-	-	-	0
C. elegans embr 6	-	1	0	0	-	-	1	1	-	-	1	-	-	-	0
C. elegans embr 7	-	1	0	0	-	-	1	1	-	-	1	-	-	-	0
C. elegans embr 8	-	1	1	0	-	-	1	1	-	-	1	-	-	-	0
C. remanei embr 1	-	1	0	0	-	-	1	1	-	-	1	-	-	-	0
C. remanei embr 2	-	1	0	0	-	-	1	1	-	-	1	-	-	-	0
C. remanei embr 3	-	1	0	0	-	-	1	1	-	-	1	-	-	-	0
M. longespiculosa embr 1	0	1	0	-	0	0	1	-	1	1	-	1	1	1	1
M. longespiculosa embr 2	0	1	1	-	0	0	1	-	0	1	-	1	1	1	1
M. longespiculosa embr 3	?	1	0	-	0	0	1	-	1	1	-	1	0	1	1
M. miotki embr 1	0	1	1	-	0	0	1	-	1	1	-	1	1	1	1
M. miotki embr 2	1	1	1	-	0	0	1	-	1	1	-	1	1	1	1
M. miotki embr 3	1	1	1	-	0	0	1	-	1	1	-	1	1	1	1
O. dolichuroides embr 1	1	1	0	-	0	0	1	-	1	1	-	1	1	1	1
O. dolichuroides embr 2	1	1	0	-	0	0	1	-	1	1	-	1	1	1	1
O. dolichuroides embr 3	0	1	0	-	0	0	1	-	1	-	-	1	1	1	1
P. marina embr 1	-	1	1	0	-	-	0	1	-	-	1	-	-	-	0
P. marina embr 2	-	1	1	0	-	-	0	1	-	-	1	-	-	-	0
P. strongyloides embr 1	-	1	1	0	-	-	1	1	-	-	0	-	-	-	0
P. strongyloides embr 2	-	1	1	0	-	-	1	1	-	-	0	-	-	-	0
P. strongyloides embr 3	-	1	1	0	-	-	1	1	-	-	0	-	-	-	0
R. axei embr 1	-	1	0	0	-	-	1	1	-	-	1	-	-	-	0
R. axei embr 2	-	1	0	0	-	-	1	1	-	-	1	-	-	-	0
R. axei embr 3	-	1	1	0	-	-	1	1	-	-	1	-	-	-	0
T. palmarum embr 1	-	1	0	0	-	-	0	1	-	-	1	-	-	-	0
T. palmarum embr 2	-	1	0	0	-	-	0	1	-	-	1	-	-	-	0
P. pacificus embr 1	-	1	0	0	-	-	1	1	-	-	1	-	-	-	0
P. pacificus embr 2	-	1	0	0	-	-	1	1	-	-	1	-	-	-	0
P. pacificus embr 3	-	1	0	0	-	-	1	1	-	-	1	-	-	-	0
P. pacificus embr 4	-	1	0	0	-	-	1	1	-	-	1	-	-	-	0
P. pacificus embr 5	-	1	0	0	-	-	1	1	-	-	1	-	-	-	0
P. pacificus embr 6	-	1	0	0	-	-	1	1	-	-	1	-	-	-	0
P. pacificus embr 7	-	1	0	0	-	-	1	1	-	-	1	-	-	-	0
P. pacificus embr 8	-	1	0	0	-	-	1	1	-	-	1	-	-	-	0
P. pacificus embr 9	-	1	0	0	-	-	1	1	-	-	1	-	-	-	0
P. pacificus embr 10	-	1	0	0	-	-	1	1	-	-	1	-	-	-	0
P. pacificus embr 11	-	1	0	0	-	-	1	1	-	-	1	-	-	-	0
P. pacificus embr 12	-	1	0	0	-	-	1	1	-	-	1	-	-	-	0
Rhabditophanes sp. embr 1	-	1	1	0	-	-	1	1	-	-	1	-	-	-	0
Rhabditophanes sp. embr 2	1	1	1	-	0	0	1	-	1	1	-	1	1	1	1
H. gingivalis embr 1	-	1	0	0	-	-	1	1	-	-	1	-	-	-	0
H. gingivalis embr 2	-	1*	0	0	-	-	1	1	-	-	1	-	-	-	0
H. gingivalis embr 3	-	1	0	0	-	-	1	1	-	-	1	-	-	-	0
P. redivivus embr 1	1	1	1	-	0	0	1	-	1	1	-	1	0	1	1
P. redivivus embrc 2	1	1	1	-	0	0	1	-	1	1	-	1	0	1	1
P. detritophagus embr 1	0	1	0	-	0	0	1	-	1	1	-	1	0	1	1
P. detritophagus embr 2	0	1	0	-	0	0	1	-	1	1	-	1	0	1	1
P. detritophagus embr 3	0	1	0	-	0	0	1	-	1	1	-	1	0	1	1
P. rigidus embr 1	1	1	0	-	0	0	1	-	1	1	-	1	1	1	1
P. rigidus embr 2	0	1	0	-	0	0	1	-	1	1	-	1	0	1	1
P. rigidus embr 3	0	1	0	-	0	0	1	?	1	1	-	1	0	1	1
Procephalobus sp. embr 1	0	1	0	-	0	0	1	-	1	1	-	1	0	1	1
Procephalobus sp. embr 2	1	1	1	-	0	0	1	-	1	1	-	1	0	1	1
Procephalobus sp. embr 3	1	1	0	-	0	0	1	-	1	1	-	1	0	1	1
A. butschlii embr 1	0	1	1	-	0	0	1	-	1	1	-	1	1	1	1
A. butschlii embr 2	0	1	1	-	0	0	1	-	1	1	-	1	1	1	1
A. butschlii embr 3	1	1	1	-	0	0	1	-	1	1	-	1	1	1	1
A. nanus embr 1	0	1	1	-	0	0	1	-	1	1	-	1	1	1	1
A. nanus embr 2	0	1	1	-	0	0	1	-	1	1	-	1	1	1	1
A. thornnei embr 1	1	1	1	-	0	0	1	-	1	1	-	1	1	1	1
A. thornei embr 2	0	1	1	-	0	0	1	-	1	1	-	1	1	1	1
A. thornei embr 3	0	1	1	-	0	0	1	-	1	1	-	1	1	1	1
C. cubaensis embr 1	0	1	0	-	0	0	1	-	1	1	-	1	1	1	1
C. cubaensis embr 2	0	1	0	-	0	0	1	-	1	1	-	1	1	1	1
C. cubaensis embr 3	0	1	0	-	0	0	1	-	1	1	-	1	1	1	1
M. incognita embr 1	0	1	0	-	0	0	1	-	1	1	-	1	1	1	1
M. incognita embr 2	0	1	0	-	0	0	1	-	1	1	-	1	1	1	1
M. incognita embr 3	0	1	0	-	0	0	1	-	0	0	-	1	1	1	1

Figure 4.6 Parsimonious reconstruction of the contact ABarp-C (character 43) onto the phylogenetic tree

This tree is a combination of the nematode phylogeny presented by Holterman *et al.* (2006) and newly obtained consensus phylogenies based on SSU rDNA data of clades 9, 10 and 11. When data from literature was not available, the species are shown in grey. The numbering of the clades (1-12) refers to the phylogeny of Holterman *et al.* (2006). Black: contact is present in all recordings, yellow: contact is absent in all recordings, black and yellow: variable contact.

Fig. 4.6

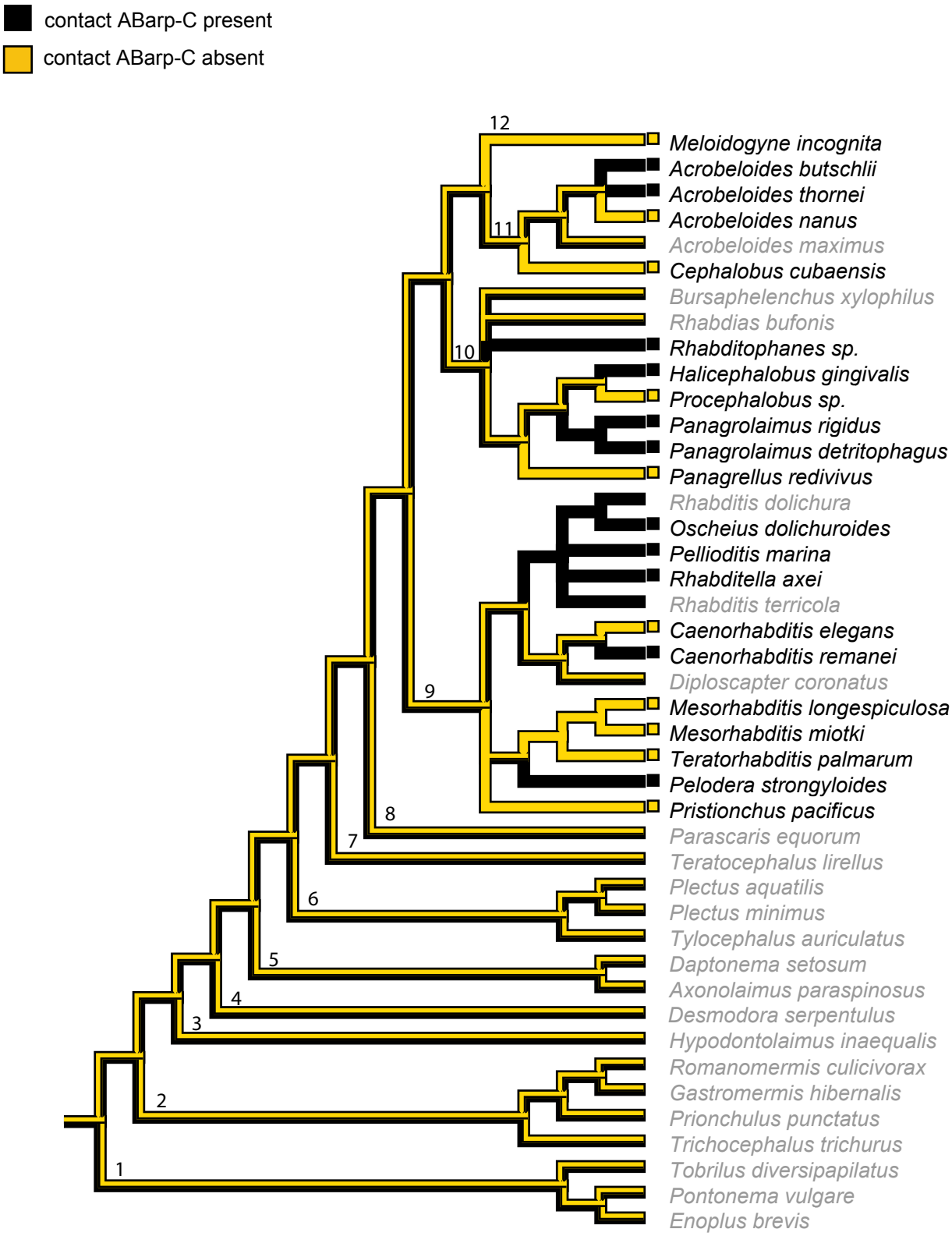
contact ABarp-C present
contact ABarp-C absent
12
11
10
9
8
7
6
5
4
3
2
1
Meloidogyne incognita
Acrobeloides butschlii
Acrobeloides thornei
Acrobeloides nanus
Acrobeloides maximus
Cephalobus cubaensis
Bursaphelenchus xylophilus
Rhabdias bufonis
Rhabditophanes sp.
Halicephalobus gingivalis
Procephalobus sp.
Panagrolaimus rigidus
Panagrolaimus detritophagus
Panagrellus redivivus
Rhabditis dolichura
Oscheius dolichuroides
Pellioditis marina
Rhabditella axei
Rhabditis terricola
Caenorhabditis elegans
Caenorhabditis remanei
Diploscapter coronatus
Mesorhabditis longespiculosa
Mesorhabditis miotki
Teratorhabditis palmarum
Pelodera strongyloides
Pristionchus pacificus
Parascaris equorum
Teratocephalus lirellus
Plectus aquatilis
Plectus minimus
Tylocephalus auriculatus
Daptonema setosum
Axonolaimus paraspinosus
Desmodora serpentulus
Hypodontolaimus inaequalis
Romanomermis culicivorax
Gastromermis hibernalis
Prionchulus punctatus
Trichocephalus trichurus
Tobrilus diversipapilatus
Pontonema vulgare
Enoplus brevis

Figure 4.7 Parsimonious reconstruction of the contact ABpla-MS (character 50) onto the phylogenetic tree

This tree is a combination of the nematode phylogeny presented by Holterman *et al.* (2006) and newly obtained consensus phylogenies based on SSU rDNA data of clades 9, 10 and 11. When data from literature was not available, the species are shown in grey. The numbering of the clades (1-12) refers to the phylogeny of Holterman *et al.* (2006). Black: contact is present in all recordings, yellow: contact is absent in all recordings, black and yellow: variable contact.

Fig. 4.7

contact ABpla-MS present

contact ABpla-MS absent

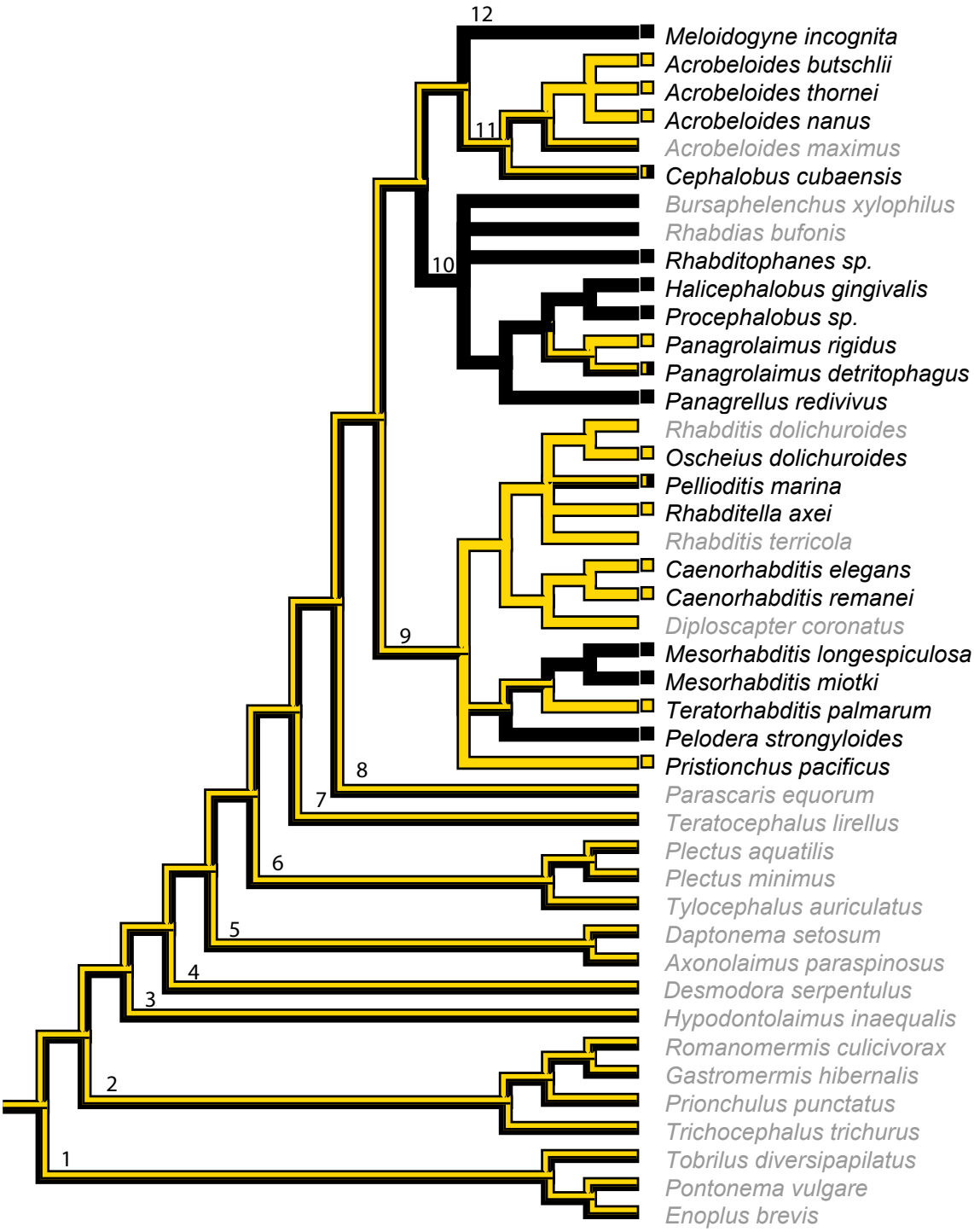

Figure 4.8 Parsimonious reconstruction of the contact ABarp-ABplp (character 38) onto the phylogenetic tree

This tree is a combination of the nematode phylogeny presented by Holterman *et al.* (2006) and newly obtained consensus phylogenies based on SSU rDNA data of clades 9, 10 and 11. When data from literature was not available, the species are shown in grey. The numbering of the clades (1-12) refers to the phylogeny of Holterman *et al.* (2006). Black: contact is present in all recordings, yellow: contact is absent in all recordings, black and yellow: variable contact.

Fig. 4.8

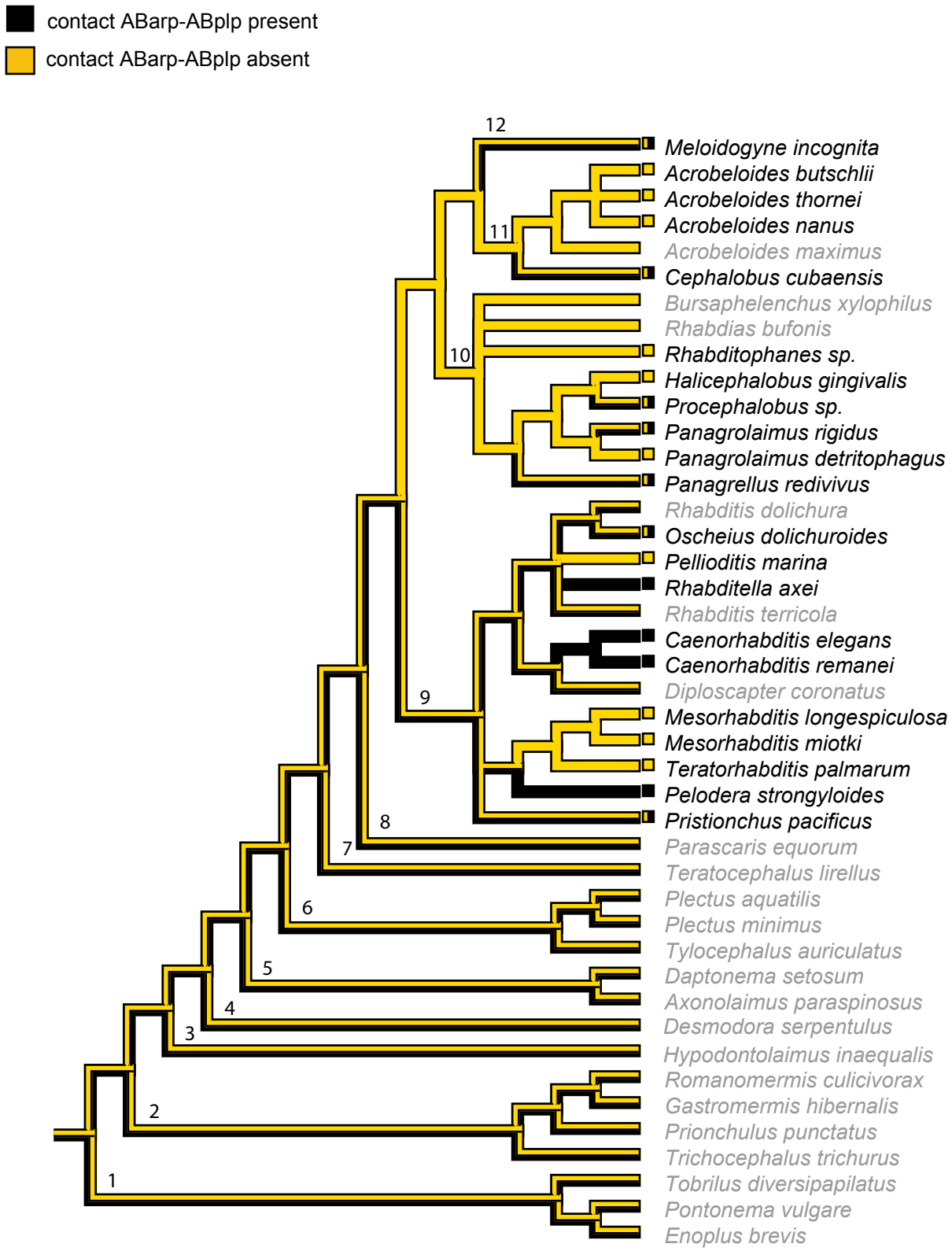
contact ABarp-ABplp present
contact ABarp-ABplp absent
12
11
10
9
8
7
6
5
4
3
2
1
Meloidogyne incognita
Acrobeloides butschlii
Acrobeloides thornei
Acrobeloides nanus
Acrobeloides maximus
Cephalobus cubaensis
Bursaphelenchus xylophilus
Rhabdias bufonis
Rhabditophanes sp.
Halicephalobus gingivalis
Procephalobus sp.
Panagrolaimus rigidus
Panagrolaimus detritophagus
Panagrellus redivivus
Rhabditis dolichura
Oscheius dolichuroides
Pellioditis marina
Rhabditella axei
Rhabditis terricola
Caenorhabditis elegans
Caenorhabditis remanei
Diploscapter coronatus
Mesorhabditis longespiculosa
Mesorhabditis miotki
Teratorhabditis palmarum
Pelodera strongyloides
Pristionchus pacificus
Parascaris equorum
Teratocephalus lirellus
Plectus aquatilis
Plectus minimus
Tylocephalus auriculatus
Daptonema setosum
Axonolaimus paraspinosus
Desmodora serpentulus
Hypodontolaimus inaequalis
Romanomermis culicivorax
Gastromermis hibernalis
Prionchulus punctatus
Trichocephalus trichurus
Tobrilus diversipapilatus
Pontonema vulgare
Enoplus brevis

Figure 4.9 Phylogenetic reconstruction based on cell-cell contacts

Maximum parsimony (MP) analysis of cell-cell contacts. Species belonging to the same family are marked in the same colour.

Fig. 4.9

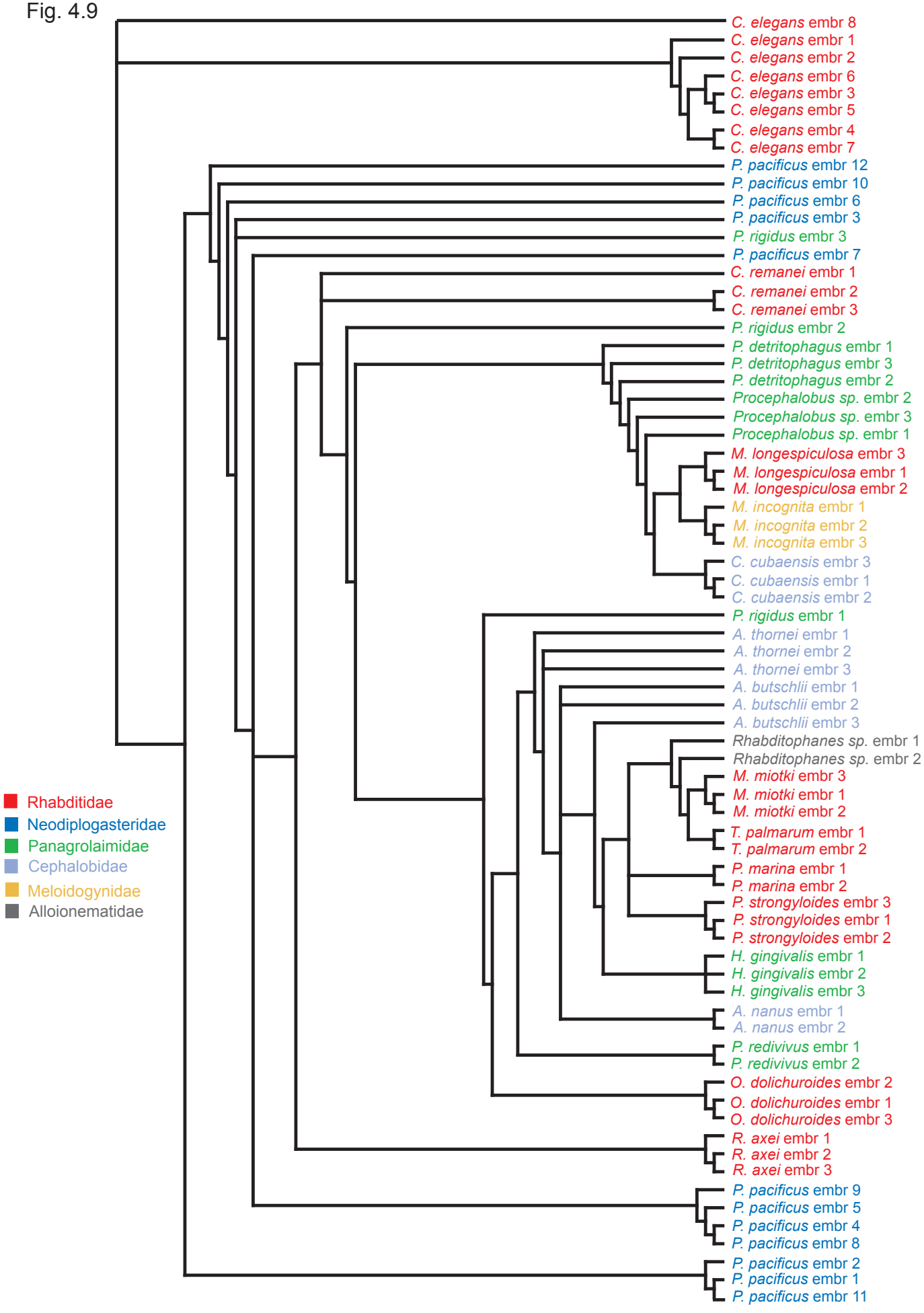
C. elegans embr 8
C. elegans embr 1
C. elegans embr 2
C. elegans embr 6
C. elegans embr 3
C. elegans embr 5
C. elegans embr 4
C. elegans embr 7
P. pacificus embr 12
P. pacificus embr 10
P. pacificus embr 6
P. pacificus embr 3
P. rigidus embr 3
P. pacificus embr 7
C. remanei embr 1
C. remanei embr 2
C. remanei embr 3
P. rigidus embr 2
P. detritophagus embr 1
P. detritophagus embr 3
P. detritophagus embr 2
Procephalobus sp. embr 2
Procephalobus sp. embr 3
Procephalobus sp. embr 1
M. longespiculosa embr 3
M. longespiculosa embr 1
M. longespiculosa embr 2
M. incognita embr 1
M. incognita embr 2
M. incognita embr 3
C. cubaensis embr 3
C. cubaensis embr 1
C. cubaensis embr 2
P. rigidus embr 1
A. thornei embr 1
A. thornei embr 2
A. thornei embr 3
A. butschlii embr 1
A. butschlii embr 2
A. butschlii embr 3
Rhabditophanes sp. embr 1
Rhabditophanes sp. embr 2
M. miotki embr 3
M. miotki embr 1
M. miotki embr 2
T. palmarum embr 1
T. palmarum embr 2
P. marina embr 1
P. marina embr 2
P. strongyloides embr 3
P. strongyloides embr 1
P. strongyloides embr 2
H. gingivalis embr 1
H. gingivalis embr 2
H. gingivalis embr 3
A. nanus embr 1
A. nanus embr 2
P. redivivus embr 1
P. redivivus embr 2
O. dolichuroides embr 2
O. dolichuroides embr 1
O. dolichuroides embr 3
R. axei embr 1
R. axei embr 2
R. axei embr 3
P. pacificus embr 9
P. pacificus embr 5
P. pacificus embr 4
P. pacificus embr 8
P. pacificus embr 2
P. pacificus embr 1
P. pacificus embr 11
Rhabditidae
Neodiplogasteridae
Panagrolaimidae
Cephalobidae
Meloidogynidae
Alloionematidae

Figure 4.10 DIC images of four-cell configurations

A Linear pattern, observed in *M. incognita*. **B** Partial linear pattern, observed in *A. thornei*. **C** Rhomboidal pattern, observed in *P. pacificus*. **D** Tetrahedral pattern, observed in *P. aquatilis*: left scheme, corresponding to the picture; right scheme, clearly showing that in this configuration each cell contacts 3 cells. Below each picture a schematic representation is shown. Scale bar = μm.

Fig. 4.10

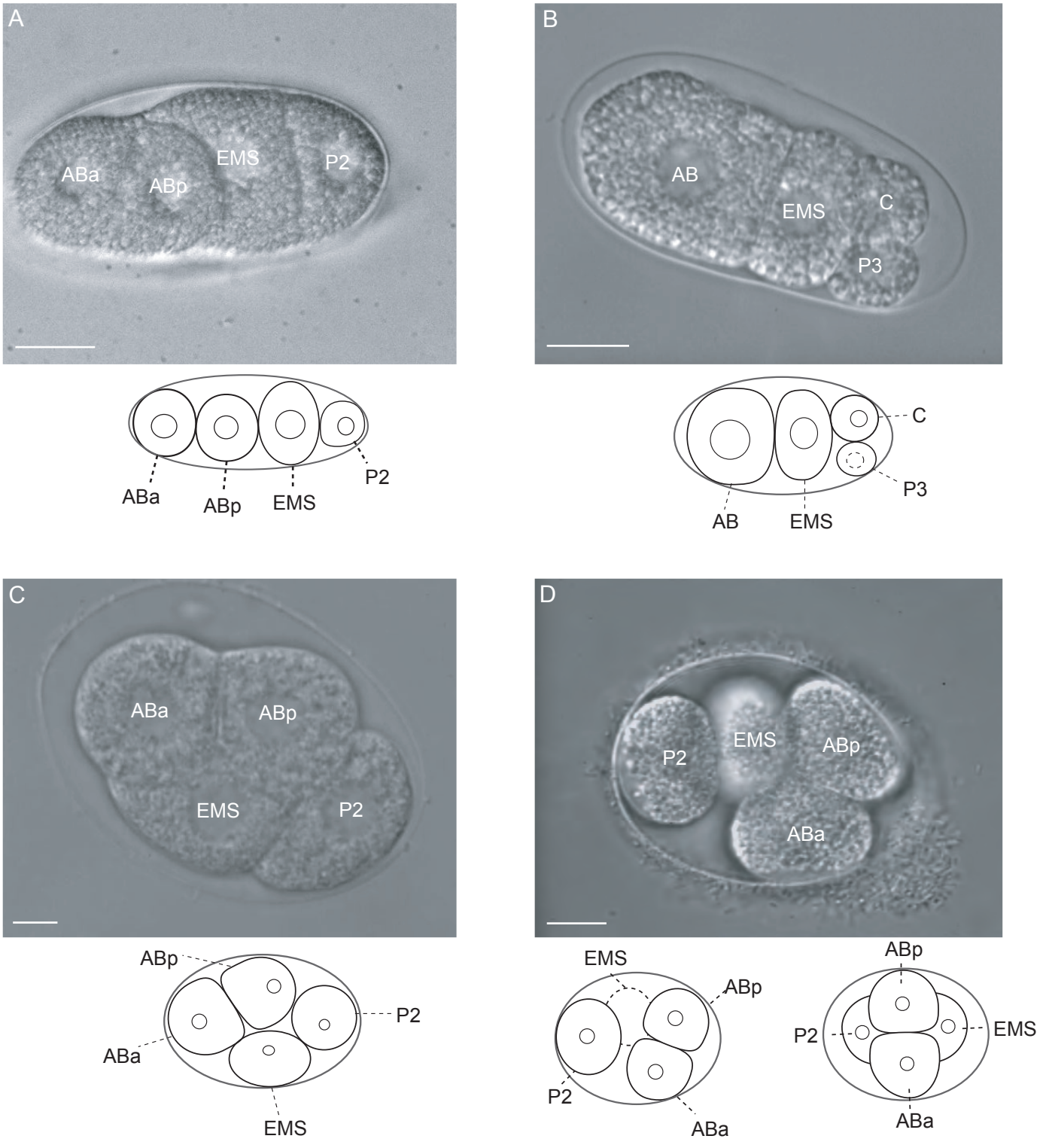
A
ABa
ABp
EMS
P2
ABa
ABp
EMS
P2
B
AB
EMS
C
P3
C
P3
AB
EMS
C
ABa
ABp
EMS
P2
ABp
P2
ABa
EMS
D
P2
EMS
ABp
ABa
EMS
ABp
P2
ABa
ABp
P2
EMS
ABa

Figure 4.11 Parsimonious reconstruction of the spatial configuration of the four-cell embryo onto the phylogenetic tree

This tree is a combination of the nematode phylogeny presented by Holterman *et al.* (2006) and newly obtained consensus phylogenies based on SSU rDNA data of clades 9, 10 and 11. Newly obtained SSU rDNA sequences are marked with an asterisk. Data obtained from literature are marked in blue (for references of *E. brevis*: Voronov and Panchin (1998), Voronov (1999); *P. vulgare*: Malakhov (1994), Malakhov (1998), Voronov *et al.* (1999); *Tobrilus diversipappilatus*, Schierenberg (2005); *Trichocephalus trichurus*, Malakhov and Spiridinov (1981), Malakhov (1994); *Romanomermis culicivorax*, Schulze and Schierenberg (2008); *Gastromermis hibernalis*, Malakhov (1994); *Desmodora serpentulus*, Malakhov (1994); *Hypodontolaimus inaequalis*, Malakhov (1994); *Axonolaimus paraspinosus*, Malakhov (1994); *Daptonema setosum*; Malakhov (1994); *Teratocephalus lirellus*, Dolinski *et al.* (2001), Lahl *et al.* (2003); *Parascaris equorum*, Boveri (1888, 1899), zur Strassen (1896, 1906), Muller (1903); *Rhabditis terricola*, Laugsch and Schierenberg (2004); *Rhabditis dolichura*, Laugsch and Schierenberg (2004); *Diploscpater coronatus*, Lahl (2007); *Rhabdias bufonis*, Spieler and Schierenberg (1995); *Bursaphelenchus xylophilus*, Hasegawa *et al.* (2004). When data from literature was not available, the species are shown in grey. The numbering of the clades (1-12) refers to the phylogeny of Holterman *et al.* (2006).

Fig. 4. 11

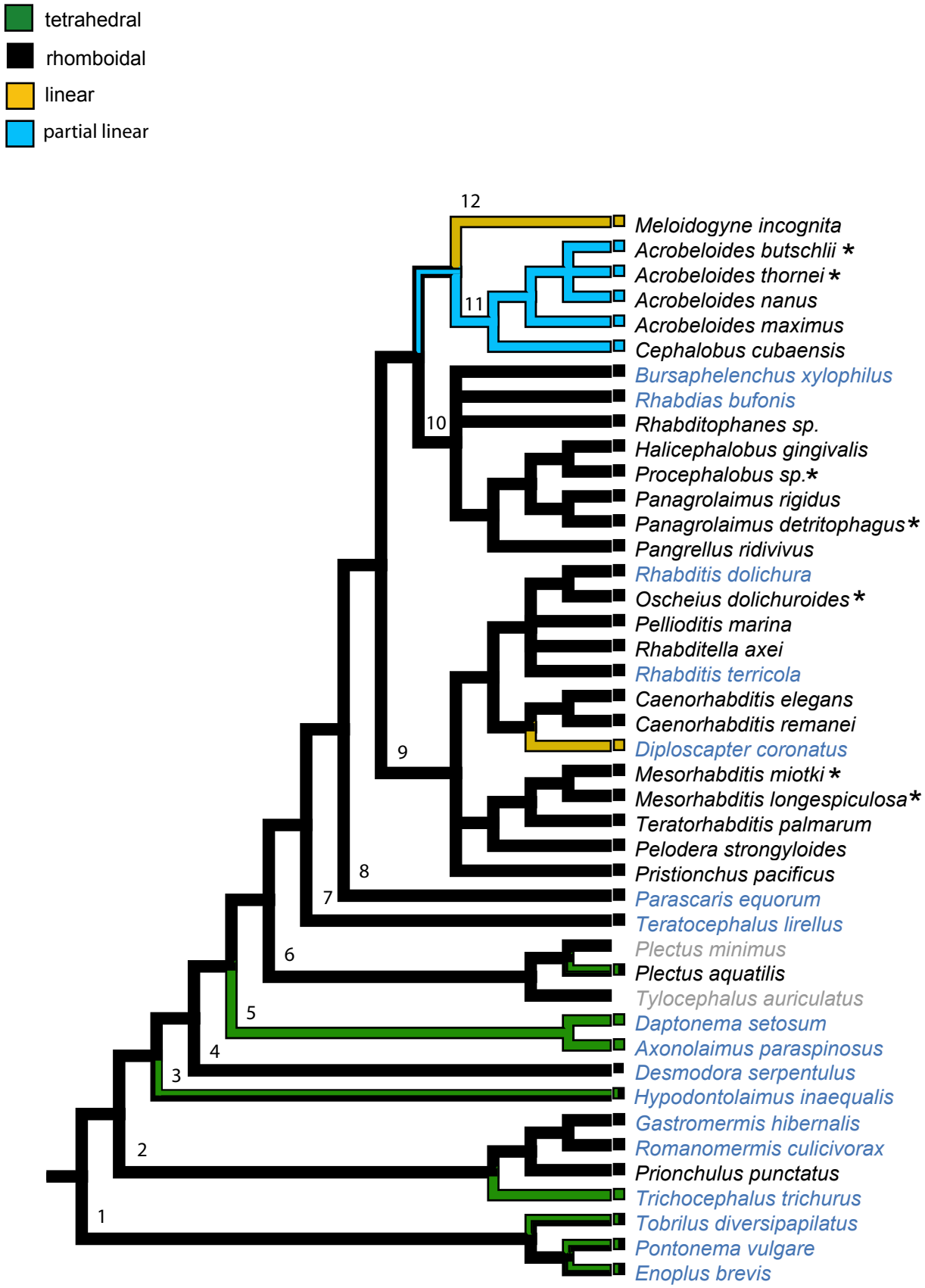
tetrahedral
rhomboidal
linear
partial linear
12
11
10
9
8
7
6
5
4
3
2
1
Meloidogyne incognita
Acrobeloides butschlii *
Acrobeloides thornei *
Acrobeloides nanus
Acrobeloides maximus
Cephalobus cubaensis
Bursaphelenchus xylophilus
Rhabdias bufonis
Rhabditophanes sp.
Halicephalobus gingivalis
Procephalobus sp.*
Panagrolaimus rigidus
Panagrolaimus detritophagus*
Pangrellus ridivivus
Rhabditis dolichura
Oscheius dolichuroides*
Pellioditis marina
Rhabditella axei
Rhabditis terricola
Caenorhabditis elegans
Caenorhabditis remanei
Diploscapter coronatus
Mesorhabditis miotki*
Mesorhabditis longespiculosa*
Teratorhabditis palmarum
Pelodera strongyloides
Pristionchus pacificus
Parascaris equorum
Teratocephalus lirellus
Plectus minimus
Plectus aquatilis
Tylocephalus auriculatus
Daptonema setosum
Axonolaimus paraspinosus
Desmodora serpentulus
Hypodontolaimus inaequalis
Gastromermis hibernalis
Romanomermis culicivorax
Prionchulus punctatus
Trichocephalus trichurus
Tobrilus diversipapilatus
Pontonema vulgare
Enoplus brevis

Figure 4.12 Parsimonious reconstruction of the spatial configuration of the four-cell embryo onto clade 9-12

Tree according to Holterman *et al*. (2006). Data for Anguinidae, Tylenchidae, Aphelenchidae and Aphelenchoididae are obtained from Dolinski *et al*., 2001.

Fig. 4.12

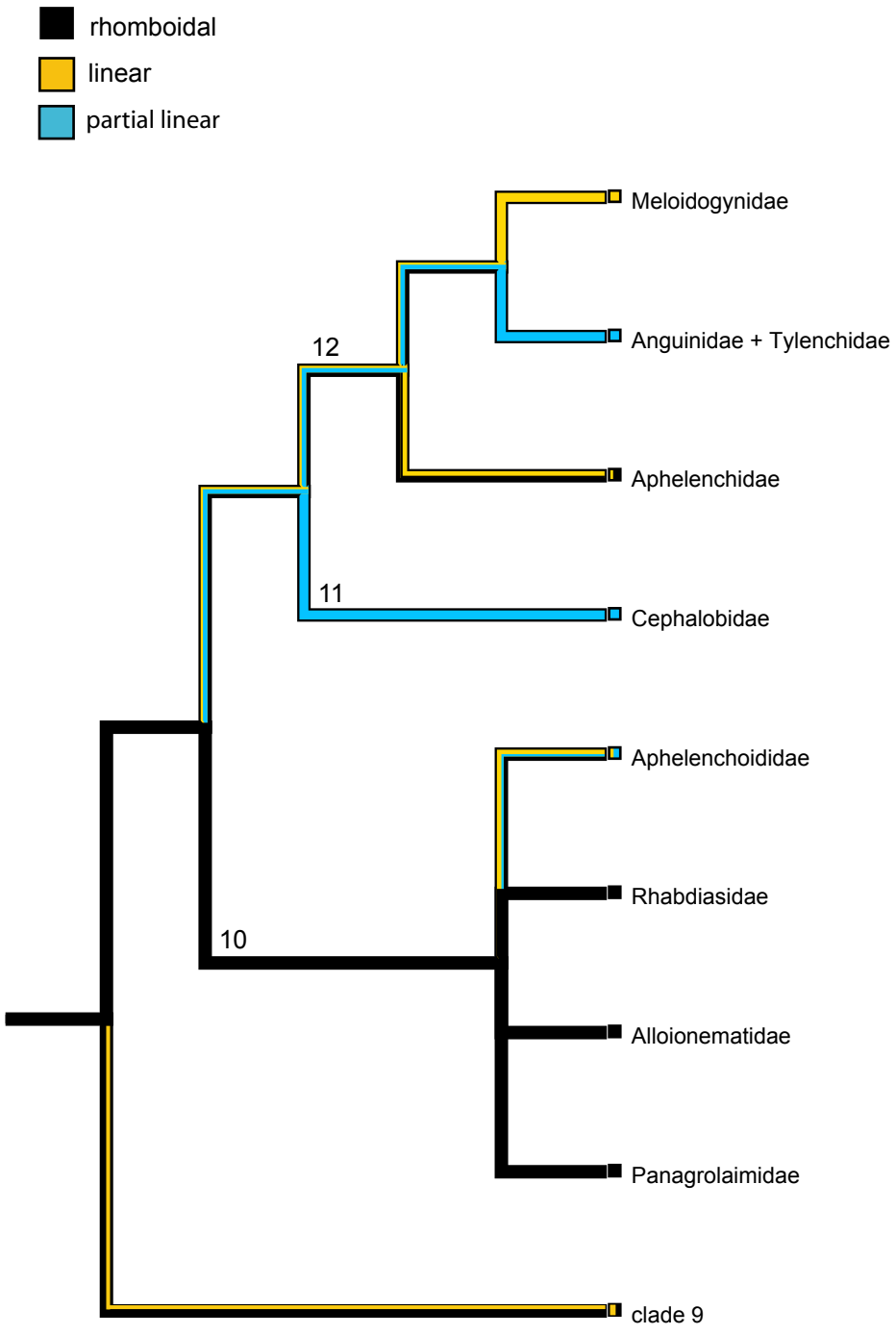
rhomboidal
linear
partial linear
Meloidogynidae
Anguinidae + Tylenchidae
12
Aphelenchidae
11
Cephalobidae
Aphelenchoididae
Rhabdiasidae
10
Alloionematidae
Panagrolaimidae
clade 9

Figure 4.13 Parsimonious reconstruction of the configuration of the posterior cells configuration onto the phylogenetic tree

This tree is a combination of the nematode phylogeny presented by Holterman *et al.* (2006) and newly obtained consensus phylogenies based on SSU rDNA data of clades 9, 10 and 11. Newly obtained SSU rDNA sequences are marked with an asterisk. Data obtained from literature are marked in blue (for references of *Desmodora serpentulus*, Malakhov (1994); *Hypodontolaimus inaequalis*, Malakhov (1994); *Axonolaimus paraspinosus*, Malakhov (1994); *Daptonema setosum*; Malakhov (1994); *Tylocephalus auriculatus*, Lahl *et al.* (2003); *Plectus minimus*, Lahl *et al.* (2003); *Teratocephalus lirellus*, Dolinski *et al.* (2001), Lahl *et al.* (2003); *Parascaris equorum*, Boveri (1888, 1899), zur Strassen (1896, 1906), Muller (1903); *Diploscpater coronatus*, Lahl (2007); *Rhabdias bufonis*, Spieler and Schierenberg (1995); *Bursaphelenchus xylophilus*, Hasegawa *et al.* (2004). When data from literature was not available, the species are shown in grey. The numbering of the clades (1-12) refers to the phylogeny of Holterman *et al.* (2006).

Fig. 4.13

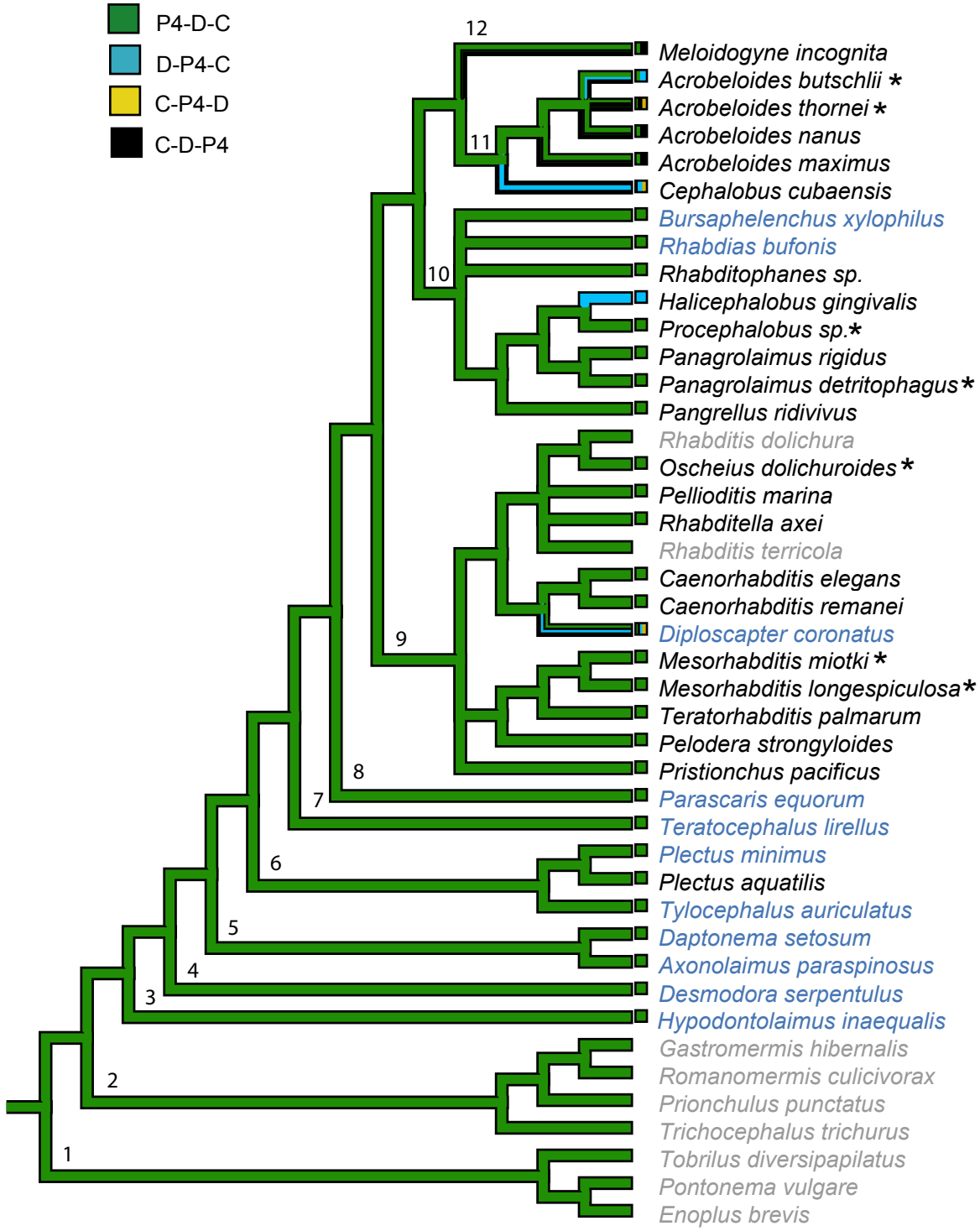
P4-D-C
D-P4-C
C-P4-D
C-D-P4
12
11
10
9
8
7
6
5
4
3
2
1
Meloidogyne incognita
Acrobeloides butschlii *
Acrobeloides thornei *
Acrobeloides nanus
Acrobeloides maximus
Cephalobus cubaensis
Bursaphelenchus xylophilus
Rhabdias bufonis
Rhabditophanes sp.
Halicephalobus gingivalis
Procephalobus sp.*
Panagrolaimus rigidus
Panagrolaimus detritophagus*
Pangrellus ridivivus
Rhabditis dolichura
Oscheius dolichuroides*
Pellioditis marina
Rhabditella axei
Rhabditis terricola
Caenorhabditis elegans
Caenorhabditis remanei
Diploscapter coronatus
Mesorhabditis miotki*
Mesorhabditis longespiculosa*
Teratorhabditis palmarum
Pelodera strongyloides
Pristionchus pacificus
Parascaris equorum
Teratocephalus lirellus
Plectus minimus
Plectus aquatilis
Tylocephalus auriculatus
Daptonema setosum
Axonolaimus paraspinosus
Desmodora serpentulus
Hypodontolaimus inaequalis
Gastromermis hibernalis
Romanomermis culicivorax
Prionchulus punctatus
Trichocephalus trichurus
Tobrilus diversipapilatus
Pontonema vulgare
Enoplus brevis

Table 4.3 Early developmental characters and their evolutionary changes within the phylum

Table 4.3

characters	nr of states	states	nr of changes
rate of developement	2	synchronous	1 change:
		asynchronous	1 from synchronous to asynchronous
division sequence	6	AB-P1-2AB	9 changes:
		AB-P1-P2	1 from P1/AB-EMS/ABa to AB-P1-2AB or from AB-P1-2AB to P1/AB-EMS/Aba
		P1/AB-EMS/Aba	2 from AB-P1-2AB to AB-P1-P2
		P1-P2-AB	1 from AB-P1-2AB to P1/AB-P2 + 1 from AB-P1-2AB or AB-P1-2AB to P1-AB-P2 + P1-AB-P2 to P1/AB-P2
		P1-AB-P2	2 from AB-P1-2AB to P1-AB-P2 or 1 from AB-P1-2AB to P1-AB-P2 + 1 from P1-AB-P2 to AB-P1-2AB
		P1/AB-P2	1 from AB-P1-2AB to P1-P2-AB + 1 from P1-P2-AB to P1-AB-P2
			or from AB-P1-2AB to P1-AB-P2 + from AB-P1-2AB to P1-P2-AB
nr of gastrulating cells	4	1	8 changes:
		2	2 from 2 to 4
		4	1 from 4 to 2
		large group	1 from 1 to 2
			1 from 2 to more than 4 or from 1 to more than 4
			1 from 2 to 1 or from 1 to 2
			1 from 1 to 2
			1 from 2 to 4 or from 1 to 4
spatial configuration in 4-cell embryo	4	tetrahadral	10 changes:
		rhomboidal	6 from rhomboidal to tetrahedral
		linear	2 from rhomboidal to linear
		partial linear	1 from rhomboidal to partial linear
			1 from rhomboidal to linear or from partial linear to linear
spatial configuration of posterior cells	2	fixed	2 changes
		variable	2 from fixed to variable

Figure 4.14 Relative early developmental tempo versus asynchronous/ synchronous development

Time is measured from of the zygote's second division until the division of the endodermal precursor cell E.

Figure 4.15 Relative early developmental tempo versus division sequence

Time is measured from of the zygote's second division until the division of the endodermal precursor cell E.

Fig. 4.14

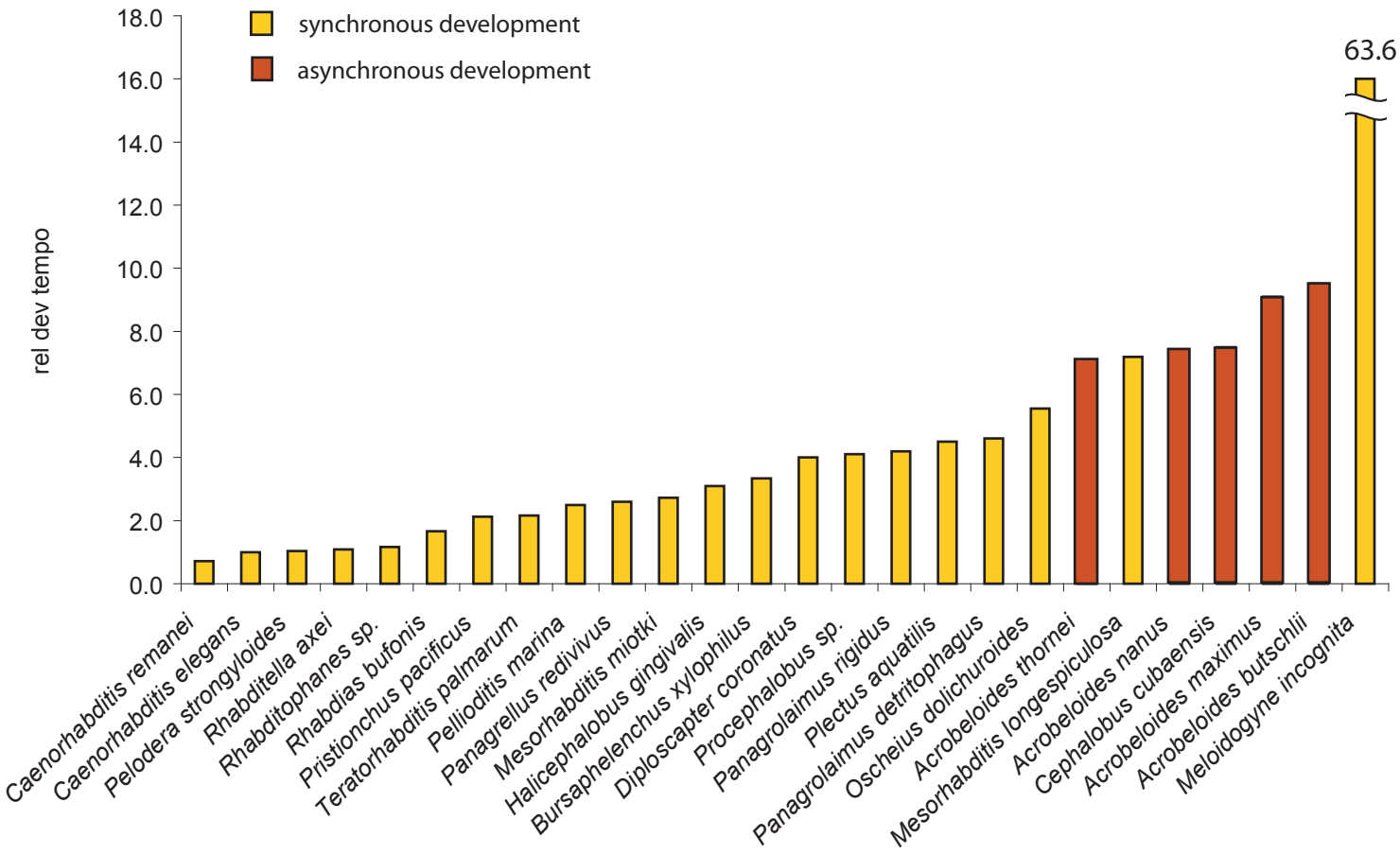

Fig. 4.15

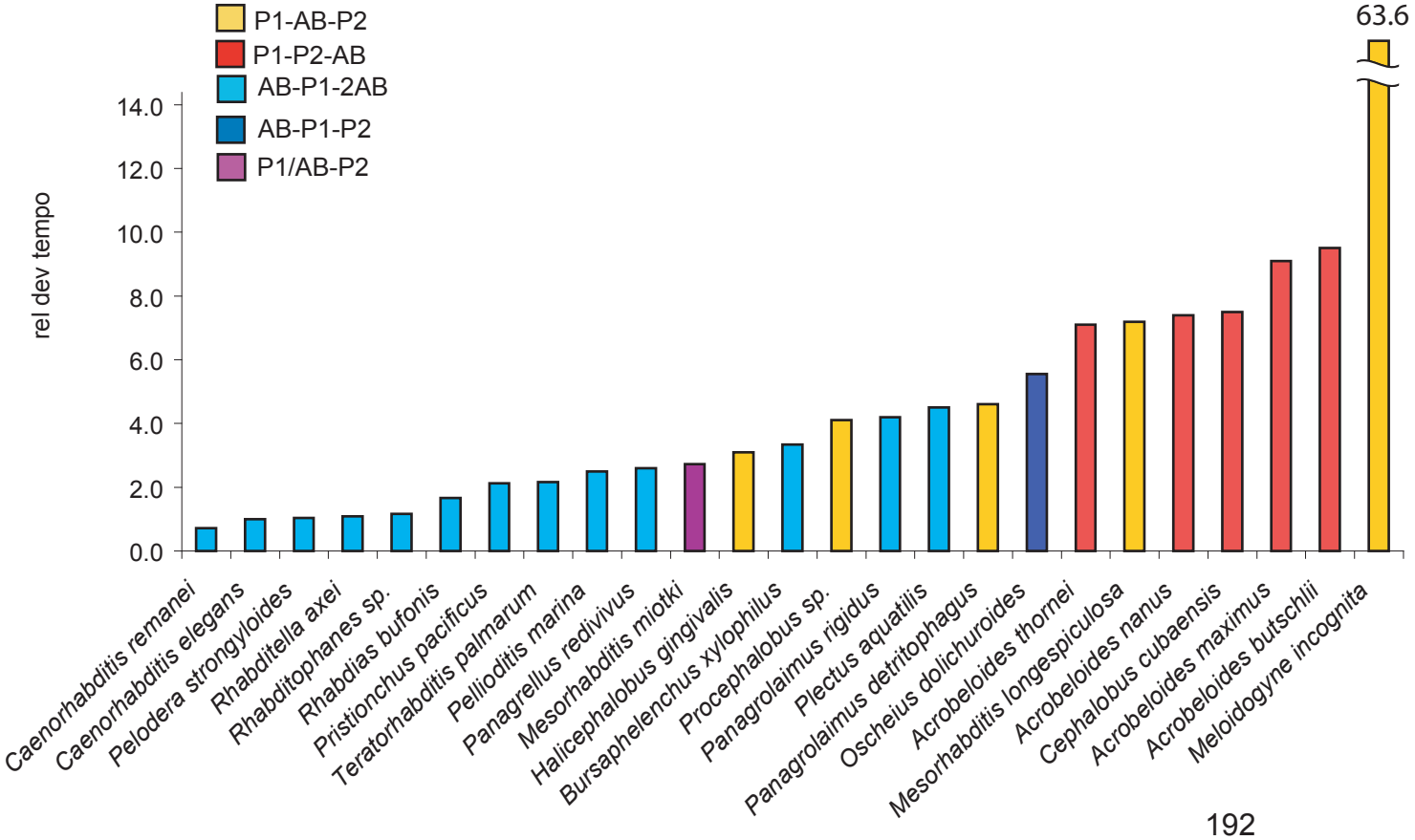

Figure 4.16 Relative early developmental tempo versus configuration in the four cell stage

Time is measured from of the zygote's second division until the division of the endodermal precursor cell E.

Figure 4.17 Relative early developmental tempo versus configuration of the posterior cells

Time is measured from of the zygote's second division until the division of the endodermal precursor cell E.

Fig. 4.16

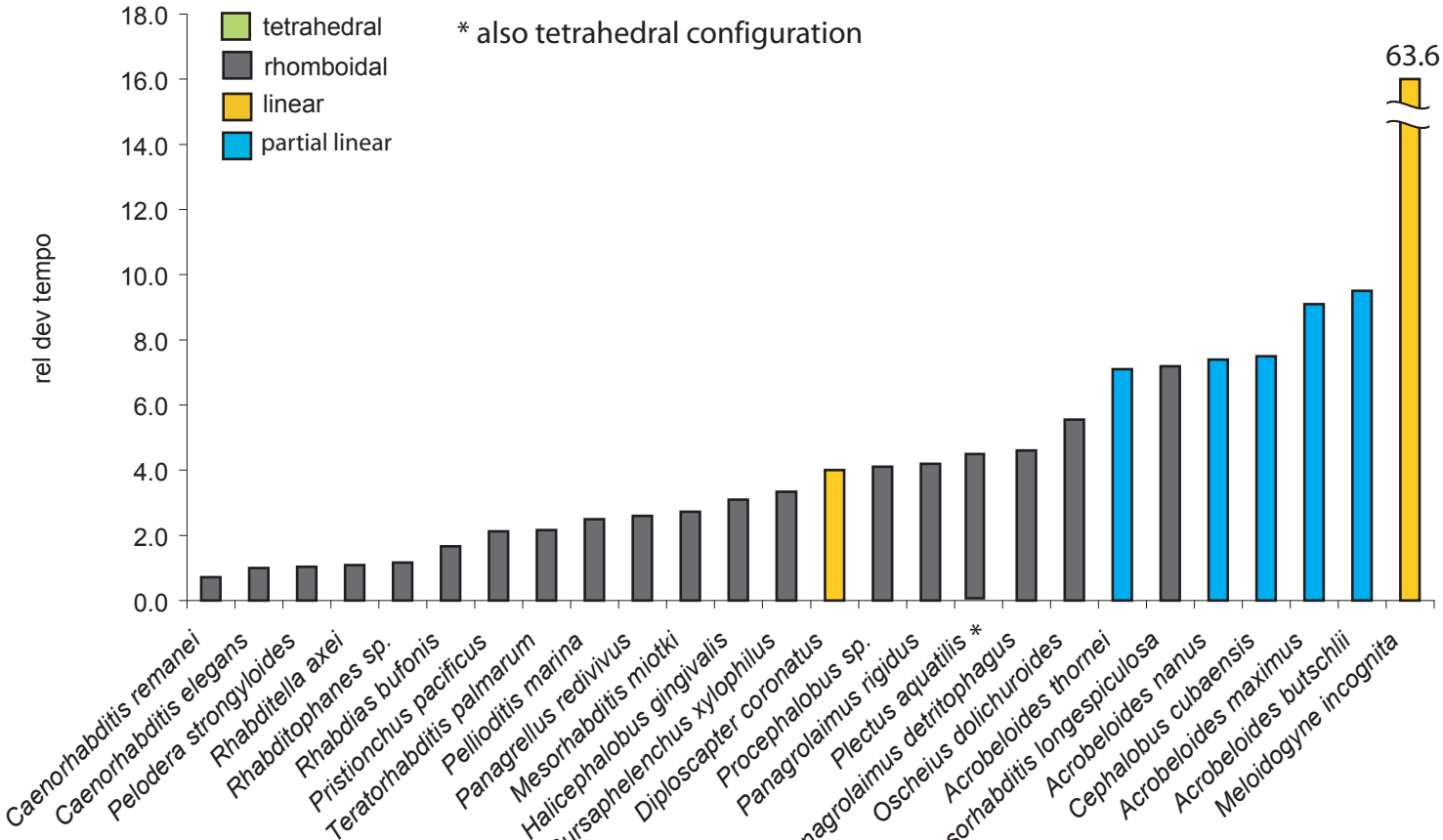

Fig. 4.17

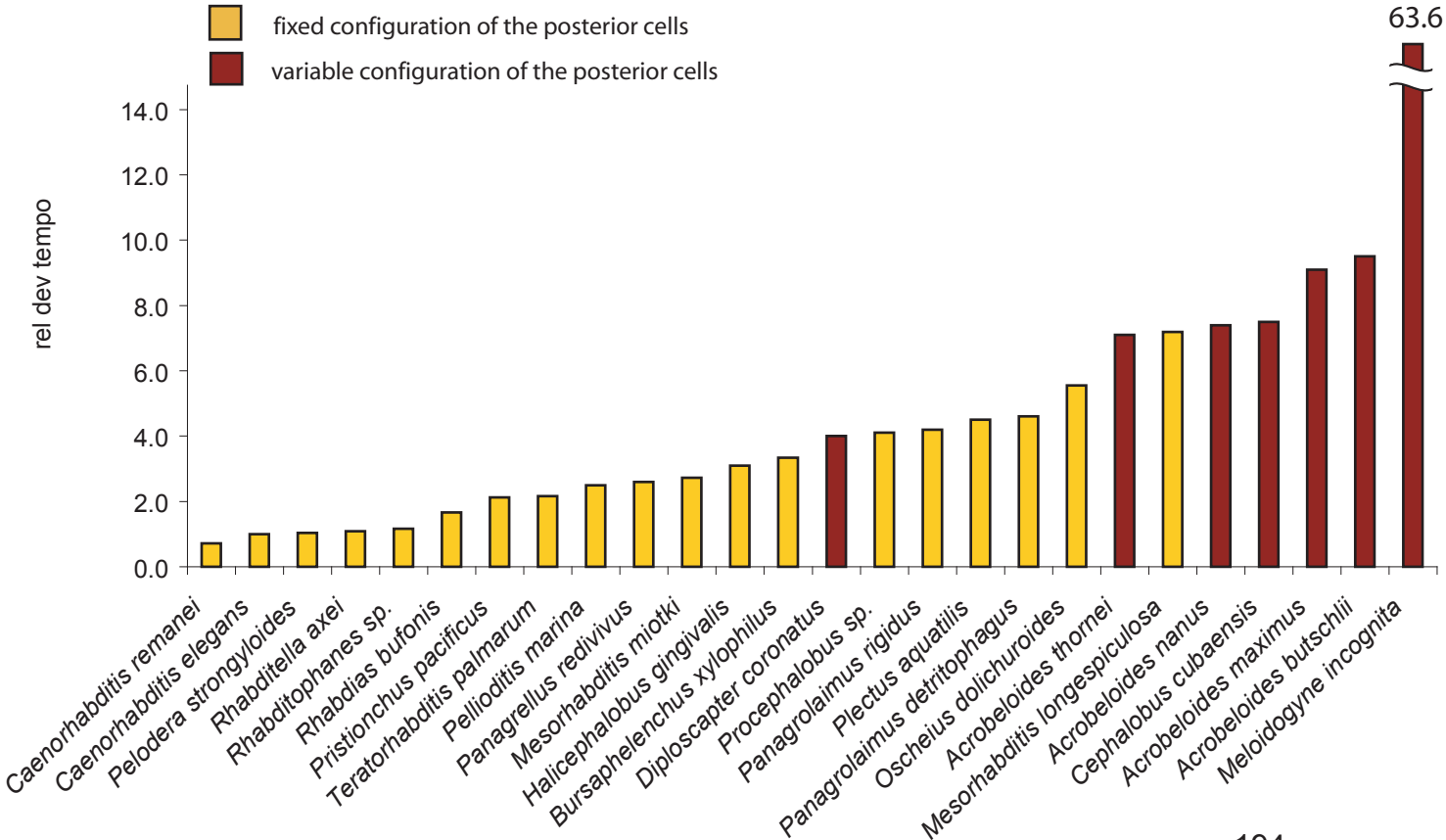

Figure 4.18 Egg shape index (ESI) versus division sequence

Figure 4.19 Egg shape index (ESI) versus configuration in the four cell stage

Fig. 4.18

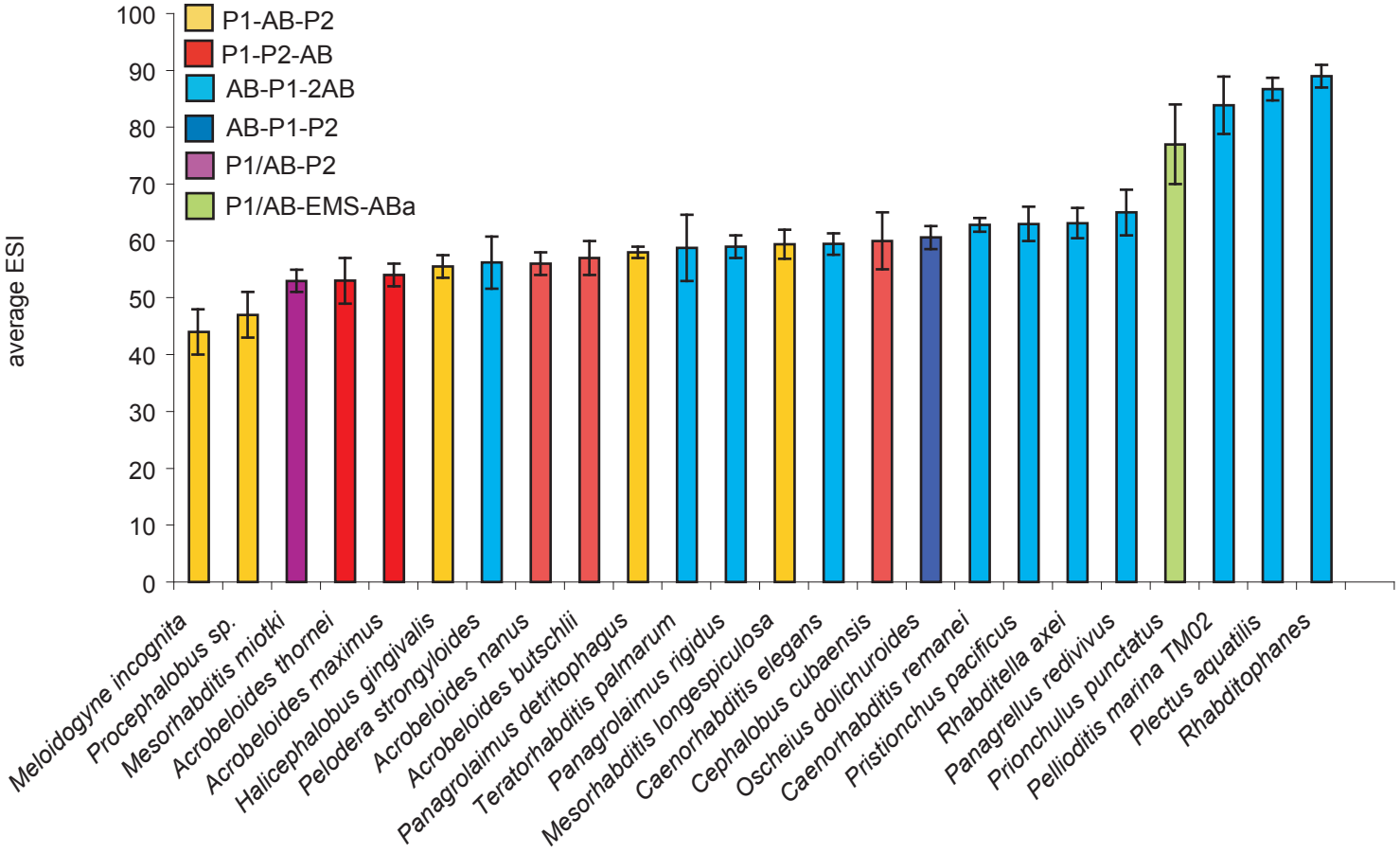

Fig. 4.19

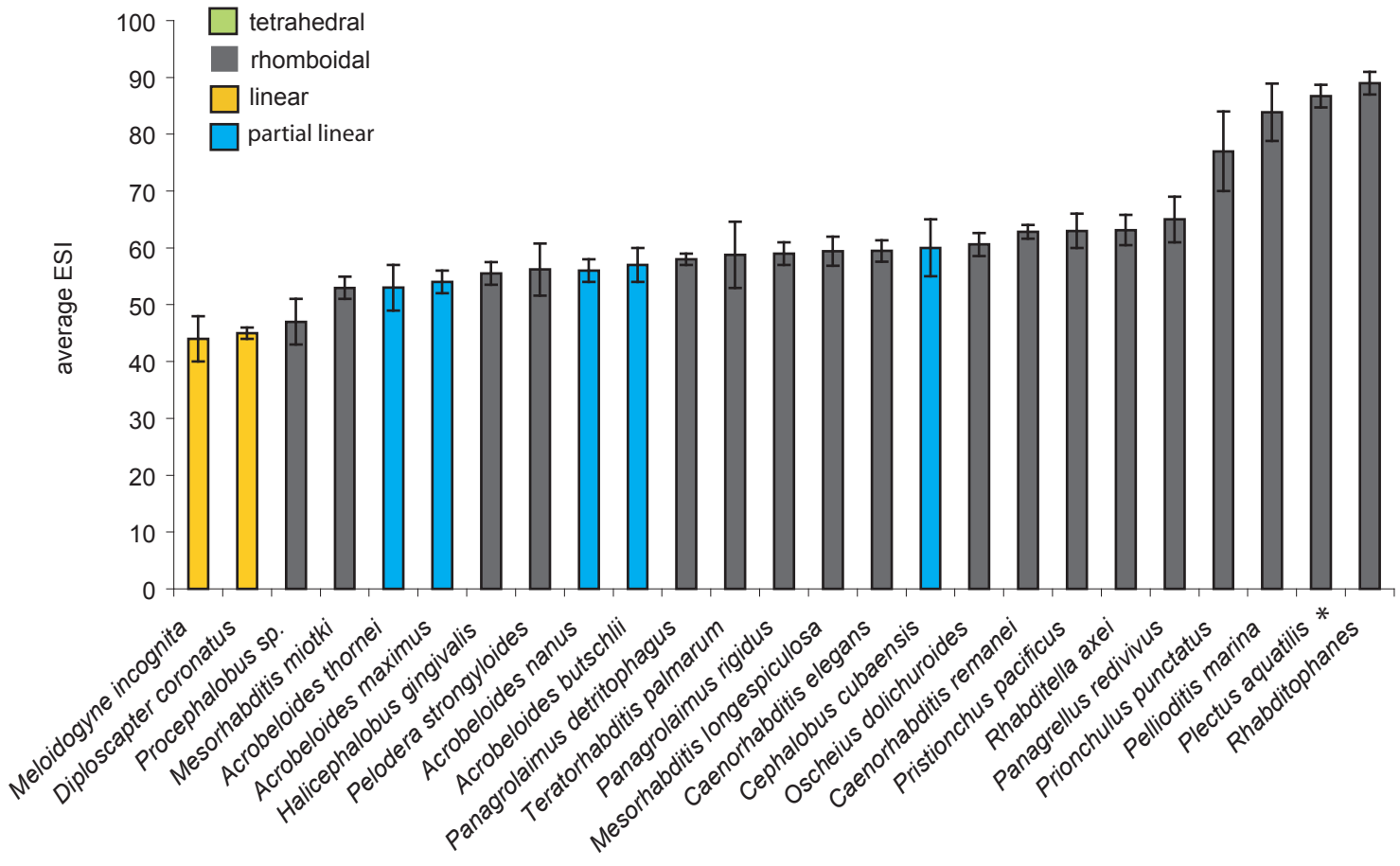

Figure 4.20 Egg shape index (ESI) versus configuration of the posterior cells

Fig. 4. 20

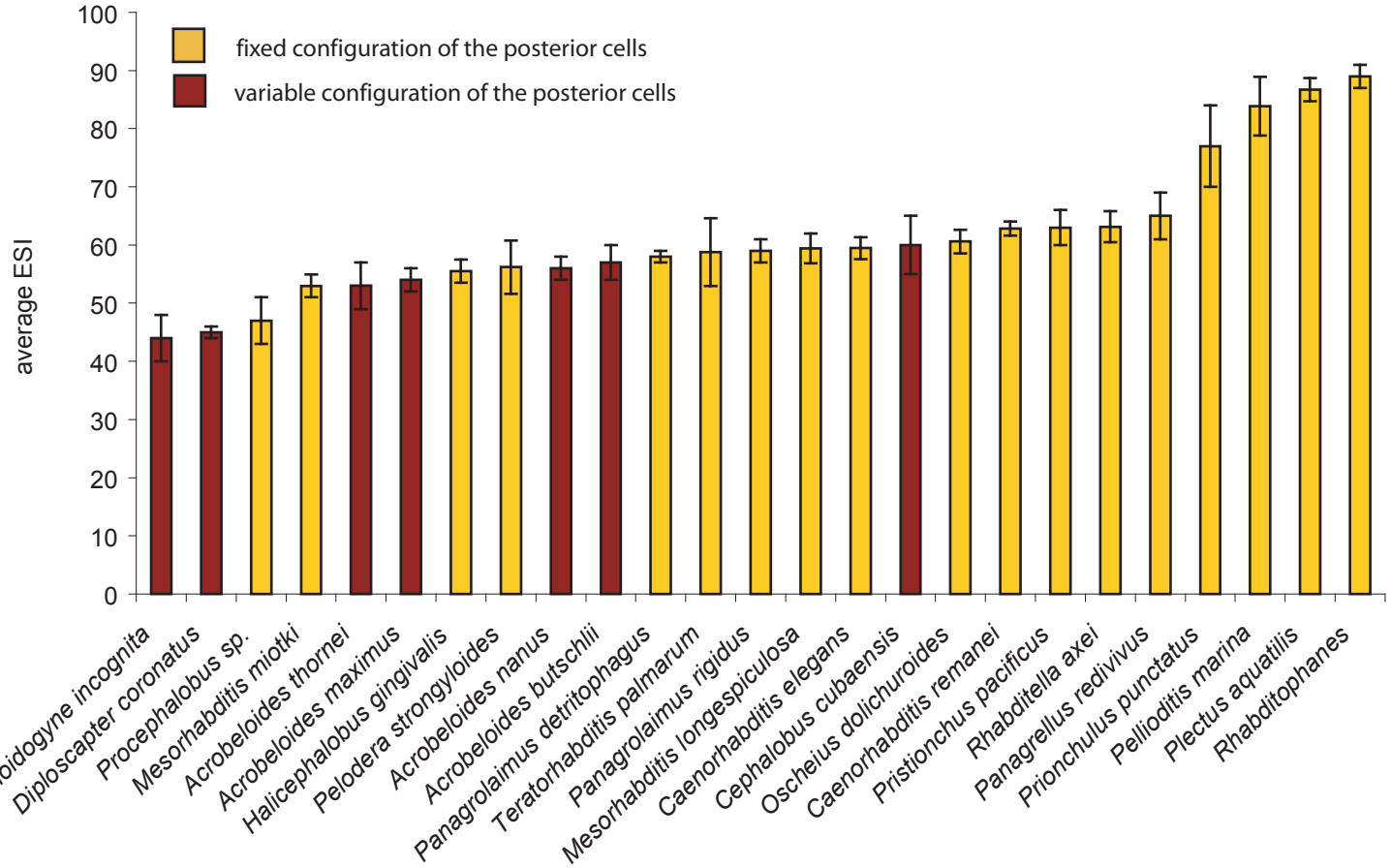
fixed configuration of the posterior cells
variable configuration of the posterior cells
average ESI
100
90
80
70
60
50
40
30
20
10
0
Meloidogyne incognita
Diploscapter coronatus
Procephalobus sp.
Mesorhabditis miotki
Acrobeloides thornei
Acrobeloides maximus
Halicephalobus gingivalis
Pelodera strongyloides
Acrobeloides nanus
Acrobeloides butschlii
Panagrolaimus detritophagus
Teratorhabditis palmarum
Panagrolaimus rigidus
Mesorhabditis longespiculosa
Caenorhabditis elegans
Cephalobus cubaensis
Oscheius dolichuroides
Caenorhabditis remanei
Pristionchus pacificus
Rhabditella axei
Panagrellus redivivus
Prionchulus punctatus
Pellioditis marina
Plectus aquatilis
Rhabditophanes

Table 4.4 p-values for the comparison of developmental tempo between the observed character states for 5 analyzed characters

After each character the p-value deduced from the Kruskal-Wallis-test is given. For each pairwise comparison of character states the p-value from the Mann- Mann-Whitney test is given. Values between brackets are sequential Bonferoni corrections.

Table 4.5 p-values for the comparison of the egg shape index between the observed character states for 5 analyzed characters.

After each character the p-value deduced from the Kruskal-Wallis test is given. For each pairwise comparison of character states the p-value from the Mann-Whitney test is given. Values between brackets are sequential Bonferoni corrections.

Table 4.4

Character 1	**p**
synchronous versus asynchronous rate	0.0003
Character 2	0.0007
AB-P1-2AB versus AB-P1-P2	0.1429
AB-P1-2AB versus P1-P2-AB	0.0001 **(0.0005)**
AB-P1-2AB versus P1-AB-P2	0.0143 **(0.0572)**
AB-P1-P2 versus P1-P2-AB	0.2857
AB-P1-P2 versus P1-AB-P2	0.8
P1-P2-AB versus P1-AB-P2	0.2571
Character 3	0.6026
Character 4	0.0009
rhomboidal versus partial linear	<0.0001
rhomboidal versus linear	0.0994
partial linear versus linear	1
Character 5	
Fixed versus variable	<0.0001

Table 4.5

Character 1	**p**
synchronous versus asynchronous rate	0.2133
Character 2	0.004
AB-P1-2AB versus AB-P1-P2	0.75
AB-P1-2AB versus P1-P2-AB	0.0091 **(0.0455)**
AB-P1-2AB versus P1-AB-P2	0.0029 **(0.0116)**
AB-P1-P2 versus P1-P2-AB	0.2857
AB-P1-P2 versus P1-AB-P2	0.4
P1-P2-AB versus P1-AB-P2	0.2762
Character 3	0.1692
Character 4	0.0206
rhomboidal versus partial linear	0.092
rhomboidal versus linear	0.0131 **(0,0393)**
partial linear versus linear	0.0714
Character 5	
Fixed versus variable	0.0147